From strains to communities: an omics approach to study the diversity and adaptation of Antarctic cyanobacteria
VALENTINA SAVAGLIA
Ph.D. Thesis

GHENT UNIVERSITY

LIÈGE université

fnrs LA LIBERTÉ DE CHERCHER

belspo

FROM STRAINS TO COMMUNITIES: AN OMICS APPROACH TO STUDY THE DIVERSITY AND ADAPTATION OF ANTARCTIC CYANOBACTERIA

VALENTINA SAVAGLIA

Ph.D. Thesis

August 2023

GHENT UNIVERSITY
Ghent University

Faculty of Sciences
Department of Biology
Research Group Protistology & Aquatic Ecology

LIÈGE université
University of Liège

Faculty of Sciences
Department of Life Sciences
InBioS-Molecular Diversity and Ecology of Cyanobacteria

From strains to communities: an omics approach to study the diversity and adaptation of Antarctic cyanobacteria

Valentina Savaglia

Promotor: Dr. Annick Wilmotte

Co-promotor: Prof. Dr. Elie Verleyen

Thesis manuscript submitted in fulfilment of the requirements for the degree of Doctor (Ph.D.) in *Sciences: Biology of Organisms and Ecology* at the University of Liège and the degree of Doctor (Ph.D.) in *Sciences: Biology* at the University of Ghent.

Academic year 2022 – 2023

belspo
MICROBIAN
BI - HABITAT
fnrs LA LIBERTÉ DE CHERCHER

Titre du doctorat en Français : Des souches aux communautés : une approche omique pour étudier la diversité et l'adaptation des cyanobactéries antarctiques

Titel van het doctoraat in het Nederlands: Van stammen tot gemeenschappen: een omics-benadering om de diversiteit en adaptatie van Antarctische cyanobacteriën te bestuderen

Members of the examination committee

Dr. Annick Wilmotte (Promotor, University of Liège, Belgium)

Prof. Dr. Elie Verleyen (Co-promotor, Ghent University, Belgium)

Prof. Dr. Koen Sabbe (Chairman, Ghent University, Belgium)

Prof. Dr. Denis Baurain (Co-chairman, University of Liège, Belgium)

Prof. Dr. Anne Willems (Ghent University, Belgium)

Dr. Bjorn Tytgat (Ghent University, Belgium)

Prof. Dr. Marc Hanikenne (University of Liège, Belgium)

Dr. Aline Frossard (Eidg. Forschungsanstalt WSL, Switzerland)

Prof. Dr. David Velazquez (Universidad Autonoma de Madrid, Spain)

This research was financially supported by the Fonds de la Recherche Scientifique (FNRS-FRIA), BelSPO MICROBIAN project, Ghent University and University of Liège. BCCM/ULC cyanobacterial collection is also thanked for the use of the ULC 180 and 008 strains.

Jonathan Kendrick,
Conferences of Cambridge "Antarctica
The alive continent,"
March the 17th, 1995

Imagine for a moment a continent that for three months a year doubles its volume. A continent in constant movement; a movement that is imperceptible for a human eye, but that, however, is devastating.

Imagine that you could see from the sky this immense mass covered by snow. You would therefore see the marks of this movement: enormous waves hurling against the glaciers, surrounding the mountains and falling as captured waterfalls in a photographic film.

This is the "imposing inertia" of which Eugene Linden spoke about. And if we, as Linden, imagine that we are looking at this image through a time-lapse photography taken during thousands of years, then yes, we would see this movement.

Thirty centimeters of movement every year doesn't seem too much in real time, but with predetermined intervals, the glaciers become rivers of ice; ice that move gracefully and freely, with an impressive and unstoppable power.

Impressive? From here I perceive your incredulity. Thirty centimeters over a year. What damage could it cause?

Well, let me tell you: a lot. Did you know that the British Government had to replace Halley station four times? You will see, as many of other research stations in the Antarctic, Halley station has been built underground, buried within the ice, but a shift of only thirty centimeters over a year would crack its walls and considerably bend its roofs.

The issue here is that the walls of Halley station are under lots and lots of pressure. All this ice moving towards the exterior, inexorably advancing towards the ocean, it is willing to reach the sea (to know the world in an iceberg form, you could say), and it is not willing to that something so insignificant as a research station would interpose to its path.

Even so, Great Britain did not come out bad from these ice displacements if we compare to other countries' stations.

Think to what happened in 1986, when the ice platform Flichner lighted up an iceberg of the size of Luxembourg in the Weddell Sea. Thirteen thousand square kilometers of ice would separate from the continental mass... taking with it the Belgrano I station, an abandoned Argentinean station, and the Soviet summer station Druzhnaya. Apparently, Soviets were foreseeing using Druzhnaya that summer. They spent the three following months looking for their misplaced station between the three enormous icebergs that originated from the displacement of the ice. And they found it. With time. But they found it.

United States was even less lucky. In the decade of the sixties, this country saw how their five stations Little America remained isolated in icebergs.

Ladies and gentlemen, the message that we can take from all this is very simple. What it seems barren, it could be not. What it looks inanimate, it could be not.

No. When you look to the Antarctic, don't let yourself fool. We are not looking to a rock covered by ice. We are looking to an alive continent, a continent that breathes.

AKNOWLEDGMENTS

It is not easy to start this paragraph, maybe it is the most difficult one of the entire thesis.

I have felt so lucky during these years of Ph.D., to be surrounded of inspiring and kind people upon which I could always count. It has not been an easy journey, with COVID-19 in between, but I will always remember that even during the difficult times, I had extraordinary people around me.

First, I would like to thank my supervisors for giving me the opportunity to start a Ph.D. in your laboratory and supported me throughout this journey, to participate to the three Antarctic field campaings foreseen within the MICROBIAN project, and trust me enough to ask me to take part of the next one. Dr. Annick Wilmotte, you gave me the opportunity to participate to conferences of international level since the very beginning of my Ph.D., you supported me during the FRIA preparation as well as during all the outreach activities within the APECS Belgium association - I will always be grateful to you for this. Prof. Elie Verleyen, among the wisest teaching I got from you are: to never sleep during the field campaigns (24h of light are not there for nothing ☺), always support each other in the difficult moments, that there are things that just take the time they take (snow storms, Ph.D. thesis...). Jokes aside, I felt very lucky to have been able to write the thesis at your laboratory, where I could confront myself with several other researchers and Ph.D. students, and could always ask you for brainstorming and suggestions. Thank you very much for always be there! Finally, thank you for teaching me how to be a good field scientist and (hopefully one day) a good scientific writer as well. I also thank Dr. Bjorn Tytgat for your co-supervision during my PhD. I would have probably not made through it if it wasn't for your support and advices when I was stuck and I asked you. I also thank all the other MICROBIAN team members and collaborators, Sam Lambrechts and Quinten Vanhellemont with whom I shared the laboratory work and the field campaigns, Prof. Anne Willems and Prof. Wim Vyverman for, among other things, your insightful comments on the second chapter of this thesis, Prof. Bart Van de Vijver, Prof. Josef Elster and Dr. Anton Van de Putte.

Per la prima volta mi ritrovo ad avere l'opportunità di ringraziare le persone che mi sono state vicine durante questi anni lunghissimi di tesi. In realtà ne ringrazierò meno di quelle che dovrei e spenderò meno parole di quelle che vorrei perché se no dovrei scrivere un'altra tesi. Però, anche se con tutte le imperfezioni di questo mondo, due persone più di tutte hanno contribuito alla mia riuscita, e queste sono mamma e papà. Vi ringrazio per avermi dato l'opportunità di studiare all'estero, quell'esperienza è stata fondamentale per riuscire a guardare il mondo con altri occhi, e sopratutto per credere in me stessa. Papi, un grazie speciale per avermi supportato (e sopportato!), per quelle sere in terrazza quando ero piccola in cui ti torturavo di perché con la testa all'insú mentre guardavamo le galassie e tu rispondevi sempre. Chissà che la mia curiosità verso il mondo là fuori non sia nato proprio da lì. Are, tu sei sempre pronta a disfare tutto il mio stress quando ti chiamo, grazie tortellina. So che non smettete mai di credere in me e per me è importante. Grazie anche a zia Angela, Luca, Andrea e zio Giovanni, per assupparvi da sempre tutte le mie storie sull'Antartide (ma una cosa più semplice no?!), nonna Agata per i suoi teatrini che fanno sempre un sacco ridere e infine alle due persone che se anche non sono più fra noi porto sempre un pezzettino di loro con me, nonno Prospero e zia Fides.

Jens, Bea, Yaprak, Benoit, Souk, you have been the dearest people to me during these years, vous avez fait de ces années sur Liège les meilleurs qu'ils vont me manquer pour toujours, j'en suis sure. Une turque, une

espagnole, une italienne et una marocaine traversent la route, qui sait comment ça se terminera (si ça terminera) cette histoire.. ☺

Alessia, Jojo e Gaietta, Mari, Gaë, Rorina & Neri, I couldn't have wished for better people around me ❤ Richard, Elyse, Jean-Louis, Alix et Isidor pour être toujours là, mon cocon imaginaire, ma "boulle" :-P Les tomato sessions avec Alice, Gwendo, Justine, Emeline, Charlotte, et d'autres déjà mentionnés.. tellement contente d'avoir partagé ce bout de chemin ensemble. Igor and Yannick, thanks for having been there when I needed you giving me another perspective (a "bird view") to my work. Mes professeurs et collègues photographes, Pascal Loup, Alain, Denis, Olivier, Maurice qui m'ont accompagnée et supporté mes histoires de these lors de ces derniers trois ans. Merci pour m'avoir fait découvrir ce monde magnifique dans lequel je peux laisser la créativité à libre ésprit. Liège n'aurait pas été la même sans Saint-Luc. E poi Cecio e Giorgia per essere sempre state compagne d'avventure e di storie dal liceo ad ora, Eddie e la piccola Norah as well, per i suoi sorrisoni. Fabrizie, per le nostre passeggiate (virtuali e in presenza) davanti al mare. Fabio per le faticate, che valevano sempre la pena con paesaggi mozzafiato e Laura per tutte le avventure fatte insieme per mari e monti (letteralmente) tra bici ed escursioni bellissime. The Canardo team – I am still crying for all our laughs. A mis amigas argentinas, Caro y Mica que siempre estuvieron a mi costado aunque lejas. Last but not least, all past and present APECS BE members, especially Ming, Caro, Henrik, Marie, Lotte, Marina, Jill, Louise, Mieke, it has been wonderful shaping APECS BE together! And in general to APECS international for all the great opportunities and network that gives to ERCs, such as participating to scientific publications and to IPCC review groups. I care about thanking Dr. Clare Eayrs who helped me finding a solution during COVID-19 pandemics with the storage of my samples from Antarctica that remained stuck in Cape Town for months. Unfortunately, I could not use those samples for my PhD, but people met within APECS international demostrated to be a strong network upon which ERCs could count even during difficult situations. I felt lucky to be part of it. It also gave me the chance to be a rapporteur for the European Polar Board during two policy makers' meetings, getting to know the inspiring Dr. Renuka Badhe and collaborating also with Joseph E. Nolan.

A special thanks also to Dr. Katharina Zacher for having taught me how to "do" science, not only during the Master Thesis but also supporting me during the one-week of intense writing of my firts first-author publication with coffee and croissants ☺ even though I already started my PhD, you did your best to get it done together. I hope I will be even 1/10 as good as you as a supervisor.

I am also grateful to Dr. Jana Kvíderova for having teached me everything about photosynthetic measurements in the field. For all your kindness and patience in taking the time for training me in Třeboň, thank you.

Alain Hubert, Gigi, Henri Robert, Pierre-Yves Terrettaz and Raphaël Mayoraz and all the Princess Elisabeth Antarctica station team of IPF, thank you for the support provided during the Antarctic field campaigns and beyond.

Finally, I thank the Presidents of my Ph.D. jury, Prof. Koen Sabbe and Prof. Denis Baurain, and the members of my Ph.D. jury, Prof. Marc Hanikenne, Prof. Anne Willems, Dr. Bjorn Tytgat, Prof. David Velazquez and Dr. Aline Frossard for reading and providing constructive commentaries on my Ph.D. manuscript, that truly improved the quality of the final version.

Grazie mille.

CONTENT

ABBREVIATIONS & ACRONYMS

ACBR	Antarctic Conservation Biogeographic Regions
ANOVA	Analysis of Variances
ASPA	Antarctic Specially Protected Areas
ASV	Amplicon Sequence Variants
ATCM	Antarctic Treaty Consultative Meeting
BCCM	Belgian Coordinated Collections of Microorganisms
BSC	Biological Soil Crusts
Chl *a*	Chlorophyll *a*
CSS	Cumulative-Sum Scaling
db-RDA	Distance-Based Redundancy Analysis
DEG	Differentially Expressed Gene
DNA	Deoxyribonucleic Acid
EC	Electric Conductivity
EPS	Exopolysaccharide
FC	Fold Change
HPLC	High-Performance Liquid Chromatography
IPCC	Intergovernmental Panel on Climate Change
ITS	Internal Transcribed Spacer
MAA	Mycosporine-like Amino Acid
nMDS	Non-Multidimensional Scaling
OTU	Operational Taxonomic Unit
PAM	Pulse Amplitude Modulation
PAR	Photosynthetically Active Radiation
PCNM	Principal Coordinates of Neighbourhood Matrix
PCoA	Principal Coordinate Analysis
PES	Princess Elisabeth Station
PSI	Photosystem I
PSII	Photosystem II
QY	Quantum Yield
RDA	Redundancy Analysis
ROS	Reactive Oxygen Species
RF	Random Forest
rRNA	Ribosomal Ribonucleic Acid
SRM	Sør Rondane Mountains
SSU	Small Subunit
TN	Total Nitrogen
TOC	Total Organic Carbon
TP	Total Phosphorus
UVR	Ultraviolet Radiation
VIF	Variance Inflation Factor

SUMMARY

Ice-free areas cover less than 0.5 % of the Antarctic, yet they host most of the terrestrial biodiversity of the whole continent. These terrestrial habitats are characterized by truncated and simple food webs consisting almost uniquely of microbial communities. Cyanobacteria are among the main primary producers in these habitats where they are often regarded as 'ecosystem engineers. Despite the important ecological role cyanobacteria play, our understanding of the factors shaping their diversity and community structure, as well as their adaptions to cope with the extreme abiotic conditions in the Antarctic remains limited.

The main aims of this Ph.D. were to (1) characterize the community structure and distribution of bacteria and micro-eukaryotes in a variety of substrates from different nunataks and valleys of the Sør Rondane Mountains region (East Antarctica); (2) identify keystone taxa in these food-webs and the main abiotic factors structuring these communities (**Chapter 2**); (3) provide a detailed understanding of the cyanobacterial diversity and community structure in these regions (**Chapter 3**); (4) identify the main physiological and genetic adaptation mechanisms that a pair of species of *Nostoc* (cyanobacteria) employ under desiccation – rehydration events which frequently occur the terrestrial environments of the Antarctic (**Chapter 4**). To achieve these goals, a multidisciplinary approach was applied combining ecophysiological and several omics analyses.

In **Chapter 2,** the composition of bacterial and micro-eukaryotic communities was examined using high-throughput sequencing of parts of the 16S rRNA and 18S rRNA genes in 105 soil samples across 9 sites within a 100 km radius in the Sør Rondane Mountains (East Antarctica), differing in substrate type and associated physical and chemical conditions. In moraine soils, Actinomycetota and Cercozoa were among the most abundant bacterial and eukaryotic phyla, whereas on gneiss, granite and marble bedrock, Cyanobacteriota and Metazoa were the among the dominant bacterial and eukaryotic phyla. A distinct differentiation was observed within the Cyanobacteriota phylum at a higher taxonomic resolution depending on bedrock type, with

granite being dominated by the Nostocaceae family and marble by the Chroococcidiopsaceae family. Surprisingly, metazoans reached a relatively high abundance in the eukaryotic dataset even in samples from the most arid sites, such as moraines in Austkampane and Widerøefjellet. Overall, this study showed that different substrate types support distinct microbial communities in inland Antarctic nunataks and valleys, and that lithological diversity is a major determinant of terrestrial microbiome biodiversity.

In **Chapter 3**, the cyanobacterial community structures of the same sampled sites as in Chapter 2 were further investigated based on the use of cyanobacterial-specific primers targeting the V3-V4 region of the 16S rRNA gene in a high-throughput sequencing approach. The latest cyanobacterial taxonomic insights used in the recently released CyanoSeq database were applied to these sequences. Ordination analyses revealed that these different substrates harbour distinct cyanobacterial communities. Differences in community structure were significantly related to differences in pH, concentration of TN and $N\text{-}NO_3^-$, and electrical conductivity. The granitic soils of the Pingvinane nunataks hosted the highest richness followed by those from the granitic Utsteinen ridge. Granitic substrates were characterized by high TN concentrations and a neutral pH and hosted a variety of filamentous Cyanobacteria, such as Leptolyngbyaceae, Gomontiellaceae, Microcoleaceae, Oculatellaceae, Nostocaceae, but also unicellular taxa (Cyanothecaceae). The moraine samples from Austkampane and Widerøefjellet were dominated by Microcoleaceae and Gomontiellaceae, respectively. They were characterized by a high dry weight and low TN, and the diversity and abundance of cyanobacteria was low. The taxonomic richness was also low in soils from the alkaline marble bedrock and the gneiss bedrock from the Perlebandet nunatak, which were both characterized by high TN. Marble bedrock was dominated by *Alitarella* sp. (Chroococcidiopsaceae), whereas gneiss by *Cyanothece* sp. (Cyanothecaceae). Overall, our data show that different substrate types host distinct cyanobacterial communities.

Cyanobacteria need to deal frequently with desiccation and rehydration events in Antarctic terrestrial and lacustrine habitats as well as during dispersal between habitats. In **Chapter 4**, the response to short-term desiccation exposure and rehydration of a terrestrial and

freshwater strain belonging to the same *Nostoc* species was investigated. To achieve this, the pigments and osmolytes (trehalose and sucrose) concentrations as well as the photosynthetic efficiency were measured in combination to a metatranscriptomic (RNA-seq) analysis of the two *Nostoc* strains after 3h of desiccation, followed by rehydration after 10 min, 24h and up to 72h. Both strains reacted to dehydration by accumulating sucrose, whereas trehalose was present in lower concentrations. Only the freshwater strain showed a recovery in chlorophyll a content after 72h of rehydration. However, the photosynthetic efficiency remained below the original levels measured before desiccation in both strains. Transcriptomics profiles showed that both strains protected their cells during dehydration by inducing stress-related genes, such as those for the production of carotenoids, trehalose synthase and nitrogen fixation-related genes. The terrestrial strain responded with the up-regulation of a higher number of genes compared to the freshwater strain. The photosynthetic metabolism, however, slowly decreased after 24h of rehydration as evidenced by the down-regulation of genes related to phycobilisomes and photosystems, whilst *psbA2* gene, encoding the D1 protein synthase necessary for PSII, was found to be significantly up-regulated under desiccation in the terrestrial ULC180, but not in the freshwater ULC008. These results suggest habitat specific adaptions to environmental stress in cyanobacteria, and provide novel insights into the strategies related to survival and adaptation of non-model Antarctic *Nostoc* strains to desiccation and rehydration events during the first 3 days experienced in extreme environments.

In the final chapter the main findings of this Ph.D. thesis were discussed and a number of future research perspectives are formulated. These include the use of shotgun metagenomics over amplicon sequencing or the use of more specific primers in bacterial and micro-eukaryotic surveys, the characterization of biotic interactions and the integration of non-model organisms in experiments concerning their abiotic tolerance. Overall, the importance of integrating both ecophysiology and 'omics' disciplines is highlighted throughout this Ph.D. thesis, with the aim of maximizing our understanding about the ecologic role of microbial communities inhabiting the extreme Antarctic ice-free areas.

SAMENVATTING

IJsvrije gebieden beslaan minder dan 0,5 % van Antarctica, maar herbergen toch het grootste deel van de terrestrische biodiversiteit van het hele continent. Deze terrestrische habitats worden gekenmerkt door korte en eenvoudige voedselwebben die bijna uitsluitend uit microbiële gemeenschappen bestaan. Cyanobacteriën behoren tot de belangrijkste primaire producenten in deze habitats en worden vaak beschouwd als "ecosysteemingenieurs". Ondanks de belangrijke ecologische rol die cyanobacteriën vervullen, hebben we nog steeds een beperkte kennis over welke de factoren hun diversiteit en gemeenschapsstructuur bepalen, alsook welke adaptaties ze bezitten om te overleven in de extreme omgevingscondities die Antarctica kenmerken.

De belangrijkste doelstellingen van dit doctoraat waren (1) het karakteriseren van de gemeenschapsstructuur en distributie van bacteriën en micro-eukaryoten in verschillende substraten van een aantal nunataks en valleien van het Sør Rondanegebergte (Oost-Antarctica); (2) het identificeren van sleuteltaxa in deze voedselwebben en de belangrijkste abiotische factoren die deze gemeenschappen structureren (**Hoofdstuk 2**); (3) een gedetailleerd inzicht verschaffen in de cyanobacteriële diversiteit en gemeenschapsstructuur in deze regio's (**Hoofdstuk 3**); (4) de belangrijkste fysiologische en genetische adaptaties identificeren die twee stammen van dezelfde Nostoc soort (cyanobacteriën) hebben om te weerstaan aan uitdroging en rehydratie. Uitdroging en rehydratie kommen immers frequent voor in de terrestrische habitats van Antarctica (**Hoofdstuk 4**). Om deze doelstellingen te bereiken werd een multidisciplinaire aanpak toegepast die ecofysiologische en verschillende omics-analyses combineert.

In **Hoofdstuk 2** werd de samenstelling van bacteriële en micro-eukaryotische gemeenschappen onderzocht met behulp van high-throughput sequencing van delen van de 16S rRNA en 18S rRNA genen in 105 bodemmonsters op 9 locaties binnen een straal van 100 km in

het Sør Rondane gebergte (Oost-Antarctica). De stalen verschillen in substraattype en bijbehorende fysische en chemische omstandigheden. In morenebodems behoorden Actinomycetota en Cercozoa tot de meest voorkomende bacteriële en eukaryotische fyla, terwijl op gneis, graniet en marmeren gesteentes Cyanobacteriota en Metazoa tot de dominante bacteriële en eukaryotische fyla behoorden. Binnen het fylum Cyanobacteriota werd een duidelijke differentiatie waargenomen op verschillende gesteentetypes, waarbij graniet werd gedomineerd door de Nostocaceae familie en marmer door de Chroococcidiopsaceae familie. Verrassend genoeg bereikten Metazoa een relatief hoge abundantie in de eukaryotische dataset, zelfs in monsters van de meest droge locaties, zoals morenes in Austkampane en Widerøefjellet. In het algemeen toonde deze studie aan dat verschillende substraattypes, verschillende microbiële gemeenschappen ondersteunen in Antarctische nunataks en valleien in het binnenland, en dat de lithologische diversiteit een belangrijke determinant is van de terrestrische microbiële biodiversiteit.

In **Hoofdstuk 3** werden de cyanobacteriële gemeenschapsstructuur van dezelfde locaties als in hoofdstuk 2 verder onderzocht door gebruik te maken van primers specifiek voor cyanobacteriën. De V3-V4 regio van het 16S rRNA-gen werd gesequeneerd met behulp van Illumina high-throughput sequencing. De sequenties werden geïdentificeerd door gebruik te maken van de meest recente cyanobacteriële taxonomie uit de onlangs vrijgegeven CyanoSeq database. Uit ordinatie-analyses bleek dat deze verschillende substraten verschillende cyanobacteriële gemeenschappen herbergen. Deze verschillen in gemeenschapsstructuur waren significant gerelateerd aan verschillen in pH, concentratie van TN en N-NO3, en elektrische geleidbaarheid. De granietbodems van de Pingvinane nunataks herbergen de hoogste rijkdom, gevolgd door die van de granietrug van Utsteinen. Granieten substraten werden gekenmerkt door hoge TN-concentraties en een neutrale pH. Zij herbergen een verscheidenheid aan filamenteuze cyanobacteriën, zoals Leptolyngbyaceae, Gomontiellaceae, Microcoleaceae, Oculatellaceae, Nostocaceae, maar ook eencellige taxa (Cyanothecaceae). De cyanobacteriële gemeenschappen in de morenes van Austkampane en Widerøefjellet werden gedomineerd door respectievelijk Microcoleaceae en Gomontiellaceae. Ze werden gekenmerkt door een hoog

drooggewicht en een lage totale stikstofconcentratie, en de diversiteit en abundantie van cyanobacteriën was er laag. De taxonomische rijkdom was ook laag in bodems van het alkalisch marmergesteente en het gneisgesteente van de Perlebandet nunatak, die beide werden gekenmerkt door een hoge TN. Bodems bestaande uit marmer werden gedomineerd door *Alitarella* sp. (Chroococcidiopsaceae), terwijl gneis werd gedomineerd door *Cyanothece* sp. (Cyanothecaceae). In het algemeen tonen onze gegevens aan dat verschillende substraattypes verschillende cyanobacteriële gemeenschappen herbergen.

Cyanobacteriën moeten in Antarctische terrestrische en lacustrische habitats en tijdens de verspreiding tussen habitats vaak uitdroging en rehydradatie weerstaan. In **Hoofdstuk 4** werd de respons onderzocht op kortdurende blootstelling aan uitdroging en rehydratie van een terrestrische en zoetwaterstam die tot dezelfde *Nostoc*-soort behoren. Hiertoe werden de concentraties van pigmenten en osmolyten (trehalose en sucrose), alsook de fotosynthese-efficiëntie gemeten en gecombineerd met een metatranscriptoom (RNA-seq) analyse van de twee *Nostoc*-stammen na 3 uur uitdroging, gevolgd door rehydratie na 10 minuten, 24 uur en tot 72 uur. Beide stammen reageerden op uitdroging door sucrose te accumuleren, terwijl trehalose in lagere concentraties aanwezig was. Alleen de zoetwaterstam vertoonde een herstel van het chlorofyl a-gehalte na 72 uur rehydratie. De fotosynthetische efficiëntie bleef echter bij beide stammen onder het oorspronkelijke niveau van vóór de uitdroging. Uit transcriptomische profielen bleek dat in beide stammen de cellen beschermd werden tijdens uitdroging door stressgerelateerde genen te induceren, zoals genen voor de productie van carotenoïden en trehalosesynthase alsook genen betrokken bij stikstoffixatie. De terrestrische stam reageerde met de up-regulatie van een groter aantal genen dan de zoetwaterstam. Het fotosynthetisch metabolisme nam echter langzaam af na 24 uur rehydratie, zoals blijkt uit de down-regulatie van genen die verband houden met fycobilisomen en fotosystemen, terwijl het *psbA2*-gen, dat codeert voor het D1-eiwitsynthase dat nodig is voor PSII, bij de terrestrische ULC180, maar niet bij de zoetwater ULC008, significant up-gereguleerd bleek te zijn onder uitdroging. Deze resultaten wijzen op habitat-specifieke aanpassingen aan milieustress bij cyanobacteriën, en bieden nieuwe inzichten in de strategieën voor overleving en aanpassing van niet-model

organismen, zoals de Antarctische *Nostoc*-stammen aan uitdroging en rehydratie tijdens de eerste 3 dagen in extreme omgevingen.

In het laatste hoofdstuk worden de belangrijkste bevindingen van dit proefschrift besproken en een aantal toekomstige onderzoeksperspectieven geformuleerd. Deze omvatten het gebruik van shotgun metagenomics boven ampliconsequencing of het gebruik van meer specifieke primers in bacteriële en micro-eukaryotische studies, alsook de karakterisering van biotische interacties en de integratie van niet-modelorganismen in experimenten betreffende adaptaties in extreme omstandigheden. In het algemeen wordt het belang van de integratie van zowel ecofysiologie als 'omics' disciplines benadrukt doorheen dit doctoraat, met als doel de ecologische rol van microbiële gemeenschappen en dan vooral cyanobacteriën in de extreme Antarctische ijsvrije gebieden beter te begrijpen.

RÉSUMÉ

Les zones libres de glace couvrent moins de 0,5 % de l'Antarctique, mais elles abritent la majeure partie de la biodiversité terrestre de l'ensemble du continent. Ces habitats terrestres sont caractérisés par des réseaux trophiques tronqués et simples, constitués presque uniquement de communautés microbiennes. Les cyanobactéries comptent parmi les principaux producteurs primaires de ces habitats, où elles sont souvent considérées comme des "ingénieurs de l'écosystème". Malgré le rôle écologique important que jouent les cyanobactéries, notre compréhension des facteurs qui déterminent leur diversité et la structure de leur communauté, ainsi que leurs adaptations pour faire face aux conditions abiotiques extrêmes de l'Antarctique, reste limitée.

Les principaux objectifs de ce doctorat sont les suivants (1) caractériser la structure et la distribution des communautés de bactéries et de micro-eucaryotes dans une variété de substrats provenant de différents nunataks et vallées de la région des monts Sør Rondane (Antarctique de l'Est) ; (2) identifier les taxons clés de ces réseaux trophiques et les principaux facteurs abiotiques qui structurent ces communautés (**Chapitre 2**) ; (3) fournir une compréhension détaillée de la structure des communautés bactéries et des micro-eucaryotes dans les nunataks et les vallées de la région des monts Sør Rondane (Antarctique de l'Est) (**Chapitre 3**); (4) identifier les principaux mécanismes d'adaptation physiologiques et génétiques qu'une paire d'espèces de Nostoc (cyanobactéries) utilise lors d'événements de dessiccation - réhydratation qui se produisent fréquemment dans les environnements terrestres de l'Antarctique (**Chapitre 4**). Pour atteindre ces objectifs, une approche multidisciplinaire a été appliquée, combinant des analyses écophysiologiques et plusieurs analyses omiques.

Dans le **Chapitre 2**, la composition des communautés bactériennes et de micro-eucaryotes est examinée en utilisant le séquençage à haut débit de parties de gènes de l'ARN ribosomique 16S et 18S dans 105 échantillons de sol sur 9 sites dans un rayon de 100 km dans les monts Sør Rondane (Antarctique de l'Est), qui diffèrent par le type de substrat et les conditions

physiques et chimiques qui y sont associées. Dans les sols morainiques, les phyla Actinomycetota et Cercozoa figurent parmi les groupes bactériens et eucaryotes les plus abondants, tandis que sur le gneiss, le granit et le marbre, le phyla Cyanobacteriota et Metazoa figurent parmi les groupes bactériens et eucaryotes dominants. Une différenciation distincte est observée au sein de l'embranchement des Cyanobacteriota à une résolution taxonomique plus élevée en fonction du type de substrat, le granite étant dominé par la famille des Nostocaceae et le marbre par la famille des Chroococcidiopsaceae. De manière surprenante, les métazoaires atteignent une abondance relativement élevée au sein des eucaryotes, même dans les échantillons provenant des sites les plus arides, tels que les moraines d'Austkampane et de Widerøefjellet. Dans l'ensemble, cette étude a montré que différents types de substrat abritent des communautés microbiennes distinctes dans les nunataks et les vallées de l'Antarctique intérieur, et que la diversité lithologique est un déterminant majeur de la biodiversité du microbiome terrestre.

Dans le **Chapitre 3**, les structures des communautés de cyanobactéries des sites échantillonnés dans le chapitre 2 sont étudiées plus en détail grâce à l'utilisation d'amorces spécifiques aux cyanobactéries ciblant la région V3-V4 du gène de l'ARN ribosomique 16S dans le cadre d'une approche de séquençage à haut débit. Les dernières connaissances taxonomiques sur les cyanobactéries utilisées dans la base de données CyanoSeq récemment publiée sont appliquées à ces séquences. Les analyses d'ordination révèlent que ces différents substrats abritent des communautés cyanobactériennes distinctes. Les différences dans la structure des communautés sont significativement liées aux différences de pH, de concentration de TN et de $N\text{-}NO_3^-$, et de conductivité électrique. Les sols granitiques des nunataks de Pingvinane abritent la plus grande richesse, suivis par ceux de la crête granitique d'Utsteinen. Les substrats granitiques se caractérisent par des concentrations élevées en TN et un pH neutre et abritent une variété de cyanobactéries filamenteuses, telles que celles appartenant aux familles Leptolyngbyaceae, Gomontiellaceae, Microcoleaceae, Oculatellaceae, Nostocaceae, mais aussi des taxons unicellulaires (Cyanothecaceae). Les échantillons de moraine d'Austkampane et de Widerøefjellet sont dominés par les Microcoleaceae et les Gomontiellaceae, respectivement. Ils sont caractérisés par un poids sec élevé, un faible TN, et une diversité et abondance faibles de

cyanobactéries. La richesse taxonomique est également faible dans les sols provenant du substrat marbrier alcalin et du gneiss provenant du nunatak Perlebandet, tous deux caractérisés par un TN élevé. Le substrat marbrier est dominé par *Alitarella sp.* (Chroococcidiopsaceae), tandis que le gneiss était dominé par *Cyanothece sp.* (Cyanothecaceae). Dans l'ensemble, nos données montrent que les différents types de substrat abritent des communautés cyanobactériennes distinctes.

Les cyanobactéries doivent fréquemment faire face à des événements de dessiccation et de réhydratation dans les habitats terrestres et lacustres de l'Antarctique, ainsi que lors de la dispersion entre les habitats. Dans le **Chapitre 4**, la réponse à une exposition à la dessiccation de courte durée et à la réhydratation d'une souche terrestre et d'une souche d'eau douce appartenant à la même espèce de Nostoc a été étudiée. Pour ce faire, les concentrations de pigments et d'osmolytes (tréhalose et saccharose) ainsi que l'efficacité photosynthétique sont mesurées en combinaison avec une analyse métatranscriptomique (RNA-seq) des deux souches de *Nostoc* après 3h de dessiccation, suivie d'une réhydratation après 10 min, 24h et jusqu'à 72h. Les deux souches ont réagi à la déshydratation en accumulant du saccharose, tandis que le tréhalose était présent en plus faibles concentrations. Seule la souche d'eau douce montre une récupération de la teneur en chlorophylle a après 72h de réhydratation. Cependant, l'efficacité photosynthétique resteinférieure aux niveaux originaux mesurés avant la déshydratation dans les deux souches. Les profils transcriptomiques ont montré que les deux souches protègent leurs cellules pendant la déshydratation en induisant des gènes liés au stress, tels que ceux de la production de caroténoïdes, de la tréhalose synthase et des gènes liés à la fixation de l'azote. La souche terrestre a réagi en régulant un plus grand nombre de gènes que la souche d'eau douce. Le métabolisme photosynthétique diminue toutefois lentement après 24 heures de réhydratation, comme le montre la régulation négative des gènes liés aux phycobilisomes et aux photosystèmes, tandis que le gène *psbA2*, codant pour la protéine synthase D1 nécessaire au PSII, se révèle être significativement régulé positivement en cas de dessiccation chez la souche terrestre ULC180, mais pas chez la souche dulçaquicole ULC008. Ces résultats suggèrent des adaptations spécifiques à l'habitat et, donc, au stress environnemental chez les cyanobactéries,

et fournissent de nouvelles informations sur les stratégies liées à la survie et à l'adaptation des souches antarctiques de *Nostoc* aux événements de dessiccation et de réhydratation au cours des trois premiers jours dans des environnements extrêmes.

Dans le dernier chapitre, les principaux résultats de cette thèse de doctorat sont discutés et un certain nombre de perspectives de recherche futures sont formulées. Celles-ci comprennent l'utilisation de la métagénomique par rapport au séquençage d'amplicons ou l'utilisation d'amorces plus spécifiques dans les études bactériennes et de micro-eucaryotes, la caractérisation des interactions biotiques et l'intégration d'organismes non-modèles dans les expériences concernant leur tolérance abiotique. Dans l'ensemble, l'importance de l'intégration des disciplines de l'écophysiologie et des sciences omiques est soulignée tout au long de cette thèse de doctorat, dans le but de maximiser notre compréhension du rôle écologique des communautés microbiennes vivant dans les zones glacées extrêmes de l'Antarctique.

CHAPTER 1

GENERAL INTRODUCTION

1.1 ANTARCTIC-ICE FREE AREAS

Antarctica is the coldest place on Earth with the lowest temperature estimates reaching 98 °C (Scambos et al. 2018). It is also the windiest, driest, and highest continent. Around 99.6 % of the landmass is covered with snow or ice (Brooks et al. 2019), accounting for ca. 90 % of the world's total ice volume (Fox and Cooper 1994). The only parts of the continent that are not covered by ice are coastal areas, exposed mountain peaks (nunataks) and valleys, where winds are intense and continuous. These permanently ice-free areas constitute isolated patches of edaphic habitat within a matrix of ice, analogous to islands in an ocean (Convey 2010). They stretch from less than 1 km^2 to thousands of km^2, and can be separated by meters to hundreds of kilometers (Convey et al. 2014; Fig. 1.1).

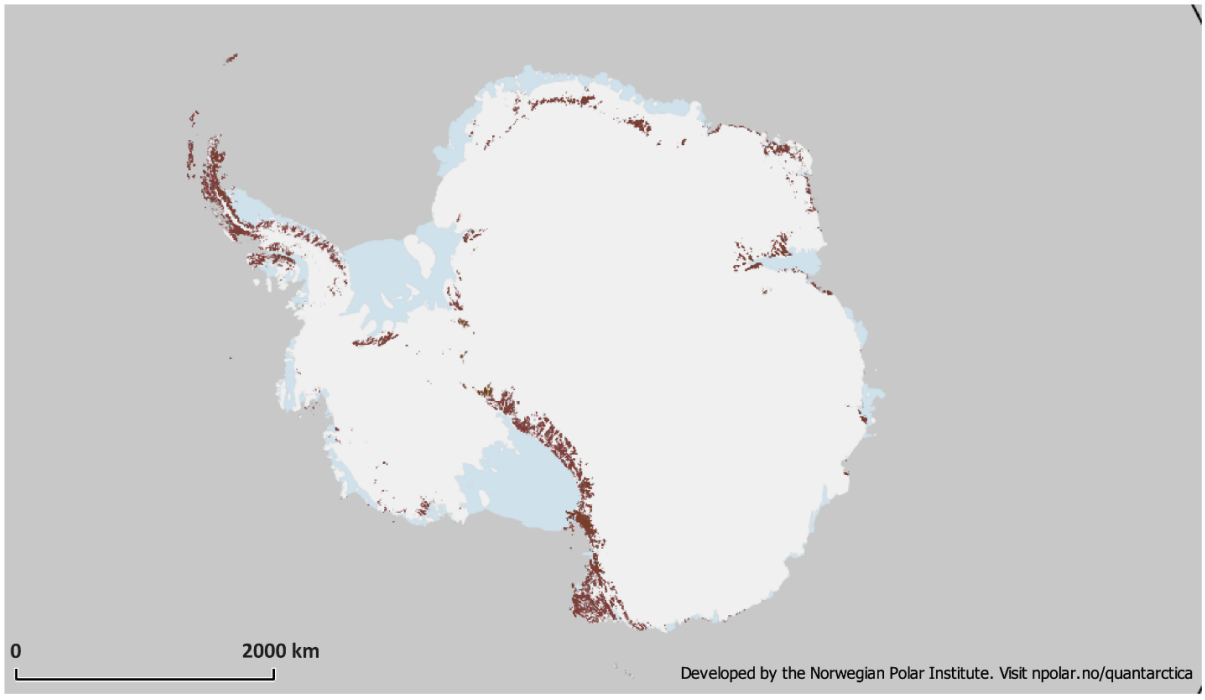

Fig. 1.1 Map of Antarctic continent showing the ice-free areas (in brown). *The map was drawn with QGIS (QGIS.org 2021) package Qantarctica (Matsuoka et al. 2021).*

The Antarctic ice-free areas are among the most extreme environments on Earth with permanently low temperatures, high irradiance during the summer months versus completely darkness during the winter months and general low nutrient availability (Fig. 1.2; Bockheim and Hall 2022, Cowan and Tow 2004). These extreme environmental conditions inevitably steer the evolution and adaptation of species, as they colonize the few available environmental niches.

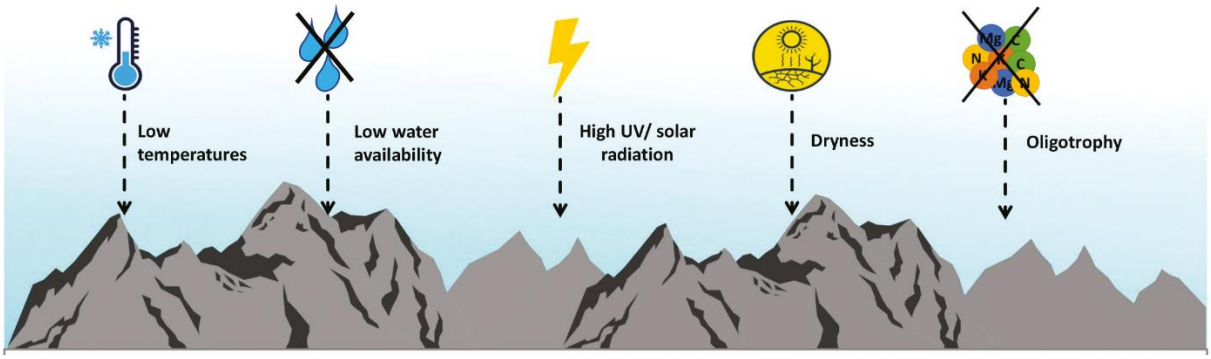

Fig. 1.2 Schema summarizing the main extreme abiotic conditions of the Antarctic terrestrial ice-free areas (from Coleine et al. 2021).

Following two climate forcing scenarios from the Intergovernmental Panel on Climate Change (IPCC) Fifth Assessment Report (AR5), Lee et al. (2017) quantified the impact of twenty-first century climate change on ice-free areas using temperature-index melt modelling. They predict that melt across the Antarctic continent will lead to the emergence of 2100 to 17,267 km^2 of new ice-free area by the end of this century, close to a 25 % increase, meaning that the total ice-free areas will increase their coverage from 0.4 to 0.5 % of the whole continent. More than 85 % of this new ice-free areas will emerge in the North Antarctic Peninsula, which will see the emergence of > 9,000 to 14,500 km^2, while the rest of the Antarctic continent will likely be less endangered (apart from a few coastal areas of East Antarctica). This is however likely to change as warming effects will continue well beyond the end of the century, even with strong mitigation measures (IPCC 2021). Indeed, current long-term climate projections are unable to incorporate the impacts of extreme events, which will increase in frequency with warming (IPCC 2021). Bergstrom, Woehler et al. (2018) describe a heatwave event that occurred in the Dry Valleys during the austral summer 2001/2002 and its consequences. On that occasion, air

temperatures on some days exceeded 10 °C with consequent significant loss of glacial mass leading to 3- to nearly 6000-fold increase in annual stream flows, melting of sub-surface ice and an increase in lake water levels that reversed, in just three months, the results of the regional cooling that had extended over the 14 previous years. As mentioned by Robinson et al. (2020), this heatwave ended a decade of drought, with subsequent dramatic consequences. Over the next 13 years, they observed shifts in populations, e.g. of soil nematodes to favour those preferring wetter conditions (such as *Eudorylaimus* sp.; Gooseff et al. 2017) or in the productivity of the cyanobacterial *Nostoc* spp. that greatly increased within streams (Gooseff et al. 2017). They also highlighted the unprecedented heatwave recorded at Casey station, East Antarctica, with minimum positive temperatures over three consecutive days and maximum temperatures of 7 °C higher than the recorded summer means since 30 years. That same summer, maximum temperatures over 20 °C were recorded. Such warm summers have strong impacts on the whole Antarctic biology, probably leading to long-term disruptions at population, community and ecosystem levels. The increase in ice-free area could utterly change the availability and connectivity of habitats with coalescing of what previously were isolated ice-free areas, with uncertain effects due to the complexity of the system. This expansion of habitats will undoubtedly enable some native species to access to new resources and to colonize new space, as already observed in the Antarctic Peninsula in which there is the risk of non-native species invading the region (Hughes et al. 2019). Also in the marine ecosystem, shifts in the benthic assemblages from a “filters-ascidian domination” to a “mixed assemblage” were observed due to glacier retreats and the consequent higher sedimentation rate (Sahade et al. 2015). Increasing connectivity could have therefore destabilizing impacts on ecological communities with the increasing regional-scale biotic homogenization as genetic variation will likely be lost (Collins and Hoggs 2016), the extinction of less-competitive species and the spread of invasive species, which already pose a substantial threat to native biota (Chown et al. 2007, 2012). Moreover, on-ground observations also show that communities are already being impacted by climate change across the continent (Andriuzzi et al. 2018, Cannone et al. 2022, Robinson et al. 2018), suggesting more subtle changes may be occurring at the microclimate scale than those reflected in broad scale

models. With the increase of ice-free areas, the availability of liquid water (from glacial and permafrost melting, and from precipitation) is expected to increase with changes in microbial biomass, microbial productivity and community structure, among which cyanobacteria would be one of the most rapid growing organisms (Cowan and Tow 2004). All in all, continued monitoring and modelling of Antarctic ecosystems is of increasing need as the anthropogenic signal of climate change progresses and longer-term projections become available (Lee et al. 2022). Baseline knowledge about microbial community diversity and structure within the current Antarctic ice-free areas is therefore of primary importance to predict and observe any future changes.

1.2 STUDY AREA: THE SØR RONDANE MOUNTAINS, EAST ANTARCTICA

The Sør Rondane Mountains (SRM) are located within Dronning Maud Land, East Antarctica (22 - 28° E, 71°30’ - 72°40’ S) and are characterized by a variety of nunataks located within an area of *ca*. 2000 km^2 (Suganuma et al. 2014), with main peaks rising up to 3400 m. The SRM were geologically produced by the collision of the African plate assembly and the Antarctic Coats Land Block ~ 650 - 540 Mya that caused the accretion of multiple arc terranes (Ruppel et al. 2015). These mountains are situated in the East African-Antarctic Orogen (EAAO; Jacobs and Thomas 2004) and are characterized by the Main Shear Zone that separates the northern metamorphic rocks SRM with ocean affinity (viz. the presence of marble veins in between gneiss bedrock), from the southern metamorphic rocks presenting igneous intrusions (e.g. granite outcrops), characteristic of island arc or continental margin arc features (Fig. 1.3). These geological features may influence the microbiota distribution that inhabits the different substrate types. Porosity (water retention), albedo, translucidity, pH, elemental compositions, salinity are examples of how the geologic features can significantly impact the inhabiting microbial communities. The variety of bedrock types may therefore consitute different habitats for microbial communities (Tytgat et al. 2016).

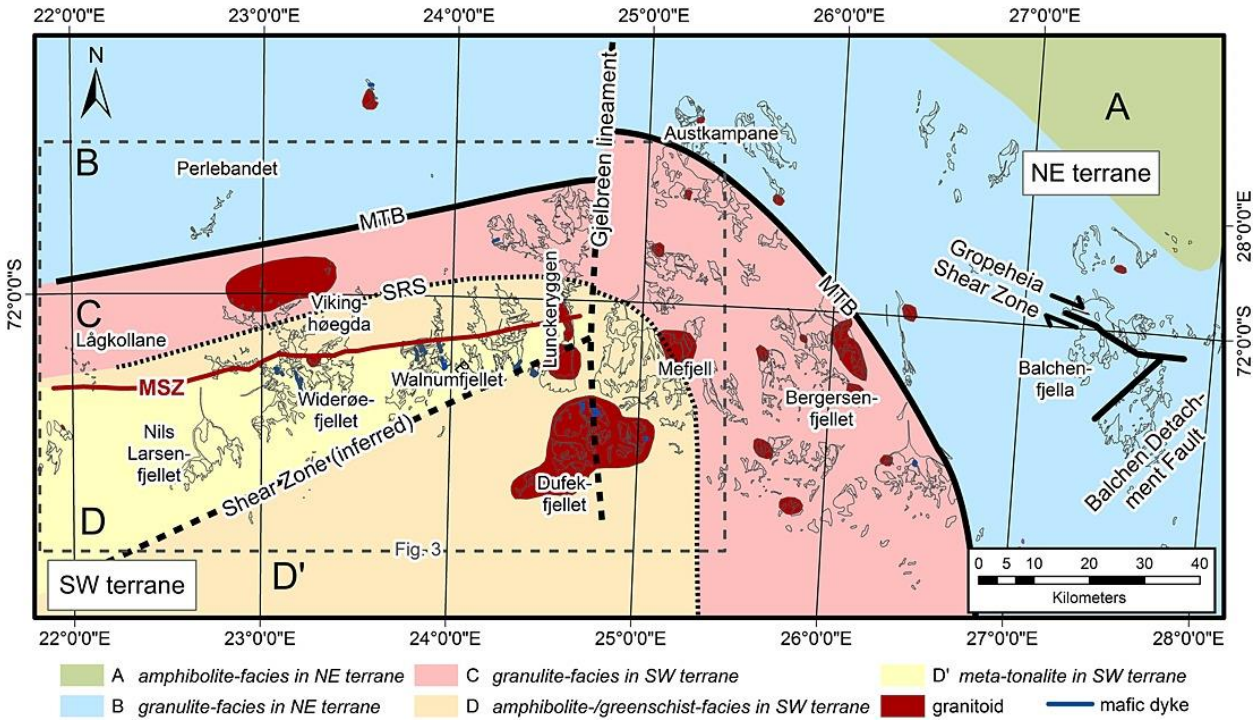

Fig. 1.3. Geological overview of Sør Rondane indicating the subdivision of tectonic terranes and units (modified after Osanai et al. [2013]) including representative place names. *Units A and B belong to the NE terrane and units C, D, and D' to the SW terrane. The Main Tectonic Boundary (MTB) separates NE and SW terranes. The previously assumed boundary between these terranes, the Sør Rondane Suture (SRS), is redefined as part of a frontal fold zone of the MTB within the SW terrane [Osanai et al. 2013]. The gabbro-tonalite-trondhjemite-granodiorite (GTTG) complex is separated from the northern greenschist- to granulite-facies rocks by the Main Shear Zone (MSZ). An inferred shear zone is indicated in the south of the GTTG complex [Shiraishi et al. 1992, Osanai et al. 1996]. Another structural feature trending N-S with as yet unknown characteristics is termed the Gjelbreen lineament [Mieth et al. 2014]. Age relation of Gropeheia Shear Zone and Balchen Detachment Fault based on aerogeophysical data [Mieth et al. 2014]. From Ruppel et al. [2015].*

Northern SRM are mainly composed of nunataks, which are summits or ridges of mountains that protrude from the ice fields, whilst the southern continental SRM are mainly characterized by valleys where strong winds impede snow accumulation on the soil surface (Fig. 1.4). In this thesis, our sampling efforts spanned across 6 nunataks and 3 valleys within *ca*. 70 km radius from the Belgian Princess Elisabeth Antarctica (PEA) station (71°57' S, 23°21' E, 1372 m a.s.l.) that are deeply described in the material and methods sections of Chapters 2 and 3.

Because of its east-west orientation, the SRM act as a barrier north of the ice plateau, forcing the katabatic winds and the ice to flow around the mountain range. As a consequence, the northern escarpment zone of the western SRM, where the PEA is located, is rather sheltered. Relatively mild winters occur with mean winter air temperatures at PEA between -20 and -25 °C while mean December and January air temperatures are between -15 and +5 °C (Pattyn, Matsuoka and Berte 2010, Gorodetskaya et al. 2013). Conditions near the main mountain range are more extreme, with Austkampane to the east being the windiest and harshest site of all sampled locations.

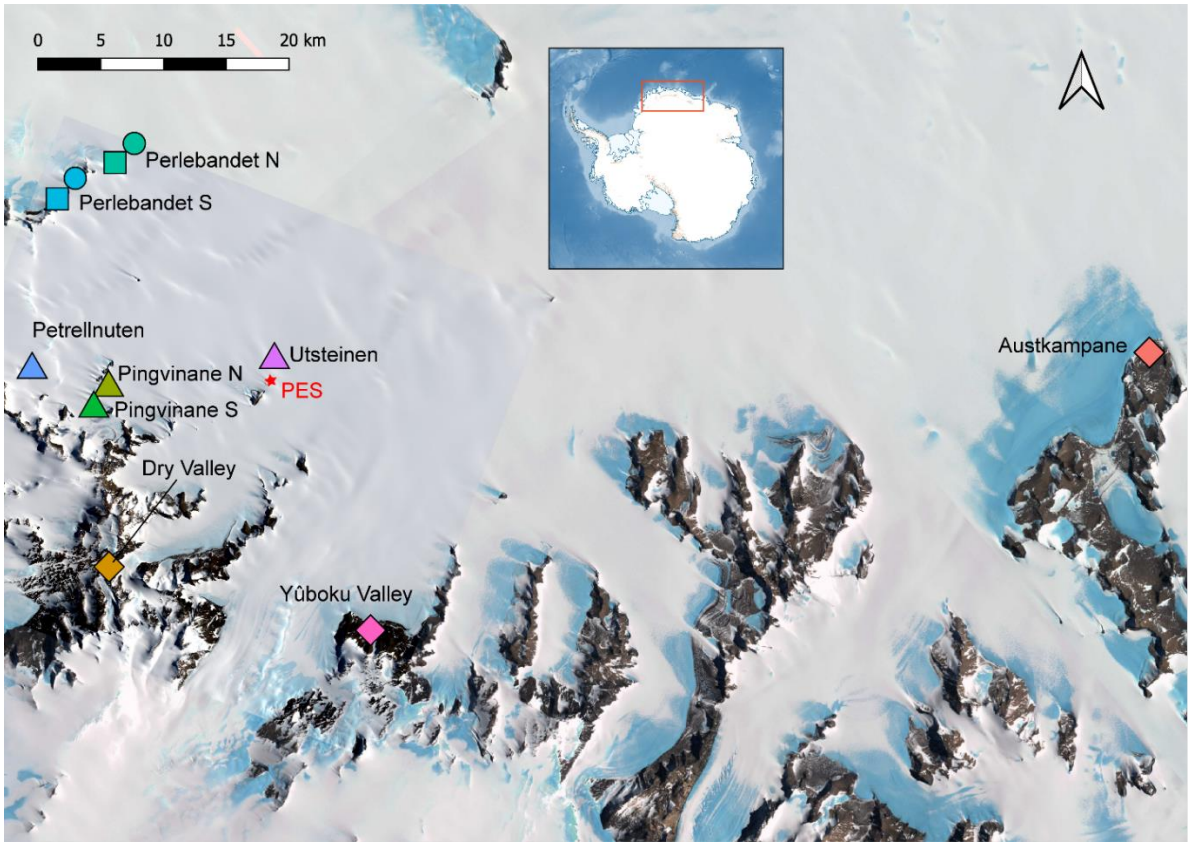

Fig. 1.4 Satellite image of the Sør Rondane Mountains and sampled sites. *Contains modified Copernicus Sentinel-2 data [2020] and Landsat Image Mosaic of Antarctica (LIMA). Colors differ by sampled site. Circles represent gneiss bedrock; squares represent marble bedrock; triangles represent granite bedrock; diamonds represent moraine substrates.*

1.3 MICROBIOME DIVERSITY OF THE ANTARCTIC ICE-FREE AREAS

At a first glance, Antarctic terrestrial ecosystems (i.e. 'true soil habitats', excluding lakes and wetlands) may appear devoid of any life, however they host diverse and more or less rich assemblages of microscopic life (Fig. 1.5). Indeed, despite representing only ~ 0.4 % of the whole continent, ice-free areas surprisingly host nearly all the continent's biodiversity, both in terrestrial and aquatic habitats, including arthropods, nematodes, microbes, vegetation (lichen, fungi, mosses and algae), rotifers tardigrades and, in the Antarctic Peninsula, two species of vascular plants (Chown and Convey 2007, Chown et al. 2015). Finally, coastal ice-free areas are also essential breeding grounds for seals (Chown et al. 2015) and, until as much as 300 kilometers from the open sea, seabirds (Løvenskiold 1960). Especially in the inland ice-free areas where abiotic conditions are the most extreme (Fig. 1.2), terrestrial food webs are characterized by a simplified trophic structure, encompassing a lower diversity at the highest taxonomic levels. However, diversity increases at a higher taxonomic resolution, mirroring the abundance of highly specialized taxa (Pointing et al. 2009). In particular, at the basis of the food web chains are often the autotrophic cyanobacteria and microalgae, which are widely distributed and can grow to large population sizes where they are key primary producer and drive food webs and biogeochemical fluxes of carbon, nitrogen and other elements (Jungblut and Vincent 2017). Recently, other autotrophic organisms have been found to be genetically equipped for the consumption of molecular hydrogen (H_2), CO_2 and CO from the atmosphere as energy and carbon sources (Ji et al. 2017, Greening et al. 2022, Ray et al. 2022, Ortiz et al. 2020), which may constitute the basis of the food web chains where conditions are too severe (i.e. extreme aridity or oligotrophy) for other autotrophs survival (i.e. cyanobacteria or microalgae).

Fig. 1.5 Developed biocrust on the granitic Utsteinen ridge (71◦57'S, 23◦21'E; 1372 m a.s.l.) from the West Sør Rondane Mountains, Dronning Maud Land (East Antarctica). *Petri dish for scale reference. © Beatriz Roncero Ramós.*

Similarly to macroscopic organisms, it has been discovered that a relatively high number of microbial taxa is endemic to the Antarctic as a result of evolution in isolation on multi-million-year timescales (Convey et al. 2020, Pinseel et al. 2020). This implies that some regions must have been ice-free during the multiple glacial cycles that took place since the formation of the Antarctic Ice Sheets ca. 35 Mya, so they could act as refugia for terrestrial and lacustrine biota (Convey et al. 2008, Pugh and Convey 2008, Stevens and D'Haese 2014, Convey et al. 2020, Pinseel et al. 2021). Among the eukaryotes, many species of tardigrades, rotifers and nematodes have been recorded in only one region or single ice-free areas (Velasco-Castrillónet al. 2014, Guidetti et al. 2014, De Smet and Gibson 2008). Yet, it is still uncertain whether these species are

limited to these specific regions because of lack of dispersal potential or opportunities, or whether there is still a limited understanding of their distribution (Chown 2015). Nonetheless, the differences existing in the terrestrial fauna led to the identification of 16 Antarctic Conservation Biogeographic Regions—ACBRs or bioregions (Fig. 1.6; Terauds et al. 2012, Terauds and Lee 2016).

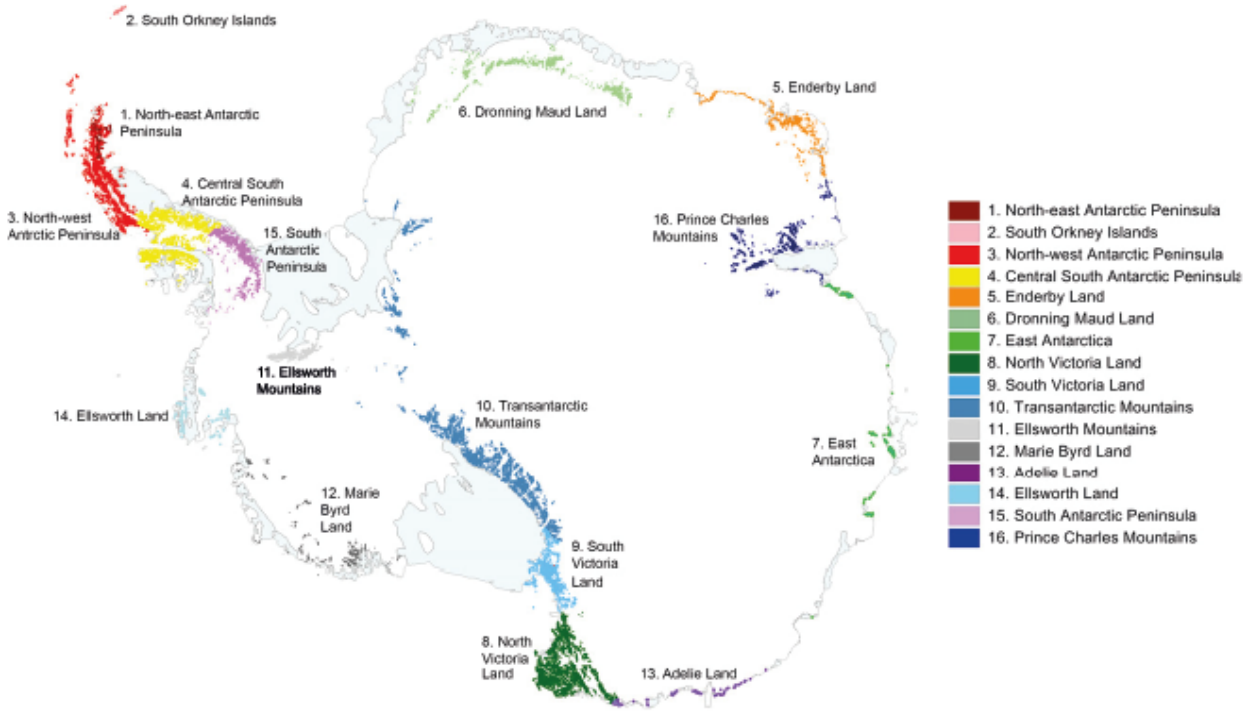

Fig. 1.6 Updated version of the Antarctic Conservation Biogeographic Regions (ACBRs v2). *From Terauds and Lee [2016].*

Recent studies showed that spatial patterns of benthic cyanobacterial lake mat communities may be associated to other factors rather than the proposed bioregions. For instance, Pessi et al. (2018) and Durieu et al. (in prep.) showed that water chemistry is a highly important structuring factor compared to the physical barrier in Antarctic lakes. This suggests that communities as those described may appear more constrained in dispersal by the availability of suitable habitats than by the geographic barriers since their dispersal may be facilitated by wind currents and animal vectors such as migratory birds (Wynn-Williams 1991, Pearce et al. 2009). Despite the structuring role of water chemestry for benthic microbial communities of both

Antarctic and Arctic lakes also found by Tygtat et al. (submitted), biogeography was encountered to be a more important structuring factor at their scale. Other studies conducted on microbial assemblages from terrestrial ice-free areas showed that the environmental variables have a more significant effect than the spatial distance (e.g. Kim et al. 2015). It is also to be noted that at the time that these bioregions were defined, not many taxa were yet investigated using modern molecular phylogenetic methods and therefore a comprehensive biogeographic study including all taxa variability was not yet possible (Terauds et al. 2012). Moreover, the cyanobacterial diversity data included was based on morphological records and outdated taxonomy. However, such bioregionalization formed the basis of a 'systematic environmental-geographical framework' for conservation management of the terrestrial Antarctic and was therefore of particular importance to the enforcement of the Antarctic Specially Protected Areas (ASPA). Although ACBRs can indeed increment our understanding of very large-scale biodiversity trends (i.e. maritime vs. continental Antarctica), local-scale phylogeographic variation cannot be revealed by such broad bioregionalization (e.g. Stevens et al. 2007, Hawes et al. 2010).

Indeed, terrestrial ice-free areas comprise areas with varying altitudes and environmental conditions, such as moisture, vegetation, exposure to PAR and UVR, and host a plethora of communities that can vary greatly, even at small distances (Kim et al. 2015, Van Horn et al. 2014). With the reduced predation pressure and competition unlike many other regions of the world, species distribution in Antarctica is therefore mostly driven by abiotic factors (Lee et al. 2019). The relation between environmental factors and microbial community structure in terrestrial Antarctic ice-free regions is yet poorly understood, with a few exceptions, such as those in the McMurdo Dry Valleys in Victoria Land that is the largest ice-free region of Antarctica, spanning an area of 4000 km^2 (Solon et al. 2021, Thompson et al. 2020, Severgnini et al. 2021, Coleine et al. 2021, Kim et al. 2015, Van Horn et al. 2014). This lack of knowledge is even more eminent for microbial eukaryotes (Cucini et al. 2022, Franco et al. 2021) and even more for the combined study of both communities (i.e. bacterial and eukaryotes; see for example Obbels et al. 2016, Niederberger et al. 2015). Bacterial communitiy structure seems to be the most affected by soil moisture, pH, salinity, nitrogen availability, soil physical stability, solar irradiance intensity and to

a lesser degree temperature and organic matter content (Niederberger et al. 2008, Convey et al. 2014, Tytgat et al. 2016, Goordial et al. 2017, Alekseev et al. 2020, Severgnini et al. 2021, Dragone et al. 2022) whereas micro-eukaryotic community structures were found to be importantly affected by pH, salinity, organic carbon content, nitrates concentration and moisture availability (Franco et al. 2022, Poage et al. 2008, Barrett et al. 2004, Courtright et al. 2001) but also latitude (Convey et al. 2020). This is particularly true for micro-inverterbrates showing a higher endemicity degree with the latitude increase (Convey et al. 2020 and references therein). Also, biotic interactions are often not taken into consideration, nonetheless primary producers such as cyanobacteria strongly influence the abundance of both fungi and, together, of micro-invertebrates (Lee et al. 2019). Only a few studies characterize specifically the cyanobacterial communities of the terrestrial Antarctic environments (Broady 1996, Woods et al. 2008, Namsaraev et al. 2010, Pushkareva et al. 2018) but at a lower taxonomic resolution they are also described in bacterial surveys (see previous examples). Cyanobacteria do not seem to be ubiquitously present in soil samples of all the ice-free areas. For example, in the McMurdo Dry Valleys cyanobacteria were only detected in some of the studied soil samples (Lee et al. 2012, Magalhaes et al. 2012, Van Horn et al. 2013). This absence may not only be linked to low humidity of soils. Wood et al. (2008) indeed pointed out that moisture content of Antarctic Dry Valley soils was a poor indicator of cyanobacterial distribution and that other variables such as soil elemental composition may play a role in influencing edaphic cyanobacterial habitat suitability. In the surface soils of hyper-arid areas, Chlorophyta, Ciliophora and Cercozoa were the most abundant eukaryotic phyla recorded, while Actinomycetota, Acidobacteriota, Bacillota and Chloroflexota were often the dominant bacterial phyla. The archaea in soils showed very limited richness, with often only a few phylotypes per sample, which structure seems to be mainly driven by water content (Richter et al. 2014) and Euryarchaeota seems to be one of the dominating taxa found in glacial samples (Bendia et al. 2018). Nitrogen and methane cycles also appear to have a pivotal role in Antarctic glaciers, where bacteria from the phyla Verrucomicrobia and Patescibacteria are found in high abundance and co-occur with the possibly methanogenic *Methanomassiliicoccus*.

Although polar ecosystems are mainly driven by abiotic factors, biotic interactions (biotic filtering) and co-occurrences of specific organisms via co-occurrence network analysis may exert a critical control on the complexity of these communities (Lee et al. 2019). Microbial co-occurrence patterns can thus help defining ecologically meaningful interactions between species and across domains (Vick-Majors et al. 2014) with the identification of groups, or modules, of co-occurring species with functional significance (Chaffron et al. 2010, Barberán et al. 2012). These analysis can also be used to statistically identify keystone taxa (Berry and Widder 2014) for which consensus in their definition within microbial ecology is still matter of discussion. However, microbial keystone taxa can be defined as individuals or in a guild of individuals, exerting a considerable influence on microbiome structure and functioning irrespective of their abundance across space and time. These taxa have a unique and crucial role in microbial communities, and their removal can cause a dramatic shift in microbiome structure and functioning (Banerjee et al. 2018). For instance, cyanobacteria are often defined as "ecosystem engineers" because they support ecosystems with energy sources, such as fixed carbon and nitrogen (Chrismas et al. 2015, Jungblut and Vincent 2017). These and other features of cyanobacteria will be more extensively presented in the next sections.

Another issue that can dominate the microbial surveys is related to the taxonomic resolution (Hanson et al. 2012). The advent of environmental amplicon sequencing widened even more this problem. This approach consists in the amplification of fragments of a particular molecular taxonomic marker gene from the DNA extracted from an environmental sample via polymerase chain reaction (PCR), that is subsequently sequenced on a High-Throughput Sequencing (HTS) platform, such as Illumina MiSeq. Micro-eukaryotic surveys predominantly focus on the V4 or V9 region of the ribosomal gene 18S rRNA (Vaulot et al. 2021) whilst bacterial surveys generally employ the V1-V3 regions of 16S rRNA (Sinclair et al. 2010). However, exclusive use of the V1-V3 region of 16S may be insufficient to uncover the variety of cyanobacterial taxa, therefore amplification of the V3-V4 region of 16S is recommended for cyanobacterial-focused surveys (Nübel et al. 1997). Data processing of amplicon datasets include grouping them into operational taxonomic units (OTUs) or amplicon sequence variants (ASVs) on the basis of their

similarity and the taxonomic assignment is performed on the basis of either phylogenetic interference or percentage similarity match to public databases (Taton et al. 2006a, b, Komárek et al. 2012, Martineau et al. 2013, Jancusova et al. 2016).

This culture-independent method gives a broad overview of the main microbial taxa inhabiting the environmental samples. Nowadays, other omics techniques exist to depict the whole taxonomic diversity as well as the functioning of the microbial communities which do not require PCR, such as shotgun metagenomics and metatranscriptomics (see Quince et al. 2017 and Shakya et al. 2019 for an overview).

Overall, Antarctic biodiversity is characterized by relatively simple and undisturbed ecosystems where fundamental ecologic processes (i.e. how organisms interact with themselves and the surrounding environment, the roles they play in nutrient cycling, the overall functioning of ecosystems) can gain a better understanding. Moreover, since the diversity of primary producers directly influences the diversity of other organisms (Lee et al. 2019), their presence and abundance may have cascade effects on other organisms (c.f. 1.1 paragraph of this thesis). Studying these organisms overall enhances our understanding of the physiological and genetic mechanisms that enable life to thrive in extreme environments, and gathering essential baseline data on the endemic species and their distribution is crucial for conservation efforts, as it helps identify areas of high ecological importance for the establishment of protected areas.

1.4 GENERAL FEATURES OF CYANOBACTERIA

Cyanobacteria (Kingdom: Bacteria; phylum: Cyanobacteriota) comprises a wide diversity of functionally and morphologically distinct Gram-negative bacteria (Paerl et al. 2000). They are the only known prokaryotes capable of oxygen-evolving photosynthesis from which they obtain energy (photoautotrophs). They are commonly referred to as cyanobacteria or blue-green algae since their blueish coloration (from Ancient Greek κύανος (kúanos) 'blue') due to the phycobiliprotein phycocyanin. Cyanobacterial record extends back to 3500 Ma (Lenton and Daines 2017) and today they represent one of the most diverse prokaryotic groups. Cyanobacteria had a key role in the oxygenation of the atmosphere ~ 2450 Ma - the so-called

"Great Oxygenation Event" – which is considered as one of the first mass extinction events in the Earth's history (Whitton and Potts 2012). This is also the period in which cyanobacteria multicellularity is thought to have arisen (2450 - 2220 Ma; Schirrmeister et al. 2011).

1.5 MORPHOLOGY

Cyanobacteria show considerable morphological diversity. They may be unicellular (e.g. *Chroococcus*) or filamentous (e.g. *Phormidesmis*), which may occur freely or grouped to colonial forms (e.g. *Nostoc*; Fig. 1.7). Filamentous forms may exhibit functional cell differentiation such as heterocysts (for nitrogen fixation), a thick-walled cell often with a nodule of cyanophycin that is a polymer of two amino-acids occurring at one or both sides of the cell (Whitton and Potts 2012), akinetes (resting stage cells), and hormogonia (reproductive, motile filaments).

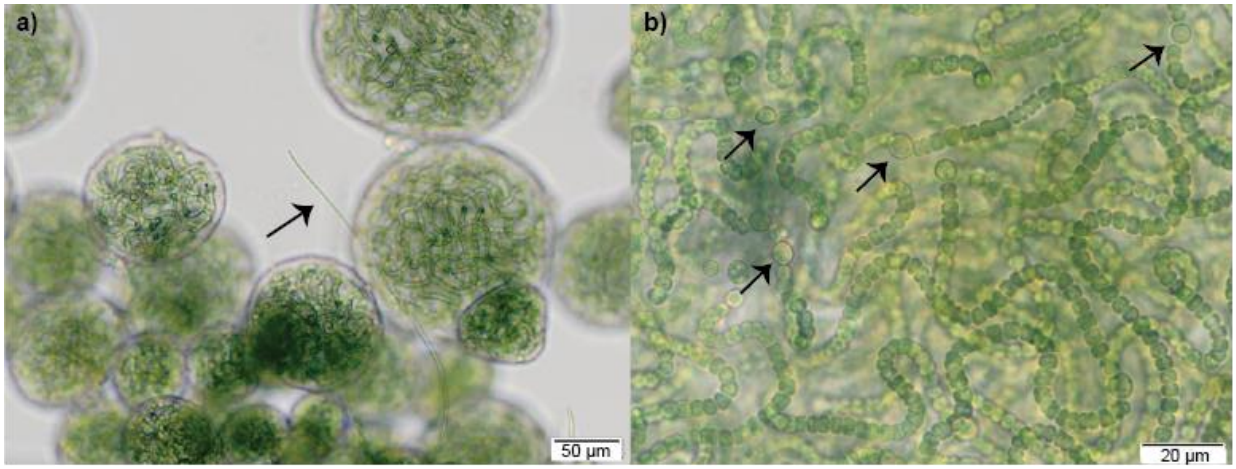

Fig. 1.7 Nostoc sp. strains under microscope with arrows indicating hormogonia (little motile filament; a) and heterocysts (cells where nitrogen fixation occurs; b). *© Valentina Savaglia.*

Cyanobacteria employ water as the electron donor during photosynthesis and present several light-harvesting pigments, being chlorophyll *a* the main one (Whitton and Potts 2012). Other pigments are the carotenoids, which also protect against excessive light by quenching (Colyer et al. 2005), or the phycobiliproteins, such as phycocyanin or allophycocyanin. Another phycobiliprotein type that is only present in some cyanobacteria and algae is phycoerythrin (Cohen-Bazire and Bryant 1982). The protein-pigment complexes are organized into specialized

light-capturing structures called phycobilisomes, which transfer their absorbed energy to the reaction centers of photosystem II (PSII). In a few taxa, other chlorophylls have been observed, including chlorophylls *b*, *d* and *f* (Miyashita et al.1996; Chen and Scheer2013). Photosystems I (PSI) and II (PSII) are located on internal membranes called thylakoids (except in the genus *Gloeobacter*, a primitive thylakoid-free cyanobacteria). Cyanobacteria fix CO_2 through photosynthesis in thylakoids and several species are also known to produce toxic secondary compounds (Castenholz 2001). Cyanobacterial endosymbiosys enabled the acquisition of photosynthesis in eukaryotes through the rise of plastids (Archibald 2015).

Some cyanobacteria are also able to fix atmospheric nitrogen. Nitrogen fixation requires anaerobic conditions. Some filamentous nitrogen fixing cyanobacteria (e.g. *Nostoc*) are able to develop specialized cells, i.e. heteocysts, under nitrogen depleted conditions, where nitrogen fixation can occur. A few cyanobacteria (e.g. *Cyanothece*) are able to perform nitrogen fixation in the absence of heterocysts. These species are able to temporarily shift between nitrogen fixation and photosynthesis, with photosynthesis occurring during the day under aerobic conditions and nitrogen fixation occurring during the night under micro-oxic or anaerobic (Belnap 2003). Atmospheric nitrogen (N_2) represents 78 % of the atmosphere. This gaseous nitrogen form is not bioavailable to heterotrophic organisms, except for those having endosymbiotic nitrogen-fixing bacteria, such as. *Pseudomonadotas* phylotypes. Hence, they enable the transformation of nitrogen gas into ammonia (NH_3) or more commonly into ammonium in neutral pH soils (NH_4^+). which process is mediated by the nitrogenase enzyme complex (Burgess and Lowe 1996). In the presence of oxygen, nitrogenase activity is inhibited (Howard and Rees 1996) and this is why nitrogen fixation only occur in anaerobic or micro-aerobic conditions. Examples of nitrogen fixing cyanobacterial genera are *Nostoc*, *Cyanothece*, *Prochlorococcus*, *Stigonema*, *Rivularia*, *Tolypotrhix*, *Aphanizomen*, *Gloeotrichia*, *Mycrocistis*, *Chamaesiphon*, *Coleosphaerium*, *Anabaena*.

1.6 TAXONOMY

Cyanobacterial taxonomy remains hitherto particularly problematic and is the subject of many researches and continuous updating studies. This led to the consequently inaccurate curation of their taxonomy within the commonly used reference databases such as Greengenes (DeSantis et al. 2006) and SILVA (Quast et al. 2012), with consequent problematic taxonomic assignment during diversity studies. With the current increasing advances in omics technologies we face the generation of thousands of sequences which need adequate taxonomy classification and revisions of inaccurate assignations are required for clarifications (Strunecký et al. 2023). The assessment of phylogenetic and taxonomic relationships among these numerous, often highly divergent new entities is an urgent task to avoid growing taxonomic confusion. Here below we show the newly proposed taxonomic classification by Strunecký et al. (2023) (Fig. 1.8-1.10) based on phylogenetic analysis of the most recently available genomic data combined with the 16S rRNA gene phylogeny. This up-to-date taxonomy was also included within the newly released CyanoSeq database (Lefler et al. 2023) that was used for the identification of cyanobacterial sequences in Chapter 3 of this thesis.

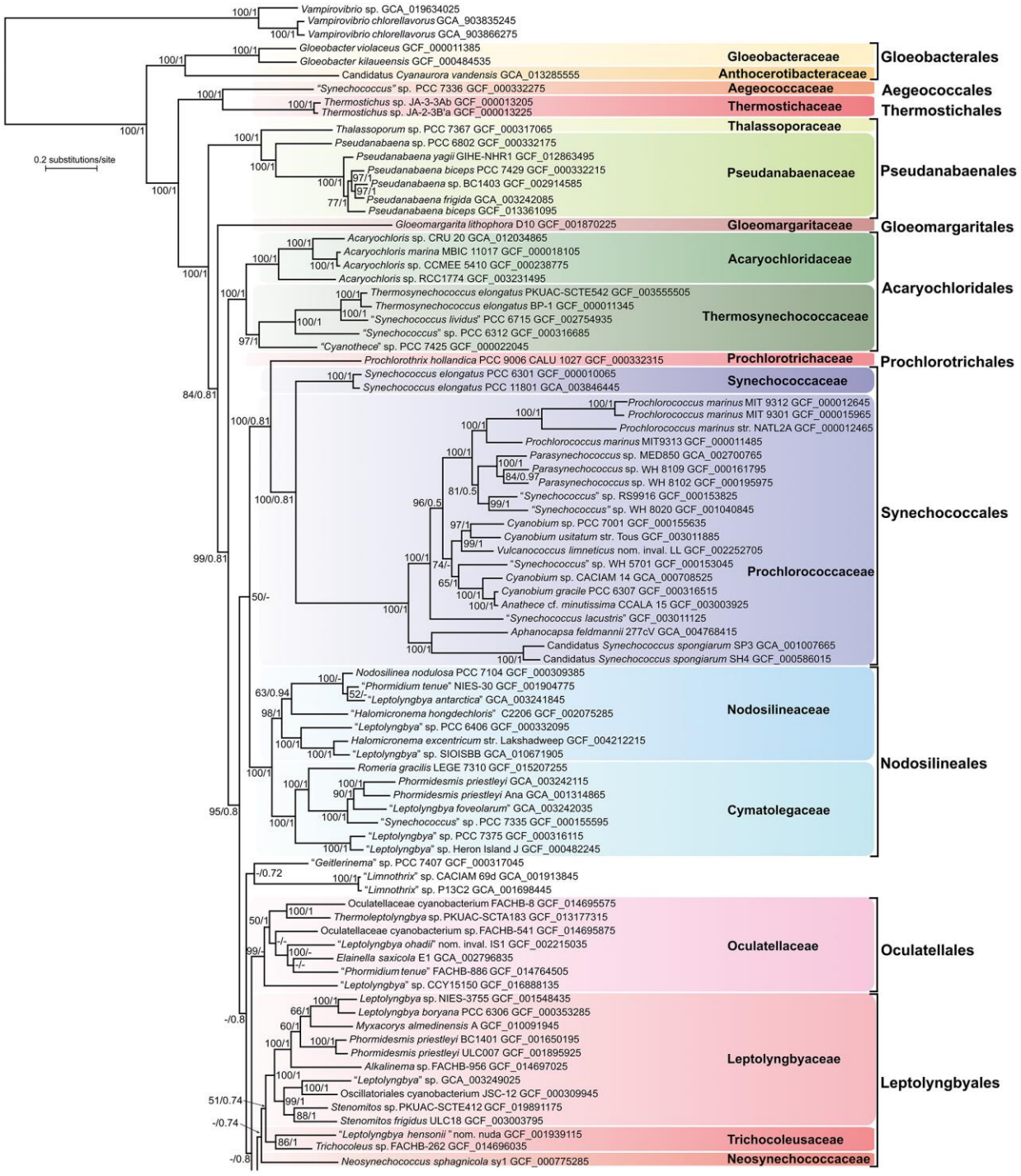

Fig. 1.8 Phylogenomic tree of cyanobacteria—part 1 (Gloeobacterales to Leptolyngbyales). *The tree was inferred from 120 housekeeping proteins using a maximum likelihood (ML) algorithm. ML bootstrap values are given at the nodes (1000 repetitions) together with Bayesian posterior probabilities. Cyanobacterial orders and families that have representatives with sequenced genomes are highlighted on the tree. From Strunecký et al. [2023].*

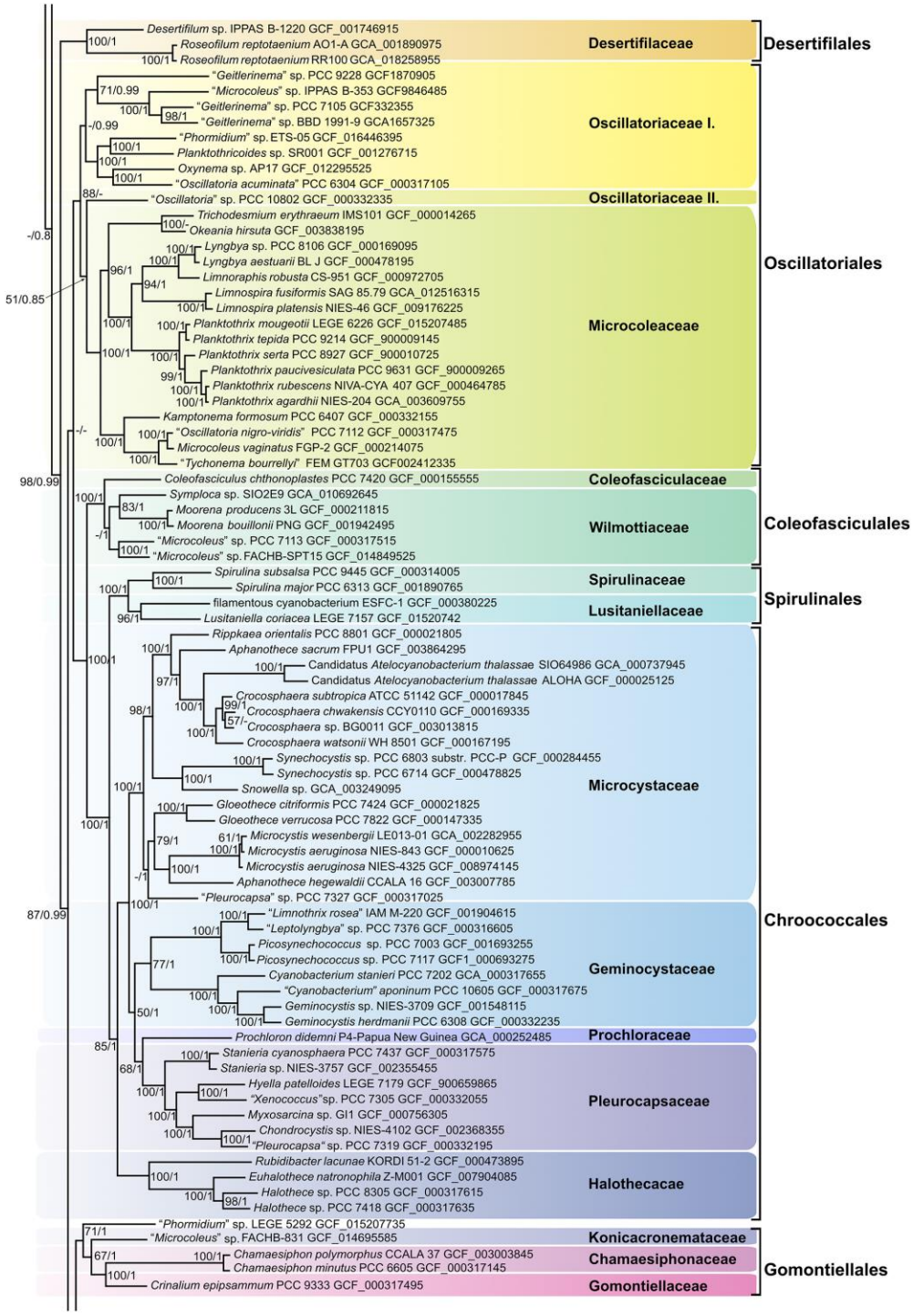

Fig. 1.9 Phylogenomic tree of cyanobacteria—part 2 Desertifilales to Gomontiellales). *The tree was inferred from 120 housekeeping proteins using a maximum likelihood (ML) algorithm. ML bootstrap values are given at the nodes (1000 repetitions) together with Bayesian posterior probabilities. Cyanobacterial orders and families that have representatives with sequenced genomes are highlighted on the tree. From Strunecký et al. [2023].*

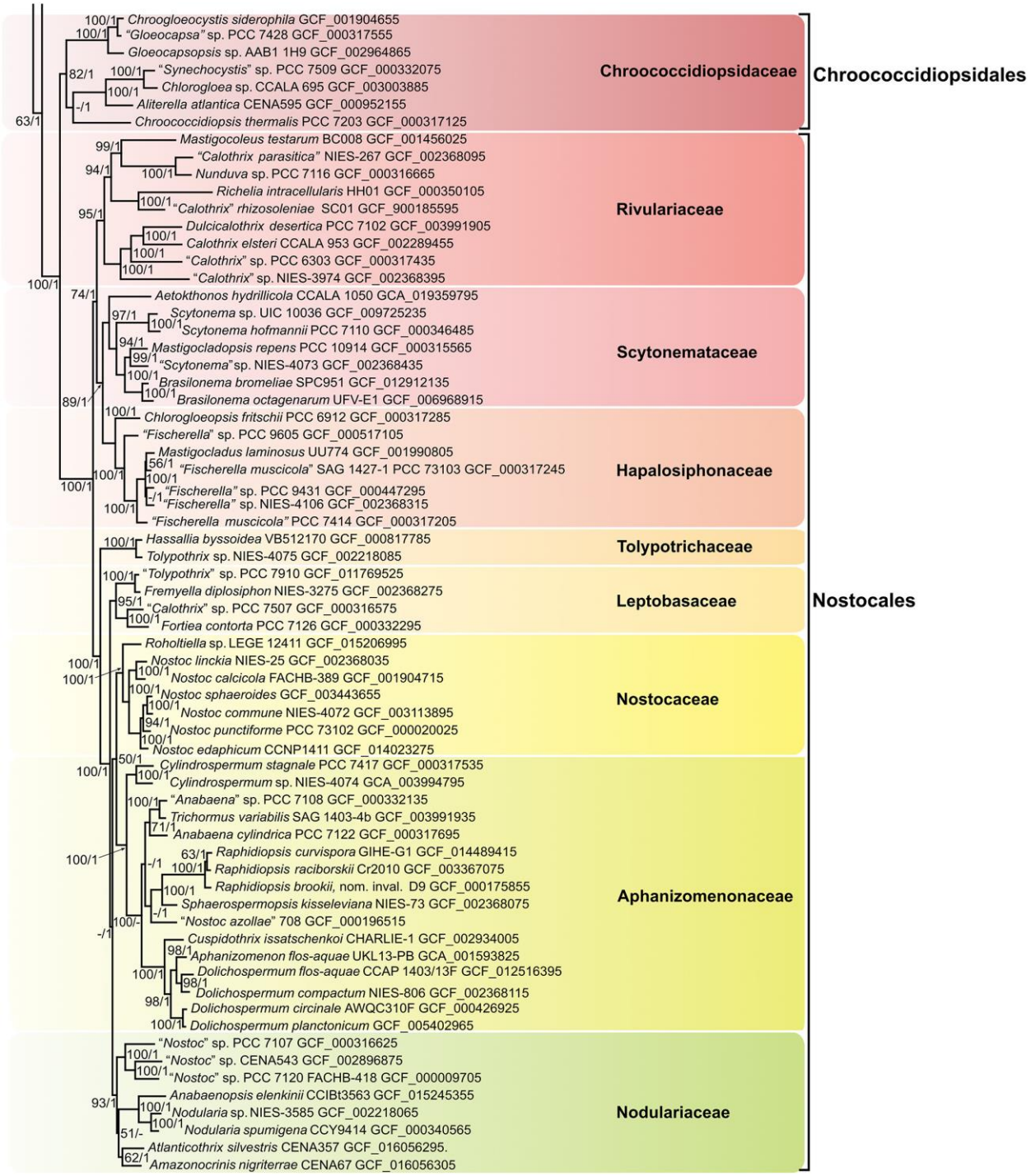

Fig. 1.10 Phylogenomic tree of cyanobacteria—part 3 Phylogenomic tree of cyanobacteria—part 3 (Chroococcidiopsidales to Nostocales). *The tree was inferred from 120 housekeeping proteins using a maximum likelihood (ML) algorithm. ML bootstrap values are given at the nodes (1000 repetitions) together with Bayesian posterior probabilities. Cyanobacterial orders and families that have representatives with sequenced genomes are highlighted on the tree. From Strunecký et al. [2023].*

1.7 ECOLOGY

Cyanobacteria are ecologically highly successful, thriving in marine, freshwater (lakes, ponds, streams) and dry terrestrial environments in polar, temperate and tropical regions. They are among the most important primary producers in oceans – where vascular plants cannot develop. The picocyanobacteria *Prochlorococcus* are the most widespread photoautotrophic organisms of the oceans and they account for up to 50 % of the chlorophyll in oligotrophic ocean regions (Partensky et al. 2019, 2021). They are responsible for around 8.5 % of global ocean primary productivity (Flombaum et al. 2013), where phytoplankton is responsible for ~ 50 % of global net primary productivity (Field et al. 1998). Cyanobacteria are central regulators of both carbon and nitrogen cycling in depauperate environments and can be viewed as 'ecosystem engineers' (Chrismas et al. 2018). The contributions of this key bacterial phylum to biogeochemical cycling, especially in oligotrophic environments, such as in diverse cold desert ecosystems where soil microbial communities mediate core functional processes relating to soil nutrient turnover because of the absence of complex food webs (Barrow 1992, Delgado-Baquerizo et al. 2018). In Antarctica, the absence of vascular plants places more importance on the cyanobacteria in shaping the ecology of the continent at local scales (Cary et al. 2010), and on the key functional roles mediated by soil-based photoautotrophs. The unique diversity and physiologies used by the cyanobacteria to cope with the worldwide extreme conditions, such as desiccation, are beginning to be understood through improved sequencing technologies and direct observations, some novel insights are collated and discussed in this thesis.

Cyanobacteria harbour numerous physiological adaptations to contend with climatic stress and are capable of colonizing, adapting and growing in broad environmental ranges across geographical space and time. They are not only genetically and therefore physiologically equipped to acclimate to UVR, desiccation and freezing stresses, by producing i.e. exopolysaccharides (EPS), mycosporine-like amino acids (MAAs), pigments such as carotenoids and scytonemin and also osmolytes (i.e. trehalose and sucrose) but some filamentous species are also able to migrate vertically downwards through the Biological Soil Crusts (BSCs) in order to protect from the high irradiance or *viceversa* when irradiance is too weak (Bebout and Garcia-

Pichel 1995, Tamaru et al. 2005, Effendi et al. 2023). Another protection strategy is to hide within lithic habitats (Chan et al. 2012). The Antarctic cryosphere is thus a model system for studies aimed at exploring the diverse and multifaceted interactions between cyanobacteria and associated microorganisms (heterotrophic bacteria, archaea, fungi, microinvertebrates) that shape their ecology at the cold, dry and oligotrophic limits of life. As primary producers, their diversity plays a central role in driving that of the other organisms (Pointing et al. 2019) and shifts in their abundance or presence due to, i.e. climate change effects (c.f. paragraph 1.1 of this thesis), may lead to cascade effects affecting also the presence of other organisms. As also mentioned for the general Antarctic biodiversity, having a baseline understanding of their distribution and of their adaptation mechanisms to the extreme abiotic conditions that they face is pivotal for conservation efforts.

1.7.1 Physiological, genetic and morphological adaptation mechanisms

In general, Antarctic cyanobacteria tend to be cold tolerant (psychrotolerant), with suboptimal growth at low temperatures, rather than psychrophiles that grow optimally at low temperature (Tang et al. 1997, Tang and Vincent 1999, Nadeau et al. 2001). They have a variety of mechanisms that allows them to tolerate and continue to grow, albeit often at slow rates, in the cold and to tolerate freeze-thaw conditions (Vincent 2007). To maintain membrane fluidity at low temperatures, polyunsaturated fatty acids with decreased chain lengths are incorporated into the membrane. In addition, the production of compatible solutes (e.g. trehalose) help to reduce the freezing point of the intracellular fluid as well as to avoid osmotic stress under desiccation (Jungblut and Vincent 2017). Genomic and metagenomic analysis of cyanobacteria inhabiting within microbial mats from the Arctic and the Antarctic such as *Phormium priestleyi* and the *Nostoc* sp. SO-36 strain showed the presence of several genes potentially implicated in the adaptation to cold stress, such as those linked to DNA replication, translation initiation factors for protein biosynthesis, chaperones for protein folding and EPS production (Varin et al. 2012, Chrismas et al. 2016, Effendi et al. 2022). Also, the segmentation into short filaments was observed as a consequence of low temperature (Effendi et al. 2022). Terrestrial cyanobacteria in Antarctica must also withstand prolonged seasonal desiccation and freezing. *Phormidesmis*-

dominated microbial mats in the Arctic have been shown to be perennial and appear to survive the winter in the vegetative state as they were metabolically active shortly before and after freezing (Tashyreva and Elster 2016). Similarly, Antarctica microbial mats have been shown to resume photosynthesis within minutes to hours after rehydration (Vincent 2007). However, the tolerance to desiccation varies between genera and the habitat of origin. While taxa belonging to *Nostoc* are anhydrobiotic, *Microcoleus* was found not to be truly anhydrobiotic as it survived extensive dehydration (to 0.23 g water g^{-1} dry mass) but not complete desiccation (to 0.03 g water g^{-1} dry mass). Laboratory experiments also suggested that nitrogen starvation prior to desiccation increased the tolerance to reduced water availability in Arctic *Microcoleus* strains (Tashyreva and Elster 2016). However, not many studies have yet been conducted with Antarctic strains and especially using omics techniques to have broader insights about their adaptation mechanisms to desiccation.

1.7.2 Life strategies as an adaptation mechanism

Cyanobacteria are often the primary colonizers of permafrost soils in areas where meltwater flushes occur through snowmelt or glacial meltwater (Pointing et al. 2015). Colonization by cyanobacteria can increase soil stability and contribute to nutrient concentrations (Niederberger et al. 2015).

In order to adapt to the very intense abiotic factors of the terrestrial ice-free areas of Antarctica, such as high UV radiation, temperature extremes, desiccation and physical removal by wind in hyperarid polar deserts, cyanobacteria are usually found in different ecotypes:

1. **BSCs**: cyanobacteria-dominated BSCs show often a ‘dark’ color and they are found throughout the Antarctic ice-free areas, especially in wind protected environments (e.g. close to relatively big boulders). Cyanobacteria can be also present in BSCs dominated by lichens or mosses.
2. **Biofilms**: cyanobacteria also form biofilms below and within the gravel where the microclimate is milder than open soils.
3. Lithic-associated habitats: they can also hide below the rock surface, depending on the optical characteristics of the rocks and the level of PAR intensity. Depending on the spatial

location of the communities, they are **hypolithic** (beneath rocks, often translucent, i.e. quarzitic), **endolithic** (in pore spaces of rocks), **chasmoendolithic** (in cracks and fissures of rocks) or **cryptoendolithic** (in the pore space between mineral grains forming sedimentary rocks) (Pointing et al. 2009, De Los Ríos 2014, Coleine et al. 2021).

1.8 MAIN AIMS & GOALS OF THIS THESIS

Despite the significant advances in the field, our knowledge on the diversity-levels, community structure, physiological, genetic adaptation of microbiota within the terrestrial and freshwater environments of Antarctica remains limited. The reasons for such limitations are multiple. First, the majority of studies focusing on the bacterial (and therefore also the cyanobacterial) and the microbial eukaryotic spatial diversity patterns have used relatively coarse taxonomic resolutions which substantially underestimate or misidentify these communities. Detailed taxonomic level surveys of cyanobacteria and micro-eukaryotes are very limited in these environments. Moreover, many studies focused on the microbiome diversity occurring in relatively stable freshwater habitats but very few focus on the extreme terrestrial habitats of Antarctica. Finally, besides the lithic-associated cyanobacterial communities, many soils also host an important cyanobacterial diversity and understanding which factors shape their structure remains one of the most important questions concerning their ecology. A thorough understanding of the variety of cyanobacterial communities and the subsequent associated bacteria and eukaryotes inhabiting different niches of the terrestrial ice-free areas can only be achieved when their diversity assessment is not biased and many of the abiotic factors characterizing their habitats are also available to link them to their spatial distribution. Which species are keystone taxa and how these interact with the whole community has yet to be elucidated.

Many questions about the ecology of cyanobacteria thriving in polar environments still remain open. A broader genome sequencing effort and the use of multidisciplinary approaches are of need to elucidate adaptation mechanisms to connect the knowledge about gene,

environment and biotic interactions. While there have been some studies on adaptation mechanisms, there does not seem to be a single metabolic characteristics or gene that provide universal tolerance to stresses imposed by extreme cold, desiccation and irradiance conditions. However, mechanisms to cope to such stressors are often similar.

Overall, the aims of this Ph.D. thesis aligned with those of the two funding projects, the Belspo "MICROBIAN" project that had as main objective the characterization of the microbiome diversity and function in the Sør Rondane Mountains (East Antarctica) and the F.N.R.S. FRIA "BI-HABITAT" project which main aim was to individuate the major genetic and ecophysiological adaptation traits developed by Antarctic cyanobacteria to desiccation conditions. In particular, the following research questions were addressed:

1) Would substrate types be responsible of driving the soil microbial community composition and structure of the SRM?
2) Would certain taxa co-occur more within certain conditions that are typical of specific substrate types and which would be the "keystone taxa" for each ecological clusters?
3) How could cyanobacteria thrive to the loss of water content, which is one of the major abiotic limiting factors affecting their distribution in Antarctic environments?

Microbial diversity and abundance, especially of primary producers, are expected to be higher within granitic soils, due the presence of crevices, pores and irregularities which represent sheltered micro-habitats compared to the smoother surface of gneiss (Obbels et al. 2016, Tytgat et al. 2016) or the porose marble soils, in which liquid water is drained faster. The coarse texture of granitic soils probably enhance also the colonization by filamentous cyanobacteria and other organisms forming BSCs. In contrast, unicellular cyanobacteria such as Chroococcidiopsaceae, are expected to be abundant in more arid soils, such as moraine and marble, because of their high resistance to xeric conditions (Jung et al. 2019). Also, Actinomycetota are expected to be widely present within the most arid soils (Pointing et al. 2009). A higher amount of micro-eukaryotes such as Rotifers and Tardigrada is also expected within communities where primary producers are particularly abundant (Lee et al. 2019). In general, nitrogen-fixer cyanobacteria such as

Nostocaceae are expected to be key taxa within these oligotrophic soils because of, e.g. their ability to provide bioavailable nitrogen to other microorganisms. Terrestrial cyanobacteria belonging to *Nostoc* sp. originated from hot deserts have been observed to be particularly resistant to desiccation conditions compared to freshwater *Nostoc* sp. (e.g. Wang et al. 2018, Katoh et al. 2014), therefore also Antarctic *Nostoc* sp. are expected to have several physiological and genetic adaptation mechanisms that would allow them to cope with complete desiccation, especially compared to a freshwater strain.

The answers to the above-mentioned research questions and hypothesis are contained within this Ph.D. thesis that is divided as follows: an introduction (Chapter 1), three research chapters (Chapters 2-4) and Chapter 5, where the results of the research chapters are discussed, and final perspectives are given.

1. **CHAPTER 2**: *Geology defines microbiome structure and composition in nunataks and valleys of the Sør Rondane Mountains, East Antarctica*. This chapter relates to the utilization of HTS to investigate the spatial distribution of bacterial and micro-eukaryotic communities within different substrate types across a range of nunataks and valleys of the Sør Rondane Mountains. More specifically, the aims were to verify whether (i) the different substrate types supported specific bacterial and micro-eukaryotic communities, characterized by different keystone phylotypes and possessing alternative primary production strategies (photosynthesis versus chemosynthesis), as well as if (ii) metazoans were restricted to environments with relatively high primary production by photosynthetic Cyanobacteriota.

2. **CHAPTER 3**: *Soil substrate drives cyanobacterial diversity in the Sør Rondane Mountains, East Antarctica.* In this chapter, HTS is used to investigate the spatial patterns of cyanobacterial communities within the different soil habitats already described in chapter 2. However, in this case, cyanobacterial specific primers were used and a more in depth characterization of cyanobacterial communities at a high taxonomic resolution was performed. More specifically, the aims were to verify whether (i) our cyanobacterial communities would differ between granite, gneiss, marble and moraine substrates sampled from different areas, (ii)

certain taxa would be highly abundant within a certain bedrock type and if (iii) their diversity would effectively be affected by hyper-dry conditions.

3. **CHAPTER 4**: *Ecophysiological and transcriptomic response to desiccation and re-wetting of Nostoc sp. from Antarctic freshwater and terrestrial habitats.* This chapter focuses on the genomic characterization and transcriptomic response to desiccation and re-hydration of a pair of *Nostoc* sp. strains belonging to the same species, isolated from two divergent habitats of the Antarctic ice-free areas: a freshwater and a terrestrial. The main aims of this chapter were (i) to verify whether both the terrestrial and the freshwater strain would possess genetic and ecophysiological mechanisms to protect themselves from desiccation and react relatively quickly to re-hydration due to their specific adaptation to Antarctic environments, and (ii) whether the freshwater and the terrestrial strain would still have a different response to both desiccation and re-hydration, with the former responding less quickly compared to the latter strain despite their close relatedness.

CHAPTER 2

GEOLOGY DEFINES MICROBIOME STRUCTURE AND COMPOSITION IN NUNATAKS AND VALLEYS OF THE SØR RONDANE MOUNTAINS, EAST ANTARCTICA

VALENTINA SAVAGLIA[1,2], SAM LAMBRECHTS[2,3], BJORN TYTGAT[2], QUINTEN VANHELLEMONT[4], JOSEF ELSTER[5], ANNE WILLEMS[3], ANNICK WILMOTTE[1], ELIE VERLEYEN[2], WIM VYVERMAN[2]

[1]InBioS, University of Liège, 4000 Liège, Belgium

[2]Laboratory of Protistology & Aquatic Ecology, Ghent University, 9000 Ghent, Belgium

[3]Laboratory of Microbiology, Ghent University, 9000 Ghent, Belgium

[4]Royal Belgian Institute for Natural Sciences, 1000 Brussels, Belgium

[5]Centre for Polar Ecology, Faculty of Science, University of South Bohemia, České Budějovice and Institute of Botany, AS CR, Třeboň, Czechia

Author contribution of VS: sampling, wetlab, bioinformatics analysis, multivariate analysis, network analysis, writing

Manuscript in preparation

2.1 ABSTRACT

Understanding the relation between terrestrial microorganisms and edaphic factors in the Antarctic can provide insights into their potential response to environmental changes. Here we examined the composition of bacterial and micro-eukaryotic communities using high-throughput sequencing of parts of the 16S rRNA and 18S rRNA genes in 105 soil samples across 9 sites in the Sør Rondane Mountains (East Antarctica), differing in bedrock type and associated physical and chemical conditions. Although the two most widespread phyla (Acidobacteriota and Chlorophyta) were relatively abundant in each sample, multivariate analysis and co-occurrence networks revealed pronounced differences in community structure depending on substrate type. In moraine soils, Actinomycetota and Cercozoa were the most abundant bacterial and eukaryotic phyla, whereas on gneiss, granite and marble substrates, Cyanobacteriota and Metazoa were the dominant bacterial and eukaryotic phyla. However, at lower taxonomic level a distinct differentiation was observed within the Cyanobacteriota phylum depending on bedrock type, with granite being dominated by the Nostocaceae family and marble by the Chroococcidiopsaceae family. Surprisingly, metazoans reached a relatively high abundance in the eukaryotic dataset even in samples from the most arid sites, such as moraines in Austkampane and Widerøefjellet. Overall, our study shows that different substrate types support distinct microbial communities in inland Antarctic nunataks and valleys, and that lithological diversity is a major determinant of terrestrial microbiome biodiversity.

KEYWORDS

microbial community composition – 16S rRNA sequencing – 18S rRNA sequencing – Antarctica – bedrock

2.2 INTRODUCTION

Ice free-regions cover only a minute fraction of the Antarctic continent (0.4 % of its surface area; Brooks et al. 2019) and occur as geographically isolated patches along the coastline, inland nunataks and mountain chains. They represent some of the most extreme environments on Earth, with a general lack of moisture due to very low amounts of precipitation and unpredictable and sporadic snow and ice melt, strong katabatic winds that scour surfaces and result in the build-up of snow banks, high levels of ultraviolet radiation, and extremely low and daily/seasonally fluctuating temperatures (Bockheim and Hall 2022, Cowan and La Tow 2004). It is now well known that despite these extreme conditions, the arid and hyper-arid Antarctic soils host a much higher microbial diversity than previously thought (Lukashanets et al. 2021, Ortiz et al. 2021, Cowan et al. 2014). In addition, there is culminating evidence that similar to macroscopic organisms, a relatively high number of microbial taxa is endemic to the Antarctic as a result of evolution in isolation on multi-million-year timescales (Convey et al. 2020; Pinseel et al. 2020). This implies that some regions must have been exposed during the multiple glacial (re-)advances that took place since the formation of the Antarctic Ice Sheets c. 35 Mya, so they could act as refugia for terrestrial and lacustrine biota (Convey et al. 2008, Pugh and Convey 2008, Stevens and D'Haese 2014, Convey et al. 2020, Pinseel et al. 2021).

In addition to their high number of endemic taxa, Antarctic terrestrial food webs are also characterized by a reduced representation or even absence of major vertebrate, invertebrate and plant groups. These soil ecosystems are therefore mainly driven by microorganisms, and have truncated and simple food webs. Despite this, the relation between environmental factors and microbial community structure in Antarctic ice-free regions is poorly understood, with the exception of those in the arid deserts of the McMurdo Dry Valleys and the Transantarctic region of Victoria Land (Dragone et al. 2022, Solon et al. 2021, Thompson et al. 2020, Severgnini et al. 2021, Coleine et al. 2021). This lack of knowledge is particularly eminent for microbial eukaryotes (Cucini et al. 2022, Franco et al. 2021, Obbels et al. 2016). The few existing studies revealed that soil moisture, pH, salinity, nitrogen concentration, soil physical stability and to a lesser degree temperature and organic matter content of the soils can explain a significant portion of the

spatial variability in Antarctic microbial soil communities (Niederberger et al. 2008, Tytgat et al. 2016, Goordial et al. 2017, Alekseev et al. 2020, Severgnini et al. 2021, Dragone et al. 2022). In the surface soils of hyper-arid areas, Chlorophyta, Ciliophora and Cercozoa were the most abundant eukaryotic phyla recorded, while Actinomycetota, Acidobacteriota, Bacillota and Chloroflexota were often the dominant bacterial phyla. Some phylotypes of these bacterial phyla were recently found to be genetically equipped for the consumption of molecular hydrogen (H_2), CO_2 and CO from the atmosphere as energy and carbon sources (Ji et al. 2017, Greening et al. 2022, Ray et al. 2022, Ortiz et al. 2020). Actinomycetota are also abundant in environments with a higher organic carbon and moisture content, such as biological soil crusts (BSCs) or lithic niche refugia (i.e. hypolithic, endolithic habitats or wind protected rock cavities). However, in these less extreme habitats other bacterial taxa such as Cyanobacteriota, Pseudomonadota and Bacteroidota are also abundant. Among the eukaryotes lichen-symbiotic and free-living Fungi, and Chlorophyta may be abundantly present, as well as the metazoans Rotifera, Tardigrada, Nematoda and Arthropoda.

In addition to identifying the structuring role of abiotic factors on microbial communities, co-occurrence networks between bacterial and (micro)eukaryotic phylotypes potentially can reveal biotic interactions which may exert an unexpected, yet critical control on the complexity of these abiotically driven polar ecosystems (Lee et al. 2019). Co-occurrence networks can also be used to identify keystone taxa, which are those phylotypes that form a link between two hubs of taxa and/or that highly co-occur with other taxa, and are expected to play a pivotal role in the ecological cluster (or module) to which they belong. Identifying the key taxa performing crucial ecosystem functions such as nitrogen and carbon fixation is pivotal to understand the threats these communities may face in response to anthropogenic and climate disturbances.

Here we analyzed environmental conditions and microbial community structure in 105 soil samples collected from 9 different sites in the Sør Rondane Mountains, East Antarctica (Fig. 2.1). This region (22 to 28° E, 71°30′ to 72°40′ S) includes several isolated ice-free nunataks and associated moraines, encompassing a variety of substrate types and local environmental conditions (Tytgat et al. 2016). We hypothesized that (i) different substrate types support

particular bacterial and micro-eukaryotic communities (i.e. a higher abundance of filamentous cyanobacteria within granitic compared to gneiss substrates as it was already observed in Tygtat et al. (2016) and Pushkareva et al. (2018)), and different keystone phylotypes possessing alternative primary production strategies (i.e. photosynthetic cyanobacteria within the most wet soils versus chemosynthetic Actinobacteriota within the driest soils), and (ii) metazoans are restricted to environments with relatively high primary production by photosynthetic Cyanobacteriota and micro-eukaryotes.

2.3 MATERIALS & METHODS

2.3.1 Sampling and site descriptions

The Sør Rondane Mountains (SRM; 22 - 28° E, 71°30′ - 72°40′ S) encompass a large number of nunataks covering an area of ca 2000 km^2 (Suganuma et al. 2014) within Dronning Maud Land, East Antarctica. The SRM are geologically situated in the East African-Antarctic Orogen (EAAO; Jacobs and Thomas 2004) that was formed by the collision of the African plate assembly and the Antarctic Coats Land Block around 650–540 Ma, causing the accretion of multiple arc terranes (Ruppel et al. 2015). In between these two plates, the Main Shear Zone separates the northern SRM with ocean affinity (viz. the presence of marble veins) and characterized by metamorphic rocks (i.e. gneiss), from the southern metamorphic rocks that exhibit island arc or continental margin arc features (igneous intrusions, e.g. granite outcrops). In this study, nine sites originating from these two plates were sampled to cover the main geological features in the western SRM (Fig. 2.1). The granitic Utsteinen ridge (“UT”) north of the Utsteinen nunatak was sampled, close to the Belgian Station Princess Elisabeth Antarctica (“PEA”; 71°57′ S, 23°21′ E; 1372 m a.s.l.). Perlebandet to the northwest of PEA is a mountain range composed of three nunataks mainly characterised by gneiss soils interlayered with some marble veins in the two northernmost nunataks (designated here as “Perlebandet N” or “PB_N”, and “Perlebandet S” or “PB_S”). To the southwest of PEA, near the main mountain range, Petrellnuten is located, which is a granitic nunatak close to the Pingvinane mountain subrange. Pingvinane is characterised by five granitic nunataks, two of which were sampled (named “Pingvinane 4th” or “PA4”, and “Pingvinane 6th” or

"PA6"). Furthermore, three moraine sites were sampled: Widerøefjellet (here referred to as "Dry Valley" or "DV") to the south-west, Yûboku Valley ("YO") to the south-east and Austkampane ("AU") to the east of PEA. Gneiss and granitic bedrock types are chemically similar but physically different. Because of the high compression gneiss has been subjected to during metamorphism, it is composed of layers of minerals (silicates, aluminium, potassium, etc.) which make the rock very hard and of low porosity. By contrast, granitic rocks are characterized by randomly dispersed minerals within the rock matrix, causing the rock to be more porous and less hard. Marble, on the other hand, is a metamorphosed limestone, mainly composed of calcium carbonates and magnesium, characterized by an even higher porosity and lower hardness than both granite and gneiss bedrock types. The moraines consist of a mixture of fragments of different types of rocks, thus with different physical and chemical characteristics. The sampled moraine soils were characterized by amphibolite (Austkampane) or greenschist-facies origins (Yûboku Valley and Dry Valley) with gneiss, quartz and/or meta-tonalite inclusions (see supplementary Table S2.1 for details).

The SRM have a east-west orientation, constituting a barrier to the northern ice plateau. This position is of particular advantage to the northern escarpment zone where most of the nunataks are located. Here, the strong north-facing katabatic winds are naturally deviated, resulting in rather sheltered areas, including Perlebandet and Utsteinen where PEA is located. Winters are relatively mild, with temperatures oscillating between -25 to -20 °C during winter and summer temperatures between - 15 and + 5 °C (Pattyn et al. 2010, Gorodetskaya et al. 2013). In opposition, conditions near the southern main mountain range are more extreme, with Austkampane to the east being the windiest site among all the sampled locations, followed by the Dry Valley area. Because of the continuous winds, these two sites are particularly harsh and microbial communities are often not visible.

During the Belgian Antarctic Research Expeditions (BELARE) 2017-18 and 2018-19 field campaigns, 105 samples from 9 sites (Fig. 2.1) were taken along gradients in bedrock type, moisture content, exposure and microclimatic conditions (Table S2.1). In each sampled site we

retrieved the diversity of surface communities observed *in situ*, by collecting the most heterogeneous kind of communities, ranging from exposed barren bedrock to protected substrates close to boulders (when present) where diverse development stages of biological soil crusts consisting of macroscopic biota such as lichens, mosses, microalgae and/or cyanobacteria, were present. This sampling design was chosen in order to have a representative overview of the biota inhabiting the surface substrate (first 1-2 cm) of the sampled nunataks or valleys, consisting mainly of gravel soil. Nonetheless, difficulties about the access to specific nunataks or the low extension of biomass partly contributed to the unbalanced sampling design, which resulted in several samples from a location compared to very few samples from other sites. All samples were collected aseptically using a sterilized spoon (70 % ethanol), immediately stored in sterile Whirl-Pak® sample bags and transported in a cool box with ice-packs (-20 °C) until arrival at the station. All the samples were stored at -80 °C at the station and brought to Belgium at -20 °C where they were stored at -20 °C until further processing at the Laboratory of Protistology and Aquatic Ecology (Ghent University). When sufficient material was collected for the analysis of soil characteristics, which included pH, electric conductivity, moisture content and the concentrations of nutrients ($N\text{-}NO_3^-$, $N\text{-}NH_4^+$, $P\text{-}PO_4^{3-}$, total nitrogen, total phosphorus) and organic matter (soil total organic carbon, TOC). Insufficient material for DNA and soil characteristics affected the overall number of samples that could be used for downstream analysis and therefore further contributed to the resulting unbalanced design.

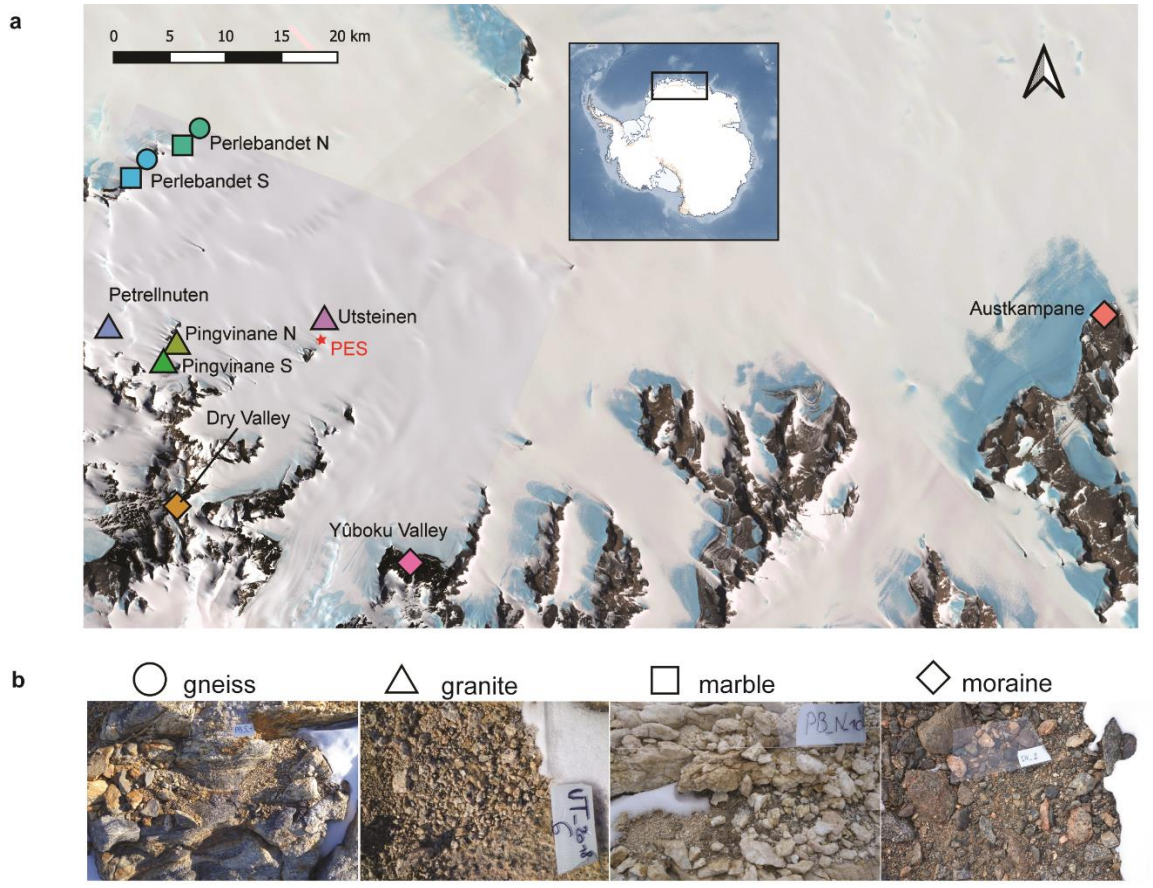

Fig. 2.1 (a) Satellite image of Sør Rondane Mountains and sampled sites. (b) In situ photographs of the four types of soil ecosystems investigated. *More information about the samples can be found in Table S2.1. Contains modified Copernicus Sentinel-2 data [2020] and Landsat Image Mosaic of Antarctica (LIMA). Colors differ by sampled site.*

2.3.2 DNA extraction and sequencing

High-quality bacterial 16S and eukaryotic 18S rRNA gene libraries were successfully constructed for 96 and 97 soil samples, respectively. Each sample was first thoroughly homogenized and between 0.2 to 1 g was used for DNA extraction with the Qiagen DNeasy Powersoil kit (Valencia, CA). For bacteria, PCRs targeting the V1-V3 hypervariable regions of the 16S rRNA gene were performed using the general forward pA (5'-AGAGTTTGATCCTGGCTCAG-3', positions 8-27) (Edwards et al. 1989) and reverse BKL1 (5'-GTATTACCGCGGCTGCTGGCA-3', positions 536-516) (Cleenwerck et al. 2007) primers. For eukaryotes, the V4 region of the 18S rRNA gene was amplified using the general forward TAReuk454FWD1 (5'-

CCAGCASCYGCGGTAATTCC-3') and reverse TAReukREV3 (5'-ACTTTCGTTCTTGATYRA-3') (Stoeck et al. 2010) eukaryotic primers. The PCR mixture consisted of 2.5 µl buffer (FastStart High Fidelity PCR System, Roche), 5 µl (2 mM) dNTP (Thermo Fisher), 2.5 µl (10 µM) of each primer, 0.25 µl (1 u μl^{-1}) Taq polymerase (FastStart High Fidelity PCR System, Roche), 1 µl template DNA and 14.75 µl sterile milliQ water. An initial denaturation step of 5 min at 94 °C was followed by 25 or 35 cycles for bacterial or eukaryotic primers, respectively, of 1 min denaturation at 94 °C, 1 min annealing at 65 to 60 °C or 57 to 52 °C for bacterial or eukaryotic primers, respectively, with a decrease of 0.5 °C per cycle, and an elongation step at 72 °C for 3 min. After a final elongation of 20 min at 72 °C, PCR products were visualized on TBE 1 % agarose gel. If amplification was successful, PCR duplicates for each sample were pooled to minimize potential biases. The pooled PCR products were subsequently purified with Agencourt AMPure XP beads (Beckman Coulter Inc.) according to the manufacturer's instructions. Twelve to sixteen-cycle (depending on the amount of DNA) index PCRs using Nextera XT (Illumina Inc.) barcodes were performed as described in the Illumina 16S rRNA metagenomics library prep guide using 25 µl of PCR grade water, 5 µl of 5x buffer, 5 µl of dNTP (10 mMol), 0.5 µl Taq Polymerase (FastStart High Fidelity PCR System, Roche), 3.5 µl of both index 1 and index 2, and 7.5 µl of PCR template. The library prep was again purified using AMPure Beads XP (Beckman Coulter Inc.) as above. The DNA concentration of the cleaned PCR products was measured using a Qubit fluorometer (ThermoFisher) with the Qubit dsDNA BR assay kit (ThermoFisher), and the samples were equimolarly pooled based on their molecular weight and DNA concentrations in a total volume of 15 µl and a final concentration of at least 5 nM. Amplicon libraries were sequenced on an Illumina Miseq platform (2 × 300 bp paired-end, v3 chemistry) at Genewiz (Azenta Life Sciences, Leipzig, Germany). Each run with either eukaryote or bacteria samples contained two replicates of a positive control sample (mock community), respectively containing 16 eukaryote (Table S2.2) and 20 bacterial species (20 Strain Even Mix Genomic Material, ATCC, Cat. No. MSA-1002, Manassas, VA), two negative controls (each composed by a mixture of two PCR blanks) to check overall run quality and benchmark processing variables, as well as 2-3 PCR replicate samples. Sequences were deposited to NCBI Sequence Read Archive under accession number.

2.3.3 Data processing

Raw reads were processed using the DADA2 package version 3.10 (Callahan et al. 2016) within R version 4.0 (R Core Team 2021). For 16S and 18S rRNA genes, primers were removed from the raw reads by trimming the first 20 and 21 (18 for 18S rRNA) nucleotides from the forward and reverse reads, respectively, using the *trimLeft* command. Based on visual inspection using Fastqc (Andrew 2010), forward and reverse reads were then truncated at base pair 297 and 257 (267 for eukaryotic reads), respectively, using the *truncLen* command and filtered with a maximum number of 'expected errors' (*maxEE*) threshold of 2 for both forward and reverse reads. Reads not matching these criteria were discarded. After sequence dereplication, sequence variants for the forward and reverse reads were inferred based on an error matrix constructed from the first 1e8 bp of the sequences. Singletons were discarded, and paired-end reads were merged with no mismatch allowed and a required minimum overlap of 20 bp. Sequence tables for each sequencing run were constructed using *makeSequenceTable*, and subsequently merged with *mergeSequenceTables* commands. Finally, chimeric sequences were removed using *removeBimeraDenovo*. Taxonomic classification of the resulting sets of ASVs was done using *classify.seqs* in Mothur with the SILVA v138.1 (Pruesse et al. 2007) and PR2 version 4.14.0 (Guillou et al. 2012) databases for the 16S and 18S ASV sets, respectively.

2.3.4 Environmental data collection

Geographical coordinates of each sampled location were taken with a Garmin 62nd/64st/Montana® 680 GPS. Elevation data were retrieved from the geographical coordinates as described in Vanhellemont et al. (2021) and are shown in Fig. 2.1 and in Supplementary Table 2.1. Soil was passed through a sterile 3 mm sieve for homogenization and to remove large particles before analysis. Analysis of geochemical and geophysical soil properties such as pH (H_2O), soil total organic carbon (TOC, %), N-NO_3^- (mg kg^{-1}), N-NH_4^+ (mg kg^{-1}), total nitrogen (TN, %), P-PO_4^{3-}(mg kg^{-1}), total phosphorus (TP, %) and soil dry weight (%) and electric conductivity (EC, µS cm^{-1}) were conducted following established methods at the Institute of Botany, AS CR in Třeboň (Czech Republic). Analyses were performed according to Czech and European Union standards (ISO 10390, ISO 10523, ČSN EN 27888, ISO 11465, ČSN EN ISO 11732, ČSN EN ISO

13395, and ČSN EN ISO 15681–1). Conductivity (µS cm^{-1}) and pH were evaluated in demineralized and distilled water, respectively. The samples were further dried at 105 °C to constant weight and then combusted at 450 °C. Soil organic matter content (SOM) was calculated as difference between two weights. Total phosphorus (TP) was estimated using spectrometric determination of phosphorus soluble in sodium hydrogen carbonate solution. Mineral nitrogen (Nmineral) was calculated as a sum of N–NH_4, N–NO_3 and N-NO_2 concentrations, which were measured using a QuikChem®8500FIA automated ion analyser (Lachat Instruments, Loveland, USA). In addition to elevation, these parameters were included as "environmental variables" for each sample (Fig. S2.3 and Supplementary Table 2.1). The different bedrock types that characterized each sample were defined as in Shiraishi et al. 1997 and confirmed with the pictures taken in field. Bedrock type variables were binary coded (1: sampled type of bedrock; 0: other types of bedrock).

2.3.5 Statistical analysis

All statistical calculations were conducted in R 4.0 (R Core Team 2021).

Singletons (defined as an ASV with a sequence that is present exactly once per sample), mitochondrial, chloroplast-related sequences and potential contaminants (following Fullerton et al. 2021) were removed. After occurrence inspection, mock communities, blanks and replicate samples were removed from the ASV tables and only one sample with the highest read number was kept among the replicates of the same sample (Fig. S2.1-2.2).

Diagnostic plots, skewness and kurtosis (0.14 version of the moments package; Komsta and Novomestky 2015) were used to identify the necessary transformations in order to improve the unimodal distribution of the environmental variables. To this purpose, the environmental variables were centered and scaled after square root (P-PO_4^{3-}) or log (elevation, TOC, N-NO_3^-, N-NH_4^+, TN, TP, dry weight, conductivity) transformations. Pearson's coefficients with 999 permutations and the variance inflation factor (VIF) with a stepwise calculation were used to check for collinearity among the transformed environmental parameters. Pearson's coefficients were calculated using the *cor* function in the 0.92 version of the corrplot package (Wei and Simko 2021). VIF factors were calculated using the *vistep* function of the 1.1.18 version of the usdm

package (R Core Team 2021). No strong correlations between any of the environmental variables were observed with both methods (Pearson's $|r| < 0.8$ and VIF < 10), hence all were kept during further analysis. Kruskal-Wallis rank sum tests were performed with the *kruskal.test* function of the 4.0.5 version of the stats package to detect significant differences in the values of geochemical variables in relation to the bedrock type (Table S2.3). Multiple pairwise-comparisons between groups were performed with the *pairwise.wilcox.test* function of the stats package to calculate pairwise comparisons between the bedrock types with Bonferroni corrections for multiple testing.

PCoA ordination and cluster analyses were conducted in phyloseq (version 1.34; McMurdie and Holmes 2013) and were used to assess differences in community structure between the samples as well as to identify the potential explanatory environmental variables for the observed community patterns between the samples.

Pearson's correlations between the environmental variables, elevation, the sampled sites, the substrate types, and, separately, the main bacterial and eukaryotic phyla were assessed in order to investigate a supplemental occurrence between all the measured variables.

Sampling plot coordinates were recorded as latitude and longitude. To test the influence of geographic distance at different spatial scales on the bacterial and eukaryotic community structure, we used the spatial variables created by principal coordinates of neighborhood matrix (PCNMs) of the geographic coordinates of the samples (Borcard and Legendre 2002), following Sakaeva et al. (2016). Briefly, using PCNMs allows to analyze the impact of spatial parameters on the communities at different spatial scales, ranging from large (PCNM1) to fine spatial scale (in our case, PCNM5). Therefore, geospatial coordinates of the samples were first used to calculate a geographic distance matrix using the 1.5.14 version of the package geosphere (Hijmans 2021). Then, PCNM eigenvectors were calculated from the geographic distance matrix using the *pcnm* function implemented in the version 2.5.7 of the vegan package in R. We determined which PCNM were significantly correlated with the environmental variables using a cutoff of $p < 0.05$. Then, from the pool of significantly correlated PCNMs, we used a stepwise model selection to

select the most parsimonious linear model (Venables and Ripley 2002) linking the environmental and bedrock type variables to PCNM eigenvectors, as shown in Sokol et al. (2013).

To explain variation in community structure associated with explanatory variables, a distance-based redundancy analysis (dbRDA; McArdle and Anderson 2001) was used to model variation in community structures as a function of either environmental (elevation, pH, TOC, N-NO_3^-, N-NH_4^+, TN, P-PO_4^{3-}, TP, dry weight, conductivity), spatial (PCNM) variables or bedrock type (as dummy variables for marble, granite, gneiss, moraine) after Euclidean transformation. The spatial variables and bedrock type were included to cover potentially important unmeasured environmental factors. Forward stepwise model selection (Blanchet et al. 2008) based on adjusted R^2 values (Beisner et al. 2006, Peres-Neto et al. 2006, Nabout et al. 2009, Legendre et al. 2012) was used to select the variables that best explained the variation in community structures.

To identify modules of strongly associated soil ASVs, a correlation network, i.e. co-occurrence network, was established, similarly to Delgado-Baquerizo et al. (2018a, b) and Fullerton et al. (2021). These analyses were done with 85 samples for which amplicon and environmental data were available for both bacteria and eukaryotes. To reduce the complexity of network visualization, rare ASVs were filtered out by defining thresholds based on a relative abundance > 0.1 %, a global abundance of more than 5 reads, and presence in more than 3 samples (performed independently for the bacterial and eukaryotic datasets). These bacterial and eukaryotic ASVs were then merged into a single relative abundance table. We then calculated all pairwise Spearman's rank correlations between all soil ASVs with a coefficient (ρ) > 0.7. We focused exclusively on positive correlations as they provide information on microbial taxa that may respond similarly to environmental conditions. A Spearman rank correlation was chosen over microbiome-specific correlation metrics (Friedman et al. 2012, Kurtz et al. 2015, Schwager et al. 2017) because, with n = 85, a Spearman coefficient equal to or above 0.355 is already sufficient (Zar 1972) to retain the relationships that have a $P < 0.001$ and Spearman rank correlations have been used extensively in similar studies (Fullerton et al. 2021, Delgado-Baquerizo et al. 2018a, b). Potential false-discovery rates were controlled through this strict alpha

level, while maintaining good power with the high Spearman rank coefficient. Finally, the network was visualized with the interactive platform gephi (Bastian et al. 2009) such that ASVs served as “nodes” or vertices, and absolute correlation values as the “edges” between OTUs. A modularity analysis using different clustering algorithms in the R package igraph (1.2.6 version, Csardi and Nepusz 2006) was performed (random walks, label propagation and Louvain clustering algorithms). A module is a cluster of highly interconnected nodes. While the total number of modules changed, the main modules identified by the tested algorithms converged and the 11 modules identified by the Louvain clustering algorithms (modularity of 0.79) were retained for downstream analysis. Identified modules represented ecological modules of ASVs showing a cohesive distribution across the sampled bedrock types. To investigate emergent patterns in the responses of these communities to soil-driven geochemical variables across the bedrock types, we coupled the co-occurrence network of ASVs to random forest (RF) variable ranking and correlations with Spearman and Pearson statistics. We then computed the relative abundance of each module by averaging the standardized relative abundances (z-score) of the ASVs that belong to each module, and we plotted them against the substrate type. By standardizing our data, we ruled out any effect of merging data from bacteria and eukaryotes. Kruskal-Wallis rank sum tests were performed to detect significant differences in the values of relative abundances per module in relation to the substrate type. Furthermore, the relationship between each module’s ASVs cumulative relative abundance and environmental predictors was investigated using an RFs regression analysis using the 1.1. version of the VSURF package (Genuer et al. 2015). The validity of the identified environmental predictors was further tested by correlating the cumulative abundance of each module, using both Pearson moment correlations and Spearman rank correlations, against all the environmental factors. Holm correction for multiple hypothesis testing was applied to all P values (Holm 1979). Afterwards, scatterplots were used to manually inspect and confirm the statistically identified correlations in order to identify possible nonlinear relationships. With a consistent overlap of the identified environmental predictors by each different approach (RFs analysis, scatterplot inspection, Pearson moment and Spearman rank correlations), we consider that modules cohesively responding to variations in specific

geochemical parameters might correspond to taxa that share habitat preferences that could be correlated to a specific bedrock type. The most biologically informative environmental variables that were associated with the distribution of each module were selected for plotting. Finally, the vertex degree and betweenness centrality of each node from the networks were measured for potential keystone taxa detection. Vertex degree represents the number of direct connections of a node with other ASVs in the whole community. Betweenness centrality reveals the role of a node as a bridge between components of a network. We considered ASVs with highest betweenness centrality and vertex degree in the network as potential keystone taxa (Martin González et al. 2010; Vick-Majors et al. 2014; Banerjee et al. 2016).

2.4 RESULTS

2.4.1 Community structure and diversity in relation to substrate type

In total, Illumina sequencing resulted in 3,236,875 and 9,670,564 bacterial and eukaryotic reads which, after filtering and downsampling, resulted in 3,852 to 111,385 reads for bacteria and 10,886 to 613,991 for eukaryotes. After bioinformatic data processing and removal of sample replicates, the remaining ASVs represented 78 and 75 % of the original bacterial and eukaryotic reads, respectively. A total of 27,398 Bacterial ASVs were found in the 96 studied samples and these were mainly classified as Actinomycetota (35 %), Bacteroidota (15 %) and Acidobacteriota (11 %). Cyanobacteriota, Pseudomonadota, Abditibacteriota (formerly known as candidate division FBP) and Chloroflexota accounted for 8, 7, 5 and 4% of the total reads, respectively, while the remaining phyla consisted of Armatimonadota, Candidatus Patescibacteria, Planctomycetota and Deinococcota representing between 2 and 1 %. Bdellovibrionota, Candidatus Dependentiae, Desulfobacterota, Elusimicrobiota, Bacillota, Gemmatimonadota, Myxococcota, Nitrospirota, Candidatus Sumerlaeota, Verrucomicrobiota and WPS-2 represented less than 1 %.
A total of 1,696 eukaryotic ASVs were detected in the 97 samples giving eukaryotic yields. The ASVs mainly belonged to the phyla Chlorophyta (28 %), Cercozoa (27 %) and Metazoa (11 %), followed by Ciliophora (7 %), Streptophyta (4 %) and Ochrophyta (2 %). Less abundant phyla were represented by Opisthokonta and Lobosa accounting for less than 2 %, and Apicomplexa,

Archaeplastida, Centroheliozoa, Conosa, Cryptophyta, Dinoflagellata, Discoba, Opalozoa, and Pseudofungi represented less than 1 % of the total reads. Interestingly, 8 % of the bacterial (Fig. 2.2) and eukaryotic reads (Fig. 2.3) remained unclassified at the phylum level and thus might represent a significant fraction of novel diversity.

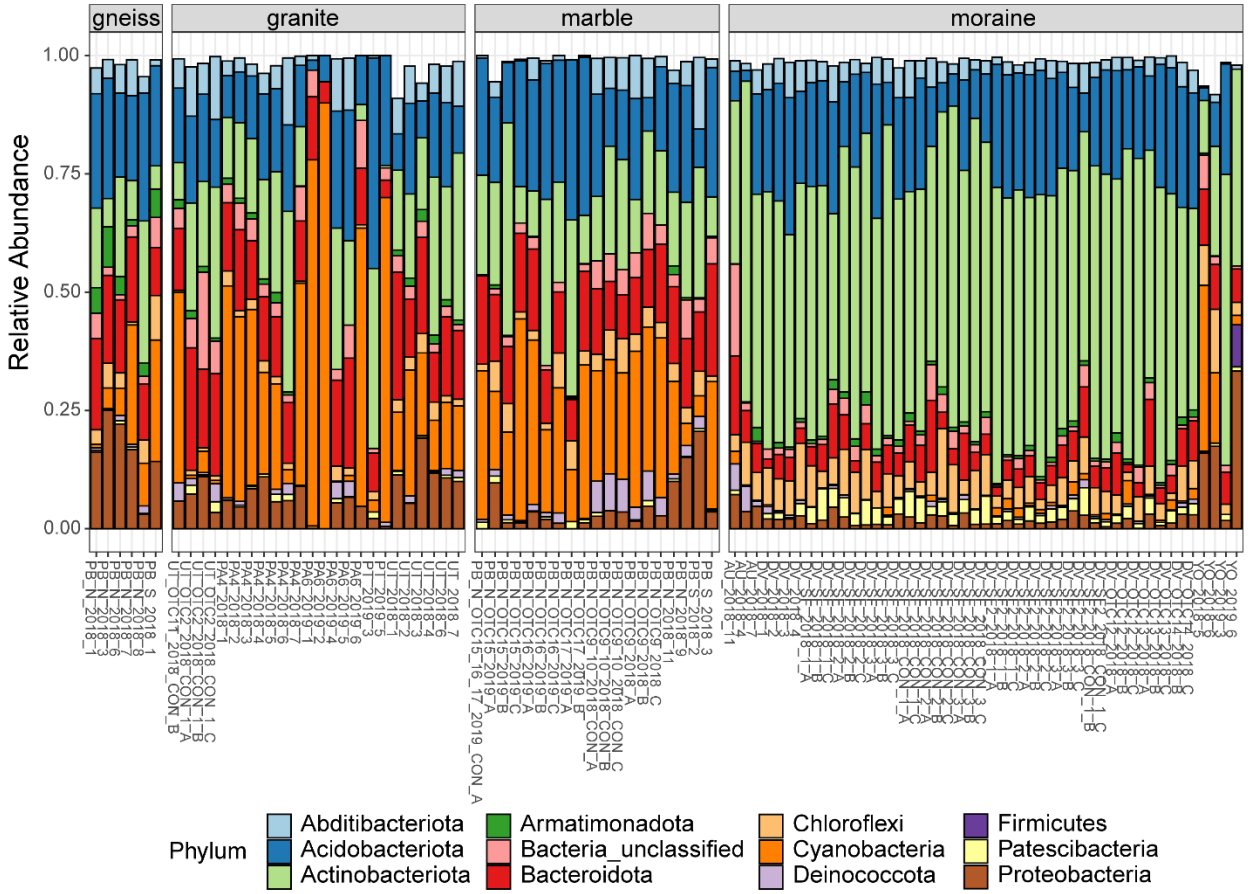

Fig. 2.2 Relative abundances of the most abundant phyla (> 1 % of total abundances) of bacteria per sample, grouped per substrate type. *Colors are according to the Phylum (see legend). Sample names indicate the site of origin (see Table S2.1 for details).*

The relative abundance of several bacterial and eukaryotic phyla differed between the different substrate types (Fig. 2.2-2.3 and Supplementary Tables 2.4-2.7). Actinomycetota were more abundant in moraine samples (49 % of the total read counts in moraines) compared to the other bedrock types (ranging from 9 % in marble soils to 12 and 16 % in gneiss and granite samples, respectively). Cyanobacteriota were dominant in granite, gneiss and marble samples, being represented by Nostocaceae (granite and gneiss: 20 and < 1 %, respectively), Phormidaceae

(granite and gneiss: 4 and 2 %, respectively) and Chroococcidiopsaceae (marble, granite and gneiss: 31, 4 and 17 %). Cyanobacteriota were present in moraine soils as well, but less abundant compared with the other substrate types (2 % in Austkampane, 1 % in Dry Valley and 32% in Yûboku Valley) while Patescibacteria were more abundant in the moraine soils (2.6 %), compared with marble (0.2 %), gneiss (0.1 %) and granite (0.8 %). Metazoa (mainly Rotifera and Tardigrada) were abundant in marble (33 %), gneiss (31 %) and granite (24 %). Rotifera were also abundant in moraine soils of Yûboku Valley (25%). Together with other unclassified Metazoa Rotifera were also found in the extreme soils of the Dry Valley (unclassified: 4 %; Rotifera: 2 %) and of Austkampane (unclassified: 5 %). Other abundant eukaryotic phyla were Ciliophora (granite: 11 %; marble: 4 %; moraine: 3 %; gneiss: < 1 %), Cercozoa (marble and moraine: 14 %; gneiss: 3 %; granite: 1 %) and Lobosa (moraine: 4 %; granite, gneiss and marble: < 1 %). At the phylum level, the bacterial communities appeared to differ more between the different substrate types compared with eukaryotic communities.

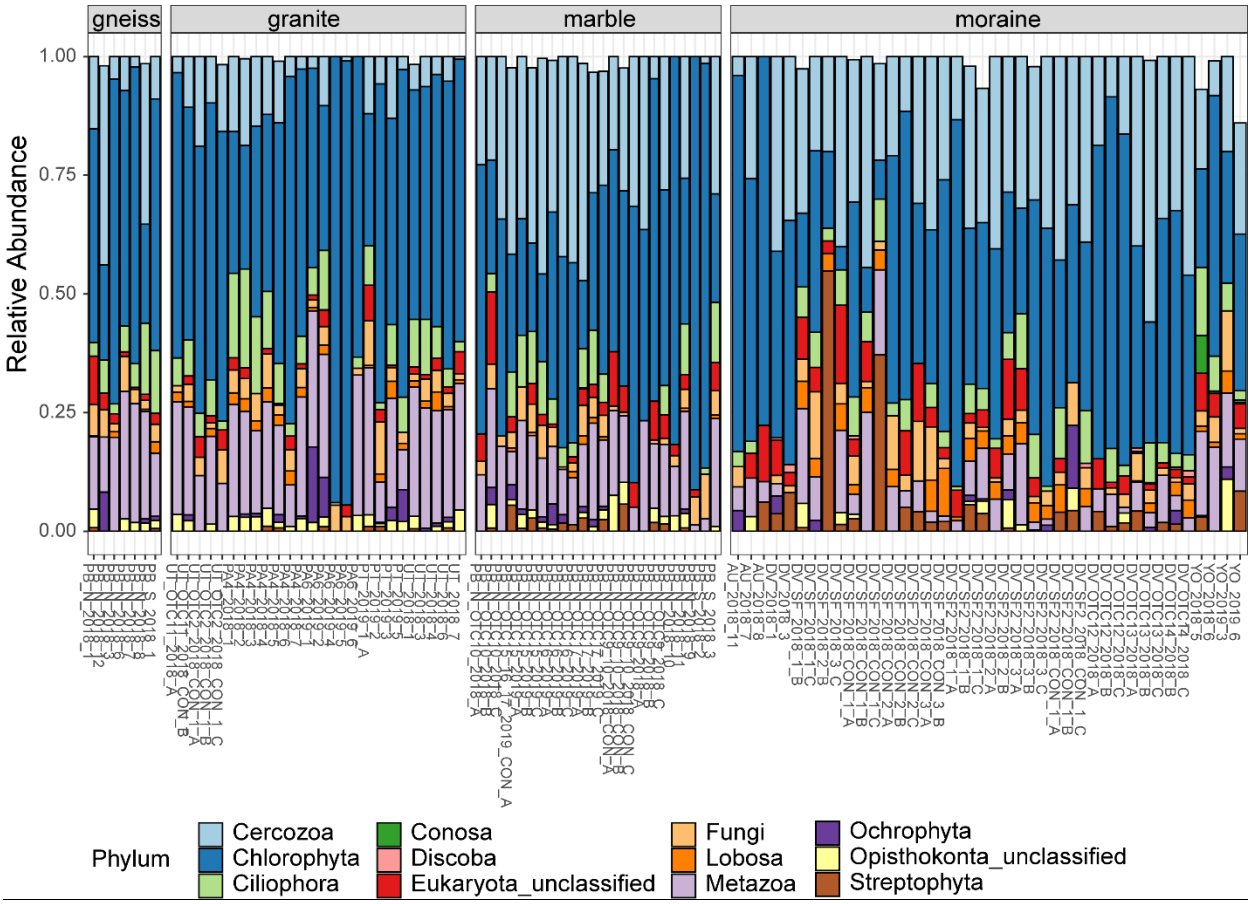

Fig. 2.3 Relative abundances of the most abundant phyla (> 1 % of total abundances) of eukaryotes per sample, grouped per substrate type. *Colors are according to the Phylum (see legend). Sample names indicate the site of origin (see Table S2.1 for details).*

The PCoA on the ASV level confirmed that samples from different sampling locations with the same bedrock type tended to have similar bacterial and eukaryotic communities (Fig. 2.4). Samples from Pingviane and Petrellnuten nunataks (PA and PT regions, respectively) and Utsteinen ridge (UT region) clustered together. Similarly, bacterial and eukaryotic communities on the marble soil from the two nunataks of Perlebandet (PBN and PBS) also clustered together. However, gneiss bedrock from Perlebandet had communities that were more similar to those observed in samples from granite bedrock. The Dry Valley (DV) bacterial communities appeared to be rather unique (Fig. 2.4a) compared to the other sites. With a few exceptions, this was also the case for the eukaryotic communities in the Dry Valleys (Fig. 2.4b).

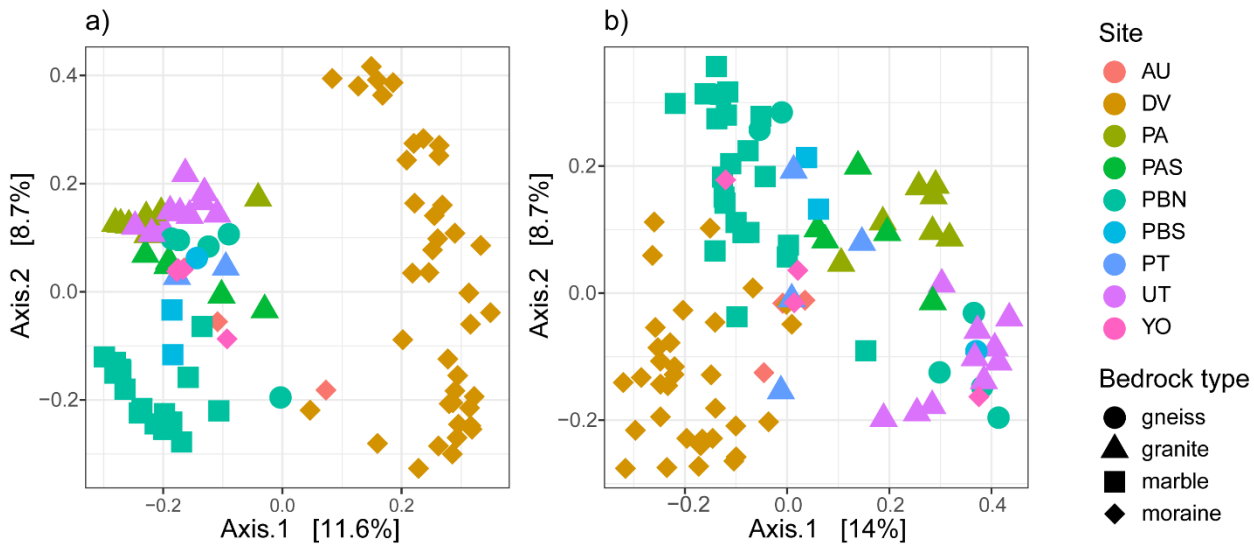

Fig. 2.4 PCoA of 96 and 97 samples of (a) bacteria and (b) eukaryotes. *Circles represent gneiss, triangles granite, squares marble and diamonds moraine samples. The percentage explained by the first two axes is given between brackets.*

2.4.2 Community structure in relation to environmental factors, location and bedrock type

Distance-based redundancy analysis (db-RDA) of the ASV relative abundance data showed a significant effect of environmental factors (P=0.001), PCNMs (P=0.001) and bedrock type (P=0.001) on the microbial community structure. Best-fit environmental models showed that the combined environmental variables (pH, elevation, total nitrogen, conductivity, total phosphorus, ammonia, nitrates, total organic carbon and only for bacteria dry weight) accounted for 19 and 21 % of the total variation in bacterial and eukaryotic community structure, respectively. Overall, four key factors (elevation, pH, total nitrogen and conductivity) had the most influence on the community structure, explaining together 14 and 16 % of the total variation in bacterial and eukaryotic community structure, respectively, while all other environmental factors individually explained 1 % or less of the total variation (Table S2.5-2.6). Of the selected environmental properties, pH was the variable explaining the highest variation (7 %). In addition, elevation appeared to be an important structuring factor for both bacteria and eukaryotes (5 %) and nearly the same geographical distance-based and the bedrock type-selected variables were selected for both datasets (Table S2.5-2.6). Out of the four selected Principal Component of Neighbourhood Matrix (PCNM) vectors built using (x,y) geographic coordinates, four and three PCNMs (PCNM3,

PCNM4, PCNM1, PCNM2 and PCNM3, PCNM4, PCNM1) explained 10 and 11 % of the total variation in bacterial and eukaryotic community structure, respectively. Selected scales reflect both short (PCNM3, PCNM4) and large (PCNM1, PCNM2) spatial scale differences and similarities between communities. Finally, among substrate type factors, three significantly explained variation in the bacterial and eukaryotic community structures, namely moraine, marble, gneiss, explaining 16 and 14 % of the total difference in bacterial and eukaryotic community structure, respectively.

2.4.3 Network analysis

A co-occurrence network enabled us to identify modules of strongly co-occurring ASVs which might represent co-existing soil taxa. Based on our criteria, only 4 % of the bacterial ASVs (1063 out of 27,398 ASVs) and 12 % of the eukaryotic ASVs (205 out of 1696) were kept for the network analyses (Fig. 2.7a, Fig. S2.6). However, this small number of ASVs accounted for 67.5 % and 93.8 % of 16S rRNA and 18S rRNA gene sequences across all samples, respectively. Together, our results suggest that soil bacterial as well as micro-eukaryotic communities, are typically dominated by a relatively small subset of ASVs. The final network included 552 nodes (91 % of bacteria and 9 % of eukaryotic ASVs) with 5181 edges, and had an average clustering coefficient of 0.669 and an overall diameter of 18.4 edges. Within the 5181 edges, 4675 indicated bacteria-bacteria co-occurrence, 452 bacteria-eukaryote co-occurrence and 76 eukaryote-eukaryote co-occurrence. Using this approach, we identified 11 modules of co-occurring ASVs (Fig. 2.7, Supplementary Tables 2.9-2.11), comprising multiple taxa (Supplementary Fig. 2.8) and which were divided in 3 main hubs. One hub was composed by five connected modules (1, 4, 5, 10 and 11). The relative abundances of ASVs present in Modules 1, 4 and 5 was highest in granitic soils (Supplementary Fig. 2.9), while in Module 10 this was in gneiss and in Module 11 in both granitic and gneiss bedrock types. A second hub was composed of two modules, namely Modules 3 and 7 of which the ASVs were mostly abundant in marble soils. The third hub included three connected modules (Modules 2, 6 and 8) with ASVs mostly abundant in moraine bedrock type. Finally, Module 9 was isolated from the three hubs and encompassed only eukaryotic ASVs (Chlorophyta) which were mostly dominant in granitic soils, but also present in all the other

bedrock types (Supplementary Fig. 2.9 and Supplementary Table 2.10). Overall, Actinomycetota and Cyanobacteriota were the most abundant phyla, representing 27 and 24 %, respectively, of the network nodes, whereas Chlorophyta, Cercozoa and Metazoa were the most represented eukaryotic phyla, accounting for 4, 2 and 1 % of the network nodes (Supplementary Table 2.10). According to the bedrock types, different microbial consortia were observed (Fig. S2.6-2.7). Photoautotrophs such as filamentous Cyanobacteriota and/or Chlorophyta were often dominant in granitic and gneiss soils (representing between 15 to 85 % of the total reads of Modules 1, 4, 5, 10 and 11) whereas the eukaryotic heterotrophs Ciliophora and Metazoa were the second most abundant category in these modules. Ciliophora dominated Module 1 (Nassulida), accounting for 56.2 % of its total read count and represented 5 % in Module 4 (Sessilida), whilst Metazoa (Rotifera) accounted for 15, 13 and 9 % of the total reads count of Modules 1, 4 and 10. Moreover, otherbacterial phyla were represented by Pseudomonadota (6 and 8 % of the total read counts of Modules 5 and 11, respectively), Bacteroidota (9 and 5 % of the total reads count of Modules 5 and 11, respectively) and Actinomycetota (5 and 7 % of the total reads count of Modules 4 and 11, respectively; Supplementary Tables 9 and 10). Moraine modules 2, 6 and 8 were dominated by the bacterial Actinomycetota phylum (75, 67 and 27 %, respectively; Supplementary Tables 2.9 and 2.10) followed by Acidobacteriota (11 % in M2 and M8) or Chloroflexota (16 % in M6) and the eukaryote Cercozoa phylum which dominated M8 (54 %; Supplementary Tables 2.9 and 2.10) and was minorly present in M2 (13 %) and M6 (2 %).

The nodes whose betweenness centrality and vertex degree indices were the highest for each module were considered as keystone taxa. Among the granitic and marble modules, Cyanobacteriota (of the Nostocaceae and Chroococcidiopsaceae families, respectively) were identified as keystone taxa candidates. This is consistent with granitic and gneiss modules sharing putative keystone taxa of the phylum Pseudomonadota, a cyanobacteria predator ASV representative belonging to the Sphingomonadaceae family showing the highest betweennes centrality of the granitic module 4 (as well as of the whole network) and the nitrogen-fixer *Rhizobacter* in the gneiss module 11 (Supplementary Table 2.15). Gneiss Module 10 and gneiss & granitic Module 11 shared putative keystone taxa such as Acidomycetota (*Blastocatella*) and

Chlorophyta (*Trebouxia jamesii* in Module 10 and unclassified representatives in Module 11), whereas Module 10 was also characterized by Cyanobacteriota (*Nostoc*) despite its very low abundance in the module (only 0.6 %, Supplementary Table 2.9). Granitic modules correlated with decreasing conductivity values (M1 and 4), or total N concentration (M5; Fig. 2.7; Supplementary Table 2.4). Gneiss Module 10 correlated with increasing TOC concentrations whilst gneiss & granitic Module 11 correlated with increasing TOC, N-NH_4^+ and TN concentrations (Fig. 2.7; Supplementary Table 2.14). Although the ASVs of Module 3 were more abundant in "pure" marble samples, the ones of Module 7 were more abundant in marble soils with some gneiss intrusions which reflected a difference in the microbial consortia. Both marble modules correlated with increasing pH values and decreasing P-PO_4^{3-} values, whilst Module 3 also correlated with increasing total N (Supplementary Table 2.14). Keystone taxa in moraine Modules were represented mainly by Actinomycetota (*Crossiella* and 67-14 in Module 2; Solirubrobacterales in Modules 6 and 8), Chloroflexota (JG30-KF-CM45) in Module 6 and Patescibacteria (uncultured) in Module 8 (Supplementary Table 2.15). Module 2, 6 and 8 correlated best with decreasing total N concentrations, although Modules 6 and 8 were also inversely correlated with decreasing pH values and TOC concentrations (Supplementary Table 2.14).

(see Figure on the next page)

Fig. 2.7 a) Co-occurrence network analysis based on bacterial and eukaryotic ASVs (dots) across all sampling sites*, colored according to the major identified modules in the different substrate types, with positive Spearman correlations > 0.7 plotted as edges. Size of nodes corresponds to the betweenness centrality degree.* ***b) Phylum-level taxonomic log-transformed abundance of those ASVs associated with each of the 11 modules****, colors represent the abundance of ASVs per module, grey rectangles highlight eukaryotic phyla****. c) Relative abundance (z-score) of ASVs in each module plotted against the most important substrate geochemical variables*** *identified by RF, Spearman correlation and Pearson correlation as the major explanatory variable for that module (P < 0.01, Holm-corrected). Module 5 represented a low number of samples. Modules 2 and 6 correlated well with decreasing TN values, similar to the plotted module 8.*

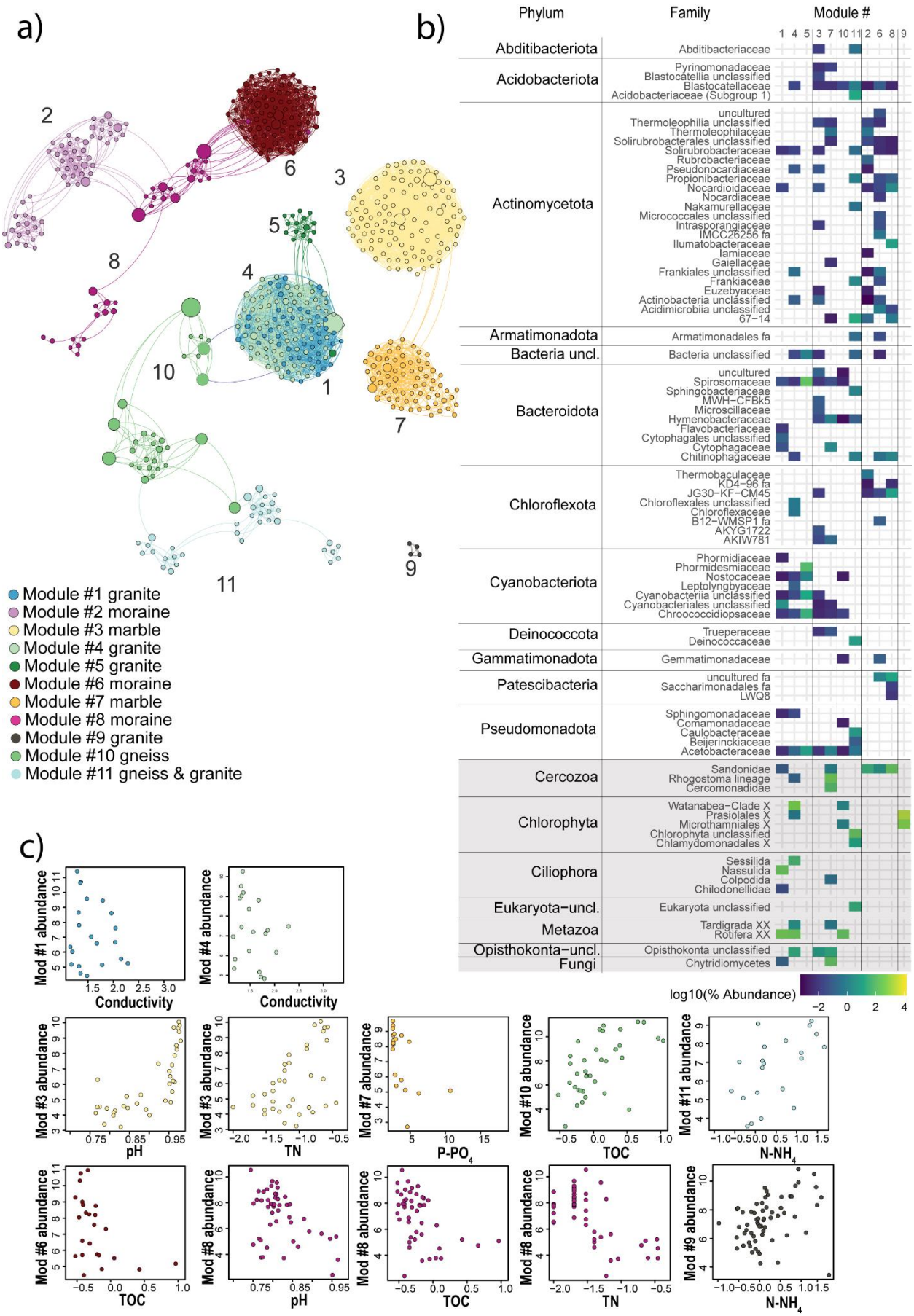
a)
b)
c)
Module #1 granite
Module #2 moraine
Module #3 marble
Module #4 granite
Module #5 granite
Module #6 moraine
Module #7 marble
Module #8 moraine
Module #9 granite
Module #10 gneiss
Module #11 gneiss & granite
Phylum
Family
Module #
Abditibacteriota
Acidobacteriota
Actinomycetota
Armatimonadota
Bacteria uncl.
Bacteroidota
Chloroflexota
Cyanobacteriota
Deinococcota
Gammatimonadota
Patescibacteria
Pseudomonadota
Cercozoa
Chlorophyta
Ciliophora
Eukaryota−uncl.
Metazoa
Opisthokonta−uncl.
Fungi
log10(% Abundance)
Mod #1 abundance
Mod #4 abundance
Mod #3 abundance
Mod #7 abundance
Mod #10 abundance
Mod #11 abundance
Mod #6 abundance
Mod #8 abundance
Mod #9 abundance
Conductivity
pH
TN
P-PO4
TOC
N-NH4

2.5 DISCUSSION

Our findings indicate, as hypothesized, that the composition of terrestrial bacteria and micro-eukarya of the inland ice-free areas of the Sør Rondane Mountains (East Antarctica) largely co-vary with the four substrate types, namely granite, marble, moraine and gneiss, even at meter-scale distances as evidenced by the different communities being present on gneiss and marble in Perlebandet. This is in agreement with Tytgat et al. (2016) who observed significant differences in bacterial community structure between granite and gneiss substrates in the region. In the present study, we show that both bacterial and eukaryotic communities of marble and moraine substrates are even more distinct compared to those on granite and gneiss. Indeed, three disconnected ecological clusters (modules) could be discerned in our co-occurrence network analysis (i.e. granite-gneiss, marble and moraine) in which putative and well known primary producers were designated as the main keystone taxa which co-occurred with different other bacterial and eukaryotic taxa. These ecological modules were correlated with important physical and chemical parameters characterizing the different substrate types (Fig. 2.7; Supplementary Tables 2.8–2.15). This is very likely because substrate type may directly affect soil chemistry (e.g. the presence of weathering products, pH and ion and nutrient concentration), as well as micro-habitat conditions such as soil temperature, and the water retention capacity. In turn, particular soil biota may also alter micro-habitat conditions by, for example, providing a habitat and buffer against environmental extremes, altering the concentration and form of nutrients, and producing organic carbon for heterotrophs and mixotrophs (e.g. Belnap et al. 2003, Colesie et al. 2014). The diversity of particular biota may therefore impact the diversity and abundance of other members of soil food webs via trophic interactions. Below we discuss the three main co-occurrence modules based on the dominance of particular taxa and or the presence of keystone ASVs. A keystone ASV is considered as an important community member crucial for network stability and therefore highly correlated with other phylotypes (highest vertex degree) and/or connects with other ASVs being present in different hubs (highest betweenness centrality) (Martin González et al. 2010; Vick-Majors et al. 2014; Banerjee et al. 2016).

2.5.1 The filamentous Nostocaceae family (Cyanobacteriota) is abundant in the granitic bedrock type

Granite hosted the highest relative abundance of diazotrophic phylotypes of the filamentous Nostocaceae family (20 % of bacterial relative abundance), which is consistent with Tytgat et al. (2016). Because of its igneous origin, granite provides a hard substrate with poor permeability. This, in combination with the exopolysaccharide matrix produced by cyanobacteria, could result in water accumulation on the bedrock surface creating favorable microenvironmental conditions for other organotrophic bacteria and micro-eukaryotes. Nostocaceae phylotypes were designated as putative keystone taxa of the granitic modules 4 and 5. Notably, also an ASV of *Polymorphobacter* (Pseudomonadota, Sphingomonadaceae family) was defined as putative keystone phylotype of module 4 because of its high betweenness centrality (the highest of the entire network; Table S2.17), although it belongs to one of the least abundant families in all the granitic samples (0.71 %; Table S2.7). Nostocaceae and Sphingomonadaceae are known to be nitrogen-fixing families (Coyne et al. 2020), and thrive under oligotrophic stress, which may explain why their presence, though in low abudance, may be critical in sustaining life. The characteristic eukaryotes on granite substrate were Metazoa and Ciliophora. For the first, these were mainly Rotifera and Tardigrada, which, together with Ciliata, are taxa commonly observed in Antarctic desert soils, as well as terrestrial and lacustrine habitats in more coastal regions of the continent (Obbels et al. 206, Thompson 2019). In addition to these characteristic taxa, the bacterial Acidobacteriota (~ 31 % in all substrate types, Table S2.4) and the photoautotrophic eukaryotic Chlorophyta (especially of the Microthamniales order) (Tables S6 and S7) phyla were abundant in granite soils, but also on the other bedrock types, which is in agreement with other studies (Moniz et al. 2012, Obbels et al. 2016). Indeed, Chlorophyta are pioneers in the colonization of soils in the Antarctic (Wynn-Williams 1996). Acidobacteriota constitute one of the most abundant phyla dominating bacterial communities in all kinds of soils (Lee and Cho 2009) including in Antarctica (Tytgat et al. 2016), and contain phylotypes able to be active at low temperatures and resilient to multiple freeze-thaw cycles (Männistö et al. 2009).

2.5.2 The unicellular Chroococcidiopsaceae family (Cyanobacteriota) dominates the marble bedrock type

As on the granitic bedrock, Cyanobacteriota also dominated communities on the marble substrates (33 % of total bacteria read counts), however, the phylotypes there belonged to the unicellular Chroococcidiopsaceae family (31 %). Phylotypes of the Chroococcidiopsaceae (*Alitarella* sp.; Table S2.15) were also recognized as putative keystone taxa in the marble modules. Chroococcidiopsaceae are known to resist prolonged periods with moisture deficit as a result of the production of EPS (Chan et al. 2012; Pointing 2016). Phylotypes of this family also represented 51 % and 15 % of the total nodes of marble modules 3 and 7, respectively. These modules positively correlated to pH and to TN (Fig. 2.7c). In addition, Bacteroidota, a phylum that is commonly found in high pH soils (Lauber et al. 2009), attained their highest abundance in the marble soils (Fig. 2.2, Table S2.4). Marble bedrock is known to be particularly alkaline, and we measured pH values of up to 9 in the marble samples from Perlebandet. For bacteria, differences in soil pH may help explain the variation in their diversity and structure (Fierer and Jackson 2006). Hence, the difference at family level between granite and marble samples could already be explained by the different pH values encountered in these two bedrock types. Moreover, *Chroococcidiopsis*-like phylotypes form small coccoid cells which makes them well adapted to entering pore spaces within the rock matrix making them a dominant component of endolithic communities (Pointing et al. 2009). Because of its metamorphic origin, marble is a softer bedrock type compared to granite, leading to a more porous rock matrix. Liquid water could therefore be retained less on the surface of the substrate, which may lead to a drier habitat for the inhabiting microbial communities as reflected in the high dry weight values of these samples (up to 99.9 %). Again, Chlorophyta and Metazoa (Rotifera and Tardigrada) were the dominant eukaryotes of marble soils. However, in contrast to the granite samples, Cercozoa were more abundant than Ciliophora, which is likely related to the dry conditions encountered in the marble soils, consistent with findings in soils from the McMurdo Dry Valleys (Thomson 2021).

2.5.3 The Acidobacteriota phylum dominates the gneiss bedrock type

On gneiss, the Acidobacteriota were the dominant bacteria (Table S2.4), together with Cyanobacteriota, and, for the latter phylum, particularly members of the unicellular Chroococcidiopsaceae. ASV1328, here identified as closely related to the Nostoc_PCC-73102 strain, was identified as putative keystone taxon of gneiss module 10 (Table S2.15) although its abundance was generally low in gneiss samples (Nostocaceae family: 0.46 %; Table S2.5). Because of their ability to fix atmospheric N_2, this phylum might contribute significantly to the N cycle of gneiss food web despite its low abundance. The eukaryotic communities were again dominated by Chlorophyta and among the Metazoa, Rotifera and Tardigrada were dominant groups.

2.5.4 The Actinomycetota phylum dominates the moraine substrate type

Moraine soils, especially from Austkampane and the Dry Valley, were the most arid and oligotrophic among the investigated substrates. Moraines are characterized by a mixture of different bedrock types. Actinomycetota were found to be conspicuously more abundant than photoautotrophs in moraine substrates, with abundances up to 50 % of the bacterial reads, which is consistent with other studies from hyper-arid regions of Antarctica (Ortiz et al. 2020, Bay et al. 2021, Ray et al. 2022). Species of this phylum are known to be able to outcompete other dominant groups under the most arid conditions in low organic soils, likely due to their high resistance to desiccation and starvation conditions (Battistuzzi and Hedges 2009, Lennon and Jones 2011). They are furthermore metabolically active at subzero temperatures and form cyst-like resting structures or spores (Soina et al. 2004). Other highly abundant bacteria of moraine substrates belonged to the Chloroflexota phylum, which is also often encountered in extremely arid and ultra-oligotrophic Antarctic environments (Ji et al. 2016). The co-occurrence network analysis revealed three connected moraine modules, whose ASVs mainly belonged to the Pseudonocardiaceae, Solirubrobacteraceae, Frankiales, and Nocardioidaceae families (Actinomycetota, Fig. S2.8) and whose putative keystone taxa belonged to the Actinomycetota and the Chloroflexota phyla. In such cyanobacteria-poor soils, part of the bacterial primary production could also be attributed to atmospheric H_2, CO_2 and CO consumption by phylotypes

of the Actinomycetota (including the order Solirubrobacterales), Chloroflexota and other taxa (Greening et al. 2022, Ray et al. 2022, Ji et al. 2017, Ortiz et al. 2020). Even in these very dry conditions, Chlorophyta were the dominant eukaryotes, together with Cercozoa. Interestingly, also Metazoans attained a considerable relative abundance (9 %), with Rotifera and unclassified taxa being the most abundant groups. For Rotifera, this is probably because of their ability to produce a drought-resistant dormant stage (resting egg), which can remain viable for a long time, survive desiccation and frost, and is well adapted for passive dispersal (Artois et al. 2011). However, the presence of Metazoa implies that the primary production by these bacteria and the dry and cold adapted Chlorophyta is sufficiently high to support these relatively diverse communities.

2.6 CONCLUSION

Our analyses revealed that the composition of terrestrial bacterial and micro-eukaryote communities in the inland ice-free areas of the Sør Rondane Mountains (East Antarctica) largely co-vary with substrate type. Three disconnected ecological clusters (modules) could be discerned in our co-occurrence network analysis (i.e. granite-gneiss, marble and moraine) in which putative and well-known primary producers were designated as the main keystone taxa which co-occurred with different other bacterial and eukaryotic taxa. These ecological modules were correlated with important physical and chemical parameters characterizing the different substrate types. Our study provides new insights into the microbial ecology of terrestrial microbial communities in inland regions of the most extreme cold deserts on Earth.

2.7 ACKNOWLEDGMENTS

This work was funded by the Federal Belgian Science Policy Office (BELSPO) under the BRAIN-BE program MICROBIAN project (BR/165/A1/MICROBIAN). The authors would like to acknowledge Sofie D'Hondt for help with the library preparations. The authors also thank the crew of the Princess Elisabeth Antarctica (PEA) station for the operation of the base and providing the necessary support during the field activities, in particular Alain Hubert for leading the Belgian

Antarctic Research Expedition (BELARE) and our field guides for the 2018 campaign, Pierre-Yves Terrettaz, and the 2019–2020 campaigns, Raphaël Mayoraz. The STEREO team at BELSPO and AIRBUS are thanked for the acquisition of Pléiades imagery which was used to create digital elevation models for our study sites. ESA/Copernicus is thanked for the free and open access to Sentinel-2 imagery used in Fig. 2.1a. A. Wilmotte is Senior Research Associate of the FRS-FNRS. Josef Elster was funded by the Ministry of Education, Youth and Sport of the Czech Republic [projects LTAIN 19139]; by the Czech Science foundation [project 22-08680 l] and by the Czech Academy of Sciences [long-term research development project No. RVO 67985939].

2.8 AUTHOR CONTRIBUTION

Conceived and designed the study: EV, WV, BT. Performed the sampling: VS, EV, QV, SL. Performed the laboratory analysis: VS, SL, JE. Analyzed the data: VS. Contributed analysis tools: SL, BT. Supervision: EV, BT, AWillems, AWillmotte, WV. Secured the funding WV, AWillmotte, AWillems, QV and EV. Wrote the paper: VS, EV, BT. All authors reviewed and commented on previous versions of the manuscript and approved the final version.

2.9 REFERENCES

Alekseev, I., Zverev, A. and Abakumov, E., 2020. Microbial communities in permafrost soils of Larsemann Hills, eastern Antarctica: environmental controls and effect of human impact. Microorganisms, 8(8), p.1202.

Andrews, S. (2010). FastQC: A Quality Control Tool for High Throughput Sequence Data [Online]

Artois, T., Fontaneto, D., Hummon, W.D., McInnes, S.J., Todaro, M.A., Sørensen, M.V. and Zullini, A., 2011. Ubiquity of microscopic animals? Evidence from the morphological approach in species identification. Biogeography of microscopic organisms: Is everything small everywhere, pp.245-249.

Banerjee, S., Baah-Acheamfour, M., Carlyle, C. N., Bissett, A., Richardson, A. E., Siddique, T., et al. (2016). Determinants of bacterial communities in Canadian agroforestry systems. Environ. Microbiol. 18, 1805–1816. doi: 10.1111/1462-2920.12986

Bastian, M., Heymann, S. and Jacomy, M., 2009, March. Gephi: an open source software for exploring and manipulating networks. In *Proceedings of the international AAAI conference on web and social media* (Vol. 3, No. 1, pp. 361-362).

Battistuzzi, F.U. and Hedges, S.B., 2009. A major clade of prokaryotes with ancient adaptations to life on land. Molecular biology and evolution, 26(2), pp.335-343.

Bay, S.K., Dong, X., Bradley, J.A., Leung, P.M., Grinter, R., Jirapanjawat, T., Arndt, S.K., Cook, P.L., LaRowe, D.E., Nauer, P.A. and Chiri, E., 2021. Trace gas oxidizers are widespread and active members of soil microbial communities. *Nature microbiology*, *6*(2), pp.246-256.

Belnap, J., Büdel, B. and Lange, O.L., 2003. Biological soil crusts: characteristics and distribution. Biological soil crusts: structure, function, and management, pp.3-30.

Bindschadler, R., Vornberger, P., Fleming, A., Fox, A., Mullins, J., Binnie, D., Paulsen, S.J., Granneman, B. and Gorodetzky, D., 2008. The Landsat image mosaic of Antarctica. *Remote Sensing of Environment*, *112*(12), pp.4214-4226.

Bockheim, J.G. and Hall, K.J., 2002. Permafrost, active-layer dynamics and periglacial environments of continental Antarctica: periglacial and permafrost research in the Southern Hemisphere. South African Journal of Science, 98(1), pp.82-90.

Borcard, D., & Legendre, P. (2002). All-scale spatial analysis of ecological data by means of principal coordinates of neighbour matrices. Ecological modelling, 153(1-2), 51-68.

Brooks, S.T., Jabour, J., van den Hoff, J., Bergstrom, D.M., 2019. Our footprint on Antarctica competes with nature for rare ice-free land. Nat. Sustain. 2, 185–190.

Callahan, B. J., McMurdie, P. J., Rosen, M. J., Han, A. W., Johnson, A. J. A., & Holmes, S. P. (2016). DADA2: High-resolution sample inference from Illumina amplicon data. Nature methods, 13(7), 581-583.

Chan, Y., Lacap, D.C., Lau, M.C., Ha, K.Y., Warren-Rhodes, K.A., Cockell, C.S., Cowan, D.A., McKay, C.P. and Pointing, S.B., 2012. Hypolithic microbial communities: between a rock and a hard place. *Environmental microbiology*, *14*(9), pp.2272-2282.

Cleenwerck, I., Camu, N., Engelbeen, K., De Winter, T., Vandemeulebroecke, K., De Vos, P., & De Vuyst, L. (2007). Acetobacter ghanensis sp. nov., a novel acetic acid bacterium isolated from traditional heap fermentations of Ghanaian cocoa beans. International journal of systematic and evolutionary microbiology, 57(7), 1647-1652.

Coleine, C., Biagioli, F., de Vera, J.P., Onofri, S. and Selbmann, L., 2021. Endolithic microbial composition in Helliwell Hills, a newly investigated Mars-like area in Antarctica. Environmental Microbiology, 23(7), pp.4002-4016.

Colesie, C., Gommeaux, M., Green, T.A. and Büdel, B., 2014. Biological soil crusts in continental Antarctica: Garwood Valley, southern Victoria Land, and Diamond Hill, Darwin Mountains region. Antarctic Science, 26(2), pp.115-123.

Convey, P., Biersma, E.M., Casanova-Katny, A. and Maturana, C.S., 2020. Refuges of Antarctic diversity. In Past Antarctica (pp. 181-200). Academic Press.

Convey, P., Gibson, J.A., Hillenbrand, C.D., Hodgson, D.A., Pugh, P.J., Smellie, J.L. and Stevens, M.I., 2008. Antarctic terrestrial life–challenging the history of the frozen continent?. Biological Reviews, 83(2), pp.103-117.

Cowan, D.A. and Tow, L.A., 2004. Endangered antarctic environments. Annu. Rev. Microbiol., 58, pp.649-690.

Cowan, D.A., Makhalanyane, T.P., Dennis, P.G. and Hopkins, D.W., 2014. Microbial ecology and biogeochemistry of continental Antarctic soils. *Frontiers in microbiology*, *5*, p.154.

Coyne, K. J., Parker, A. E., Lee, C. K., Sohm, J. A., Kalmbach, A., Gunderson, T., León-Zayas, R., Capone, D. G., Carpenter, E. J., & Cary, S. C. (2020). The distribution and relative ecological roles of autotrophic and heterotrophic diazotrophs in the McMurdo Dry Valleys, Antarctica. FEMS Microbiology Ecology, 96(3). https://doi.org/10.1093/femsec/fiaa010

Csardi, G., and Nepusz, T. (2006). The igraph software package for complex network research. InterJ. Complex Syst. 1695, 1–9.

Cucini, C., Nardi, F., Magnoni, L., Rebecchi, L., Guidetti, R., Convey, P. and Carapelli, A., 2022. Microhabitats, macro-differences: a survey of temperature records in Victoria Land terrestrial and freshwater environments. Antarctic Science, pp.1-10.

Delgado-Baquerizo, M., Oliverio, A.M., Brewer, T.E., Benavent-González, A., Eldridge, D.J., Bardgett, R.D., Maestre, F.T., Singh, B.K. and Fierer, N., 2018a. A global atlas of the dominant bacteria found in soil. Science, 359(6373), pp.320-325.

Delgado-Baquerizo, M., Reith, F., Dennis, P.G., Hamonts, K., Powell, J.R., Young, A., Singh, B.K. and Bissett, A., 2018b. Ecological drivers of soil microbial diversity and soil biological networks in the Southern Hemisphere. Ecology, 99(3), pp.583-596.

Dragone, N.B., Henley, J.B., Holland-Moritz, H., Diaz, M., Hogg, I.D., Lyons, W.B., Wall, D.H., Adams, B.J. and Fierer, N., 2022. Elevational Constraints on the Composition and Genomic Attributes of Microbial Communities in Antarctic Soils. Msystems, 7(1), pp.e01330-21.

Fierer, N., Leff, J.W., Adams, B.J., Nielsen, U.N., Bates, S.T., Lauber, C.L., Owens, S., Gilbert, J.A., Wall, D.H. and Caporaso, J.G., 2012. Cross-biome metagenomic analyses of soil microbial communities and their functional attributes. Proceedings of the National Academy of Sciences, 109(52), pp.21390-21395.

Fierer, N. and Jackson, R.B., 2006. The diversity and biogeography of soil bacterial communities. *Proceedings of the National Academy of Sciences*, *103*(3), pp.626-631.

Franco, A.L., Adams, B.J., Diaz, M.A., Lemoine, N.P., Dragone, N.B., Fierer, N., Lyons, W.B., Hogg, I. and Wall, D.H., 2022. Response of Antarctic soil fauna to climate-driven changes since the Last Glacial Maximum. Global Change Biology, 28(2), pp.644-653.

Friedman, J. & Alm, E. J. Inferring correlation networks from genomic survey data. PLoS Comput. Biol. 8, e1002687 (2012).

Fullerton, K.M., Schrenk, M.O., Yücel, M., Manini, E., Basili, M., Rogers, T.J., Fattorini, D., Di Carlo, M., d'Errico, G., Regoli, F. and Nakagawa, M., 2021. Effect of tectonic processes on biosphere–geosphere feedbacks across a convergent margin. Nature Geoscience, 14(5), pp.301-306.

Genuer, R., Poggi, J.M. and Tuleau-Malot, C., 2015. VSURF: an R package for variable selection using random forests. *The R Journal*, *7*(2), pp.19-33.

Geyer, K.M., Altrichter, A.E., Takacs-Vesbach, C.D., Van Horn, D.J., Gooseff, M.N. and Barrett, J.E., 2014. Bacterial community composition of divergent soil habitats in a polar desert. FEMS microbiology ecology, 89(2), pp.490-494.

Goberna, M., Navarro-Cano, J.A., Valiente-Banuet, A., García, C. and Verdú, M., 2014. Abiotic stress tolerance and competition-related traits underlie phylogenetic clustering in soil bacterial communities. Ecology letters, 17(10), pp.1191-1201.

Goordial, J., Davila, A., Greer, C.W., Cannam, R., DiRuggiero, J., McKay, C.P. and Whyte, L.G., 2017. Comparative activity and functional ecology of permafrost soils and lithic niches in a hyper-arid polar desert. Environmental microbiology, 19(2), pp.443-458.

Gorodetskaya, I. V., Van Lipzig, N. P. M., Van den Broeke, M. R., Mangold, A., Boot, W., & Reijmer, C. H. (2013). Meteorological regimes and accumulation patterns at Utsteinen, Dronning Maud Land, East Antarctica: Analysis of two contrasting years. Journal of Geophysical Research: Atmospheres, 118(4), 1700-1715.

Greening, C., Islam, Z.F. and Bay, S.K., 2022. Hydrogen is a major lifeline for aerobic bacteria. Trends in Microbiology, 30(4), pp.330-337.

Guillou, L., Bachar, D., Audic, S., Bass, D., Berney, C., Bittner, L., ... & Christen, R. (2012). The Protist Ribosomal Reference database (PR2): a catalog of unicellular eukaryote small sub-unit rRNA sequences with curated taxonomy. Nucleic acids research, 41(D1), D597-D604.

Hijmans, R. J. (2021). Introduction to the" geosphere" package (Version 1.5-14).

Holm, S., 1979. A simple sequentially rejective multiple test procedure. Scandinavian journal of statistics, pp.65-70.

Jacobs, J. and Thomas, R.J., 2004. Himalayan-type indenter-escape tectonics model for the southern part of the late Neoproterozoic–early Paleozoic East African–Antarctic orogen. *Geology*, *32*(8), pp.721-724.

Ji, M., van Dorst, J., Bissett, A., Brown, M.V., Palmer, A.S., Snape, I., Siciliano, S.D. and Ferrari, B.C., 2016. Microbial diversity at Mitchell Peninsula, Eastern Antarctica: a potential biodiversity "hotspot". Polar Biology, 39(2), pp.237-249.

Ji, M., Greening, C., Vanwonterghem, I., Carere, C.R., Bay, S.K., Steen, J.A., Montgomery, K., Lines, T., Beardall, J., Van Dorst, J. and Snape, I., 2017. Atmospheric trace gases support primary production in Antarctic desert surface soil. *Nature*, *552*(7685), pp.400-403.

Komsta, L. and Novomestky, F., 2015. Moments, cumulants, skewness, kurtosis and related tests. *R package version*, *14*(1).

Kurtz, Z. D., Muller, C. L., Miraldi, E. R., Littman, D. R., Blaser, M. J., and Bonneau, R. A. (2015). Sparse and compositionally robust inference of microbial ecological networks. PLoS Comput. Biol. 11:e1004226. doi: 10.1371/journal.pcbi.1004226

Lauber, C.L., Hamady, M., Knight, R. and Fierer, N., 2009. Pyrosequencing-based assessment of soil pH as a predictor of soil bacterial community structure at the continental scale. *Applied and environmental microbiology*, *75*(15), pp.5111-5120.

Lee, C.K., Laughlin, D.C., Bottos, E.M., Caruso, T., Joy, K., Barrett, J.E., Brabyn, L., Nielsen, U.N., Adams, B.J., Wall, D.H. and Hopkins, D.W., 2019. Biotic interactions are an unexpected yet critical control on the complexity of an abiotically driven polar ecosystem. *Communications biology*, *2*(1), p.62.

Lee, S.H. and Cho, J.C., 2009. Distribution patterns of the members of phylum Acidobacteria in global soil samples. *Journal of microbiology and biotechnology*, *19*(11), pp.1281-1287.

Lukashanets, D.A., Convey, P., Borodin, O.I., Miamin, V.Y., Hihiniak, Y.H., Gaydashov, A.A., Yatsyna, A.P., Vezhnavets, V.V., Maysak, N.N. and Shendrik, T.V., 2021. Eukarya biodiversity in the Thala Hills, East Antarctica. *Antarctic Science*, *33*(6), pp.605-623.

Männistö, M.K., Rawat, S., Starovoytov, V. and Häggblom, M.M., 2011. Terriglobus saanensis sp. nov., an acidobacterium isolated from tundra soil. International Journal of Systematic and Evolutionary Microbiology, 61(8), pp.1823-1828.

González, A.M.M., Dalsgaard, B. and Olesen, J.M., 2010. Centrality measures and the importance of generalist species in pollination networks. *Ecological complexity*, *7*(1), pp.36-43.

McMurdie, P.J. and Holmes, S., 2013. phyloseq: an R package for reproducible interactive analysis and graphics of microbiome census data. *PloS one*, *8*(4), p.e61217.

Moniz, M.B., Rindi, F., Novis, P.M., Broady, P.A. and Guiry, M.D., 2012. Molecular phylogeny of Antarctic *Prasiola* (Prasiolales, Trebouxiophyceae) reveals extensive cryptic diversity. *Journal of phycology*, *48*(4), pp.940-955.

Niederberger, T.D., McDonald, I.R., Hacker, A.L., Soo, R.M., Barrett, J.E., Wall, D.H. and Cary, S.C., 2008. Microbial community composition in soils of Northern Victoria Land, Antarctica. Environmental microbiology, 10(7), pp.1713-1724.

Obbels, D., Verleyen, E., Mano, M.J., Namsaraev, Z., Sweetlove, M., Tytgat, B., Fernandez-Carazo, R., De Wever, A., D'hondt, S., Ertz, D. and Elster, J., 2016. Bacterial and eukaryotic biodiversity patterns in terrestrial and aquatic habitats in the Sør Rondane Mountains, Dronning Maud Land, East Antarctica. FEMS microbiology ecology, 92(6).

Ortiz, M., Leung, P.M., Shelley, G., Jirapanjawat, T., Nauer, P.A., Van Goethem, M.W., Bay, S.K., Islam, Z.F., Jordaan, K., Vikram, S. and Chown, S.L., 2021. Multiple energy sources and metabolic

strategies sustain microbial diversity in Antarctic desert soils. Proceedings of the National Academy of Sciences, 118(45), p.e2025322118.

Ortiz, M., Leung, P.M., Shelley, G., Van Goethem, M.W., Bay, S.K., Jordaan, K., Vikram, S., Hogg, I.D., Makhalanyane, T.P., Chown, S.L. and Grinter, R., 2020. A genome compendium reveals diverse metabolic adaptations of Antarctic soil microorganisms. bioRxiv.

Pattyn, F., Matsuoka, K., & Berte, J. (2010). Glacio-meteorological conditions in the vicinity of the Belgian Princess Elisabeth Station, Antarctica. Antarctic Science, 22(1), 79-85.

Paulson, J.N., Pop, M. and Bravo, H.C., 2013. metagenomeSeq: Statistical analysis for sparse high-throughput sequencing. *Bioconductor package*, *1*(0), p.191.

Peres-Neto, P. R., Legendre, P., Dray, S., & Borcard, D. (2006). Variation partitioning of species data matrices: estimation and comparison of fractions. Ecology, 87(10), 2614-2625.

Pinseel, E., Janssens, S.B., Verleyen, E., Vanormelingen, P., Kohler, T.J., Biersma, E.M., Sabbe, K., Van de Vijver, B. and Vyverman, W., 2020. Global radiation in a rare biosphere soil diatom. Nature communications, 11(1), p.2382.

Pinseel, E., Van de Vijver, B., Wolfe, A.P., Harper, M., Antoniades, D., Ashworth, A.C., Ector, L., Lewis, A.R., Perren, B., Hodgson, D.A. and Sabbe, K., 2021. Extinction of austral diatoms in response to large-scale climate dynamics in Antarctica. Science advances, 7(38), p.eabh3233.

Pointing, S.B., 2016. Hypolithic communities. In Biological soil crusts: An organizing principle in drylands (pp. 199-213). Springer, Cham.

Pointing, S.B., Chan, Y., Lacap, D.C., Lau, M.C., Jurgens, J.A. and Farrell, R.L., 2009. Highly specialized microbial diversity in hyper-arid polar desert. Proceedings of the National Academy of Sciences, 106(47), pp.19964-19969.

Pruesse, E., Quast, C., Knittel, K., Fuchs, B. M., Ludwig, W., Peplies, J., & Glöckner, F. O. (2007). SILVA: a comprehensive online resource for quality checked and aligned ribosomal RNA sequence data compatible with ARB. Nucleic acids research, 35(21), 7188-7196.

Pugh, P.J. and Convey, P., 2008. Surviving out in the cold: Antarctic endemic invertebrates and their refugia. Journal of Biogeography, 35(12), pp.2176-2186.

Pushkareva, E., Pessi, I.S., Namsaraev, Z., Mano, M.J., Elster, J. and Wilmotte, A., 2018. Cyanobacteria inhabiting biological soil crusts of a polar desert: Sør Rondane Mountains, Antarctica. Systematic and applied microbiology, 41(4), pp.363-373.

R Core Team (2021). R: A language and environment for statistical computing. R Foundation for Statistical Computing, Vienna, Austria. URL https://www.R-project.org/.

Ray, A.E., Zaugg, J., Benaud, N., Chelliah, D.S., Bay, S., Wong, H.L., Leung, P.M., Ji, M., Terauds, A., Montgomery, K. and Greening, C., 2022. Atmospheric chemosynthesis is phylogenetically and geographically widespread and contributes significantly to carbon fixation throughout cold deserts. The ISME Journal, pp.1-14.

Ruppel, A.S., Läufer, A., Jacobs, J., Elburg, M., Krohne, N., Damaske, D. and Lisker, F., 2015. The Main Shear Zone in Sør Rondane, East Antarctica: Implications for the late-Pan-African tectonic evolution of Dronning Maud Land. *Tectonics*, *34*(6), pp.1290-1305.

Sakaeva, A., Sokol, E. R., Kohler, T. J., Stanish, L. F., Spaulding, S. A., Howkins, A., ... & McKnight, D. M. (2016). Evidence for dispersal and habitat controls on pond diatom communities from the McMurdo Sound Region of Antarctica. Polar Biology, 39(12), 2441-2456.

Schloss, P.D., Westcott, S.L., Ryabin, T., Hall, J.R., Hartmann, M., Hollister, E.B., Lesniewski, R.A., Oakley, B.B., Parks, D.H., Robinson, C.J. and Sahl, J.W., 2009. Introducing mothur: open-source, platform-independent, community-supported software for describing and comparing microbial communities. Applied and environmental microbiology, 75(23), pp.7537-7541.

Schwager, E., Mallick, H., Ventz, S. and Huttenhower, C., 2017. A Bayesian method for detecting pairwise associations in compositional data. PLoS computational biology, 13(11), p.e1005852.

Severgnini, M., Canini, F., Consolandi, C., Camboni, T., Paolo D'Acqui, L., Mascalchi, C., Ventura, S. and Zucconi, L., 2021. Highly differentiated soil bacterial communities in Victoria Land macro-areas (Antarctica). FEMS Microbiology Ecology, 97(7), p.fiab087.

Shiraishi, K., Osanai, Y., Ishizuka, H. and Asami, M., 1997. Antarctic Geological Map Series (Sheet 35, Sør Rondane Mountains). *National Institute of Polar Research, Japan*.

Soina, V.S., Mulyukin, A.L., Demkina, E.V., Vorobyova, E.A. and El-Registan, G.I., 2004. The structure of resting bacterial populations in soil and subsoil permafrost. Astrobiology, 4(3), pp.345-358.

Sokol, E. R., Herbold, C. W., Lee, C. K., Cary, S. C., & Barrett, J. E. (2013). Local and regional influences over soil microbial metacommunities in the Transantarctic Mountains. Ecosphere, 4(11), 1-24.

Solon, A.J., Mastrangelo, C., Vimercati, L., Sommers, P., Darcy, J.L., Gendron, E.M., Porazinska, D.L. and Schmidt, S.K., 2021. Gullies and moraines are islands of biodiversity in an arid, mountain landscape, Asgard Range, Antarctica. Frontiers in microbiology, 12, p.654135.

Stevens, M.I. and D'Haese, C.A., 2014. Islands in ice: isolated populations of Cryptopygus sverdrupi (Collembola) among nunataks in the Sør Rondane Mountains, Dronning Maud Land, Antarctica. Biodiversity, 15(2-3), pp.169-177.

Stoeck, T., Bass, D., Nebel, M., Christen, R., Jones, M. D., BREINER, H. W., & Richards, T. A. (2010). Multiple marker parallel tag environmental DNA sequencing reveals a highly complex eukaryotic community in marine anoxic water. Molecular ecology, 19, 21-31.

Suganuma, Y., Miura, H., Zondervan, A. and Okuno, J.I., 2014. East Antarctic deglaciation and the link to global cooling during the Quaternary: Evidence from glacial geomorphology and 10Be surface exposure dating of the Sør Rondane Mountains, Dronning Maud Land. *Quaternary Science Reviews*, *97*, pp.102-120.

Thompson, A.R., Geisen, S. and Adams, B.J., 2020. Shotgun metagenomics reveal a diverse assemblage of protists in a model Antarctic soil ecosystem. *Environmental Microbiology*, *22*(11), pp.4620-4632.

Thompson, A.R., 2021. Phagotrophic protists (protozoa) in Antarctic terrestrial ecosystems: diversity, distribution, ecology, and best research practices. Polar Biology, 44(8), pp.1467-1484.

Tytgat, B., Verleyen, E., Sweetlove, M., D'hondt, S., Clercx, P., Van Ranst, E., Peeters, K., Roberts, S., Namsaraev, Z., Wilmotte, A. and Vyverman, W., 2016. Bacterial community composition in relation to bedrock type and macrobiota in soils from the Sør Rondane Mountains, East Antarctica. FEMS Microbiology Ecology, 92(9).

Vanhellemont, Q., Lambrechts, S., Savaglia, V., Tytgat, B., Verleyen, E. and Vyverman, W., 2021. Towards physical habitat characterisation in the Antarctic Sør Rondane Mountains using satellite remote sensing. *Remote Sensing Applications: Society and Environment*, *23*, p.100529.

Venables, W.R. and Ripley, B., 2002. BD (2002). Modern Applied Statistics with S. *New York: Springer Science & Business Media*, *200*, pp.183-206.

Vick-Majors, T.J., Priscu, J.C. and A Amaral-Zettler, L., 2014. Modular community structure suggests metabolic plasticity during the transition to polar night in ice-covered Antarctic lakes. *The ISME journal*, *8*(4), pp.778-789.Wei, T., Simko, V., Levy, M., Xie, Y., Jin, Y. and Zemla, J., 2017. Package 'corrplot'. *Statistician*, *56*(316), p.e24.

Wynn-Williams, D.D., 1996. Response of pioneer soil microalgal colonists to environmental change in Antarctica. Microbial Ecology, 31, pp.177-188.

Zar, J.H., 1972. Significance testing of the Spearman rank correlation coefficient. Journal of the American Statistical Association, 67(339), pp.578-580.

CHAPTER 3

SOIL SUBSTRATE DRIVES CYANOBACTERIAL DIVERSITY OF CYANOBACTERIA IN THE SØR RONDANE MOUNTAINS, EAST ANTARCTICA

VALENTINA SAVAGLIA[1,2], BENOIT DURIEU[1], BJORN TYTGAT[2], JOSEF ELSTER[3], WIM VYVERMAN[2], ELIE VERLEYEN[2], ANNICK WILMOTTE[1]

[1]InBioS, University of Liège, 4000 Liège, Belgium

[2]Laboratory of Protistology & Aquatic Ecology, Ghent University, 9000 Ghent, Belgium

[3]Centre for Polar Ecology, Faculty of Science, University of South Bohemia, České Budějovice and Institute of Botany, AS CR, Třeboň, Czechia

Author contribution of VS: sampling, multivariate analysis, writing

Manuscript in preparation

3.1 ABSTRACT

Cyanobacteria are important primary producers in Antarctic terrestrial ecosystems, yet little is known about their diversity and distribution in these environments. Here, we studied the cyanobacterial community composition in a range of soil substrates in the western Sør Rondane Mountains, East Antarctica. We used cyanobacterial-specific primers targeting the V3-V4 region of the 16S rRNA gene in a high-throughput sequencing approach, and applied the latest cyanobacterial taxonomic insights used in the recently released CyanoSeq database. A total of 100 samples were collected from a variety of soil habitats encompassing bare soils, biofilms and biological soil crusts situated on four different substrates, namely marble, granite, gneiss and moraine which differed in environmental properties. Ordination analyses revealed that these different substrates harbour distinct cyanobacterial communities. Differences in community structure were significantly related to differences in pH, concentration of TN and N-NO_3^-, and electrical conductivity. The granitic soils of the Pingvinane nunataks hosted the highest richness followed by those from the granitic Utsteinen ridge. Granitic substrates were characterized by high TN concentrations and a neutral pH and hosted a variety of filamentous cyanobacteria, such as Leptolyngbyaceae, Gomontiellaceae, Microcoleaceae, Oculatellaceae, Nostocaceae, but also unicellular taxa (Cyanothecaceae). The moraine samples from Austkampane and Widerøefjellet were dominated by Microcoleaceae and Gomontiellaceae, respectively. They were characterized by a high dry weight and low TN, and the diversity and abundance of cyanobacteria was low. The taxonomic richness was also low in soils from the alkaline marble bedrock and the gneiss bedrock from the Perlebandet nunatak, which were both characterized by high TN. Marble bedrock was dominated by *Alitarella* sp. (Chroococcidiopsaceae), whereas gneiss by *Cyanothece* sp. (Cyanothecaceae). Overall, our data show that different substrate types host distinct cyanobacterial communities.

KEYWORDS

Cyanobacteria community composition, Antarctica, marble, granite, gneiss, moraines

3.2 INTRODUCTION

Cyanobacteria occur worldwide in a variety of terrestrial and aquatic ecosystems (Vincent 2009), including extreme environments, such as hot springs, barren rocks and desert soils (Whitton and Potts, 2000). The cold deserts in the Antarctic are among the most extreme biotopes on Earth (Brooks et al. 2019) and are characterized by low temperatures, frequent freeze-thaw cycles, high photosynthetically active radiation (PAR) and ultra-violet radiation (UVR) during half of the year, and general low nutrient concentrations (Vincent 2000). These terrestrial biotopes include exposed rocks and oligotrophic mineral soils (Ugolini and Bockheim 2008, Lee et al. 2017), which are derived from the weathering of the underlying bedrock. In these habitats, cyanobacteria are often the dominant photoautotrophs and some groups are also capable of nitrogen fixation (Broady 2005, Pointing et al. 2015, Chapter 2). Antarctic cyanobacteria are therefore regarded as true ecosystem engineers in these terrestrial habitats. Despite this, the diversity and factors shaping the community structure of terrestrial cyanobacteria in the Antarctic are far less studied compared with those in lacustrine habitats (e.g. Vincent et al. 1993; Taton et al. 2003, 2006a, 2006b, de los Ríos et al. 2004, Jungblut et al. 2005, Wood et al. 2008, Zhang et al. 2015, Pessi et al. 2018). In sheltered and more humid edaphic habitats, they are known to live as free organisms or in lichen symbioses thereby forming more or less developed communities where they facilitate the formation of biological soil crusts (BSCs; Weber et al. 2022). Instead, under the most extreme terrestrial conditions, such as the moraine soils of the McMurdo Dry Valleys, cyanobacteria may be absent or restricted to few, often unicellular taxa (Pointing et al. 2015). Here, they protect themselves by hiding from the extreme abiotic conditions within or below the lithic matrix of rocks, thereby forming endolithes, chasmoendolithes or hypolithes (Chan et al. 2012). In these cases, cyanobacteria appear to be genetically and therefore physiologically adapted to thrive under the extreme conditions in the Antarctic by producing i.a. exopolysaccharides (EPS), mycosporine-like amino acids (MAAs) and pigments such as carotenoids and scytonemin (Tamaru et al. 2005, Effendi et al. 2023, Chapter 4). In addition, some filamentous species living within BSCs are also able to migrate vertically

downwards to avoid high irradiances, or move upwards when the irradiance is too weak (Bebout and Garcia-Pichel 1995).

Most of our knowledge on the diversity and structure of Antarctic cyanobacterial communities is based on molecular surveys using general 16S rRNA primers to target bacteria (but see Taton et al. 2003, 2006a, 2006b, de los Ríos et al. 2004, Jungblut et al. 2005, Wood et al. 2008, Zhang et al. 2015, Pessi et al. 2018). In fact, this also holds true for cyanobacteria studies worldwide. While this gives a broad overview of the Bacteria present in some environments, most sequences obtained through high-throughput sequencing (HTS) belong to heterotrophic groups, which prevents to obtain detailed information on the cyanobacterial diversity. This can be circumvented by using cyanobacterial-specific primers, as shown by Taton et al. (2003). In addition to the use of general 16S rRNA primers, most studies also suffer from the lack of a detailed and up-to-date taxonomic identification, because the databases used are based on outdated taxonomic insights. Recently, Lefler et al. (2022) have constructed the CyanoSeq database that is continuously updated (Lefler et al. 2023) in order to apply the most up-to-date taxonomic identifications.

The studies in Antarctic terrestrial ecosystems based on general bacterial primers revealed that cyanobacteria constitute one of the most diverse bacterial groups, and this is particularly the case in more humid conditions. By contrast, in hyper arid edaphic habitats, they attain a lower abundance (e.g. Pointing et al. 2009). In these dry habitats, Actinomycetota are the most abundant bacterial phylum (Rego et al. 2019, Chapter 2) and cyanobacteria are almost exclusively confined to lithic habitats (Cockell and Stokes 2004, Pointing et al. 2009). These findings were recently confirmed in the western Sør Rondane Mountains, located in Dronning Maud Land (East Antarctica). This mountain chain consists of inland ice-free nunataks with different geological histories and bedrock types, and valleys occupied by moraines. Despite the very harsh climatic conditions, diverse bacterial and micro-eukaryotic communities occur in particular sites (e.g. those sheltered from katabatic winds, where liquid water is present during summer, or exposed to the North) (Chapter 2, Tytgat et al. 2016). Actinomycetota and Cercozoa dominate the moraine soils, whilst Cyanobacteriota and Metazoa dominate the granitic and marble bedrock types.

Distinct cyanobacterial genotypes were present on the different substrate types, with keystone phylotypes belonging to unicellular *Aliterella* sp. in marble soils and filamentous *Nostoc* sp. in granitic and gneiss soils (Chapter 2).

Here, we performed an in-depth study of the cyanobacterial communities from 100 soil samples from the western Sør Rondane Mountains (East Antarctica) in order to better understand what are the cyanobacterial communities structures and their main abiotic drivers of one the most understudied Antarctic ice-free areas. In order to investigate such research questions, our study is based on HTS of amplicons of the 16S rRNA gene generated using cyanobacteria specific primers (Nübel et al. 1997) and by employing the most up-to-date taxonomy used in the recently developed CyanoSeq database. Because of the variety of substrate types, we expected to have different cyanobacterial communities following the results of Chapter 2 where only general 16S primers and Silva database for the taxonomy assignment were used. In order to validate Chapter 2 results on keystone taxa, an indicator taxa analysis per substrate type was perfomed. We therefore expected (1) more diverse communities and filamentous taxa such Nostocaceae in wetter granitic soils and (2) less diverse communities and the presence of unicellular taxa such as Chroococcidiopsaceae in xeric marble and moraine soils.

3.3 MATERIALS & METHODS

3.3.1 Sampling and site descriptions

The Sør Rondane Mountains (SRM; 22 - 28° E, 71°30′ - 72°40′ S) encompass a large number of nunataks and valleys covering an area of ca. 2000 km^2 (Suganuma et al. 2014) within Dronning Maud Land, East Antarctica. The Belgian station Princess Elisabeth Antarctica ("PEA") is located in the western part of the Sør Rondane Mountains, on the granitic Utsteinen ridge (71°57′ S, 23°21′ E; 1372 m a.s.l.). For the present study, cyanobacterial communities inhabiting the most diverse geological types that could be encountered within a 70 km radius around PES were sampled (Fig. 3.1) in 5 nunataks, 1 ridge and 3 valleys. The Utsteinen ridge ("UT") is characterized by intermittent east-western katabatic winds and it was sampled on an altitudinal gradient from

north (1359 m a.s.l.) to south (1370 m a.s.l.). A total of 10 samples encompassing a variety of community development stages were collected. They ranged from north or sky facing bare soil consisting of small gravel without any visible communities, to well-developed BSCs with visible mosses and/or lichens located in wind protected areas, especially frequent on the northern part of the ridge. *Circa* 20 km to the southwest from PES and close to the main mountain range, Petrellnuten ("PT"), a single granitic nunatak (72°00′ S, 22°50′ E) was sampled on the top (472 m a.s.l.) with a northern exposure and inside its windscoop (1460 m a.s.l.) facing north-east, ranging from sites overgrown with black lichens to mineral soil without visible biomass. The bedrock was characterized by relatively small gravel (a few mm diameter). The Pingvinane range is located a few kms to the east of Petrellnuten nunatak. It consists of seven granitic nunataks, two of which were sampled for the present study. A total of 7 samples were collected from the west-southwest slope of the fourth nunatak counted from the northern top (named "PA4"; 72°00′ S, 23°00′ E; 1410 m a.s.l.), within an altitude gradient of a few meters starting from the relatively flat south-facing windscoop, mostly composed of granite gravel with no big granitic boulders and characterized by relatively small but visible communities developed below and in between the first gravel layer where black lichens could be occasionally encountered, to a steeper slope characterized by massive rocks and less developed communities. Here the sampled bedrock consisted predominantly of small-medium size granite gravel (mm-cm range). On the sixth nunatak of the Pingvinane range (named "PA6"; 72°01′ S, 22°59′ E; 1416 m a.s.l.), a total of 5 samples were collected along an altitude gradient with different exposures (north, south and east), ranging from sites overgrown with black mosses and lichens especially encountered in the lower part of the nunatak to mineral soils without visible communities at the top. The bedrock consisted mostly of small granite gravel (few mm). The Perlebandet range is located *ca*. 40 km to the northwest of PES, and it is characterized by three nunataks of gneiss rocks interlayered with marble veins in the two northernmost nunataks (designated here as "Perlebandet N'' or "PB_N" and "Perlebandet S" or "PB_S", respectively). Twenty-three samples were taken from Perlebandet N (71°50′ S, 22°50′ E) along an altitude gradient (1256 to 1310 m a.s.l.). Five samples of the gneiss bedrock include a granulometry ranging from small gravel (few mm) to big pebbles

(cm order) and encompass different degrees of community development, from mineral soils to very well-developed moss and lichen forming communities. Nine samples were characterized by 'pure' marble bedrock ranging from small gravel (few mm) where no visible biomass occurred to small communities living underneath the first layer of gravel and where black lichen could occur on the gravel surface. Nine other samples were characterized by marble gravel (few mm) mixed with gneiss pebbles (cm order) in which no communities were visible from the gravel surface. Perlebandet S nunatak (71°53' S, 22°45' E, 1354 m a.s.l.) consisted of two additional samples of marble bedrock characterized by gravel (few mm) with occasional gneiss pebbles (cm order) in which communities were not particularly prominent and only occurred under a first layer of gravel, and one gneiss sample in which black lichen communities were visible on the gravel surface. Furthermore, three moraine sites were sampled, namely one in the Northeastern part of Widerøefjellet (here referred to as "Dry Valley'' or "DV"), in Yûboku Valley ("YO") and in Tvetaggen (here referred to as "Austkampane'' or "AU"). Dry Valley is located around 30 km south from PEA (72°60' S, 23°11' E; 1666 m a.s.l.) and is characterized by very strong katabatic winds which scrub the surfaces and inhibit the development of visible microbial communities. A total of forty samples were collected from this area characterized by little to no visible biomass under the first layer of gravel. Yûboku Valley (72°41' S, 23°48' E; 1357 m a.s.l.) is located to the south-east of Dry Valley, and is also characterized by greenschist, gneiss and quartz mineral moraines. Five soil samples were analysed from this area which is up to now the only investigated site where lakes were discovered. They are generally year-round frozen and contain conspicuous benthic cyanobacterial mats. Dried mats are also present on the shores. For this study, only mineral soil samples from the shore and from sites situated deeper inside the valley were collected. Last, Austkampane (71°40' S, 25°90' E; 930 m a.s.l.) is an extremely windy site located 70 km east from PES, characterized by amphibolite on which almost no life was visible. Three collected samples were characterized by small gravel (few mm). Sample collection and the resulting unbalanced design was already described in Chapter 2. Pictures of the studied localities are shown in Fig. 3.1 and details of the collected samples are given in Table S3.1.

Because of its east-west orientation, the SRM act as a barrier against the strong northern-facing katabatic winds. As a consequence, the northern escarpment zone is rather sheltered. Mean winter air temperatures at PES are between -25 and -20 °C, while mean summer air temperatures fluctuate between -15 and +5 °C (Pattyn, Matsuoka and Berte 2010, Gorodetskaya et al. 2013). Conditions near the main mountain range are more extreme, with Austkampane to the east being the windiest and harshest site of all sampled locations.

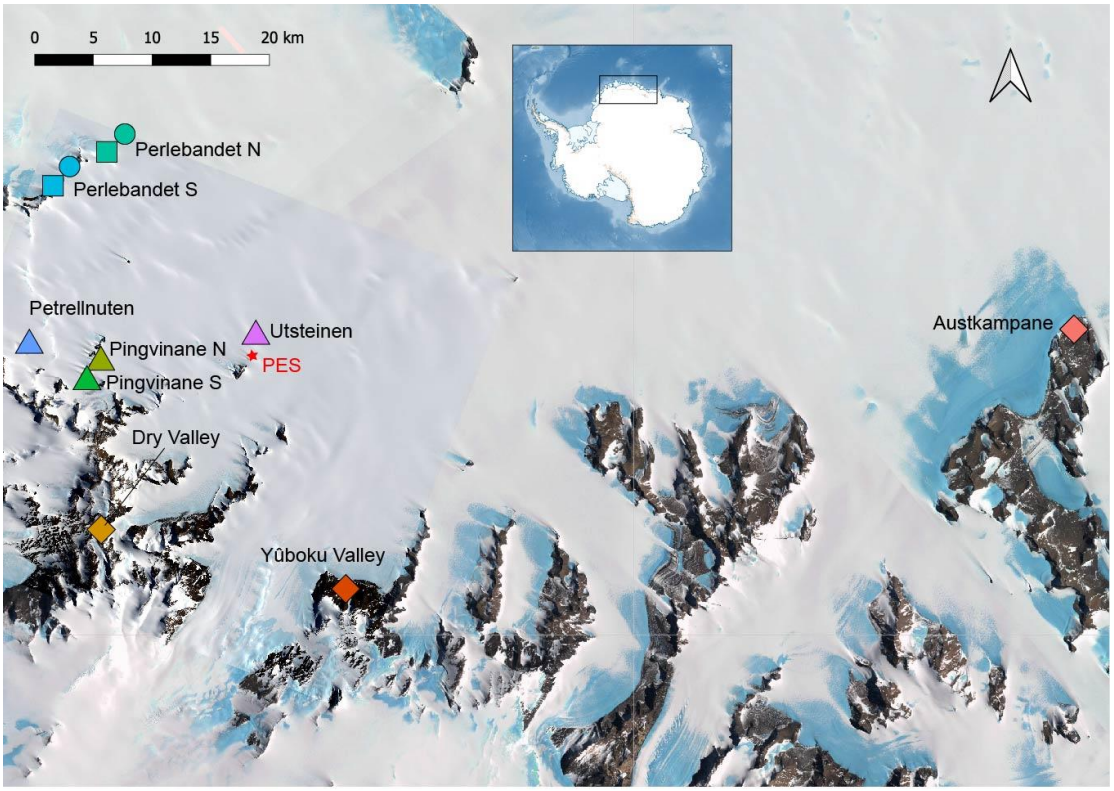
0 5 10 15 20 km
Perlebandet N
Perlebandet S
Petrellnuten
Pingvinane N
Pingvinane S
Utsteinen
PES
Dry Valley
Yûboku Valley
Austkampane

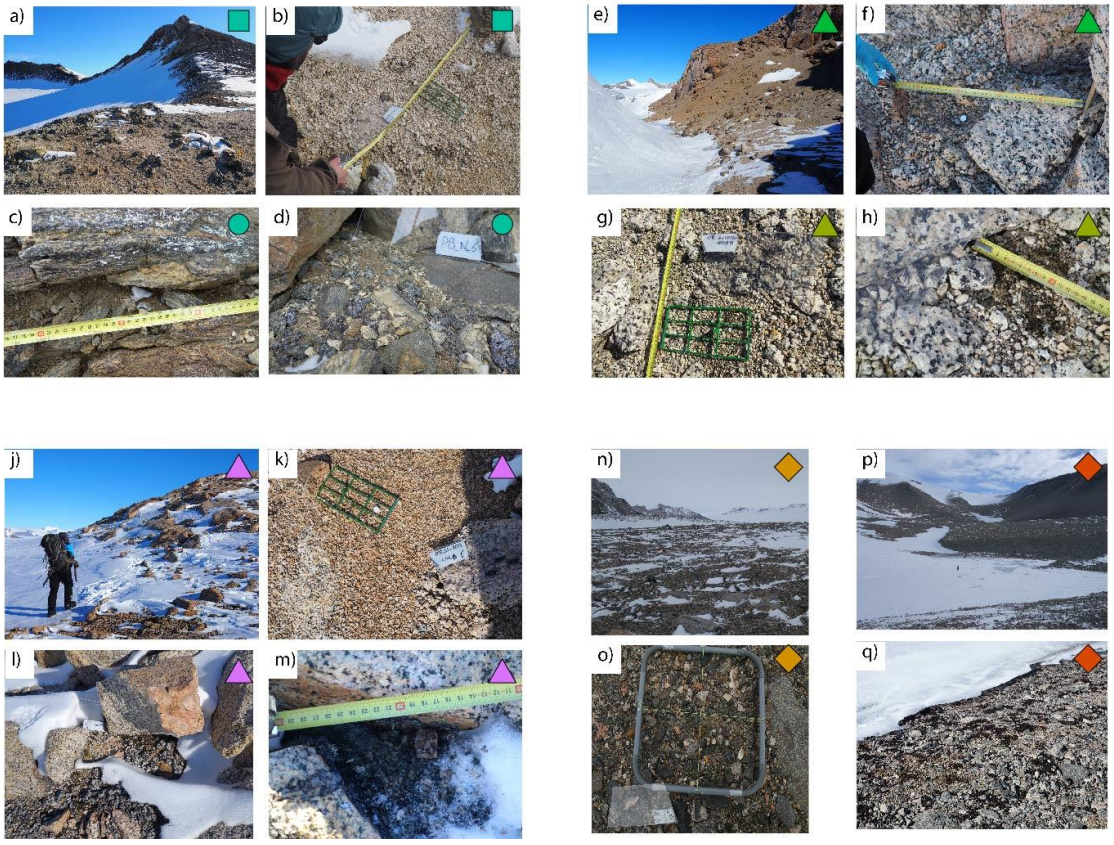
a)
b)
c)
d)
e)
f)
g)
h)
j)
k)
l)
m)
n)
o)
p)
q)

Fig. 3.1 Satellite image of Sør Rondane Mountains (up) and detail of the sampled sites (below)*: Perlebandet N nunatak overview (a) and zoom on marble (b) and gneiss (c-d) bedrock types. Pingvinane 6 nunatak overview (e) and zoom on its communities (f) and Pingvinane 4 nunatak (g-h) communities on granitic gravel. Utsteinen ridge overview (j) and zoom on bare granitic gravel (k) and developed BSCs (l-m). 'Dry Valley' overview (n) and zoom on its moraines (o). Yûboku-dani Valley overview (p) and zoom on biofilms (q) and moraines close to a frozen lake. More information about the samples can be found in Table S3.1. Contains modified Copernicus Sentinel-2 data [2020] and Landsat Image Mosaic of Antarctica (LIMA). Colors differ by sampled site; symbol by bedrock type: circles represent gneiss, triangles granite, squares marble and and diamonds moraine samples.*

3.3.2 DNA extraction and sequencing

High-quality cyanobacterial 16S rRNA gene libraries were successfully constructed for 100 soil samples. Each sample was first thoroughly homogenized and between 0.2 to 1 g was used for DNA extraction based on the amount of biomass or mineral sample with the Qiagen DNeasy Powersoil kit (Valencia, CA). Only a small amount of biomass is needed for DNA extraction when the sample was taken from, e.g. a BSC. For cyanobacteria, PCRs targeting the V3-V4 hypervariable region of the 16S rRNA gene were performed using the cyanobacteria-specific primers CYA359F and CYA781Rb (Nübel et al. 1997) following the protocol described by Pessi et al. (2016). The PCR mixture consisted of 2.5 µl buffer with 2.5 µl BSA (1 mg mL^{-1}) , 0.5 µl dNTP (200 µM), 1.25 µl of each primer (0.2 µM), 0.2 µl of 1 U $µl^{-1}$ SUPER TAQ plus DNA polymerase (HT Biotechnology, Cambridge, UK), 2 µl template DNA and completed with 0,1 µl filtered water (Sigma-Aldrich) to reach a final volume of 25 µl. PCR amplification was carried out with an initial denaturation step at 94 °C for 5 min, followed by 37 cycles of 94 °C for 1 min, 1 min annealing at 57 °C and 1 min at 72 °C and an elongation step at 72 °C for 5 min. After a final elongation of 20 min at 72 °C, PCR products were visualized on TBE 0.8 % agarose gel. If amplification was successful, PCR duplicates for each sample were pooled to minimize potential biases. The pooled PCR products were subsequently purified (NucleoSpin® Gel and PCR Clean-up, Macherey-Nagel GmbH & Co, Düren, Germany) according to the manufacturer's instructions. The DNA concentration of the cleaned PCR products was measured using Quant-iT PicoGreen dsDNA Assay Kit, Life Technologies, Carlsbad, CA, USA), and the samples were equimolarly pooled based on their molecular weight

and DNA concentrations of at least 6 ng μl^{-1} for a total quantity of 200 ng for each sample. Amplicon libraries were sequenced on an Illumina Miseq platform (2 × 300 bp paired-end, v3 chemistry) at Genewiz (Azenta Life Sciences, Leipzig, Germany) where ligation of sequencing adapters to the amplicons and sequencing were performed. Each run contained 2 replicates of a mock community containing 6 cyanobacterial species (Table S3.3), each of the latter strains separately in the same concentration used for the mock community, in order to check the effective quantity of each strain of the mock community), 2 negative controls (each composed by a mixture of PCR blanks) to check the overall run quality and benchmark processing variables, as well as 24 randomly chosen PCR replicate samples.

3.3.3 Data processing

Read quality control and chimeric sequences filtering protocol based on UPARSE (Edgar 2013) were adapted from Pessi et al. (2016). Briefly, reads that were not matching primer and barcode at the 3' and 5' ends were removed after merging and filtering the paired-end reads. Two and zero mismatches were allowed for primer and barcode sequences, respectively. Reads with a maximum expected error of more than 0.5 and a length of less than 370 bp were removed. After singletons removal, the remaining sequences were clustered into OTUs using a 99 % similarity threshold (Edgar 2013). The most abundant sequence in each OTU cluster was selected as the representative. Taxonomic classification of the resulting sets of OTUs was performed using *assignTaxonomy* in the DADA2 package version 3.10 (Callahan et al. 2016) within the R version 4.0 (R Core Team 2021) using the CyanoSeq v1.2 database (Lefler et al. 2023) with minBoot=80 parameter.

3.3.4 Environmental data collection

Environmental factors including elevation, pH (H_2O), soil total organic carbon (TOC, %), soil dry weight (%), total phosphorus (TP, %) total nitrogen (TN, %), electric conductivity (EC, µS cm^{-1}), and concentrations of N-NO_3^- (mg kg^{-1}), N-NH_4^+ (mg kg^{-1}), and P-PO_4^{3-}(mg kg^{-1}), were conducted following established methods at the Institute of Botany, AS CR in Třeboň (Czech

Republic) as described and summarized in Chapter 2 (raw data shown in Table S3.1 and summarized in Table S3.2).

3.3.5 Statistical analysis

All statistical calculations were conducted in R 4.0 (R Core Team 2021).

OTUs represented by only one sequence per sample, mitochondrial, chloroplast-related sequences and non-Cyanobacteriota OTUs were removed. After inspection of the mock community (see Table S2 for more details), blanks and replicate samples were removed from the OTU table and only one sample with the highest read number was kept among the replicates of the same sample (Fig. S3.1). To assess the differences in mean local alpha-diversity (i.e. OTU richness) between sites (Fig. S3.2) and bedrock types (Fig. S3.3), a negative binomial generalized linear model was applied cf. Tytgat et al. (submitted), thereby accounting for differences in the (log) number of sequences and evenness (defined as the Shannon index divided by the natural logarithm of the richness) between samples. Phylotypes (OTUs) significantly associated with a substrate type were determined through the indicator value index (IndVal; Table S3.7) using the *multipatt* function implemented in the indicspecies package (version 1.7.12; De Cáceres et al. 2010). The computed indicator Value (IndVal) measures the strength of the association between an OTU and a sample. For example, a value equal to 1 ("stat." column in Table S3.7) means that the OTU is found uniquely on a type of substrate. For beta-diversity, cumulative-sum scaling (CSS) was performed using the cumNorm function in the metagenomeSeq package (v1.32; Paulson et al. 2013). For $P\text{-}PO_4^{3-}$, normal distribution and homoscedasticity were investigated using the Shapiro-Wilks test and the Bartlett's test using the package *stats* in R (v4.0.5; R Core Team 2021), and skewness and kurtosis with package *moments* in R (v.0.14; Komsta and Novomestky 2015). For TOC, $N\text{-}NO_3^-$, $N\text{-}NH_4^+$, TN, TP, dry weight, conductivity, the dataset was log(x+1) transformed in order to attenuate skewness. Pearson's coefficients with 999 permutations and the variance inflation factor (VIF) with a stepwise calculation were used to check for collinearity among the transformed environmental parameters. Pearson's coefficients were calculated using the *cor* function in the 0.92 version of the corrplot package (Wei and Simko 2021; Fig. S3.4). VIF factors

were calculated using the *vistep* function of the 1.1.18 version of the usdm package (R Core Team 2021). No strong correlations between any of the environmental variables were observed with both methods (Pearson's $|r| < 0.6$ and VIF < 5), hence all were kept during further analysis. Kruskal-Wallis rank sum tests were performed with the *kruskal.test* function of the 4.0.5 version of the stats package to detect significant differences in the values of geochemical variables in relation to the substrate type (Table S3.4) as well as in the values of richness in relation to the sampled site (Table S3.5). Multiple pairwise-comparisons between groups were performed with the *pairwise.wilcox.test* function of the stats package to calculate pairwise comparisons between the substrate types with Bonferroni corrections for multiple testing.

The OTU table was converted into a dissimilarity matrix using Bray-Curtis similarity coefficient between pairs of samples after CSS-scaling in order to perform nonmetric multidimensional scaling (nMDS) ordinations using the *ordinate* function in phyloseq (version 1.34; McMurdie and Holmes 2013). Ordination plots were used to assess differences in community structure between the samples as well as to identify the potential explanatory environmental variables for the observed community patterns between the samples. A Kruskal-Wallis rank sum test was also applied to detect significant differences in the abundance of the main families of cyanobacteria in relation to substrate type and multiple pairwise-comparisons between groups were calculated as described previously (Fig S3.6).

Sampling plot coordinates were recorded as latitude and longitude. To test the influence of geographic distance at different spatial scales on the bacterial and eukaryotic community structure, we used the spatial variables created by principal coordinates of neighbourhood matrix (PCNMs) of the geographic coordinates of the samples (Borcard and Legendre 2002), following Sakaeva et al. (2016). Briefly, with PCNMs we analyse the impact of spatial parameters on the communities at different spatial scales, ranging from large (PCNM1) to fine spatial scale (in our case, PCNM5). Therefore, geospatial coordinates of the samples were first used to calculate a geographic distance matrix using the 1.5.14 version of the package geosphere (Hijmans 2021). Then, PCNM eigenvectors were calculated from the geographic distance matrix using the *pcnm*

function implemented in the version 2.5.7 of the vegan package in R. We determined which PCNM were significantly correlated with the environmental variables using a cutoff of $p < 0.05$. Then, from the pool of significantly correlated PCNMs, we used a stepwise model selection to select the most parsimonious linear model (Venables and Ripley 2002) linking the environmental and substrate type variables to PCNM eigenvectors, as shown in Sokol et al. (2013).

To explain variation in community structure associated with explanatory variables, a distance-based redundancy analysis (db-RDA; McArdle and Anderson 2001) was used to model variation in community structures as a function of either environmental (pH, $N\text{-}NO_3^-$, $N\text{-}NH_4^+$, TN, TP, dry weight, conductivity), spatial (PCNM) or substrate type (marble, granite, gneiss, moraine) variables after Euclidean transformation. Forward stepwise model selection (Blanchet et al. 2008) based on adjusted R^2 values (Peres-Neto et al. 2006) was used to select the variables that best explained the variation in community structures.

3.4 RESULTS

3.4.1 Community structure and diversity in relation to substrate type

The Illumina sequencing resulted in 2,697,299 reads which, after filtering and removing the duplicate samples, resulted in 1,168,743 reads. After bioinformatic data processing, the removal of sample replicates and of OTUs that did not belong to the Cyanobacteriota phylum, the remaining OTUs represented 43 % of the original reads in 60 samples containing more than 1000 reads (normalization step), which were selected for the downstream analyses. A total of 1551 Cyanobacteriota OTUs were found in these 60 investigated samples and they were mainly classified as Chroococcidiopsidaceae (21 %), Gomontiellaceae (19 %), Cyanothecaceae (18 %), Leptolyngbyaceae (12 %), and Oculatellaceae (10 %). Unknown families, Microcoleaceae, Nostocaceae, Tolypothrichaceae and Chamaesiphonaceae accounted for 8, 5, 3, 2 and 1 % of the total reads, respectively. The remaining families represented less than 1 % of the total selected reads and consisted of Cymatolegaceae, Stigonemataceae, Pseudanabaenaceae,

Prochlorococcaceae, Rivulariaceae, Pleurocapsaceae, Aphanizomenonaceae, Microcystaceae, Wilmottiaceae, Chroococcaceae and Oscillatoriaceae (Table S3.4).

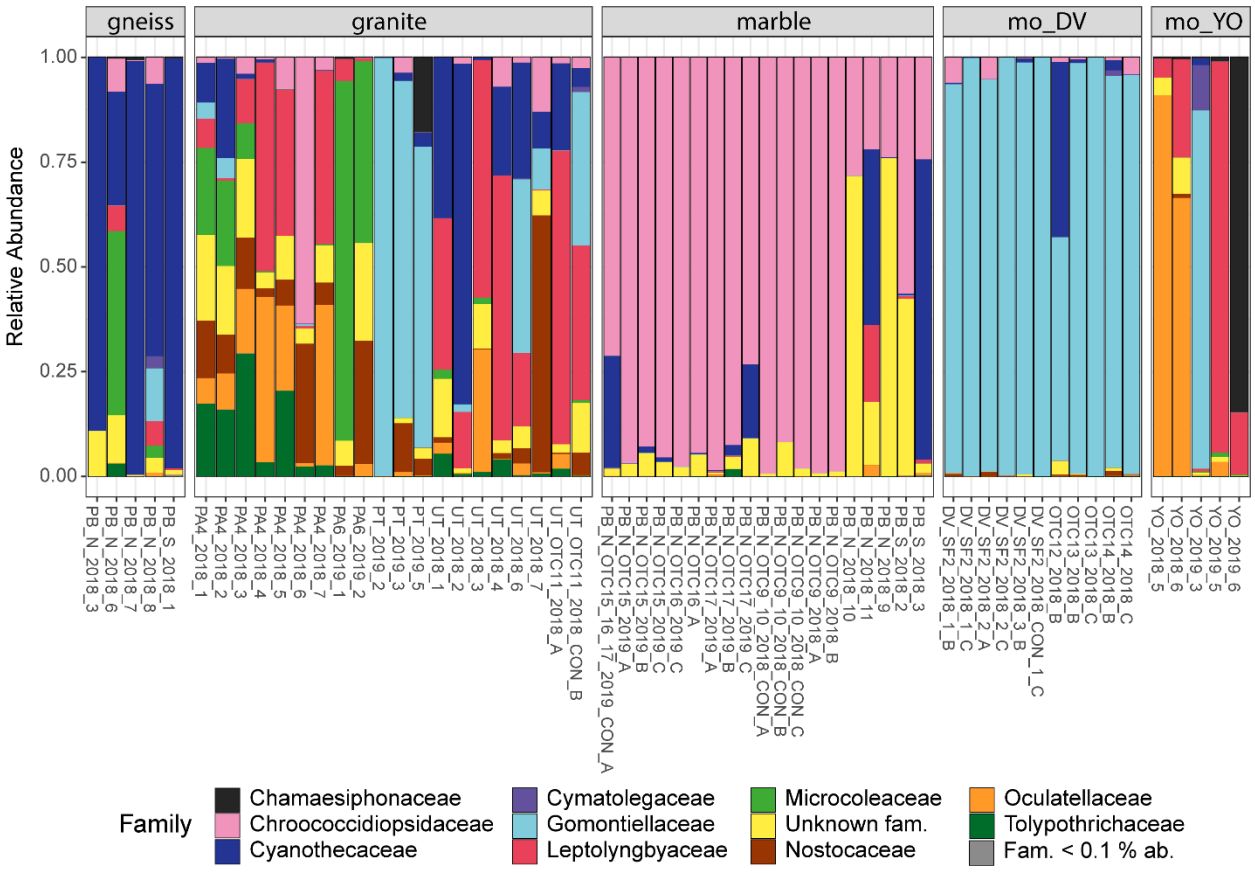

Fig. 3.2 Barplots showing the relative abundance of the most abundant cyanobacterial families in each sample. *Samples are grouped according to substrate (top) and arranged alphabetically (colors indicate cyanobacterial families - see legend below). Mo_DV: moraines of Dry Valley; mo_YO: moraines of Yûboku Valley.*

The relative abundance of cyanobacterial families varied across the different substrate types (Fig. 3.2, and Table S3.5-S3.6). Chroococcidiopsidaceae was the most abundant family with a total of 250,920 reads, of which most (94 %) were found in marble samples (236,757 reads). Gomontiellaceae was the second most abundant family (19 %) with a total of 227,516 reads that were mainly encountered in moraines from Dry Valley (67 %) where they were the dominant taxa (92 % of the moraine reads). This family was also abundant in some granite samples (second most abundant phylum, representing the 13 % of the total reads). Cyanothecaceae were the third most

represented family with 210,719 reads (18 %), which were present in all substrate types, though its OTUs represented 88 % of the reads in gneiss samples. Leptolyngbyaceae (142,134 reads) and Oculatellaceae (117,629 reads) were mainly distributed in the moraine of Yûboku Valley (59 %) and granitic bedrock (46 %). Leptolyngbyaceae represented 23 and 27 %, and Oculatellaceae 11 % and 51 % of the total read counts of granitic bedrock and the moraines in Yûboku Valley, respectively. Both families were barely present in the moraines soils of Dry Valley (< 1 %).

Significant indicator taxa were identified for all the substrate types but the moraines of Dry Valleys (Table S3.7). Granitic bedrock was characterized by 23 OTUs, mostly belonging to the Nostocales order, that are specifically encountered within these samples. Four OTUs belonging to the *Alitarella* genus were identified for marble bedrock. Five OTUs belonging to *Chamaesiphon*, *Alitarella*, *Cyanothece* and unknown taxonomic affiliations were identified for gneiss bedrock. Three OTUs belonging to *Limnospira*, *Microcoleus* and *Dolichospermum* were identified for the moraines of Austkampane. Finally, 200 OTUs, mostly belonging to Leptolyngbyaceae phylotypes and *Timaviella*, were identified for the moraines of the Yûboku Valley, suggesting a high degree of specialization of cyanobacteria within this site.

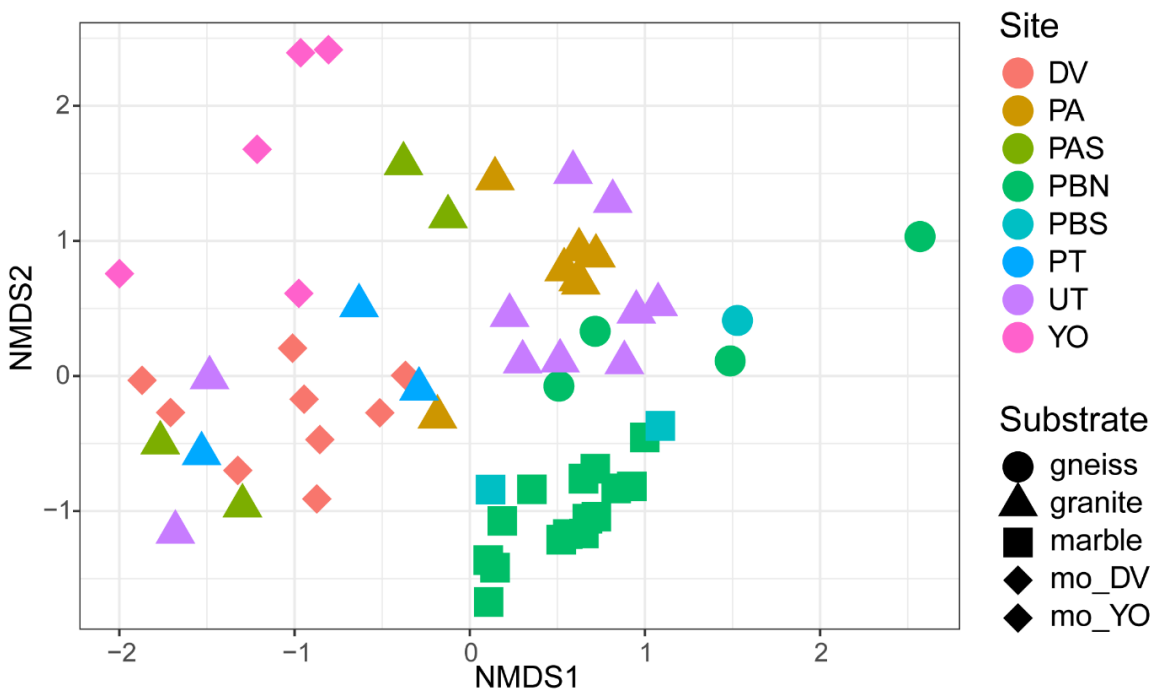

Fig. 3.3 Non-metric multidimensional scaling (nMDS) plot at the OTU level of Bray–Curtis distances for each sample (n=60). *Symbols are colored by sampling site, with different shapes representing the substrate type (see legend on right). Moraine_DV: moraine substrates of Dry Valley samples; moraine_YO: moraine substrates of Yûboku samples.*

The nMDS of the CSS-transformed Bray–Curtis dissimilarity matrices of the OTU relative abundance data showed that samples from different sites but with the same substrate type tended to have similar cyanobacterial communities (i.e. marble from different Perlebandet nunataks or granitic samples from different sites such as UT, PA and PAS; Fig. 3.3). This was not the case for some granitic samples from different sites which overlapped with moraine samples of the Dry Valley and gneiss samples. The marble cluster was characterized by several OTUs belonging to unknown genera of the Chroococcidiopsaceae family and one belonging to the *Alitarella* sp. (Fig. S3.5). The granitic/gneiss cluster was characterized by unknown genera of the Oculatellaceae family, the Cyanophyceae class, the Nostocales oder, the Leptolyngbyaceae family and *Cyanothece* genus (Fig. S3.5). The Dry Valley moraines were characterized by one OTU belonging to the *Hormoscilla* genus (Fig. S3.5).

In addition to the community structure, also ASV richness was significantly different between the different substrate types, but differences existed among the sampling sites (Fig. S3.2). The hyper arid moraine samples of DV showed the lowest richness in comparison to the granitic UT and PA4 sites. The only two PA6 samples, although characterized by granitic bedrock, had a low richness. The richness in the other sites was not significant different.

3.4.2 Community structure in relation to environmental factors, location and substrate type

Distance-based redundancy analysis (db-RDA) of the CSS-transformed Bray–Curtis dissimilarity matrices of the OTU relative abundances data showed a significant effect of environmental factors (P=0.002), PCNMs (P=0.002) and type of substrate (P=0.002) on variations in the cyanobacterial community structure. Best-fit environmental models showed that the combined environmental variables (pH, TN, N-NO_3^- and conductivity) accounted for 26 % of the total variation. Overall, pH and TN had the most influence on variation in community structure (18 %), while the other environmental factors together explained less than half percent (Table S6). Of the selected environmental variables, pH was the variable explaining the highest amount of variation (13 %). In addition, seven out of the 12 PCNMs (PCNM1, PCNM3, PCNM2, PCNM10, PCNM4, PCNM8 and PCNM9) were identified as significantly explaining variations in cyanobacterial community structure. The PCNMs explained together 32 % out of the total variation. The significant PCNMs reflect both large (PCNM1-4) and short (PCNM8-10) spatial scales, although those explaining most of the variation in community structure (22 %) reflected large spatial scales (PCNM1, PCNM3, PCNM2). Finally, four substrate types significantly explained variation in the cyanobacterial community structures, namely marble, moraines from Yûboku, moraines from Dry Valley and granite. Together these variables explained 31 % of the total variation, with marble and moraines from Yûboku explaining together up to 25 %.

3.5 DISCUSSION

Our findings show that soil cyanobacterial communities from different mountain peaks (nunataks) and valleys of the Sør Rondane Mountains largely differ among the investigated

substrate types at the family and OTU level. Sites characterized by different substrates also showed significant differences in richness levels, similarly to results of Chapter 2. Overall, the encountered differences among the studied cyanobacterial composition and structure were mainly differing among sites. Marble bedrock was characterized by high pH (and low PO_4^{3-}), granitic bedrock by high TN (positively correlating with TOC) and moraines of Dry Valley by low TN concentrations. The recently released CyanoSeq database allowed us to assign a taxonomic identification at the order level for 78 % of the encountered OTUs (1211 out of 1551). Most of these OTUs were also assigned to the genus level, allowing to classify many of the sequences that had previously been considered as 'unclassified' by the Greengenes database (data not shown). Thus, the use of this new database improves the taxonomic identification of the OTUs, and links them with the current cyanobacterial taxonomic system that has evolved quite a lot recently (Strunecký et al. 2022). Below we discuss the four major substrate types and the cyanobacterial taxa that were encountered within each of them.

3.5.1 Chroococcidiopsaceae dominates marble samples

Marble hosted the highest relative abundance of the coccoid Chroococcidiopsaceae family (up to 74 %; Fig. 3.2, Table S3.5), the majority of which belonged to the genus *Aliterella* (63 %; Table S3.6). Samples from this bedrock also had a relatively high richness (Fig. S3.3). Members of the Chroococcidiopsaceae are often found to dominate lithic habitats of hot and cold deserts (Broady 2005, Pointing et al. 2009, Chan et al. 2012, Jung et al. 2021) and especially in quartz-derived rocks which enable UV filtering but sufficient PAR to reach the biota. Chan et al. (2012) regarded members of the Chroococcidiopsaceae such as *Chroococcidiopsis* sp. as keystone taxa of hypolithic environments in hot and cold deserts. The present study confirmes our earlier findings (Chapter 2) based on the general V1-V3 bacterial primers. Chroococcidiopsaceae were also identified as the dominant family, and phylotypes identified as *Aliterella* sp. were also recognized as putative keystone taxa after a co-occurrence network analysis (Chapter 2). This highlights not only the dominance of this genus in this alkaline bedrock type but also their important ecological role in the community. Their ecological value within the marble soils was also confirmed by the indicator taxa analysis, that showed four OTUs belonging

to the *Alitarella* genus to be specifically present within this bedrock and not in other (Table S3.7). This genus has recently been described (Rigonato et al. 2016) and only a few strains have been isolated and studied so far, namely *A. shannxiensis*, *A. antarctica*, *A. atlantica, A. chasmolithica*, *A. compacta* and *A. gigantean*. Phylotypes of this genus belong to aquatic and terrestrial habitats, yet they could in fact represent different genera as already proposed by several authors (Rigonato et al. 2016, Jung et al. 2020 and 2021). Two of these species were cyanobionts (*A. compacta* and *A. gigantea*) of different fungal species with which they form lichens (*Peltula clavata* and *Peltula capensis*, respectively; Jung et al. 2021). Interestingly, in our marble samples, black lichen communities were often present, which may suggest that the phylotypes occurring in our study may form symbionthic lichen communities as well. The only species of this genus confined to lithic habitats (i.e. *A. chasmolithica*) also comes from a very extreme environment (i.e. the Atacama Desert). This is in line with the ecological features of our *Alitarella* sp. phylotypes which have to deal with extremely varying and fluctuating environmental conditions. Lithic genera of the Chroococcidiopsaceae family are able to withstand prolonged periods of drought thanks to their high production of trehalose and sucrose along with EPS (Azua-Bustos et al. 2014). Other studies focusing on marble bedrock (i.e. Timoncini et al. 2022) - despite their very distant focus compared to our study (i.e. bacterial composition of marble statues) - also found a predominance of cyanobacteria belonging to the genus *Aliterella*. These highly specialized cyanobacterial communities could be linked to the high alkalinity of marble soils, however, more research is needed in order to assess whether this taxon also occurs in other alkaline environments. Other taxa that were particularly present within the investigated marble samples but were not identfied with the general bacterial primers (Chapter 2) belonged to the *Cyanothece* genus (12 %; Fig. 3.2, Table S3.6), from the Cyanothecaceae family (Gomontiellales order). This genus is only represented by unicellular phylotypes, of which some are able to fix nitrogen (Sherman et al. 2010). Many other OTUs belonged to an “unknown" family (12 %; Fig. 3.2, Table S3.4).

3.5.2 Cyanothecaceae dominates gneiss samples

Gneiss hosted the highest relative abundance of the unicellular genus *Cyanothece*, family Cyanothecaceae (88 %; Fig. 3.2, Table S3.5, Table S3.6). Only five samples from gneiss bedrock of Perlebandet N nunatak which had visible lichen communities also generated enough sequences. The more mineral samples from this region had less than 1000 cyanobacterial reads per sample (c.f. Table S3.1). Despite the low samples number, the results were very consistent and revealed the dominance of *Cyanothece*. This dominance is likely related to their ability to fix atmospheric N_2 (Sherman et al. 2010), which also makes them important biota for other taxa in the hyper-oligotrophic soils of Antarctica. Hitherto, the only *Cyanothece* strain isolated from Antarctica was *Cyanothece aeruginosa* NIVA-CYA 258/1 (Mares et al. 2019), which was found within a lichen vegetation, yet has a different morphology compared to *C. aeruginosa,* which was previously reported from soils with visible 'algal' crusts in Victoria Valley, McMurdo Dry Valleys (Broady 2005). *Cyanothece* sp. was also present in marble and granitic bedrock, where lichen communities were more or less prominent. This may suggest that this genus could form symbionthic lichen communities. Phylotypes belonging to *Cyanothece* were also detected in the granitic Pingvinane 4th nunatak in a previous survey (Pushkareva et al. 2018), yet this taxon was absent in the gneiss samples from Teltet included in that same study. However, gneiss samples in Pushkareva et al. (2018) were collected from soils without visible communities which might explain the absence of *Cyanothece* sp. Members of the Cyanothecaceae family were also not detected as the dominant cyanobacterial genera of the gneiss samples of our earlier microbial survey conducted with general bacterial primers (Chapter 2) where instead Chroococcidiopsaceae family was recognized as the dominant family. *Cyanothece* sp. was indeed not present within the dataset of Chapter 2. Interestingly, within the Silva database the only few sequences belonging to *Cyanothece* genus were assigned to the Microcystaceae or the Thermosynechococcaceae families, but none of these families were present on the dataset of Chapter 2. We can therefore conclude that some taxa were misassigned and the two datasets cannot be compared. Other encountered reads in gneiss samples were much less abundant, with phylotypes belonging to Microcoleaceae, Gomantiellaceae, Chroococcidiopsidaceae and

Leptolyngbyaceae (between 3 and 1 % of the total reads abundance within this substrate; Fig. 3.2, Table S3.5).

3.5.3 Gomontiellaceae dominates moraine samples of Dry Valley

Moraine samples of Dry Valley had very low abundances of cyanobacterial reads and showed the lowest richness among all the investigated substrate types (Fig. S3.3). This environment is characterized by strong katabatic winds causing the microbiota to develop under the first layer of gravel. Nonetheless, and probably because of the intrinsic very harsh conditions of this site, only 9 samples were characterized by a minimum of 1000 reads. In these soils, the Cyanobacteriota was among the less abundant phyla (Chapter 2). Gomontiellaceae was the dominant cyanobacterial family encountered in these soils (92 %; Fig. 3.2, Table S3.5) represented mostly by *Hormoscilla* (74 %) and secondly by *Crinalium* (17 %; Table S3.6). Other represented taxa belonged to the family Cyanothecaceae (6 %; Table S3.5), which is however an abundant family of especially one sample (DV_OTC_12_2018_12; Fig. 3.2). Gomontiellaceae is a family encompassing peculiar non-heterocystous filamentous cyanobacteria (Bohunická et al. 2015) that were previously included in Oscillatoriales (Komarek et al. 2014, Bohunická et al. 2015). It is a rarely reported family and the uncultured strains belonging to this family have been recorded from mountain environments in Peru, Nepal, and Tibet, and also within dunes of the Baltic Sea, suggesting that members of the family Gomontiellaceae may occur in particular environments all over the world. The small number of reports on their occurrence is likely related to their low population densities (Bohunická et al. 2015, Mikhailyuk et al. 2019) and perhaps, the lack of studies in these particular environments. In Silva database no sequence belonged to the *Hormoscilla* genus, and the *Crinalium* genus belonged to the Chroococcidiopsaceae family. However, in Chapter 2 the Cyanobacteriota phylum represented only 3 % of the total reads within moraine soils, with ~ 1 % belonging to the Chroococcidiopsaceae family, that probably represented misclassified sequences. Only very few sequences belonging to the genus *Crinalium* were previously found in Taylor Valley (McMurdo Dry Valleys, Michaud et al. 2012), in a lake in the Larsemann Hills (Snowbowl Lake; Pessi et al. 2023) and soils of our sampled region in a

previous survey (Tytgat et al. 2016), as well as in cryoconite holes (Singh et al. 2021, Broady 2005) which highlight the adaptation of this genus to extremely cold and oligotrophic conditions.

3.5.4 Filamentous and heterocystous families dominate granite samples

Several families with comparable abundances were present on granitic samples, namely Leptolyngbyaceae (23 %), Gomontiellaceae (13 %), Cyanothecaceae (13 %), Microcoleaceae (12 %), Oculatellaceae (11 %), Nostocaceae (9%) (Table S3.5). Similarly to marble soils, many other OTUs belonged to an “unknown" family (10 %; Fig. 3.2, Table S3.5). In general, the granitic soils appeared to be among the richest bedrock types (Fig. S3.3) with Pingvinane 4th nunatak and Utsteinen ridge hosting the most diverse communities (Fig. S3.2). This might be related to the relatively high TOC values and the presence of visible BSCs (Chilton et al. 2018). Earlier studies in the Sør Rondane Mountains similarly showed that the granitic bedrock hosted the most diverse bacterial and cyanobacterial communities (Tytgat et al. 2016, Pushkareva et al. 2018).

However, in the present study, more locations and more substrate types were added compared with Tytgat et al. (2016) and Pushkareva et al. (2018), which allowed a more nuanced view on the cyanobacterial diversity in the region. Indeed, the granitic Petrellnuten nunatak studied for the first time, hosted one of the least diverse cyanobacterial communities (Fig. S3.2). These communities were dominated by the Gomontiellaceae family, which was also dominant in the Dry Valley samples. This could be explained by the relatively harsh conditions in this nunatak as it is not very sheltered and closely situated to the plateau of the East Antarctic Ice Sheet. The Pingvinane 6th nunatak also had a low richness compared with the other granitic sites (Fig. S3.2). This nunatak was characterized by large communities of microalgae within well-developed BSCs covering granitic gravel. Competition among the two phototrophic functional groups could explain the low cyanobacterial diversity. However, despite these sites having a lower richness, cyanobacterial communities are generally very diverse in granitic soils. This might be linked to their diverse physical structure with gravel soils alternating with large boulders which have cracks, crevices and pores, all providing a diverse range of microhabitats. The diversity of habitats in the soil could also be higher due to the presence of BSCs and hence specific microclimatic

conditions (Caster et al. 2021, Rodríguez-Caballero et al. 2012). This supports the hypothesis of Namsaraev et al. (2010) who suggested that the coarser texture of the rock and the large dimensions of most granite boulders result in a more stable environment leading to a higher diversity of cyanobacterial communities. In addition, weathering processes may lead to the addition of nutrients such as phosphorus and potassium, which can further promote the growth and diversity of cyanobacteria (Stewart and Alexander 1971). Indeed, granite had the highest phosphate content (Table S3.1) which could be an advantage for nitrogen-fixing cyanobacteria that need higher amounts compared to other organisms in order to perform diazotrophy. Furthermore, granite can also better retain moisture on the surface compared to other bedrock types. For example, marble has a high porosity possibly enabling liquid water runoff through the pores, leaving the surface particularly dry. The higher water retention in granites can create microenvironments that are favorable for the growth and survival of different species of cyanobacteria. In our study, the Leptolyngbiaceae family, which is represented by nitrogen-fixer phylotypes, was mostly represented by the genus *Phormidesmis* (14 %). Pushkareva et al. (2018) also found Leptolyngbiaceae among the most abundant families of the granitic Pingvinane 4th nunatak and Utsteinen ridge. Leptolyngbyaceae is a polyphyletic family and one among the most intensively studied within the Synechococcales order (Mai et al.2018), of which several species such as *Phormidesmis priestleyi* and *Leptolyngbya* sp. have been extensively found in Antarctic or Arctic habitats (Taton et al. 2006, Chrismas et al. 2018). Trait evolution analyses have predicted that *P. priestleyi* and *Leptolyngbya* sp. could have a cold tolerant ancestor (Chrismas et al. 2015), but these taxa are however not restricted to cold habitats (Jungblut et al. 2009, Chrismas et al. 2015). Another well represented genus from this family was *Heteroleibleinia* (8 %).

Microcoleaceae were the second most abundant family in the granitic soils and were to a high extent composed of unknown genera (43 % of the overall genera in this family) as well as the genus *Tychonema*, which only represented 3 % of the total read counts in granitic soils. *Microcoleus* sp. was found to be particularly abundant in PA4 nunatak as reported by Pushkareva et al. (2018), which was in agreement with our results (Fig. 3.2).

Gomontiellaceae were mostly represented by the genus *Hormoscilla* (9 %). This genus represents a rarely reported group of cyanobacteria found in both soils and aquatic (marine and freshwater) habitats (Bohunická et al. 2015). This genus shares > 99 % identity of the 16S rRNA with the *Crinalium* genus, well above the recommended value for the separation of genera (Stackebrandt and Goebel 1994), but their distinct morphological and ecological characteristics provide a solid basis for maintaining the two genera separated (Bohunická et al. 2015). Another important family was Cyanothecaceae represented by the genus *Cyanothece* (13 %). As discussed above, the genus *Cyanothece* is particularly abundant in granitic samples characterized by BSCs with developed lichen vegetations. In our study the Oculatellaceae family was largely represented by the genus *Timaviella* (7 %), which was recently described from a cryptic community located in a cave from the Italian Alps (Sciuto et al. 2017).

Nostocaceae was uniquely represented by the genus *Nostoc* (9 %), which is one of the most abundant cyanobacterial genera in Antarctic environments. The majority of Antarctic BSCs were indeed found to be mainly composed of filamentous cyanobacteria such as *Nostoc commune* and *Tolypothrix*, *Calothrix* and *Leptolyngbya* species (Büdel and Colesie 2014). Cyanobacteria, and especially diazotrophs, are often considered keystone taxa of hyper-arid environments, because they provide nitrogen to the entire community they inhabit (Ortiz et al. 2020, Belnap et al. 2003, Lee et al. 2016, Van Goethem et al. 2017). Phylotypes belonging to the Nostocaceae were also shown to be putative keystone taxa in the granitic soils as shown recently (Chapter 2) and, in the present study, were also the majority of indicator taxa, confirming their ecologic value within these soils.

Many phylotypes within granitic soils, similarly to other substrate types (i.e. marble and moraine of Yûboku Valley, see Table S3.5-3.6) remained unclassified at the genera (~ 20 %) and the family level (~ 8 %) that may comprehend potentially endemic lineages. This is not uncommon for desert microbial communities (Niederberger et al. 2008, Lee et al. 2012, Makhalanyane et al. 2013, Van Goethem et al. 2016) and other Antarctic environments, such as the benthic microbial

mats, where Pessi et al. 2018 also encountered a high percentage (> 37 %) of “novel” cyanobacterial sequences.

3.6 CONCLUSION

Distinct cyanobacterial communities were present on the different investigated substrate types. As hypothetized, granitic soils were the most diverse hosting a variety of filamentous cyanobacterial phylotypes, whilst other kind of substrates were characterized by a high abundance of phylotypes belonging to single families. Interestingly, many OTUs remained unclassified, which remind that a considerable effort is needed to improve the representation of Antarctic cyanobacteria in sequence databases. This work provides insights into the cyanobacterial community structures of the nunataks and valleys of the west Sør Rondane Mountains and incites into the use of specific primers as well as up-to-date databases for the correct taxonomy assignation of cyanobacterial sequences. The information here providedcan be used as a baseline cyanobacterial biodiversity reference in the sites that are now proposed to become part of an Antarctic Specially Protected Area.

3.7 ACKNOWLEDGMENTS

This work was funded by the Federal Belgian Science Policy Office (BELSPO) under the BRAIN-BE program MICROBIAN project (BR/165/A1/MICROBIAN). The authors thank the crew of the Princess Elisabeth Antarctica (PES) station for the operation of the base and providing the necessary support during the field activities, in particular Sam Lambrechts and Quinten Vanhellemont for helping in collecting the samples, Alain Hubert for leading the Belgian Antarctic Research Expedition (BELARE) and our field guides for the 2018 campaign, Pierre-Yves Terrettaz, and the 2019 campaign, Raphaël Mayoraz. ESA/Copernicus is thanked for the free and open access to Sentinel-2 imagery used in Fig. 3.1. VS and BD had a PhD FRIA fellowship from the FRS-FNRS. AW is Senior Research Associate of the FRS-FNRS.

3.8 AUTHOR CONTRIBUTION

Conceived and designed the study: EV, WV, BT, AW. Performed the sampling: VS, EV. Performed the laboratory analysis: BD. Analyzed the data: BD, VS. Supervision: EV, AW. Secured the funding WV, AW and EV. Wrote the paper: VS. All authors reviewed and commented on previous versions of the manuscript and approved the final version. BD and VS equally contributed to the work.

3.9 REFERENCE

Azua-Bustos, A., Zúñiga, J., Arenas-Fajardo, C., Orellana, M., Salas, L. and Rafael, V., 2014. Gloeocapsopsis AAB1, an extremely desiccation-tolerant cyanobacterium isolated from the Atacama Desert. Extremophiles, 18, pp.61-74.

Bebout, B.M. and Garcia-Pichel, F., 1995. UV B-induced vertical migrations of cyanobacteria in a microbial mat. Applied and Environmental Microbiology, 61(12), pp.4215-4222.

Belnap, J., Büdel, B., Lange, O.L., 2003. Biological soil crusts: characteristics and distribution. In: Belnap, J., Lange, O.L. (Eds.), Biological Soil Crusts: Structure, Function, andManagement. Springer-Verlag, Berlin, pp. 3–30.

Blanchet, F.G., Legendre, P. and Borcard, D., 2008. Forward selection of explanatory variables. Ecology, 89(9), pp.2623-2632.

Bohunická, M., Mareš, J., Hrouzek, P., Urajová, P., Lukeš, M., Šmarda, J., Komárek, J., Gaysina, L.A. and Strunecký, O., 2015. A combined morphological, ultrastructural, molecular, and biochemical study of the peculiar family Gomontiellaceae (Oscillatoriales) reveals a new cylindrospermopsin-producing clade of cyanobacteria. Journal of Phycology, 51(6), pp.1040-1054.

Broady, P.A., 1996. Diversity, distribution and dispersal of Antarctic terrestrial algae. Biodiversity & Conservation, 5, pp.1307-1335.

Broady, P.A., 2005. The distribution of terrestrial and hydro-terrestrial algal associations at three contrasting locations in southern Victoria Land, Antarctica. Algol Stud, 118(1), pp.95-112.

Brooks, S.T., Jabour, J., van den Hoff, J., Bergstrom, D.M., 2019. Our footprint on Antarctica competes with nature for rare ice-free land. Nat. Sustain. 2, 185–190.

Büdel, B. and Colesie, C., 2014. Biological soil crusts. Antarctic Terrestrial Microbiology: Physical and Biological Properties of Antarctic Soils, pp.131-161.

Callahan, B.J., McMurdie, P.J., Rosen, M.J., Han, A.W., Johnson, A.J.A. and Holmes, S.P., 2016. DADA2: High-resolution sample inference from Illumina amplicon data. *Nature methods*, *13*(7), pp.581-583.

Čapková, K., Hauer, T., Řeháková, K. and Doležal, J., 2016. Some like it high! Phylogenetic diversity of high-elevation cyanobacterial community from biological soil crusts of western Himalaya. Microbial ecology, 71, pp.113-123.

Caster, J., Sankey, T.T., Sankey, J.B., Bowker, M.A., Buscombe, D., Duniway, M.C., Barger, N., Faist, A. and Joyal, T., 2021. Biocrust and the soil surface: Influence of climate, disturbance, and biocrust recovery on soil surface roughness. Geoderma, 403, p.115369.

Cavacini, 2001. Soil algae from northern Victoria Land (Antarctica). Polar Bioscience, 14 (2001), pp. 45-60

Chan, Y., Lacap, D.C., Lau, M.C., Ha, K.Y., Warren-Rhodes, K.A., Cockell, C.S., Cowan, D.A., McKay, C.P. and Pointing, S.B., 2012. Hypolithic microbial communities: between a rock and a hard place. Environmental microbiology, 14(9), pp.2272-2282.

Chilton, A.M., Neilan, B.A. and Eldridge, D.J., 2018. Biocrust morphology is linked to marked differences in microbial community composition. Plant and soil, 429, pp.65-75.

Choe, Y.H., Kim, M. and Lee, Y.K., 2021. Distinct microbial communities in adjacent rock and soil substrates on a high Arctic polar desert. Frontiers in Microbiology, 11, p.607396.

Chrismas, N.A., Anesio, A.M. and Sánchez-Baracaldo, P., 2015. Multiple adaptations to polar and alpine environments within cyanobacteria: a phylogenomic and Bayesian approach. Frontiers in microbiology, 6, p.1070.

Chrismas, N.A., Anesio, A.M. and Sanchez-Baracaldo, P., 2018. The future of genomics in polar and alpine cyanobacteria. FEMS Microbiology Ecology, 94(4), p.fiy032.

Cockell, C.S. and Stokes, M.D., 2004. Widespread colonization by polar hypoliths. *Nature*, *431*(7007), pp.414-414.

De Cáceres, M., Legendre, P. and Moretti, M., 2010. Improving indicator species analysis by combining groups of sites. Oikos, 119(10), pp.1674-1684.

de Los Ríos, A., Ascaso, C., Wierzchos, J., Fernández-Valiente, E. and Quesada, A., 2004. Microstructural characterization of cyanobacterial mats from the McMurdo Ice Shelf, Antarctica. Applied and Environmental Microbiology, 70(1), pp.569-580.

DeSantis, T.Z., Hugenholtz, P., Larsen, N., Rojas, M., Brodie, E.L., Keller, K., Huber, T., Dalevi, D., Hu, P. and Andersen, G.L., 2006. Greengenes, a chimera-checked 16S rRNA gene database and workbench compatible with ARB. Applied and environmental microbiology, 72(7), pp.5069-5072.

Edgar, R.C., 2013. UPARSE: highly accurate OTU sequences from microbial amplicon reads. Nature methods, 10(10), pp.996-998.

Effendi, D.B., Sakamoto, T., Ohtani, S., Awai, K. and Kanesaki, Y., 2022. Possible involvement of extracellular polymeric substrates of Antarctic cyanobacterium Nostoc sp. strain SO-36 in adaptation to harsh environments. Journal of Plant Research, 135(6), pp.771-784.

Fernandes, V.M., Machado de Lima, N.M., Roush, D., Rudgers, J., Collins, S.L. and Garcia-Pichel, F., 2018. Exposure to predicted precipitation patterns decreases population size and alters community structure of cyanobacteria in biological soil crusts from the Chihuahuan Desert. Environmental Microbiology, 20(1), pp.259-269.

Fernández-Carazo, R., Namsaraev, Z., Mano, M.J., Ertz, D. and Wilmotte, A., 2012. Cyanobacterial diversity for an anthropogenic impact assessment in the Sør Rondane Mountains area, Antarctica. Antarctic Science, 24(3), pp.229-242.

Garcia-Pichel, F., Loza, V., Marusenko, Y., Mateo, P. and Potrafka, R.M., 2013. Temperature drives the continental-scale distribution of key microbes in topsoil communities. Science, 340(6140), pp.1574-1577.

Greening, C., Islam, Z.F. and Bay, S.K., 2022. Hydrogen is a major lifeline for aerobic bacteria. Trends in Microbiology, 30(4), pp.330-337.

Hijmans, R. J. (2021). Introduction to the" geosphere" package (Version 1.5-14).

Jung, P., Brust, K., Schultz, M., Büdel, B., Donner, A. and Lakatos, M., 2021. Opening the gap: rare lichens with rare cyanobionts–unexpected cyanobiont diversity in cyanobacterial lichens of the order Lichinales. Frontiers in Microbiology, 12, p.728378.

Jung, P., Mikhailyuk, T., Emrich, D., Baumann, K., Dultz, S. and Büdel, B., 2020. Shifting boundaries: Ecological and geographical range extension based on three new species in the cyanobacterial genera Cyanocohniella, Oculatella, and, Aliterella. Journal of phycology, 56(5), pp.1216-1231.

Jung, P., Schermer, M., Briegel-Williams, L., Baumann, K., Leinweber, P., Karsten, U., Lehnert, L., Achilles, S., Bendix, J. and Büdel, B., 2019. Water availability shapes edaphic and lithic cyanobacterial communities in the Atacama Desert. Journal of phycology, 55(6), pp.1306-1318.

Jungblut, A.D., Allen, M.A., Burns, B.P. and Neilan, B.A., 2009. Lipid biomarker analysis of cyanobacteria-dominated microbial mats in meltwater ponds on the McMurdo Ice Shelf, Antarctica. Organic Geochemistry, 40(2), pp.258-269.

Jungblut, A.D., Hawes, I., Mountfort, D., Hitzfeld, B., Dietrich, D.R., Burns, B.P. and Neilan, B.A., 2005. Diversity within cyanobacterial mat communities in variable salinity meltwater ponds of McMurdo Ice Shelf, Antarctica. Environmental microbiology, 7(4), pp.519-529.

Komsta, L. and Novomestky, F., 2015. Moments, cumulants, skewness, kurtosis and related tests. R package version, 14(1).

Lee, C.K., Barbier, B.A., Bottos, E.M., McDonald, I.R. and Cary, S.C., 2012. The inter-valley soil comparative survey: the ecology of Dry Valley edaphic microbial communities. The ISME journal, 6(5), pp.1046-1057.

Lee, J.R., Raymond, B., Bracegirdle, T.J., Chadès, I., Fuller, R.A., Shaw, J.D. and Terauds, A., 2017. Climate change drives expansion of Antarctic ice-free habitat. Nature, 547(7661), pp.49-54.

Lee, K.C., Archer, S.D., Boyle, R.H., Lacap-Bugler, D.C., Belnap, J. and Pointing, S.B., 2016. Niche filtering of bacteria in soil and rock habitats of the Colorado Plateau Desert, Utah, USA. Frontiers in Microbiology, 7, p.1489.

Lefler, F.W., Berthold, D.E. and Dail Laughinghouse IV, H., 2023. CyanoSeq: a database of cyanobacterial 16S rRNA sequences with curated taxonomy. Journal of Phycology.

Lefler, F.W., Berthold, D.E. and Laughinghouse, D., 2022. CyanoSeq: a new curated reference database of cyanobacterial 16S rRNA sequences.

Mai, T., Johansen, J.R., Pietrasiak, N., Bohunicka, M. and Martin, M.P., 2018. Revision of the Synechococcales (Cyanobacteria) through recognition of four families including Oculatellaceae fam. nov. and Trichocoleaceae fam. nov. and six new genera containing 14 species. Phytotaxa.

Makhalanyane, T.P., Valverde, A., Birkeland, N.K., Cary, S.C., Marla Tuffin, I. and Cowan, D.A., 2013. Evidence for successional development in Antarctic hypolithic bacterial communities. The ISME Journal, 7(11), pp.2080-2090.

Mareš, J., Johansen, J.R., Hauer, T., Zima Jr, J., Ventura, S., Cuzman, O., Tiribilli, B. and Kaštovský, J., 2019. Taxonomic resolution of the genus Cyanothece (Chroococcales, Cyanobacteria), with a treatment on Gloeothece and three new genera, Crocosphaera, Rippkaea, and Zehria. Journal of Phycology, 55(3), pp.578-610.

McArdle, B.H. and Anderson, M.J., 2001. Fitting multivariate models to community data: a comment on distance-based redundancy analysis. Ecology, 82(1), pp.290-297.

McMurdie, P.J. and Holmes, S., 2013. phyloseq: an R package for reproducible interactive analysis and graphics of microbiome census data. PloS one, 8(4), p.e61217.

Mikhailyuk, T., Vinogradova, O., Holzinger, A., Glaser, K., Samolov, E. and Karsten, U., 2019. New record of the rare genus Crinalium Crow (Oscillatoriales, Cyanobacteria) from sand dunes of the

Baltic Sea, Germany: epitypification and emendation of Crinalium magnum Fritsch et John based on an integrative approach. Phytotaxa, 400(3), p.165.

Muñoz-Martín, M.Á., Becerra-Absalón, I., Perona, E., Fernández-Valbuena, L., Garcia-Pichel, F. and Mateo, P., 2019. Cyanobacterial biocrust diversity in Mediterranean ecosystems along a latitudinal and climatic gradient. New Phytologist, 221(1), pp.123-141.

Namsaraev, Z., Mano, M.J., Fernandez, R. and Wilmotte, A., 2010. Biogeography of terrestrial cyanobacteria from Antarctic ice-free areas. Annals of Glaciology, 51(56), pp.171-177.

Niederberger, T.D., McDonald, I.R., Hacker, A.L., Soo, R.M., Barrett, J.E., Wall, D.H. and Cary, S.C., 2008. Microbial community composition in soils of Northern Victoria Land, Antarctica. Environmental microbiology, 10(7), pp.1713-1724.

Nübel, U., Garcia-Pichel, F. and Muyzer, G., 1997. PCR primers to amplify 16S rRNA genes from cyanobacteria. Applied and environmental microbiology, 63(8), pp.3327-3332.

Obbels, D., Verleyen, E., Mano, M.J., Namsaraev, Z., Sweetlove, M., Tytgat, B., Fernandez-Carazo, R., De Wever, A., D'hondt, S., Ertz, D. and Elster, J., 2016. Bacterial and eukaryotic biodiversity patterns in terrestrial and aquatic habitats in the Sør Rondane Mountains, Dronning Maud Land, East Antarctica. FEMS microbiology ecology, 92(6).

Ortiz, M., Bosch, J., Coclet, C., Johnson, J., Lebre, P., Salawu-Rotimi, A., Vikram, S., Makhalanyane, T. and Cowan, D., 2020. Microbial nitrogen cycling in Antarctic soils. Microorganisms, 8(9), p.1442.

Paulson, J.N., Pop, M. and Bravo, H.C., 2013. metagenomeSeq: Statistical analysis for sparse high-throughput sequencing. Bioconductor package, 1(0), p.191.

Peres-Neto, P. R., Legendre, P., Dray, S., & Borcard, D. (2006). Variation partitioning of species data matrices: estimation and comparison of fractions. Ecology, 87(10), 2614-2625.

Pessi, I.S., Lara, Y., Durieu, B., Maalouf, P.D.C., Verleyen, E. and Wilmotte, A., 2018. Community structure and distribution of benthic cyanobacteria in Antarctic lacustrine microbial mats. FEMS Microbiology Ecology, 94(5), p.fiy042.

Pessi, I.S., Maalouf, P.D.C., Laughinghouse IV, H.D., Baurain, D. and Wilmotte, A., 2016. On the use of high-throughput sequencing for the study of cyanobacterial diversity in Antarctic aquatic mats. Journal of Phycology, 52(3), pp.356-368.

Pessi, I.S., Popin, R.V., Durieu, B., Lara, Y., Savaglia, V., Roncero-Ramos, B., Hultman, J., Verleyen, E., Vyverman, W. and Wilmotte, A., 2023. Novel diversity of polar Cyanobacteria revealed by genome-resolved metagenomics. bioRxiv, pp.2023-02.

Pointing, S.B., Büdel, B., Convey, P., Gillman, L.N., Koerner, C., Leuzinger, S. and Vincent, W.F., 2015. Biogeography of photoautotrophs in the high polar biome. Frontiers in plant science, 6, p.692.

Pointing, S.B., Chan, Y., Lacap, D.C., Lau, M.C., Jurgens, J.A. and Farrell, R.L., 2009. Highly specialized microbial diversity in hyper-arid polar desert. Proceedings of the National Academy of Sciences, 106(47), pp.19964-19969.

Pushkareva, E., Pessi, I.S., Namsaraev, Z., Mano, M.J., Elster, J. and Wilmotte, A., 2018. Cyanobacteria inhabiting biological soil crusts of a polar desert: Sør Rondane Mountains, Antarctica. Systematic and applied microbiology, 41(4), pp.363-373.

Quast, C., Pruesse, E., Yilmaz, P., Gerken, J., Schweer, T., Yarza, P., Peplies, J. and Glöckner, F.O., 2012. The SILVA ribosomal RNA gene database project: improved data processing and web-based tools. Nucleic acids research, 41(D1), pp.D590-D596.

R Core Team (2021). R: A language and environment for statistical computing. R Foundation for Statistical Computing, Vienna, Austria. URL https://www.R-project.org/.

Rego, A., Raio, F., Martins, T.P., Ribeiro, H., Sousa, A.G., Séneca, J., Baptista, M.S., Lee, C.K., Cary, S.C., Ramos, V. and Carvalho, M.F., 2019. Actinobacteria and cyanobacteria diversity in terrestrial antarctic microenvironments evaluated by culture-dependent and independent methods. *Frontiers in microbiology*, *10*, p.1018.

Rigonato, J., Gama, W.A., Alvarenga, D.O., Branco, L.H.Z., Brandini, F.P., Genuario, D.B. and Fiore, M.F., 2016. Aliterella atlantica gen. nov., sp. nov., and Aliterella antarctica sp. nov., novel members of coccoid Cyanobacteria. International Journal of Systematic and Evolutionary Microbiology, 66(8), pp.2853-2861.

Rodríguez-Caballero, E., Cantón, Y., Chamizo, S., Afana, A. and Solé-Benet, A., 2012. Effects of biological soil crusts on surface roughness and implications for runoff and erosion. Geomorphology, 145, pp.81-89.

Sakaeva, A., Sokol, E. R., Kohler, T. J., Stanish, L. F., Spaulding, S. A., Howkins, A., ... & McKnight, D. M. (2016). Evidence for dispersal and habitat controls on pond diatom communities from the McMurdo Sound Region of Antarctica. Polar Biology, 39(12), 2441-2456.

Schulze-Makuch, D., Wagner, D., Kounaves, S.P., Mangelsdorf, K., Devine, K.G., de Vera, J.P., Schmitt-Kopplin, P., Grossart, H.P., Parro, V., Kaupenjohann, M. and Galy, A., 2018. Transitory microbial habitat in the hyperarid Atacama Desert. Proceedings of the National Academy of Sciences, 115(11), pp.2670-2675.

Sciuto, K., Moschin, E. and Moro, I., 2017. Cryptic cyanobacterial diversity in the Giant Cave (Trieste, Italy): the new genus Timaviella (Leptolyngbyaceae). Cryptogamie, Algologie, 38(4), pp.285-323.

Sherman, L.A., Min, H., Toepel, J. and Pakrasi, H.B., 2010. Better living through Cyanothece–unicellular diazotrophic cyanobacteria with highly versatile metabolic systems. In Recent advances in phototrophic prokaryotes (pp. 275-290). Springer New York.

Sokol, E. R., Herbold, C. W., Lee, C. K., Cary, S. C., & Barrett, J. E. (2013). Local and regional influences over soil microbial metacommunities in the Transantarctic Mountains. Ecosphere, 4(11), 1-24.

Stackebrandt, E. and Goebel, B.M., 1994. Taxonomic note: a place for DNA-DNA reassociation and 16S rRNA sequence analysis in the present species definition in bacteriology. International journal of systematic and evolutionary microbiology, 44(4), pp.846-849.

Stewart, W.D.P. and Alexander, G., 1971. Phosphorus availability and nitrogenase activity in aquatic blue-green algae. Freshwater Biology, 1(4), pp.389-404.

Strunecký, O., Ivanova, A.P. and Mareš, J., 2023. An updated classification of cyanobacterial orders and families based on phylogenomic and polyphasic analysis. Journal of Phycology, 59(1), pp.12-51.

Suganuma, Y., Miura, H., Zondervan, A. and Okuno, J.I., 2014. East Antarctic deglaciation and the link to global cooling during the Quaternary: Evidence from glacial geomorphology and 10Be surface exposure dating of the Sør Rondane Mountains, Dronning Maud Land. Quaternary Science Reviews, 97, pp.102-120.

Tamaru, Y., Takani, Y., Yoshida, T. and Sakamoto, T., 2005. Crucial role of extracellular polysaccharides in desiccation and freezing tolerance in the terrestrial cyanobacterium Nostoc commune. Applied and Environmental Microbiology, 71(11), pp.7327-7333.

Taton, A., Grubisic, S., Balthasart, P., Hodgson, D.A., Laybourn-Parry, J. and Wilmotte, A., 2006a. Biogeographical distribution and ecological ranges of benthic cyanobacteria in East Antarctic lakes. FEMS microbiology ecology, 57(2), pp.272-289.

Taton, A., Grubisic, S., Brambilla, E., De Wit, R. and Wilmotte, A., 2003. Cyanobacterial diversity in natural and artificial microbial mats of Lake Fryxell (McMurdo Dry Valleys, Antarctica): a morphological and molecular approach. Applied and environmental microbiology, 69(9), pp.5157-5169.

Taton, A., Grubisic, S., Ertz, D., Hodgson, D.A., Piccardi, R., Biondi, N., Tredici, M.R., Mainini, M., Losi, D., Marinelli, F. and Wilmotte, A., 2006b. Polyphasic study of Antarctic cyanobacterial strains 1. Journal of Phycology, 42(6), pp.1257-1270.

Timoncini, A., Costantini, F., Bernardi, E., Martini, C., Mugnai, F., Mancuso, F.P., Sassoni, E., Ospitali, F. and Chiavari, C., 2022. Insight on bacteria communities in outdoor bronze and marble artefacts in a changing environment. Science of The Total Environment, 850, p.157804.

Tytgat, B., Verleyen, E., Sweetlove, M., D'hondt, S., Clercx, P., Van Ranst, E., Peeters, K., Roberts, S., Namsaraev, Z., Wilmotte, A. and Vyverman, W., 2016. Bacterial community composition in relation to bedrock type and macrobiota in soils from the Sør Rondane Mountains, East Antarctica. FEMS Microbiology Ecology, 92(9).

Ugolini, F.C. and Bockheim, J.G., 2008. Antarctic soils and soil formation in a changing environment: a review. Geoderma, 144(1-2), pp.1-8.

Van Goethem, M.W., Makhalanyane, T.P., Cowan, D.A. and Valverde, A., 2017. Cyanobacteria and Alphaproteobacteria may facilitate cooperative interactions in niche communities. Frontiers in microbiology, 8, p.2099.

Venables, W.R. and Ripley, B., 2002. BD (2002). Modern Applied Statistics with S. New York: Springer Science & Business Media, 200, pp.183-206.

Vincent, W., 1993. Antarctic cyanobacteria: light, nutrients and photosynthesis in the microbial mat environment. J. Phycol., 29, pp.745-755.

Vincent, W.F., 2000. Evolutionary origins of Antarctic microbiota: invasion, selection and endemism. Antarctic Science, 12(3), pp.374-385.

Vincent, W.F., 2009. Cyanobacteria. In:Encyclopedia of Inland Waters(ed. Likens, G.E.). Elsevier Inc., Oxford, pp. 226–232.

Weber, B., Belnap, J., Büdel, B., Antoninka, A.J., Barger, N.N., Chaudhary, V.B., Darrouzet-Nardi, A., Eldridge, D.J., Faist, A.M., Ferrenberg, S. and Havrilla, C.A., 2022. What is a biocrust? A refined, contemporary definition for a broadening research community. Biological Reviews, 97(5), pp.1768-1785.

Wei, T., Simko, V., Levy, M., Xie, Y., Jin, Y. and Zemla, J., 2017. Package 'corrplot'. Statistician, 56(316), p.e24.

Whitton, B.A. and Potts, M., 2012. Introduction to the cyanobacteria. Ecology of cyanobacteria II: their diversity in space and time, pp.1-13.

Whitton, B.A. and Potts, M., 2012. Introduction to the cyanobacteria. Ecology of cyanobacteria II: their diversity in space and time, pp.1-13.

Williams, L., Loewen-Schneider, K., Maier, S. and Büdel, B., 2016. Cyanobacterial diversity of western European biological soil crusts along a latitudinal gradient. FEMS microbiology ecology, 92(10).

Wood, S.A., Mountfort, D., Selwood, A.I., Holland, P.T., Puddick, J. and Cary, S.C., 2008. Widespread distribution and identification of eight novel microcystins in Antarctic cyanobacterial mats. Applied and Environmental Microbiology, 74(23), pp.7243-7251.

Zhang, L., Jungblut, A.D., Hawes, I., Andersen, D.T., Sumner, D.Y. and Mackey, T.J., 2015. Cyanobacterial diversity in benthic mats of the McMurdo Dry Valley lakes, Antarctica. Polar Biology, 38, pp.1097-1110.

Zhang, Q.I., Zheng, L., Li, T., Li, R. and Song, L., 2018. Aliterella shaanxiensis (Aliterellaceae), a new coccoid cyanobacterial species from China. Phytotaxa, 374(3), pp.211-22

CHAPTER 4

ECOPHYSIOLOGICAL AND TRANSCRIPTOMIC RESPONSE TO DESICCATION AND RE-WETTING OF NOSTOC SP. FROM ANTARCTIC FRESHWATER AND TERRESTRIAL HABITATS

VALENTINA SAVAGLIA[1,2], BEATRIZ RONCERO-RAMOS[1,3], IGOR S. PESSI[4], LUC CORNET[1], ANNICK WILMOTTE[1], ELIE VERLEYEN[2]

[1]InBioS, Molecular Diversity and Ecology of cyanobacteria, University of Liège, Liège, Belgium

[2]Laboratory of Protistology & Aquatic Ecology, Ghent University, Ghent, Belgium

[3]Department of Plant Biology and Ecology, University of Sevilla, Sevilla, Spain

[4]Finnish Environment Institute (SYKE), Helsinki, Finland

Author contribution of VS: experiment, laboratory analysis (DNA, RNA and assisted pigments extraction), bioinformatic analysis (genomics, transcriptomics), statistical analysis, writing

Manuscript in preparation

4.1 ABSTRACT

Filamentous heterocystous cyanobacteria belonging to the genus *Nostoc* are true ecosystem engineers in dry and oligotrophic environments worldwide due to their capacity to fix atmospheric N_2. In Antarctica, the genus is often a dominant member in both terrestrial and lacustrine habitats, yet little is known about its specific adaptations to thrive in both extremely dry and wet conditions, and during its dispersal between habitats. Here we studied the response to short-term desiccation exposure and rehydration of two Antarctic terrestrial and freshwater strains belonging to the same *Nostoc* species. To achieve this, we measured concentrations of photosynthetic pigments and the osmolytes trehalose and sucrose, analysed the photosynthetic efficiency, and performed a transcriptomic (RNA-seq) analysis of the two *Nostoc* strains after 3h of desiccation, followed by rehydration after 10 min, 24h and up to 72h. Both strains reacted to dehydration by accumulating sucrose, whereas trehalose was present in lower concentrations. Only the freshwater strain showed a recovery in chlorophyll *a* content after 72h of rehydration. However, the photosynthetic efficiency remained below the original levels measured before desiccation in both strains. Transcriptomics profiles showed that both strains protected their cells during dehydration by inducing stress-related genes, such as those for the production of carotenoids, trehalose synthase and nitrogen fixation-related genes. The terrestrial strain responded with the up-regulation of a higher number of genes compared to the freshwater strain. The photosynthetic metabolism, however, slowly decreased after 24h of rehydration as evidenced by the decrease in expression of genes related to phycobilisomes and photosystems. By contrast the *psbA2* gene, encoding the D1 protein synthase necessary for PSII, was found to be significantly up-regulated under desiccation in the terrestrial ULC180, but not in the freshwater ULC008. These results suggest habitat specific adaptions to environmental stress in cyanobacteria, and provide novel insights into the strategies related to the survival and adaptation of non-model Antarctic *Nostoc* strains to desiccation and rehydration events during the first 3 days experienced in extreme environments.

KEYWORDS

Desiccation – rehydration – cyanobacteria – transcriptomics – ecophysiology – Antarctica

4.2 INTRODUCTION

Only few biota are adapted to thrive in the extreme conditions experienced in the Antarctic (Pearce 2012). The cyanobacterial genus *Nostoc* is one these taxa and is one of the dominant member of benthic microbial communities in lakes, seepages, meltwater streams and terrestrial biotopes on soils and rocks in the Antarctic (Jungblut and Warwick 2017). In these environments, *Nostoc* species are regarded as ecosystem engineers because they are one of the main producers of organic carbon and capable of atmospheric nitrogen fixation. In lakes, they are part of the benthic microbial mats (Niederberger et al. 2012, Makhalanyane et al. 2015), and in terrestrial ecosystems, *Nostoc* colonizes the soil surfaces and often forms biological soil crusts (BSCs) together with other organisms such as lichens, mosses, fungi, heterotrophic bacteria, archaea, microalgae and other cyanobacteria (Weber et al. 2022, Jungblut and Warwick 2009). Particularly in terrestrial habitats, they are exposed to several extreme abiotic conditions, including prolonged periods of darkness alternating with periods with high intensities of photosynthetically active radiation (PAR) and ultra-violet radiation (UVR), air temperatures that average well below freezing all year round often accompanied by freeze-thaw cycles, and large variations in nutrient supply and conductivity (Cowan and Tow 2004, Jungblut and Warwick 2009). In lacustrine systems, the fluctuations in these environmental conditions are less extreme as the lake water provides a buffer against temperature change and high UVR and PAR. However, it has been shown that microbial mats can be dispersed after they became detached from their substrates as a result of oxygen bubbles being formed in their extracellular matrix. These so-called 'lift-off' mats may be blown by winds once they reach the lake surface, and be transported to another aquatic or terrestrial habitat. During this dispersal, these organisms experience similar environmental conditions as those experienced by their terrestrial counterparts (Dudeja et al. 2010).

In order to cope with these environmental stressors, *Nostoc*, and Cyanobacteria in general, possess defense or ecological strategies as evidenced by molecular, physiological, biochemical studies (Tamaru et al. 2005, Morgan-Kisset et al. 2006, Sinetova and Los 2016, Pessi et al. 2023).

One such strategy is the synthesis of exopolysaccharides (EPS), which form an extracellular sheath, which is crucial for their protection against UVR, desiccation and freezing stresses (Bebout and Garcia-Pichel 1995, Tamaru et al. 2005, Effendi et al. 2023). The EPS matrix allows water to be absorbed quickly and lost slowly, and stabilizes the cellular membrane during periods of desiccation (Grilli Caiola et al. 1993 and 1996, Tamaru et al. 2005). In terrestrial environments, the EPS matrix also stabilizes soils by gluing their particles together to form soil aggregates (Büdel et al. 2016), which reduces erosion and stabilizes the substrate (Pointing and Belnap 2012). In addition, the protection strategy against photo-oxidative stress due to intense light and UV radiation, is assured by the production of mycosporine-like amino acids (MAAs), the extracellular pigment scytonemin (withinthe EPS matrix) and intracellular photoprotective carotenoid pigments (Wada et al. 2013, Gao 2017), which inhibit the formation of reactive oxygen species and dissipate the energy as heat (ROS; Conde et al. 2007, Wada et al. 2013). Frequent freeze-thaw cycles are experienced in biological soil crusts and lacustrine shorelines. These events may cause dramatic osmotic stress to cyanobacterial cells, which react by accumulating a wide range of compatible solutes, also called osmolytes, which ensure the uptake of water in order to maintain turgor and cellular growth (Brown 1976). Cyanobacteria have been classified, as low, mild or high salt or drought-tolerant, based on the osmolytes they produce. The low tolerant taxa often accumulate disaccharides (such as trehalose and sucrose), while the mild tolerant species use heterosides (such as glucosylglycerol). The high salt or drought tolerant taxa use derivatives of amino acids, such as glycine betaine and glutamate betaine (Kirsh et al. 2019 and references therein). These compounds might be transported from extracellular sources or synthetized *de novo*. In addition, other strategies may play a role in the level of drought-resistance. Similar to other desiccation-tolerant organisms, it is known that *Nostoc* members may become inactive while they are able to maintain their cellular components during desiccation, and rapidly resume metabolism once rewetted (Potts 1994 and 2001, Büdel et al. 2008). The freshwater model strain, *Anabaena* (*Nostoc*) PCC 7120 could only tolerate mild desiccation and 95 % of the cells died after 22h of desiccation (Katoh et al. 2004, Higo et al. 2007). By contrast, the terrestrial strain *Nostoc flagelliforme* could survive for many years under complete desiccation and recovered its

photosynthetic activity quickly after rehydration (Wang et al. 2018). Moreover, cells of the terrestrial taxon *N. commune* survived up to 100 years of desiccation (Katoh et al. 2012).

The genomic basis of the response of Cyanobacteria to desiccation is only recently being studied and understood. Terrestrial *Nostoc* species appear to have larger genomes and an increased copy number of the core genes compared to freshwater ones (Juyabad et al. 2022). However, the functions of only a limited number of desiccation-inducible genes of freshwater *Nostoc* sp. have been elucidated so far (Katoh et al. 2004, Higo et al. 2006, Yoshimura et al. 2007, Sen et al. 2017, Juyabad et al. 2022). For instance, genes involved in trehalose and EPS production were demonstrated to be responsible of the desiccation tolerance in both the terrestrial *Nostoc* sp. HK-0 and the freshwater strain *Anabaena* PCC 7120 (Higo et al. 2006, Yoshimura et al. 2007, Juyabad et al. 2022). Interestingly, also nitrogen fixation genes were induced by desiccation in *Anabaena* PCC 7120 (Sen et al. 2017, Katoh 2021) as well as by cold temperatures in *N. flagelliforme* (Gao et al. 2021). Overall, it seems that terrestrial *Nostoc* strains are genetically more equipped to cope with severe conditions such as short and long-term desiccation stress than their freshwater relatives. However, although desiccation-resistance of *Nostoc* strains originating from hot deserts have been widely studied (e.g. *Nostoc* sp. MG11 , *Nostoc flagelliforme*, *Anabaena* (*Nostoc*) sp. PCC 7120; Khani-Juyabad et al. 2022, Li et al. 2022, Xu et al. 2022, Yadav et al. 2021), to our knowledge, only a few studies exist on desiccation resistance of cyanobacterial strains isolated from Antarctic deserts (i.e. *Nostoc* sp. strain SO-36; Effendi et al. 2022) or cold environments (e.g. *Nostoc flagelliforme*; Gao et al. 2021). This knowledge is however needed to help underpinning their physiological and molecular strategies to successfully colonize one of the most extreme environments on Earth.

Here, we compared the ecophysiology and transcriptomic response to dehydration and rehydration for 3 days of a pair of *Nostoc* strains belonging to the same species, but originally isolated from terrestrial and lacustrine habitats from ice-free areas in Antarctica. To achieve this, we measured the concentration of the osmolytes trehalose and sucrose, the pigment concentration, as well as the photosynthetic efficiency in order to integrate physiological strategies with gene expression during dehydration and rehydration after three time points (10

min, 24h and 72h). We hypothesized that i) both the terrestrial and the freshwater strain possess genetic and ecophysiological mechanisms to protect themselves from desiccation and react relatively quickly to rehydration due to their specific adaptation to Antarctic environments, and ii) the freshwater and the terrestrial strain have a different response to both desiccation and rehydration, with the former responding less quickly compared to the latter strain despite their close relatedness.

4.3 MATERIALS & METHODS

4.3.1 CYANOBACTERIAL STRAIN AND CULTURE CONDITIONS

Unicyanobacterial strains of *Nostoc* sp. ULC008 and ULC180 from the BCCM/ULC Cyanobacterial Collection share 97.7 % of ANI similarity (see methods below) though they were collected from distant regions (ca. 2000 km apart) and different habitats (freshwater vs. soil) in Eastern Antarctica. *Nostoc* sp. ULC008 was isolated from a benthic mat (76°24' S, 69°24' E) situated in Progress Lake of the Larsemann Hills (Taton et al. 2006) that was collected in 1998 and isolated/cultivated in 1999. *Nostoc* sp. ULC180 originated from a BSC (72°01' S, 22°56' E) located on the granitic nunatak of Tanngarden in the Sør Rondane Mountains (Pushkareva et al. 2018) that was collected in 2011 and isolated/cultivated in 2012. Progress Lake has a maximum depth of 34 m and limited bioturbation (as a result of the absence of larger metazoa), low wind-induced hydrodynamic mixing due to the thick ice cover lasting more than 10 months per year and slow decomposition, which are thought to contribute to the strongly preserved nature of the laminated deposits occurring in such deep lakes (Sabbe et al. 2004). In contrast, in the terrestrial biotopes, soil temperature fluctuations occur during summer in Tanngarden where daily ranges were recorded between -2 and +12 °C (Pushkareva et al. 2018). Organisms inhabiting these soils are therefore subjected to daily freeze-thaw cycles. Prior to the experiment, both strains were cultivated in flasks of 1L containing 800 mL of BG11 without nitrogen (medium BG-11_0) culture medium (Rippka et al. 1979), for 1 month under 6 µmol photons m^{-2} s^{-1} and continuous light at 12 °C (same conditions as in the culture collection) and continuous shaking at 80 rpm (IKA KS 4000) to avoid clumps formation. These two strains were selected for the experiment because

they were rather easy to grow under laboratory conditions compared to other “pair” of strains that were similarly sampled from a freshwater and a soil habitat.

4.3.2 TESTING DESICCATION STRESS INDUCED AND RE-WETTING IN ULC008 AND ULC180

After cultivating ULC008 and ULC180 in BG-11_0 medium, the biomass was centrifuged to obtain a homogeneous and concentrated inoculum after removal of the supernatant. Three mL of this concentrated inoculum were filtered on GF/F filters of Ø 25 mm (Whatman) for each replicate. Four replicates per treatment (D, RW1, RW2 and RW3) and measurement type (RNA, pigment content, and osmolyte concentration) were set up (i.e. 12 filters per treatment). The controls consisted of analyzing samples immediately after filtration (C). In controls and during treatments, the effective quantum yield of chlorophyll *a* fluorescence of PSII (QY) was monitored using a pulse-amplitude modulated (PAM) fluorimeter (AquaPen AP-C, Photon Systems Instruments, CZ) using the QY protocol as described below. The desiccation treatment consisted of transferring the filters into a Plexiglas chamber filled with 100 g of silica gel similarly to Karsten et al. (2014). After approximately 3h, the desiccation process was considered to be finalized when the QY values immediately reached values close to zero, and 24 filters (2 strains x 4 replicates x 3 treatments) were sampled (D). Immediately afterwards, the silica gel was replaced by 100 mL of sterile water and the dried filters were wetted with 200 µL of $BG11_0$ medium. Filter replicates were harvested 10 min (RW1), 24h (RW2) and 72 h (RW3) after wetting. Twelve replicates per treatment were then stored at -80 °C until RNA, pigments and osmolytes (trehalose and sucrose) extractions were performed. However, in some cases, during RNA extractions only three replicates instead of four were sent for sequencing, i.e. those with the highest RNA quality as measured using an Agilent Technologies 2100 Bioanalyzer.

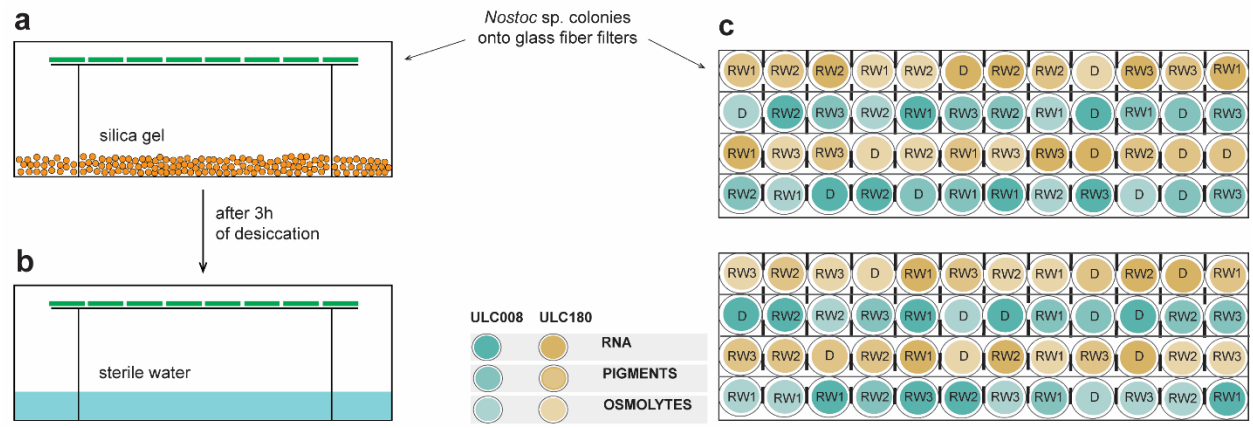

Fig. 4.2 Experimental design. *Side view of the desiccation chambers during (a) desiccation and (b) after rehydration (200 µL of sterile culture medium was also added onto the filters in order to rewet the colonies). (c) Top view of the two desiccation chambers used for the experiments. Filters with the freshwater ULC008 (in blue) and the terrestrial ULC180 (in orange) strains were randomly positioned inside both chambers. Color intensity denotes the performed analysis: 100 % is RNA extraction for transcriptomic analysis; 75 % pigments (see methods for the entire list) extraction; 50 % osmolytes (trehalose and sucrose) extraction. Continuous irradiance intensity was set at 6 µmol* m^{-2} s^{-1} *and temperature at 12 °C during 3 days, similarly to their usual culture conditions.*

4.3.3 PHOTOSYNTHESIS PERFORMANCES

Prior to the desiccation experiment (C) and during each treatment (D, RW1, RW2 and RW3), QY was monitored without disturbing the filters as an indicator of the PSII efficiency (**Fig. 4.2**). The optic fiber was placed ~ 0.5 cm above the illuminated samples and measurements were performed as a reaction to a saturating red-light pulse. QY represent measurements of the actual quantum yield (Φ_2, QY), determined using the AquaPen QY protocol. Calculations were performed according to Roháček (2002) as follows:

$$\Phi_2 = (F'_m - F_s) / F'_m$$

in which F_S is the steady-state fluorescence and F'_m is the maximum fluorescence in ambient light. The measurements were carried out on all the individual filters containing the cyanobacterial suspension that were in the chambers, prior to harvest them during each treatment. Desiccated colonies were harvested once QY values were close to zero, otherwise RNA extraction gave poor yields (data not shown).

4.3.4 PIGMENTS AND OSMOLYTES EXTRACTIONS

During the experiment at each time point (including the controls) chlorophylls and carotenoid production was monitored by quantifying the following pigment content: Chlorophyll *c3*, Chlorophyll *c2*, Chlorophyll *c1*, Chlorophyllide *a*, Pheophorbide *a*, Peridinin, 19'-Butanoyloxyfucoxanthin, Fucoxanthin, Neoxanthin, Prasinoxanthin, Violaxanthin, 19'-Hexanoyloxyfucoxanthin, Astaxanthin, Myxoxanthin, Diadinoxanthin, Mutatoxanthin, Antheraxanthin, Alloxanthin, Diatoxanthin, Zeaxanthin, Lutein, Canthaxanthin, Chlorophyll *b*, Crocoxanthin, α-cryptoxanthin, β-cryptoxanthin, Echinenone, Chlorophyll *a*, Lycopene, Pheophythin *a*, α-carotene, β-carotene via HPLC (following Van Heukelem et al. 1994; Fig. S4.1) on an Agilent 1200 system equipped with an Agilent Eclipse XDB-C8 column (temperature 60 °C), auto-sampler, pump with flow rate of 1.0/1 mL min^{-1} and binary gradient with a run time of 36 min, and diode array detection at 450 and 665nm. The mobile phase consisted of pure methanol (B) and a 7:3 methanol:TBAA mixture (A), with gradients set from 95 % to 5 % for B and from 5 % to 95 % for A. Pigments were identified from chromatograms targeting 450nm (carotenoids and chlorophylls other than chlorophyll *a*) and 665nm (chlorophyll *a* and its derivatives), based on their absorption spectra and the retention time of standards (Roy et al. 2011) using the Agilent LC/MSD ChemStation. Pigment concentrations were calculated based on known response factors of the standards derived from DHI Denmark.

Trehalose and sucrose concentrations were quantified (Fig. 4.3) in Gembloux Agro-Bio Tech facultyby freeze-drying the filters, eluting them and measuring with a Dionex System HPAED-PAD equipped with a CarboPAC PA100 column of 4*250 mm. The eluents used were: A) HPLC-grade water + 10 mM NaOH, and B) HPLC-grade water + 100 mM NaOH + 600 mM of Sodium acetate. The system was operated at 30 °C with a selected flow rate of 1 mL min^{-1}.

4.3.5 DNA EXTRACTION AND GENOME SEQUENCING

Prior to DNA extraction 200 mL of fresh cultures were centrifuged at 12,000 g and the pellets were washed in medium $BG\text{-}11_0$ several times in order to limit heterotrophic bacterial contamination during the DNA extraction. Genomic DNA was extracted in triplicates using the GenElute™ Bacterial Genomic DNA Kit (Sigma-Aldrich) following the standard protocol for Gram-

negative bacteria with one modification, i.e. a first step of lysozyme digestion for 30 mins prior to the DNA extraction. DNA quality and yield were determined via electrophoresis gel (0.8 % agar, 80 V, 100 min) and the Quant-iT^{TM} PicoGreen^{TM} dsDNA Assay (Invitrogen). Finally, the DNAs from the three extractions of each strain were mixed to obtain enough material and sent to the GIGA-Genomics sequencing platform (University of Liège) where the libraries were prepared. Two different DNA sequencing technologies were applied to obtain better quality and coverage of the genomic DNA sequences. Short paired-end reads sequencing was performed on an Illumina MiSeq v3 sequencer on libraries (2x300 bp, coverage 100x) prepared following the Nextera XT DNA Library Preparation Kit protocol (Illumina, San Diego, CA, USA). Long reads sequencing was applied on a MinION Flow Cell R9.4.1 (Oxford Nanopore Technologies, UK) after Barcoding and Ligation sequencing preparation (coverage 100x) using the Library Prep Native barcoding genomic DNA Kit (EXP-NBD114/LSK109).

4.3.6 RNA EXTRACTION AND TRANSCRIPTOME SEQUENCING

All harvested filters were instantly quenched in liquid nitrogen after retrieving them from the -80 °C freezer and quickly homogenized in a chilled sterilized mortar (in a bead-beater, retch, for 5 min at 30 hertz, info: https://www.retsch.com/products/milling/ball-mills/mixer-mill-mm-400/). The powder was immediately processed with either the RNeasy PowerSoil kit (QIAGEN) or the PowerBiofilm kit (QIAGEN), which performed better for the most stressed cultures (i.e. the desiccated and the rehydrated colonies (probably because of a higher amount of produced EPS and or osmolytes). The quality of the resulting RNA extractions was assessed on a BioAnalyzer instrument (Agilent Technologies, SantaClara, CA, United States) and subsequently sent to GENEWIZ for library prep and sequencing (i.e. RIN values > 8). Briefly, RNA samples were quantified using Qubit 4.0 Fluorometer (Life Technologies, Carlsbad, CA, USA) and RNA integrity was checked with RNA Kit on Agilent 5300 Fragment Analyzer (Agilent Technologies, Palo Alto, CA, USA). ERCC RNA Spike-In Mix kit (Cat. 4456740) from ThermoFisher Scientific, was added to normalized total RNA prior to library preparation following manufacturer's protocol. rRNA depletion was performed using NEBNext rRNA Depletion Kit (Bacteria). RNA sequencing library preparation was performed using NEBNext Ultra II RNA Library Prep Kit for Illumina by following

the manufacturer's recommendations (NEB, Ipswich, MA, USA). Briefly, enriched RNAs were fragmented according to manufacturer's instruction. First strand and second strand cDNA were subsequently synthesized. cDNA fragments were end repaired and adenylated at 3' ends, and universal adapter was ligated to cDNA fragments, followed by index addition and library enrichment with limited cycle PCR. Sequencing libraries were validated using NGS Kit on the Agilent 5300 Fragment Analyzer (Agilent Technologies, Palo Alto, CA, USA), and quantified by using Qubit 4.0 Fluorometer (Invitrogen, Carlsbad, CA). The sequencing libraries were multiplexed and loaded on the flow cell on the Illumina NovaSeq 6000 instrument according to manufacturer's instructions. The samples were sequenced using a 2x150 Pair-End (PE) configuration v1.5. Image analysis and base calling were conducted by the NovaSeq Control Software v1.7 on the NovaSeq instrument. Raw sequence data (.bcl files) generated from Illumina NovaSeq was converted into fastq files and de-multiplexed using Illumina bcl2fastq program version 2.20. One mismatch was allowed for index sequence identification. In order to test if the use of different RNA extraction kits could bias the results, we extracted the RNA from liquid cultures of ULC008 and ULC180 with both kits (Fig. S4.2).

4.3.7 BIOINFORMATIC ANALYSES

4.3.7.1 Genome assembly

The Nanopore reads were assembled using the workflow Assembly.nf v2.0.0 of the GEN-ERA toolbox (Cornet et al. 2023). Briefly, long reads were assembled using Flye (metagenome mode; v2.9b1774; Kolgomorov et al. 2020). Afterwards, short reads were trimmed with fastp (v0.23.1; Chen et al. 2018) and aligned to the assembled genome with bwa-mem v0.7.17 (Wang et al. 2019) and samtools (v1.13; Li et al. 2009). Then, the assembled genome was polished with pilon (v1.24; Walker et al. 2014) using the indexed bam files as input. Binning to remove contigs from non-cyanobacterial contaminants was performed with CONCOCT (v1.1; Alneberg et al. 2014). Qualityestimations were performed with a combination of Checkm (v1.1.3; Parks et al. 2015), GUNC (v1.0.5; Orakov et al. 2021), BUSCO (v5.3.0; Simão et al. 2015), Kraken (v2.1.2; Wood et al. 2019), EukCC (v2.1.1; Saary et al. 2021) and QUAST (v2.3; Gurevich et al. 2013).

4.3.7.2 Genome annotation

Annotation was performed with a rapid prokaryotic sequence annotation algorithm implemented in Prokka (v1.14.6; Seemann 2014) which uses Prodigal (v2.6.3; Hyatt et al. 2010). Functional annotation was further inferred using Mantis v1.5.0, with default options, (Quéiros et al. 2021) integrated in the GEN-ERA toolbox (Cornet et al. 2023).

Phylogenomic analysis of Nostoc strains

Genome sequences corresponding to the Nostocaceae family in RefSeq (Pruitt et al. 2007, O'Leary et al. 2016) and GenBank (Sayers et al. 2022; Clark et al. 2016) were downloaded on December 4, 2022. Genomes corresponding to *Gloeobacter* genus in RefSeq (Pruitt et al. 2007; O'Leary et al. 2016) were downloaded as outgroup. An average nucleotide identity (ANI) for each public genome of GenBank against our assembled genomes was performed using fastANI v1.33 (Jain et al. 2018) integrated in the GEN-ERA toolbox (Cornet et al. 2023). All Genomes from RefSeq and genomes from GenBank with an ANI greater than 85 % were kept for phylogenomics analysis. 113 Genomes were used for orthology inference with OrthoFinder (Emms & Kelly. 2019), using the workflow, Orthology.nf v1.0.3 from the GEN-ERA toolbox (Cornet et al. 2023). 331 core genes, present in unicopy in all genomes at the exception of the outgroup, were used for Phylogenomic inference. These core genes were used with the workflow Phylogeny.nf from the GEN-ERA toolbox (Cornet et al. 2023) to generate a supermatrix of 113 x 93,048 conserved positions. In brief, genes were aligned with MUSCLE v3.8.32 (Edgar 2003), unambiguous position were selected with BMGE v1.12 (Criscuolo and Gribaldo 2010) using a medium masking, concatenation of genes was performed with ScaFoS v1.15 (Roure et al. 2007) and tree was inferred with RAxML v8.2.12 (Stamatakis et al. 2008) using 100 rapid bootstrap under the PROTGAMMALGF model. The dataset was further subsampled to the largest monophyletic clade corresponding to ULC008 and ULC180, with 60 genomes. The workflows Orthology.nf and Phylogeny.nf were run again with same parameters on this dataset (60 Nostocaceae genomes + 3 Gloeobacter) producing 638 core genes, a supermatrix of 63 x 184,325 conserved position. Hundred jackknife matrices of 100,000 conserved position were generated from the same dataset and RAxML v8.2.12

(Stamatakis et al. 2008) was used with fast option, under PROGAMMALGF model, to generate 100 trees. Jackknife tree is a consensus of these 100 trees.

4.3.7.3 Transcriptome analysis during desiccation and re-hydration

The quality of raw reads was controlled by FastQC v0.11.5 (https://github.com/s-andrews/FastQC) with default parameters, rRNA sequences were removed using SortMeRNA v1.9 (Kopylova et al. 2012). The clean reads of each transcriptome were aligned with the corresponding reference annotated genome using STAR v2.7.6a (https://github.com/alexdobin/STAR) and HTSeq v2.0.2 was utilized to count the reads that are mapped to each gene (Anders 2010). For differential testing, normalization factors were computed by the DESeq2's median of ratios and together with the differentially expressed genes (DEGs) analyses were processed with DESeq R package v1.30.1 (Anders a Huber 2010). The means and standard deviations of the ratios of the transcript levels at each treatment (D, RW1, RW2, RW3) relative to those of the control (C) were calculated as base-2 logarithms. A gene was considered as up-regulated when its mean relative ratio was greater than 2 with adjusted P-value (Benjamini & Hochberg correction) of less than 0.01. A gene was considered as down-regulated when its mean relative ratio was less than -2 with adjusted P-value (padj; Benjamini & Hochberg correction) (Table 4.2, Table S4.3). Heatmap was created using the ComplexHeatmap R package v2.15.1 (Gu 2022) with the normalized, transformed and scaled counts of a selection of genes, based on their sigificant difference.

4.3.7.4 STATISTICAL ANALYSES

The effect of desiccation and rehydration treatments were investigated on the QY values, and concentrations of pigments, trehalose and sucrose for each strain. Normality and homoscedasticity of data were checked with the Shapiro-Wilk (*shapiro.test* function, stats R package, v4.0.5; Development Core Team 2021), and Levene tests (*leveneTest* function, car R package, v3.1-1; Fox and Weisberg 2011), respectively. In order to determine whether the median between treatments of every measured parameter were significantly different between them, the anova function (*aov*, stats R package) followed by the Tukey post hoc test (*TukeyHSD*

function, stats R package) were applied when data met the normality and homoscedasticity criteria, otherwise the non-parametric Kruskal-Wallis test (*kruskal.test* function, stats R package) followed by the multiple pairwise comparison Dunn's test (*dunn.test* R package, v1.3.5) were applied. PCA of the different transcriptomic samples was conducted to examine intrinsic clusters and variations using the *plotPCA* function after variance stabilizing transformation of the DESeq2 R package. Figures were plotted using the ggplot2 library (v3.4.1; Wickham 2016). All analyses were performed using R v4.0.5 (Development Core Team 2021).

4.4 RESULTS

4.4.1 ECOPHYSIOLOGICAL ANALYSES

4.4.1.1 Photosynthesis performance

We monitored the effect of the desiccation process by measuring the photosynthetic quantum yield of PSII (QY) of light-exposed cells. QY values before filtration were 0.497 ± 0.08 in ULC008 and 0.580± 0.06 in ULC180 (Fig. 4.3, Tables S4.1-2). The QY values of both strains significantly decreased on average by 96 % in ULC008 (0.019 ± 0.03) and 94 % in ULC180 (0.034 ± 0.05) under treatment D compared with the controls (Fig. 4.3, Tables S4.1-2). QY values immediately increased after rehydration (RW1: 0.226 ± 0.14 in ULC008 and 0.295 ± 0.15 in ULC180), and showed similar values during the rehydration period, with a high variability among the replicates (RW2: 0.274 ± 0.100 and 0.262 ± 0.087 in ULC008 and ULC180, respectively; RW3: 0.240 ± 0.097 and 0.332 ± 0.204 in ULC008 and ULC180, respectively). However, none of the strains was able to reach the initial QY values (C) after 72 hours (Fig. 4.3, Tables S4.1-2).

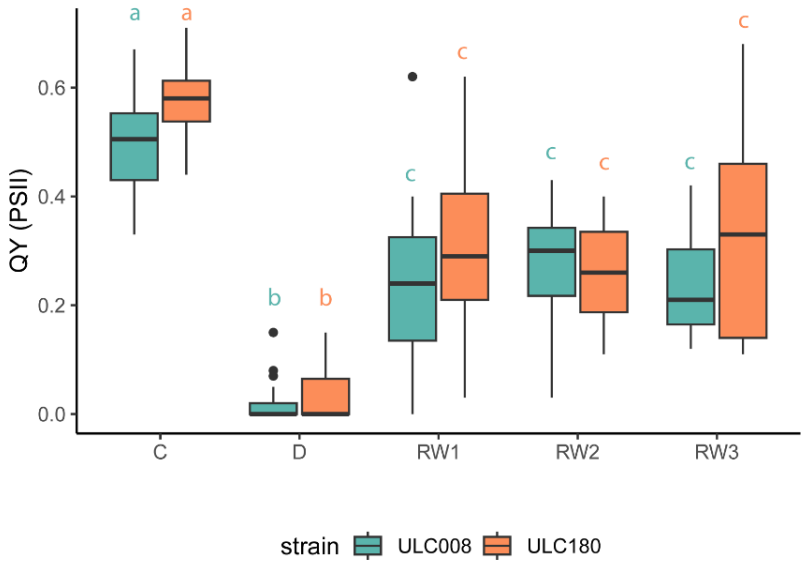

Fig. 4.3 Boxplots of the QY of PSII of the terrestrial Nostoc sp. ULC180 (in orange) and aquatic Nostoc sp. ULC008 (in blue) per treatment *(C = control, D = desiccation, RW1 = 0 min after wetting, RW2 = 24h after wetting, and RW3 = 72h after wetting). For each treatment, measurements were performed on all the available filters inside the chamber (median ± 75 to 25 percentile, n > 4). Different letters above the barplots indicate significant differences (one-way ANOVA or Kruskal-Wallis test; p < 0.05) among treatments within each strain.*

4.4.1.2 Pigments

The same pigments were detected in both strains. The most abundant pigments were the chlorophylls chlorophyllide *a* (chlide *a*), chlorophyll *a* (chl *a*) and pheophorbide *a* (phide *a*, shown in Fig. S4.1), followed by the carotenoids echinenone (echin), myxoxanthophyll (myxo) and β-carotene (b-car; Fig. 4.4). The carotenoid canthaxanthin (cantha) was present in lower abundance which is shown in Fig. S4.1 and Table S4.1. Concentrations of chl *a* and its precursor, chlorophyllide *a,* followed a different pattern in both strains (Fig. 4.4). While chlorophyllide *a* concentration decreased after 72h of rehydration in both strains (~ -80 % in both strains from D), its concentration showed a significant steep increase during desiccation in the freshwater strain (+41 %), but not in the terrestrial one (-5 %; Fig. 4.4, Tables S4.1-4.2). The steep increase of chlorophyllide *a* in the freshwater ULC008 during desiccation corresponded to a decrease in chl *a* (-13 %), although this trend was not significant (Fig. 4.4, Tables S4.1-2). Its concentration significantly decreased after 24h of rehydration (4383 ± 404 µg L^{-1}) followed by a steep increase

after 72h (5679 ± 888µg L^{-1}), suggesting a complete recovery from desiccation after three days. Similarly to the freshwater strain, also the terrestrial ULC180 showed no significant change in chl *a* concentration during desiccation (C: 5365 ± 326 µg L^{-1}; D: 5415 ± 247 µg L^{-1}), but a significant decrease was observed after 24h of rehydration (RW2: 4040 ± 816 µg L^{-1}). In contrast to the freshwater strain, however, chl *a* concentration did not show a recover after 72h of rehydration (4526 ± 383 µg L^{-1}; Fig. 4.4, Tables S4.1-4.2). Similarly, the freshwater ULC008 strain showed a decrease in chl *a* concentration and was the only one reaching the starting values of chl *a* (C: 5661 ± 240 µg L^{-1}) after 72h of rehydration (5679 ± 888 µg L^{-1}; Fig. 4.4, Tables S4.1-4.2).

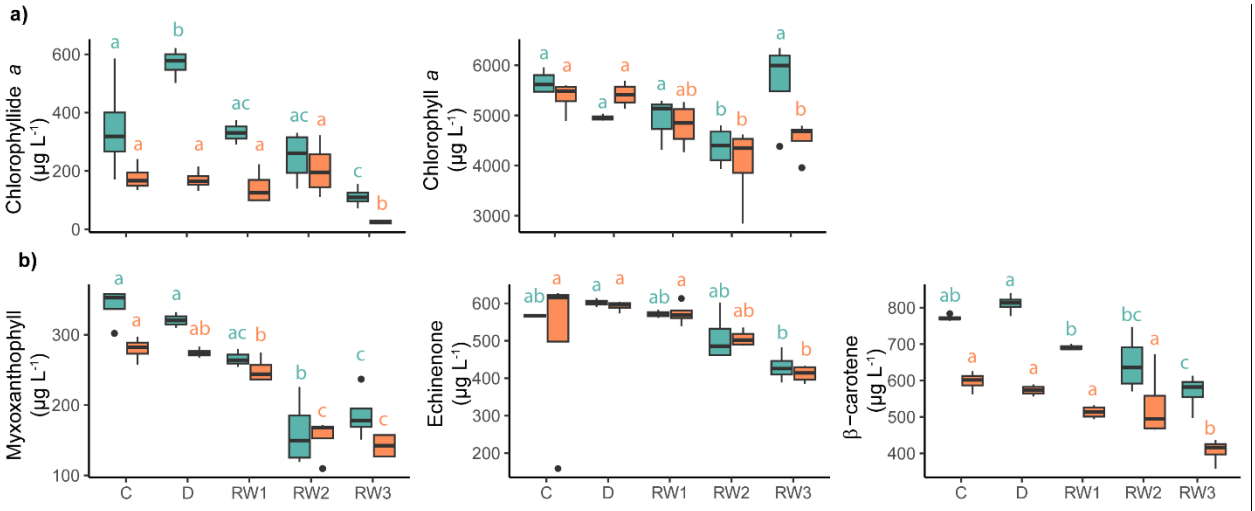

Fig. 4.4 Boxplots of the pigment content (in µg L^{-1}) of the terrestrial Nostoc sp. ULC180 (in orange) and aquatic Nostoc sp. ULC008 (in blue) per treatment. *(a) represents the chlorophyll a and its precursor chlorophyllide a and (b) the carotenoids myxoxanthophyll, echinenone, β-carotene (median ± 75 to 25 percentile, n = 4). Different letters above the barplots indicate significant differences (one-way ANOVA or Kruskal-Wallis test; p < 0.05) among treatments within each strain.*

The β-carotene concentration was higher in the freshwater strain (C: 772 ± 8.46 µg L^{-1} in ULC008 and 598 ± 26.9 µg L^{-1} in ULC180) and it was significantly lower after 72h of rehydration (RW3: 407 ± 34.0 µg L^{-1}; 569 ± 50.5 µg L^{-1} in ULC008 and ULC180, respectively) compared to the concentration under desiccation (Fig. 4.4, Tables S4.1-2). Furthermore, the concentration of two of the specific cyanobacterial carotenoids, myxoxanthophyll and echinenone, showed a similar

decrease in both strains with time. However, in the terrestrial strain the decrease of echinenone concentration was not significant until 72 hours of rehydration compared with the control (C: 504 ± 230 μg L^{-1}; RW3: 411 ± 23.1 μg L^{-1}) and a decrease was also observed in ULC008 after 72h of rehydration, although not significantly compared to the control (C: 567 ± 4.19 μg L^{-1}; RW3: 430 ± 39.1 μg L^{-1} in ULC008; Fig. 4.4, Tables S4.1-2). On the other hand, myxoxanthophyll concentrations were already significantly lower at RW2 for both strains (C: 342 ± 26.9 μg L^{-1}; RW2: 161 ± 49.0 μg L^{-1} in ULC008 and C: 280 ± 16.8 μg L^{-1}; RW2: 154 ± 29.7 μg L^{-1} in ULC180; Fig. 4.4, Tables S4.1-2). Moreover, the freshwater strain showed a significant increase of myxoxanthophyll concentrations at RW3 (186 ± 36.3 μg L^{-1}) compared with RW2, suggesting a sign of recovery, which was not observed in the terrestrial strain (RW3: 142 ± 17.9 μg L^{-1}; Fig. 4.4, Tables S4.1-2).

4.4.1.3 Osmolytes

The freshwater strain showed higher trehalose (C: 104 ± 61.4 mg mL^{-1}) and sucrose (C: 352 ± 12.6 mg mL^{-1}) concentrations compared to the terrestrial strain in the controls (C: 31.4 ± 10.9 mg mL^{-1} of trehalose and 181 ± 35.6 mg mL^{-1} of sucrose), but also under rehydration (Fig. 4.5, Tables S4.1-2). Trehalose was not significantly affected by desiccation in the freshwater strain (D: 119 ± 41.6 mg mL^{-1}), nor in the terrestrial strain (D: 103 ± 23.7 mg mL^{-1}). However, the freshwater strain significantly accumulated more trehalose at RW3 (513 ± 229 mg mL^{-1}), while the terrestrial one did not significantly accumulate trehalose with the experimental times (Fig. 4.5, Tables S4.1-2). Similarly, sucrose concentrations were not significantly affected by desiccation in both strains (D: 719 ± 209 mg mL^{-1} and 124 ± 5.79 mg mL^{-1} in the freshwater and the terrestrial strains, respectively; Fig. 4.5, Tables S4.1-2). Sucrose in the freshwater strain significantly increased at RW1 (823 ± 125 mg mL^{-1}; Tables S4.1-2) and again at RW3 (1580 ± 397 mg mL^{-1}) whilst in the terrestrial strain it significantly increased only at RW3 (643 ± 139 mg mL^{-1}; Fig. 4.5, Tables S4.1-2). Contrary to the trehalose pattern, during rehydration, the sucrose concentration increased continuously until 72h in the terrestrial strain (643 ± 139 mg mL^{-1}) and similarly to trehalose also in the freshwater strain (1580 ± 397 mg mL^{-1}; Fig. 4.5).

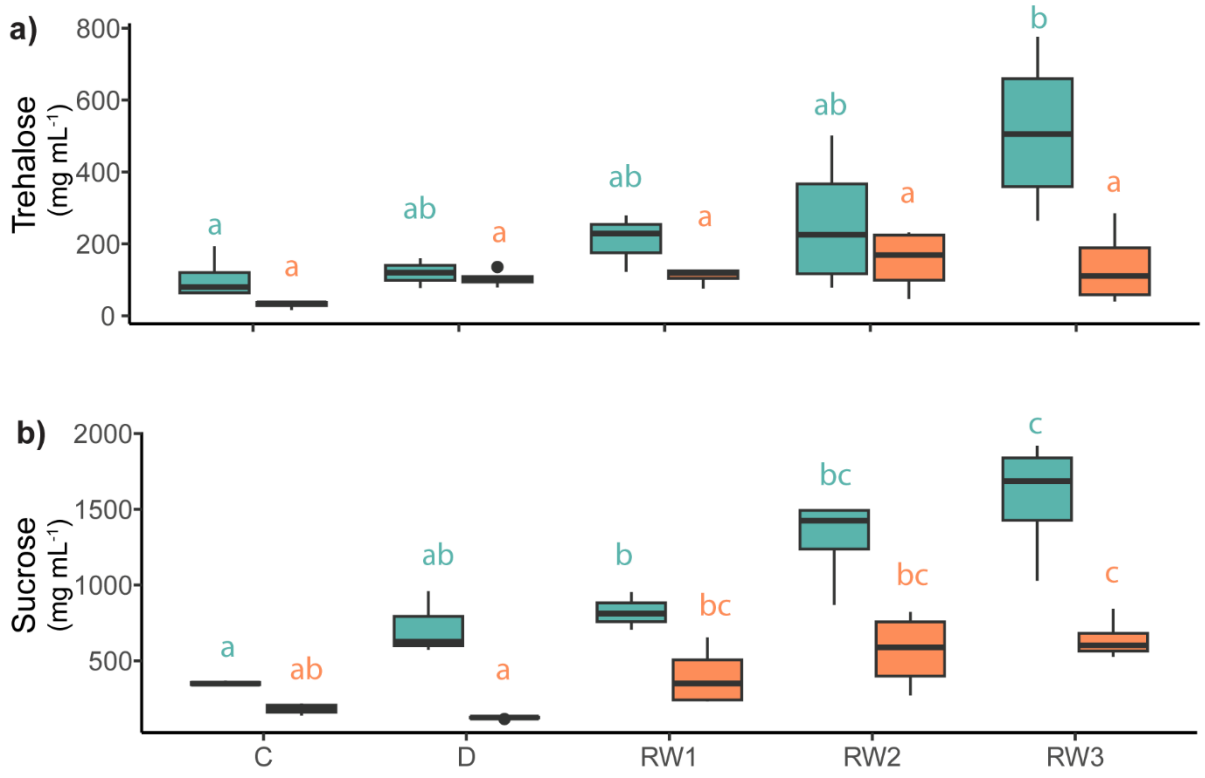

Fig. 4.5 Boxplot of trehalose (a) and sucrose (b) concentrations (mg mL^{-1}) in the terrestrial Nostoc sp. ULC180 (in orange) and aquatic Nostoc sp. ULC008 (in blue) per treatment *measured via HPAED-PAD (median ± 75 to 25 percentile, n=4). Different letters indicate significant differences (one-way ANOVA or Kruskal-Wallis test; p < 0.05) among treatments within each strain.*

4.4.2 REFERENCE GENOMES ASSEMBLY

After sequencing and assembling the long reads of the non-axenic freshwater *Nostoc* spp. ULC008 and terrestrial ULC180 cultures, we obtained 4 and 3 bins, respectively. For both strains, only one bin was identified as a cyanobacterium, and both showed a completeness of 99.11 % and a contamination of 0.44 % (computed via Checkm; Table 4.1). The non-cyanobacterial bins included 3 and 2 contigs, respectively, that were all assigned to the Pseudomonadota phylum. The freshwater strain had a larger genome size and a larger number of predicted CDS than the terrestrial strain (Table 4.1). Both genomes were assigned to *Nostoc* sp. and had a total length of 6,300,489 and 5,773,082 bp, and a GC% of 49.78 and 49.98, respectively (Table 4.1). The ULC008 bin was composed of 1 big contig (5,907,629 bp) and 2 small contigs, whereas the ULC180 bin

was composed just of 1 big contig (5,773,082 bp) (Table 4.1). Gene annotations by PROKKA resulted in 5734 CDSs, 8 rRNAs, 45 tRNAs, 1 tmRNA and 3 repeat regions for ULC008, and 5567 CDSs, 8 rRNAs and 47 tRNAs, 1 tmRNA and 3 repeat regions for ULC180 (Table 4.1). Protein-coding gene annotation was possible only for 34 and 35 % of the total CDSs in ULC008 and ULC180, respectively (Table 4.1).

Table 4.1. General features of the Nostoc spp. ULC008 (aquatic) and ULC180 (terrestrial) strains genomes.

Strains	Size (bp)	Completeness (%)	Contamination (%)	Contigs	GC (%)	Total genes	Total protein CDSs	Number / percentage of protein CDSs with function (%)	Number / percentage of protein CDSs without function (%)
Nostoc sp. ULC008	6,300,489	99.11	0.44	3	41.78	5,791	5,734	1,967 / 34	3,767 / 66
Nostoc sp. ULC180	5,773,082	99.11	0.44	1	41.98	5,626	5,567	1,941 / 35	3,626 / 65

4.4.3 PHYLOGENOMICS OF THE NOSTOCACEAE FAMILY

The two investigated genomes form a monophyletic cluster with only two other public genomes within the known biodiversity in Nostocales. This cluster is well supported by the two tested methods: 98 % by bootstrap (Fig. 4.6) and 100 % by jackknife (Fig. S4.3). This cluster shows the maximum support values for both methods. The two related public genomes (GCA_023522315.1 for *Nostoc* sp. CCCryo 231-06 and GCA_014324315.1 for *Nostoc* sp. HG1) were also isolated from Antarctica (Liu et al. 2022, Raymond et al. 2021). *Nostoc* sp. CCCryo 231-06 was isolated from permafrost soil and rock substrates in Victoria Land (70°30'S to 78°00'S, Liu et al. 2022), while *Nostoc* sp. HG1 was isolated from the Hughes glacier (77°44’S, 162°28’E; Raymond et al. 2021).

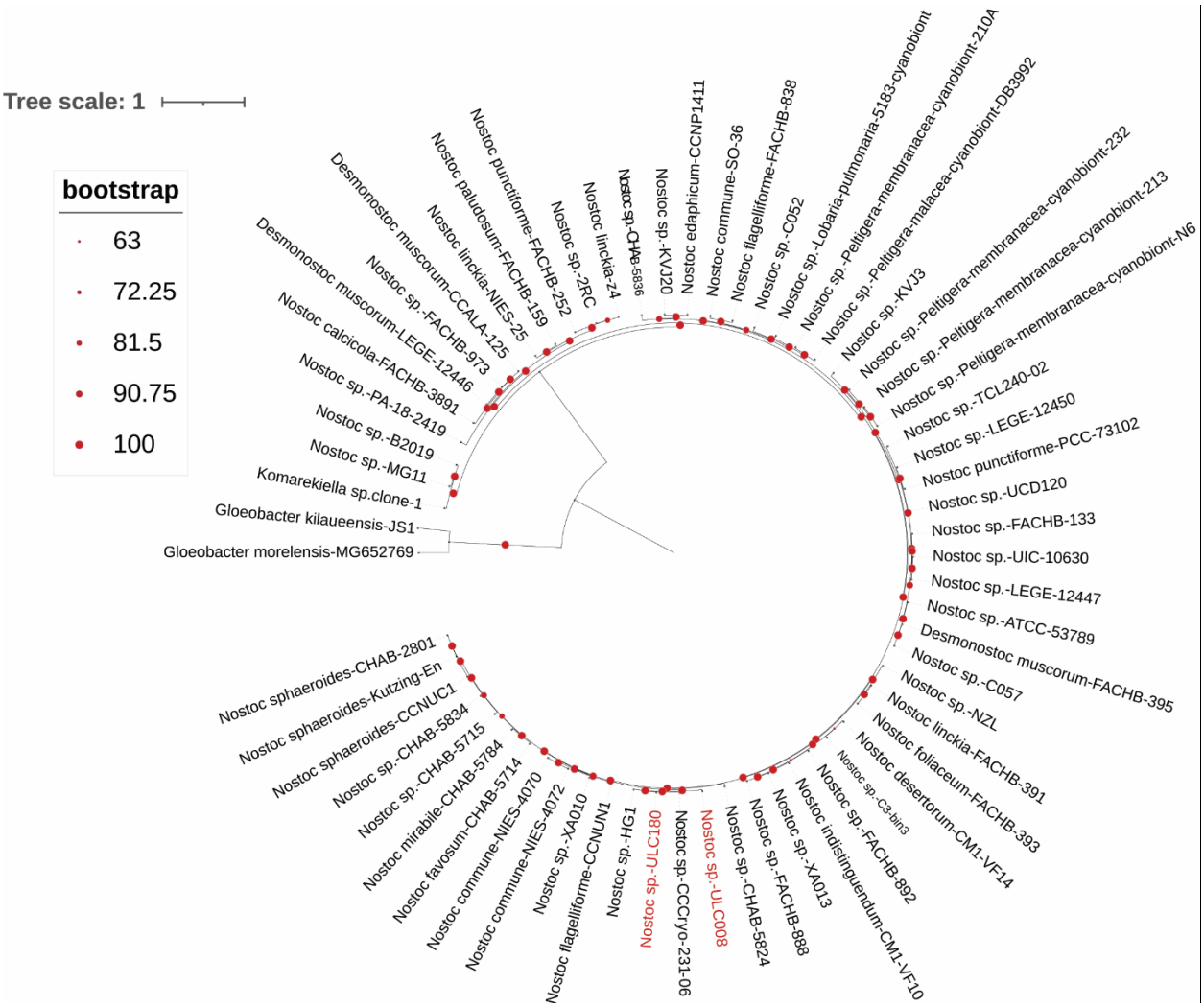

Fig. 4.6 Phylogenetic tree of all (63) the cyanobacterial genomes belonging to the Nostocaceae family downloaded from RefSeq constructed using the maximum-likelihood approach. *ULC008 and ULC180 highlighted in red, forming a cluster with other two terrestrial Antarctic genomes: Nostoc sp. HG1 (GCA_014324315.1) and Nostoc sp. CCCryo 231-06 (GCA_023522315.1).*

4.4.4 MAPPING TRANSCRIPTOMIC READS TO REFERENCE GENOMES

A total of 9,046,905 and 9,052,601 to 24,467,576 and 21,977,730 raw reads were generated for each sample of ULC008 and ULC180 strains, respectively. After the data were filtered, high quality 150-bp reads were selected for further analyses. A total of 6,764,624 to 21,062,868 and 7,355,899 to 19,741,910 clean non-rRNA reads were obtained from the raw reads in each sample of ULC008 and ULC180 strains, respectively. In total, 56 to 90 % and 53 to 80 %

uniquely mapped reads were matched to the sequenced reference genomes of ULC008 and ULC180, respectively.

4.4.5 TRANSCRIPTOME RESPONSE UNDER DESICCATION STRESS FOLLOWED BY RE-HYDRATION

The dehydration and rehydration response of the freshwater *Nostoc* sp. ULC008 involved a total of 209 DEGs, whereas the terrestrial *Nostoc* sp. ULC180 showed up to 437 DEGs. A total of 30 and 127 DEGs were identified during the desiccation treatment (D-C; Table 4.2) of the freshwater ULC008 and the terrestrial ULC180 strains, respectively, among which 21 and 118 were significantly up-regulated in ULC008 and ULC180, respectively. After 10 min of rehydration (RW1-C; Table 4.2), the number of up-regulated genes increased in both strains (50 over 60 and 202 over 218 for ULC008 and ULC180, respectively; Table 4.2). Once both strains had been rehydrated for 72 h, the number of down-regulated genes started to surpass the number of up-regulated ones, with 57 down-regulated genes over a total of 85 DEGs in ULC008, and 84 over a total of 182 in ULC180 (RW3-C; Table 4.2). Rehydration after 10 min showed a very low number of DEGs in both strains compared to desiccation (RW1-D: 3 and 0 in ULC008 and ULC180, respectively) whilst after 24h (RW2-D) and especially after 72h (RW3-D), it was evident an increased number of downregulated compared to up-regulated genes in both strains (Table 4.2).

Table 4.2. Number of DEGs per strain between the treatments with respect to controls. *Between brackets: + represents up-regulated genes; - represents down-regulated genes. The treatments compared are: control (C), desiccation (D), 10 min (RW1), 24h (RW2) and 72 h (RW3) after rehydration started.*

	D-C	RW1-C	RW2-C	RW3-C	RW1-D	RW2-D	RW3-D
	30	60	135	85	3	36	48
ULC008	(21+ ; 9-)	(50+ ; 10-)	(73+ ; 61-)	(27+ ; 57-)	(3+ ; 0-)	(12+ ; 25-)	(17+ ; 31-)
	127	218	302	182	0	96	138
ULC180	(118+ ; 9-)	(202+; 16-)	(204+ ; 98-)	(98+ ; 84-)	(0+ ; 0-)	(24+ ; 72-)	(32+ ; 106-)

Interestingly, only three DEGs in ULC008 (1.4 % of the total DEGs) and 27 DEGs in ULC180 (6.2 % of the total DEGs; Fig. 4.7) were shared across all treatments, suggesting a high variability of DEGs among treatments. In ULC008, 18 DEGs were shared between the D-C and the RW1-C treatments, of which 8 were shared also with RW2-C but 0 with RW3-C. The majority of the

shared DEGs between D-C and other treatments were up-regulated (Fig. S4.4). On the other hand, 51 DEGs were shared between RW2-C and RW3-C in ULC008, of which 19 were up-regulated and 33 down-regulated (Fig. S4.4), suggesting a common down-regulation of the transcriptome with time after rehydration. Interestingly, in ULC180, the highest number of shared DEGs was also between RW2-C and RW3-C (136) of which the majority were down-regulated (57). Also, 21 of the total DEGs were shared with the RW1-C treatment, of which the majority (14) were up-regulated (Fig. 4.7 and Fig. S4.5).

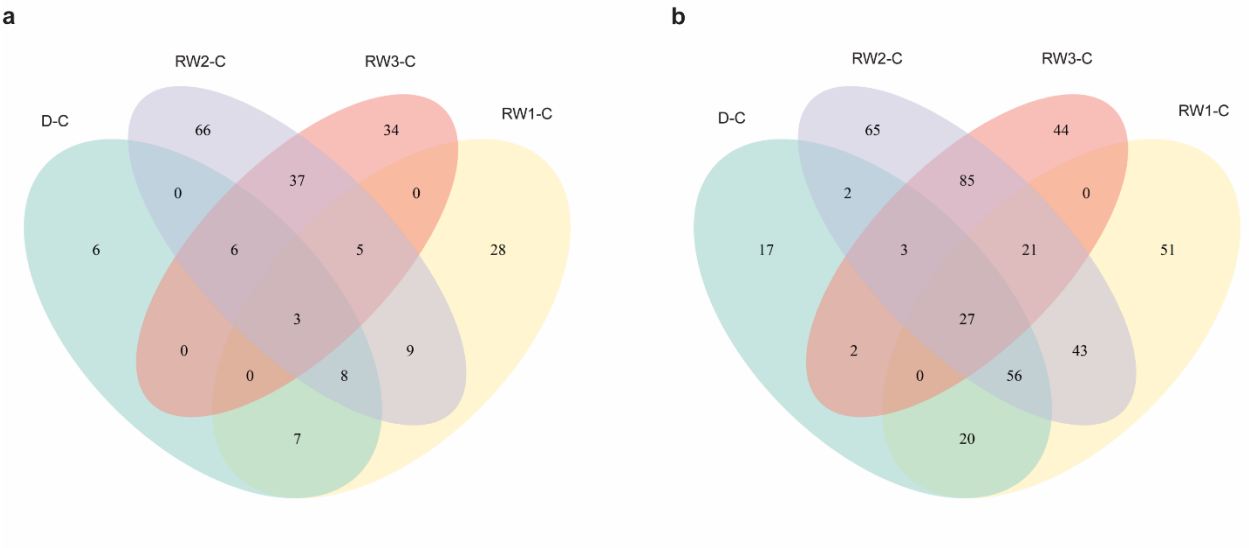

Fig. 4.7 Venn diagram of the shared DEGs between treatments of (a) freshwater ULC008 and (b) terrestrial ULC180. *The treatments compared to the same control are: desiccation (D-C), 10 min (RW1-C), 24h (RW2-C) and 72 h (RW3-C) after rehydration started.*

In the PCA of both strains, the transcriptome of the strains under the different treatments are clearly differentiated (Fig. 4.8a and b). RW3 replicates of both strains seem to return along the same y axis of C replicates, even if a high difference is observed (see the high variance explained by the x axis: ~ 50 %).

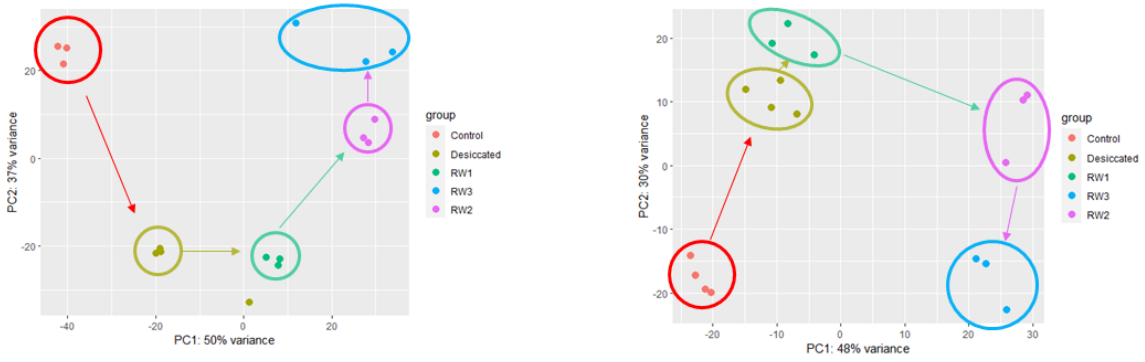

Fig. 4.8 Principal Component Analysis plot of trasncriptome of a) ULC008 and b) ULC180. *C = control, D = desiccation, RW1 = 10 min after rewetting, RW2 = 24h after rewetting, RW3 = 72h after rewetting.*

According to COG classification, almost half of the DEGs involved in the desiccation treatment did not have a clear function assigned (~ 45 %; Table S4.3). Among the annotated ones, functional categories belonging to "Cell wall/membrane/envelope biogenesis", "Energy production and conversion", "Inorganic ion transport and metabolism", and "Signal transduction mechanisms" were the most abundant (> 10 %) in the terrestrial ULC180 strain. In the freshwater ULC008 strain, the most abundant functional categories belonged to "Energy production" and "Inorganic ion transport and metabolism" (> 15 %; Fig. 4.9). The five most up-regulated genes during desiccation in the terrestrial strain were the consecutive stress-response associated genes KLONEFKL_04364, KLONEFKL_04365, KLONEFKL_04366, KLONEFKL_04367 and KLONEFKL_03427 (Table S4.3), encoding orange carotenoid-binding proteins (OCP). In the freshwater strain under desiccation, these were GNPDOPOO_00606, a RNA recognition motif (RRA) gene; GNPDOPOO4546, GNPDOPOO_01452 and GNPDOPOO_01451 of unknown function; and GNPDOPOO_04547, encoding chemotaxis proteins of methyltransferase (cheR), belonging to the Two-component system (Table S4.3). In ULC180, most of the DEGs were up-regulated, though "energy production and conversion" had two downregulated genes encoding Flavorubredoxin proteins (*norV*) and Fe-S oxidoreductase (*glpC*), and the category "Inorganic ion transport and metabolism" included only one gene corresponding to the *cmpA* gene which transports CO_2

(Table S4.3). Interestingly, among the three genes belonging to the category "Energy production and conversion" in ULC008, none was upregulated, while two were downregulated, namely *norV* and *petC,* which encodes flavorubredoxins and cytochrome b5f complex, respectively (Table S4.3). Also, within the category "Inorganic ion transport and metabolism" in ULC008, two genes were up- and two downregulated. The two downregulated genes encode for the bicarbonate ABC-transporter proteins (*cmpA* and *cmpB*), which is in agreement with the observations for the ULC180 strain (Table S4.3). The two upregulated genes encode the nitrogenase molybdenum-iron protein (*nifD*) and the Na^+/H^+ or K^+/H^+ antiporters (*nhaP*; Table S4.3).

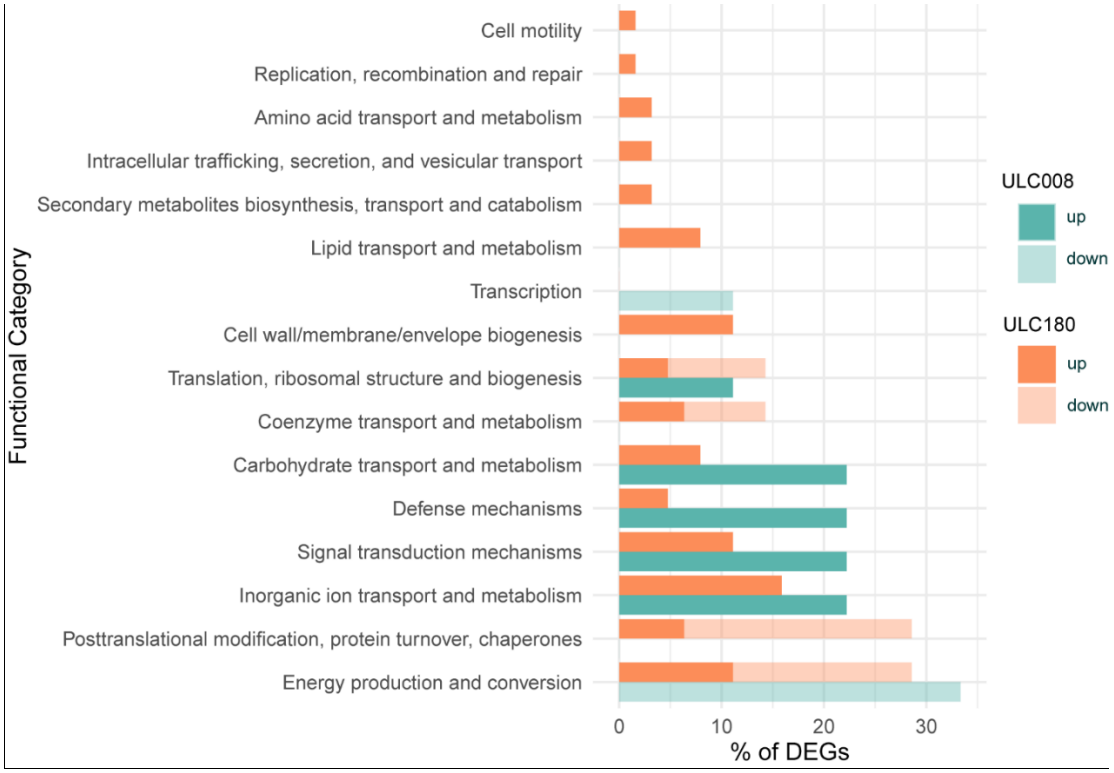

Fig. 4.9 Percentage of all the DEGs within each strain under desiccation grouped by COG functional categories. *Colors indicate the strain type and the tint of the bar indicates the up- (filled) and down- (transparent) regulated genes (see legend).*

4.4.6 MAIN PATHWAYS RESPONDING TO DESICCATION AND REHYDRATION

In the present study, we mainly focused on the pathways involved in the photosynthetic processes, carbohydrate and nitrogen metabolism, and UV protection mechanisms, because they were among the most frequent processes found within the DEGs (see Table S4.3), and evidently relevant in oligotrophic polar terrestrial habitats.

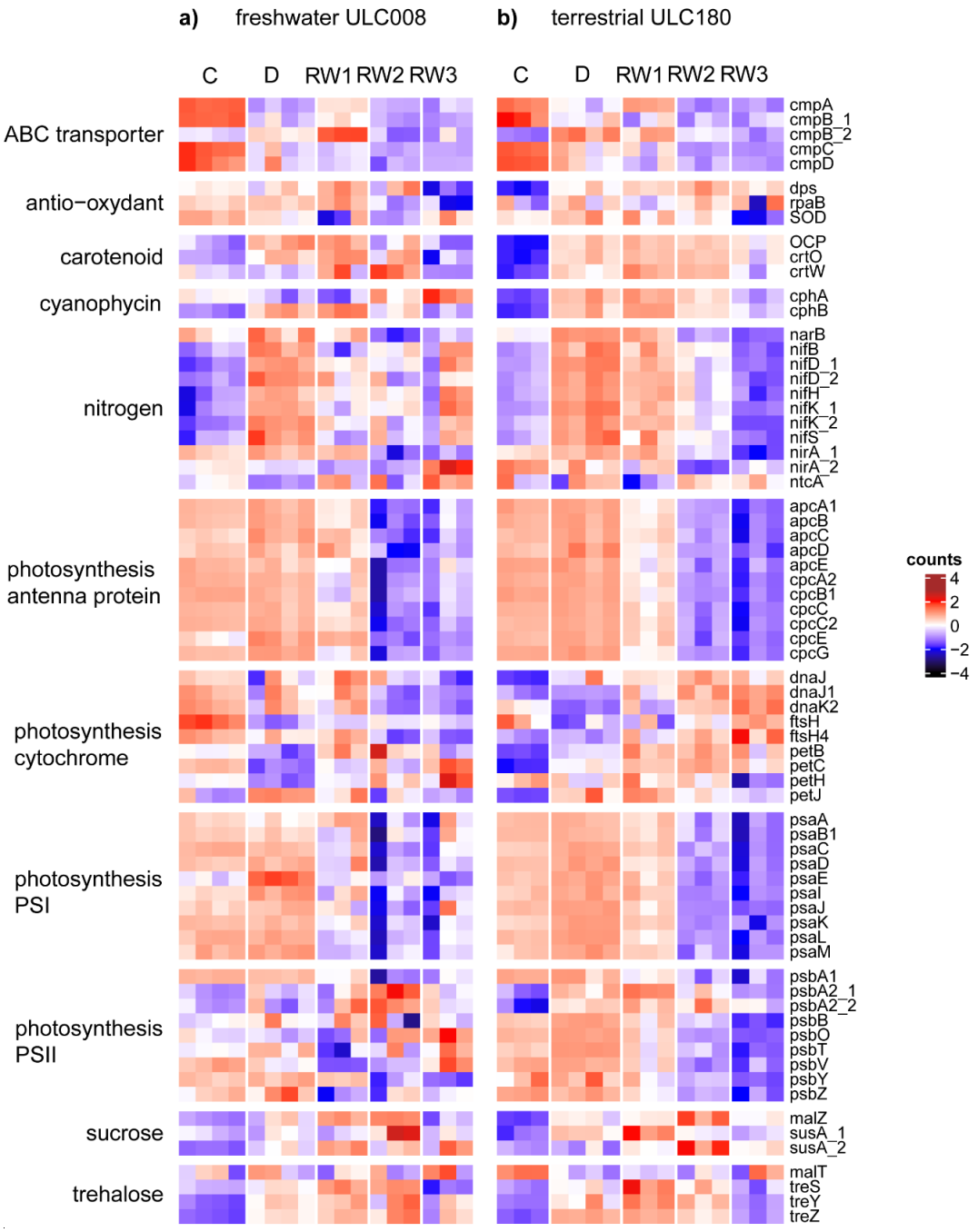

Fig. 4.10 Heatmap of gene transcript counts of freshwater ULC008 and terrestrial ULC180 strains clustered by group of metabolism/pathway categories. *Colors represent the normalized (DESeq2's median of ratios) and scaled (via a row Z-score) gene expression counts. Treatments are: controls (C), desiccation (D), 10 min (RW1), 24h (RW2) and 72 h (RW3) after rehydration started; n=3 or 4. For gene details see Table S4.3.*

4.4.7 PHOTOSYNTHESIS

The patterns in DEGs between the treatments were different between genes involved in PSI versus PSII (Fig. 4.10). First, in both strains, PSI related genes showed a high expression in controls. Interestingly, desiccation did not affect their expression as approximated by the $\log_2$ fold change. However, PSI (*psaC*, *psaL*, *psaI*, *psaJ*, *psaF*) and antenna proteins (*cpcB1*, *apcA*, *apcB*, *apcE*, *apcC*, *cpcC2*, *cpcC*, *cpcE*) were significantly down-regulated at RW2 and RW3 in the terrestrial ULC180 strain (Fig 4.10 b, Table S4.3) and only three antenna protein genes (i.e. *apcA*, *cpcC*, *cpcC2, cpcE*) were significantly down-regulated in the freshwater strain after 24h of rehydration (Fig 4.10 a, Table S4.3). On the other hand, genes related to PSII have a less homogenous behavior in both strains compared with PSI, and particularly in the freshwater ULC008 strain (Fig. 4.10). In ULC180, the *psbA2* gene was significantly up-regulated under desiccation, whilst *psbA1* started to be down-regulated after 24h of rehydration (Fig. 4.10, Table S4.3). In the terrestrial ULC180 strain the cytochrome b6 complex gene (*petC*) was significantly up-regulated only after 10 min of rewetting, compared to control, whilst the cytochrome b6 gene (*petB*) started being significantly up-regulated after 10 min of rewetting compared to control and it remained up-regulated until the end of the experiment (Fig. 4.10, Table S4.3). By contrast, *petC* in the freshwater ULC008 strain was down-regulated after 10 min of rehydration compared to controland then started to be significantly up-regulated after 72h of rehydration compared to desiccation. Ferredoxin-NADP+ reductase (*petH*) and ferrodoxin gene (p*etF*) showed a significant down-regulation in the terrestrial strain at RW1-C (*petH*), RW3-C and RW3-D (*petH*, *petF*) and in the freshwater strain at RW2-D (Fig. 4.10, Table S4.3). Chaperone gene *dnaK* was significantly up-regulated after 24h and 72h after rewetting compared to desiccation, only in the terrestrial ULC180 strain.

4.4.8 CARBOHYDRATE METABOLISM

Gene involved in the synthesis of trehalose (*treZ*) was significantly up-regulated from the desiccation experiment compared to control in the terrestrial ULC180 strain and from 10 min of rehydration in the freshwater ULC008 strain, and remained up-regulated until 24h of rehydration in both strains (RW2-C; Fig. 4.10, Table S4.3). In ULC180 *treZ* started to significantly down-

regulate after 72h of rewetting compared to desiccation (RW3-D; Fig. 4.10, Table S4.3). *TreY*, also involved in trehalose synthase, was significantly up-regulated in both strains after 10 min of rehydration compared to control (RW1-C; Fig. 4.10, Table S4.3), while treS, involved in both trehalose synthase and degradation, was significantly up-regulated only in the freshwater strain after 24h of rehydration (RW2-C, RW2-D; Fig. 4.10, Table S4.3). *SusA*, involved in the sucrose synthase, and malZ, involved in the sucrose degradation, were significantly up-regulated only in the terrestrial ULC180 strain after 24h of rehydration compared to control (RW2-C; Fig. 4.10, Table S4.3), whilst *malZ* was also significantly up-regulated already after 10 min of rehydration (RW1-C) in the freshwater strain, and remained significantly up-regulated until 24h of rehydration (RW2-C; Fig. 4.10, Table S4.3).

4.4.9 NITROGEN METABOLISM

NifDK genes were significantly upregulated under dehydration in the terrestrial ULC180 strain and only *nifD* in the freshwater ULC008 strain (D-C; Fig. 4.10, Table S4.3). Moreover, all the *nif* genes related to nitrogen fixation, including the nitrogenase reductase *nifH* gene, were highly expressed in both strains under desiccation followed by a decrease 10 minutes after rehydration in ULC008 and after 24h in ULC180, but were not statistically considered DEGs (Fig. 4.10, Table S4.3). *NifDEKNX* were significantly down-regulated in the terrestrial ULC180 after 72h of rewetting compared to desiccation (RW3-D; Fig. 4.10, Table S4.3). Other genes involved in nitrogen assimilation by transforming nitrate into nitrite (*narB*) and to ammonia (*nirA*) were already expressed in control treatments and were more expressed under desiccation in both strains (Fig. 4.10), while the gene regulating the whole nitrogen fixation and assimilation processes (*ntcA*) did not show a clear expression pattern. During rehydration, narB significantly down-regulated after 72h of rehydration compared to desiccation in both strains, and *nirA* only in ULC180 (RW3-D; Fig. 4.10, Table S4.3). *NtcA* was slightly more expressed again from 10 minutes after rehydration (RW1; Fig. 4.10). Finally, the genes for the synthesis/hydrolysis of cyanophycin (a typical nitrogen reserve; Kolodny et al. 2006), were significantly up-regulated only in the ULC180 strain under desiccation, and remained up-regulated until 24h after rehydration (*cphA*, *cphB*; Fig. 4.10 and Table S4.3).

4.4.10 PROTECTION MECHANISMS

The genes coding for the biosynthesis of echinenone and canthaxanthin (*crtO*, *crtW*) were significantly up-regulated under desiccation only in the terrestrial strain (Fig 10, Table S4.3). *CrtW* remained significantly up-regulated until 10 min after rehydration (RW1-C) whilst it was significantly up-regulated at 72h after rehydration (RW3-C; Fig. 4.10, Table S4.3). The orange carotenoid protein (OCP)-encoding gene followed the pattern of other carotenoid-encoding genes in ULC180, and its expression was significantly up-regulated under desiccation (D-C; Fig. 4.10, Table S4.3). This was similar for the freshwater strain, although not significant (Fig. 4.10). Concerning ROS scavenging systems, in the terrestrial ULC180 the *dps* gene expression was significantly up-regulated under desiccation compared to control (D-C) and again at 24h (RW2-C) and 72h after rehydration (RW3-C), whilst in the freshwater strain it was significantly down-regulated (Fig. 4.10, Table S4.3).

4.5 DISCUSSION

We combined ecophysiological and transcriptomic techniques to investigate the response mechanisms of two *Nostoc* sp. strains belonging to the same species, but originating from a terrestrial and freshwater habitat in the Antarctic. During desiccation, more genes were up-regulated in the terrestrial strain compared with the freshwater strain (Table 4.2, Table S4.3). Moreover, the desiccation treatment is characterized by a higher number of up-regulated genes in both strains, whilst the rehydration process measured during 3 times points over a 3 day's period is characterized by a larger number of down-regulated genes (Table 4.1). This is in agreement with earlier studies investigating the transcriptomics response to desiccation of drought-tolerant cyanobacteria (Wang et al. 2018, Rajeev et al. 2013, Khani-Juyabad 2022). However, it is counter to the transcriptomic response of the mild-desiccation tolerant *Anabaena* PCC7120, which showed a higher proportion of down-regulated compared with up-regulated genes in response to desiccation (Higo et al. 2007). However, this model strain is in culture since 1971 and was isolated from a temperate habitat. Below, the major pathways used to resist

dehydration stress in the two investigated strains are discussed in the light of our prior hypotheses.

4.5.1 PHOTOSYNTHESIS

Both strains showed in general a small decrease in the expression of genes related to PSI, PSII and antenna pigment starting from 10 min on after rehydration and this down-regulation was significant in the terrestrial strain after 24 and 72h (Fig. 4.10, Table S4.3). Nonetheless, the QY response of both strains significantly decreased already under dehydration, and started increasing again immediately after rehydration, although they never reached the control values after three days of rehydration (Fig. 4.3, Table S4.1-4.2). Similarly, chlorophyll *a* concentrations dropped during dehydration and started to increase again upon rehydration with only a complete recovery to control values shown by the freshwater strain (Fig. 4.2). The down-regulation of PSI, PSII and antenna-protein genes has been observed under desiccation in the desiccation-sensitive *Anabaena* (*Nostoc*) sp. PCC7120, with a recovery of the PSI and PSII observed within 2h (Katoh et al. 2004, Higo et al. 2007). Nonetheless, the drought-resistant *Microcoleus vaginatus* within a natural crust was observed to maintain the photosynthetic apparatus working under early desiccation, which was explained by the possibility of this cyanobacterium of employing unknown mechanisms that keep the water potential higher in the immediate vicinity of the cells, allowing the cyanobacteria to support photosynthesis (Rajeev et al. 2013). The long time for photosynthesis to recover as also observed in the QY values and in chl *a* concentrations, might suggest that the complete recovery of the photosynthetic process takes more than 72h in the studied *Nostoc* strains or that a longer desiccation period should be tested to observe the cease of metabolism. A faster photosynthetic recovery was observed in natural crusts compared to single cultures of cyanobacteria (Rajeev et al. 2013, Garcia-Pichel and Belnap 1996, Ohad et al. 2010), which could suggest a slightly different behaviour of our strains compared to their natural environment. In addition, we used a short-term desiccation that might have not been enough to completely dehydrate the cyanobacterial cells to the point of ceasing any photosynthetic related activity. Additionally, the terrestrial ULC180 strain showed a significant up-regulation of one of the *psbA2* genes under desiccation (Table S4.3) indicating *de novo* synthesis of the D1 protein

under stress, probably to prevent the damage of PSII, which was not observed in the freshwater ULC008 strain. The D1 protein represents a critical component of the reaction center in PSII and plays a central role in the electron transfer chain between PSII and PSI through cytochrome b6-f (Kirchhoff and Puthiyaveetil 2017). This protein was shown to be dramatically affected and damaged by ROS production under dehydration conditions (Raanan et al. 2016). FtsH protease is responsible to degrade this damaged D1 protein (Adam et al. 2006). *De novo* synthesis of the D1 protein is therefore fundamental to re-establish PSII, and hence the whole photosynthetic machinery (Ohad et al. 2011). After the significant up-regulation of the *psbA2* gene during dehydration (Fig. 4.10, Table S4.3), we observed an increase in expression in the *ftsH*, *dnaK* and *dnaJ* genes in the terrestrial ULC180 transcriptome during the whole rehydration period (Fig. 4.10, Table S4.3). This is counter to their decrease within 24h of rehydration in the freshwater ULC008 strain (Fig. 4.10). Recently, the DnaK and DnaJ chaperones were shown to interact with the FtsH protease in cyanobacteria and are thus involved in the activity and integrity of PSII during dehydration (Xu et al. 2020). Two different *psbA* genes were observed in the present *Nostoc* sp. genomes (one *psbA1* and two *psbA2* genes). Both *psbA* genes, according to Forsman et al. (2019), may be able to produce two different, yet functionally equivalent, forms of the D1 protein. Other studies also showed that the expression levels of *psbA1* and *psbA2* can differ under variable environmental conditions, such as light and nutrient availability (Mohamed et al. 1993, Summerfield et al. 2008, Sicora et al. 2009), suggesting that the production of two D1 proteins may help cyanobacteria to adapt to changing abiotic conditions. In our study, the expression of the *psbA1* gene was significantly down-regulated at RW2 and RW3, similarly to other PSI and antenna-protein genes, whilst *psbA2* genes were characterized by a low transcript counts in controls, and their expression was significantly enhanced under desiccation in the terrestrial strain (Fig. 4.10, Table S4.3). This pattern was not observed in the freshwater ULC008 strain, which indicates differences in the turnover of the D1 protein between the two strains, suggesting a potential difference in the resistance level to dehydration conditions. Indeed, the terrestrial ULC180 strain could therefore be more adapted to cope with such conditions compared to the

freshwater ULC008 strain. These patterns, however, need to be confirmed in other terrestrial and freshwater cyanobacterial lineages.

4.5.2 CARBOHYDRATE METABOLISM

In the terrestrial ULC180, expression of the gene for trehalose synthesis (*treZ*) was significantly upregulated during desiccation and until 24h of rehydration (Table S4.3), although the amount of accumulated trehalose was close to zero during this treatment step (Fig. 4.5a, Table S4.2). Overall, the expression of genes involved in the trehalose biosynthesis (i.e. *treZ*, *treY* and *treS*) increased in both strains under desiccation and decreased, significantly in some cases, after 72h of rehydration (Fig. 4.10, Table S4.3). A similar result was also found by Higo et al. (2006) who observed that during desiccation, *Anabaena* PCC 7120 highly expressed a trehalose gene cluster (*mts* gene, now called *treY*) though only small concentrations of trehalose were observed in the cells (0.05 – 0.1 % of dry weight). During this and a later study, Higo et al. (2006, 2007) proposed that trehalose has an important role during dehydration, yet they also suggested that trehalose may not directly stabilize proteins and membranes during dehydration as is the case with sucrose, but that trehalose may be rather metabolized by another enzyme, or that it may be used for the synthesis of exopolysaccharide or lipopolysaccharide. Another hypothesis was that trehalose could regulate the expression of molecular-chaperone-related genes, such as *dnaK*, which play an important role in desiccation (Higo et al. 2007). Chaperones indeed protect the structure of proteins against denaturation and aggregation under stress. This hypothesis was already supported by Bulman & Nelson (2005) who suggested that trehalose could be involved in the regulation of chaperone-involved genes in *Saccharomyces cerevisiae*.

Interestingly, both strains accumulated much more sucrose than trehalose (Fig. 4.5b), yet no significant increase in corresponding DEGs was observed during desiccation in any strain. However, there was an increase in the transcript counts of sucrose-related genes (*susA_1* and *susA_2*; Fig. 4.10), one of which was significant only in the terrestrial ULC180 after 24h of rehydration (RW2-C; Table S4.3). Cumino et al. (2007) observed that sucrose and glycogen metabolisms, as well as respiration, might be linked, and the sucrose cleavage by *sus* genes in vegetative cells would contribute to the ADP-glucose pool, which could explain why the increase

in *susA* gene expression does not coincide with sucrose accumulation. The up-regulation of the maltodextrin glucosidase gene (*malZ*) responsible of degrading the sucrose, was observed after 24h of rehydration, similarly to *susA* gene (RW2-C, Table S4.3). Higo et al. (2007) also hypothesized that high amounts of sucrose accumulation, as well as the high expression of genes related to sucrose synthase (*susA*), could be related to a specific function of sucrose as a 'chemical' chaperone – which, to work as such, it needs to be present in high quantity.

Cyanobacterial cells accumulate inorganic carbon in the cytoplasm as HCO_3^- and convert it into CO_2 in carboxysomes to elevate the CO_2 concentration around the CO_2-fixing enzyme rubisco (Pirce et al. 1998, Kaplan and Reinhold 1999). *CmpABCD* are the genes encoding the substrate-binding of the HCO_3^- transporter (Maeda et al. 2000). *CmpA* genes were significantly down-regulated in both the freshwater and the terrestrial strains during dehydration and together with other *Cmp* genes, they remained down-regulated also under the rehydration treatments (Fig. 4.10; Table S4.3) suggesting impaired carbon fixation under dehydration and also rehydration. Only one *cmpB* gene was significantly up-regulated under desiccation in the terrestrial ULC180 gene (Fig. 4.10; Table S4.3). The downregulation of such genes was also observed by several studies involving desiccation stress in cyanobacteria (Sen et al. 2017, Oren et al. 2017, Higo et al. 2007) and was proposed to be a mechanism to protect the cells under a severe stress, such as desiccation, by inhibiting respiration.

4.5.3 PROTECTION MECHANISMS

The terrestrial ULC180 showed a significant up-regulation of *crtW* and *crtO* genes, which are responsible for the biosynthesis of canthaxanthin, zeaxanthin and echinenone, as well as the orange carotenoid protein encoding gene (*ocp*; Table S4.3, Fig 10). Interestingly, the trend in carotenoid concentrations was counter to these gene expression results, because the concentrations of these pigments were slightly decreasing during treatments (Fig. 4.4, Table S4.2). This decrease coincides with a chlorophyll *a* decrease as well, which suggests that most of the carotenoids that decrease are primary and hence accessory pigments, such as zeaxanthin and echinenone, which are bound to the photosystems and involved in photosynthesis (Mulder et al. 2015, Rehakova et al. 2019). On the other hand, the levels of some secondary carotenoids and

mainly involved in photoprotection (such as canthaxanthin and orange carotenoids; Wilson et al. 2006, Mulders et al. 2015, Rehakova et al. 2019) do not significantly decrease during the rehydration period along time (Fig. 4.4 and Fig. S4.1). The increase of transcripts related to the production of these three carotenoids 24h after rehydration might suggest that the photosynthetic activity is starting to recover (primary carotenoids) and that the photoprotective system is being activated by the cells (secondary carotenoids). Moreover, the peak of chlorophyllide *a* during desiccation in the freshwater strain ULC008 (Fig. 4.4) might be linked with the increase of another secondary carotenoid, β-carotenoid, in the same strain. Carotenoids are known to perform important functions in photosynthesis, i.e. in the protection against photo-oxidative damage (Baker 2008, Lan et al. 2010). Therefore, in unacclimated cyanobacteria, a low carotenoid content could result in reduced quenching of ROS and consequent inhibition of photosynthesis (Xu et al. 2021). Gao et al. (2020) empirically showed that a transgenic *Anabaena* sp. PCC7120 strain that heterologously overexpressed *crtO* and therefore produced more echinenone and canthaxanthin, showed a stronger drought tolerance than the wild type.

In both our investigated *Nostoc* genomes, four copies of *ocp* were encountered. In earlier studies, it was observed that terrestrial cyanobacteria contain multiple copies of OCP homologs (Melnicki et al. 2016, Bao et al. 2017), however, no differences in the number of copies between the terrestrial and the freshwater strains were encountered in the present study. Their transcription was found to be under phytochrome control in *L. ohadii* and they were among the most upregulated genes during dawn, prior to any noticeable decline in water content (Oren et al. 2017). The authors also observed a down-regulation of the *ocp* genes under rehydration in both *N. flagelliforme* and *L. ohadii* (Oren et al. 2017, Yang et al. 2019). These results highlight the important role of *ocp* genes in the desiccation-tolerance of both terrestrial and freshwater cyanobacteria. Interestingly, *dps* (DNA-binding ferritin), which is another gene responsible for the protection of DNA against oxidative stress (Martinez and Kolter 1997), was also significantly induced during desiccation in the terrestrial ULC180, but not in the freshwater ULC008 (Fig. 4.10). The induction of this gene during desiccation was also observed in other terrestrial cyanobacteria, i.e. *Nostoc* sp. MG11 and *Microcoleus vaginatus*, and is probably related to its

function of DNA protection against oxidative damage (Khani-Juyabad et al. 2022, Rajeev et al. 2013). Other anti-oxidant related genes were observed in the two genomes, but they did not show a significant role in desiccation, nor exhibited a clear expression pattern over the tested treatments (Fig 10).

4.5.4 NITROGEN METABOLISM

Nitrogen fixation related genes were significantly up-regulated during dehydration in both ULC008 (only *nifD*) and ULC180 strains (*nifDK*) (Table S4.3). Moreover, the expression of all the *nif* genes, including the nitrogenase-related gene *nifH*, increased under desiccation, although this increase was not significant (Fig. 4.10). This finding is in line with Sen et al. (2017) who observed a 2.9-fold increase of the *nifH* gene during early dehydration in the moderately drought resistant *Anabaena* sp. PC7120, followed by a decrease in expression during long-term desiccation. Katoh et al. (2004) also observed an increased *nifH* gene expression after 30 min of dehydration, which is probably a strategy to mitigate the ongoing nitrogen deficiency caused by the dehydration condition. Indeed, nitrogen deficiency is linked to the decrease of media concentration, which contains nitrates among other nutrients, even those fixed by the cyanobacterial filaments.

In many cyanobacteria, cyanophycin - a nonribosomically synthesized amino acid polymer composed of aspartic acid and arginine - is produced by the cyanophycin synthetase gene (*cphA*) (Ziegler et al. 1998, Potts 1999, Zhang et al. 2018, Shang et al. 2019). Cyanophycin can accumulate during dehydration as a dynamic reservoir of carbon and nitrogen in heterocysts or vegetative cells (Sherman et al. 2000, Watzer and Forchhammer 2018). In the terrestrial ULC180 strain, the expression of the *chpA* and *cphB* genes increased upon desiccation and remained up-regulated until 24h after rehydration (D-C, RW1-C, RW2-C; Fig. 4.10, Table S4.3), which was already observed in the terrestrial *M. vaginatus* from a natural crust (Rajeev et al. 2013). Also Liang et al. (2012) and Shang et al. (2019) similarly observed an increase in *chpA* gene expression under dehydration in order to store more nitrogen, and, similarly to our study, they observed a significant up-regulation of the *cphB* gene upon rehydration as well, probably to supply the carbon and nitrogen compounds necessary to resume growth as quickly as the water stress ends.

4.5.5 UNKNOWN GENES

Although we used a cross-referencing database for gene annotation (c.f. Material & Method), 45 % of DEGs during dehydration of both strains had unknown functions, or were assigned a general function prediction only, with many genes being labeled as coding for stress-related proteins (Table S4.3). Similarly, analysis of the *Nostoc* sp. MG11 transcriptome demonstrated that 35 % of DEGs were unknown or hypothetical (Khani-Juyabad et al. 2022), and other studies also reported the differential expression of unknown genes during desiccation (i.e. Rajeev et al. 2013), highlighting the potential importance of these novel genes in the survival of cells in desiccation conditions.

4.6 CONCLUSIONS

We demonstrated that both *Nostoc* spp. strains have developed strategies to cope with desiccation, with the terrestrial *Nostoc* ULC180 strain showing a stronger degree of adaptation. For instance, by transcriptomic analysis we observed a higher number of up-regulated genes under desiccation compared to the freshwater *Nostoc* ULC008 strain, and these genes were often related to desiccation-resistance (i.e. carotenoids production, trehalose synthase, D1 protein synthase). However, upon rehydration, an immediate response of photosynthetic activity or PSI and PSII genes expression was not observed in any of the strains, suggesting that neither strain has a high resistance level to drought-rehydration events. Finally, the freshwater strain showed a higher proportion of down-regulated genes during rehydration and a recovery in chlorophyll *a* content after 72h of rehydration, which was not observed in the terrestrial strain, suggesting that the freshwater *Nostoc* sp. ULC008 might show a quicker response to rehydration compared to the terrestrial strain. From these results we can infer that even though they belong to the same species, their original environment has probably exerted a strong selection on the genetic mechanisms that these cyanobacteria developed to adapt to their environment, and left an imprint on their resistance mechanisms. This study expands our understanding on the adaptability traits of Antarctic cyanobacteria facing desiccation and rehydration events in extreme environments.

4.7 ACKNOWLEDGMENTS

The authors would like to thank Sofie D'Hondt and Ilse Daveloose for help with the RNA and pigments extractions. Yannick Lara and Bjorn Tytgat are also thanked for the helpful comments that improved the analyses of the paper. Emmanuel Mignolet kindly purified the strain ULC008. The authors also thank Aurore Richel and Isabelle Van De Vreken for the osmolytes extraction in Gembloux Agro-Bio Techfaculty (ULiège). Also, the members of the Center for Data Analysis and Statistical Science of Ghent University are thanked for providing access to the FIRE service to prepare the experimental design enabling adequate statistical analyses of the results. Samuel Rondia from the atelier of électromécanique of the University of Liège is also thanked for the construction of the experimental chambers in plexiglas. VS was supported bya PhD FRIA fellowship from the FRS-FNRS. AW is Senior Research Associate of the FRS-FNRS.BRR was supported by the Special Funds for Research (University of Liège), the IPD-STEMA Program, and the Junta de Andalucía (PAIDI-DOCTOR 21_00571).

4.8 AUTHOR CONTRIBUTIONS

Conceived and designed the experiment: VS, EV, AW. Performed the experiment and the RNA-Seq extractions: VS. Minor laboratory analysis: BRR. Major data analysis: VS. Minor data analysis: ISP, LC. Supervision: EV, AW. Secured the funding: VS, EV, AW. Wrote the paper: VS, BRR. All authors reviewed and edited the manuscript and approved the final version.

4.9 REFERENCE

Alonge, M., Lebeigle, L., Kirsche, M., Aganezov, S., Wang, X., Lippman, Z.B., Schatz, M.C. and Soyk, S., 2021. Automated assembly scaffolding elevates a new tomato system for high-throughput genome editing. BioRxiv.

Anders, S. 2010. HTSeq: analysing high-throughput sequencing data with Python. http://www-huber.embl.de/users/anders/HTSeq/doc/overview.html

Anders, S. and Huber, W., 2010. Differential expression analysis for sequence count data. Nature Precedings, pp.1-1.

Andrews, S., 2010. FastQC: a quality control tool for high throughput sequence data.

Asker, D., 2018. High throughput screening and profiling of high-value carotenoids from a wide diversity of bacteria in surface seawater. Food chemistry, 261, pp.103-111.

Avonce, N., Mendoza-Vargas, A., Morett, E. and Iturriaga, G., 2006. Insights on the evolution of trehalose biosynthesis. BMC evolutionary biology, 6(1), pp.1-15.

Badger, M.R. and Price, G.D., 2003. CO2 concentrating mechanisms in cyanobacteria: molecular components, their diversity and evolution. Journal of experimental botany, 54(383), pp.609-622.

Bahl, J., Lau, M.C., Smith, G.J., Vijaykrishna, D., Cary, S.C., Lacap, D.C., Lee, C.K., Papke, R.T., Warren-Rhodes, K.A., Wong, F.K. and McKay, C.P., 2011. Ancient origins determine global biogeography of hot and cold desert cyanobacteria. Nature communications, 2(1), p.163.

Baker, N.R., 2008. Chlorophyll fluorescence: a probe of photosynthesis in vivo. Annu. Rev. Plant Biol., 59, pp.89-113.

Barger, N.N., Weber, B., Garcia-Pichel, F., Zaady, E. and Belnap, J., 2016. Patterns and controls on nitrogen cycling of biological soil crusts. Biological soil crusts: an organizing principle in drylands, pp.257-285.

Bardou, P., Mariette, J., Escudié, F., Djemiel, C., and Klopp, C. (2014) jvenn: an interactive Venn diagram.

Bao, H., Melnicki, M.R. and Kerfeld, C.A., 2017. Structure and functions of Orange Carotenoid Protein homologs in cyanobacteria. Current opinion in plant biology, 37, pp.1-9.

Basheva, D., Moten, D., Stoyanov, P., Belkinova, D., Mladenov, R. and Teneva, I., 2018. Content of phycoerythrin, phycocyanin, allophycocyanin and phycoerythrocyanin in some cyanobacterial strains: Applications. Engineering in Life Sciences, 18(11), pp.861-866.

Bebout, B.M. and Garcia-Pichel, F., 1995. UV B-induced vertical migrations of cyanobacteria in a microbial mat. Applied and Environmental Microbiology, 61(12), pp.4215-4222.

Blighe K, Rana S, Lewis M (2022). EnhancedVolcano: Publication-ready volcano plots with enhanced colouring and labeling. R package version 1.16. 0, https://github.com/kevinblighe/EnhancedVolcano.

Brown, A., 1976. Microbial water stress. Bacteriological reviews, 40(4), pp.803-846.

Buchfink B, Reuter K, Drost HG, "Sensitive protein alignments at tree-of-life scale using DIAMOND", Nature Methods 18, 366–368 (2021). doi:10.1038/s41592-021-01101-x

Bulman, A.L. and Nelson, H.C., 2005. Role of trehalose and heat in the structure of the C-terminal activation domain of the heat shock transcription factor. Proteins: Structure, Function, and Bioinformatics, 58(4), pp.826-835.

Büdel, B., Bendix, J., Bicker, F.R. and Allan Green, T.G., 2008. Dewfall as a water source frequently activates the endolithic cyanobacterial communities in the granites of Taylor Valley, Antarctica 1. Journal of Phycology, 44(6), pp.1415-1424.

Caiola, M.G., Billi, D. and Friedmann, E.I., 1996. Effect of desiccation on envelopes of the cyanobacterium *Chroococcidiopsis* sp.(Chroococcales). European Journal of Phycology, 31(1), pp.97-105.

Chen, S., Zhou, Y., Chen, Y. and Gu, J., 2018. fastp: an ultra-fast all-in-one FASTQ preprocessor. Bioinformatics, 34(17), pp.i884-i890.

Clark, K., Karsch-Mizrachi, I., Lipman, D.J., Ostell, J. and Sayers, E.W., 2016. GenBank. Nucleic acids research, 44(D1), pp.D67-D72.

Cornet, L., Durieu, B., Baert, F., D'hooge, E., Colignon, D., Meunier, L., Lupo, V., Cleenwerck, I., Daniel, H.M., Rigouts, L. and Sirjacobs, D., 2023. The GEN-ERA toolbox: unified and reproducible workflows for research in microbial genomics. GigaScience, 12, p.giad022.

Couradeau, E., Karaoz, U., Lim, H.C., Nunes da Rocha, U., Northen, T., Brodie, E. and Garcia-Pichel, F., 2016. Bacteria increase arid-land soil surface temperature through the production of sunscreens. Nature communications, 7(1), p.10373.

Cowan, D.A. and Tow, L.A., 2004. Endangered Antarctic environments. Annu. Rev. Microbiol., 58, pp.649-690.

Criscuolo, A. and Gribaldo, S., 2010. BMGE (Block Mapping and Gathering with Entropy): a new software for selection of phylogenetic informative regions from multiple sequence alignments. BMC evolutionary biology, 10, pp.1-21.

Cytryn, E.J., Sangurdekar, D.P., Streeter, J.G., Franck, W.L., Chang, W.S., Stacey, G., Emerich, D.W., Joshi, T., Xu, D. and Sadowsky, M.J., 2007. Transcriptional and physiological responses of *Bradyrhizobium japonicum* to desiccation-induced stress. Journal of bacteriology, 189(19), pp.6751-6762.

De Coster, W., D'hert, S., Schultz, D.T., Cruts, M. and Van Broeckhoven, C., 2018. NanoPack: visualizing and processing long-read sequencing data. Bioinformatics, 34(15), pp.2666-2669.

Dubois M, Gilles KA, Hamilton JK, Rebers PA, Smith F (1956) Colorimetric Method for Determination of Sugars and Related Substances. Anal Chem 28(3), 350-356.

Dudeja, S., Bhattacherjee, A.B. and Chela-Flores, J., 2010. Microbial mats in Antarctica as models for the search of life on the Jovian moon Europa. Microbial Mats: Modern and ancient microorganisms in stratified systems, pp.543-561.

Edgar, R.C., 2004. MUSCLE: a multiple sequence alignment method with reduced time and space complexity. BMC bioinformatics, 5(1), pp.1-19.

Emms, D.M. and Kelly, S., 2019. OrthoFinder: phylogenetic orthology inference for comparative genomics. Genome biology, 20, pp.1-14.

Eren, A.M., Esen, Ö.C., Quince, C., Vineis, J.H., Morrison, H.G., Sogin, M.L. and Delmont, T.O., 2015. Anvi'o: an advanced analysis and visualization platform for 'omics data. PeerJ, 3, p.e1319.

Eren, A.M., Vineis, J.H., Morrison, H.G. and Sogin, M.L., 2013. A filtering method to generate high quality short reads using Illumina paired-end technology. PloS one, 8(6), p.e66643.

Eren, A.M., Kiefl, E., Shaiber, A., Veseli, I., Miller, S.E., Schechter, M.S., Fink, I., Pan, J.N., Yousef, M., Fogarty, E.C. and Trigodet, F., 2021. Community-led, integrated, reproducible multi-omics with anvi'o. Nature microbiology, 6(1), pp.3-6.

Fawaz, M.N., 2013. Revealing the ecological role of Gemmatimonadetes through cultivation and molecular analysis of agricultural soils.

Forsman, J.A., Winter, R.T. and Eaton-Rye, J.J., 2019. An improved system for the targeted mutagenesis of the psbA2 gene in *Synechocystis* sp. PCC 6803: mutation of D1-Glu244 to His impairs electron transfer between QA and QB of Photosystem II. New Zealand Journal of Botany, 57(2), pp.125-136.

Fox, J. and Weisberg, S., 2011. An R companion to applied regression. Sage publications.

Frankenberg, N., Mukougawa, K., Kohchi, T. and Lagarias, J.C., 2001. Functional genomic analysis of the HY2 family of ferredoxin-dependent bilin reductases from oxygenic photosynthetic organisms. The Plant Cell, 13(4), pp.965-978.

Gao, Q. and Garcia-Pichel, F., 2011. Microbial ultraviolet sunscreens. Nature Reviews Microbiology, 9(11), pp.791-802.

Gao, K. and Ye, C., 2007. Photosynthetic insensitivity of the terrestrial cyanobacterium *Nostoc flagelliforme* to solar UV radiation while rehydrated or desiccated. Journal of Phycology, 43(4), pp.628-635.

Gao, X., Zhu, Z., Xu, H., Liu, L., An, J., Ji, B. and Ye, S., 2021. Cold adaptation in drylands: transcriptomic insights into cold-stressed *Nostoc flagelliforme* and characterization of a hypothetical gene with cold and nitrogen stress tolerance. Environmental Microbiology, 23(2), pp.713-727.

Gong, M. and Bassi, A., 2016. Carotenoids from microalgae: A review of recent developments. Biotechnology advances, 34(8), pp.1396-1412.

Grilli Caiola, M., Ocampo-Friedmann, R. and Friedmann, E.I., 1993. Cytology of long-term desiccation in the desert cyanobacterium *Chroococcidiopsis* (Chroococcales). Phycologia, 32(5), pp.315-322.

Grossman, A.R., Schaefer, M.R., Chiang, G.G. and Collier, J., 1993. The phycobilisome, a light-harvesting complex responsive to environmental conditions. Microbiological reviews, 57(3), pp.725-749.

Gu Z (2022). “Complex Heatmap Visualization.” iMeta. doi: 10.1002/imt2.43.

Gurevich, A., Saveliev, V., Vyahhi, N. and Tesler, G., 2013. QUAST: quality assessment tool for genome assemblies. Bioinformatics, 29(8), pp.1072-1075.

Hagemann, M., 2011. Molecular biology of cyanobacterial salt acclimation. FEMS microbiology reviews, 35(1), pp.87-123.

Haldrup, A., Jensen, P.E., Lunde, C. and Scheller, H.V., 2001. Balance of power: a view of the mechanism of photosynthetic state transitions. Trends in plant science, 6(7), pp.301-305.

Higo, A., Suzuki, T., Ikeuchi, M. and Ohmori, M., 2007. Dynamic transcriptional changes in response to rehydration in *Anabaena* sp. PCC 7120. Microbiology, 153(11), pp.3685-3694.

Higo, A., Katoh, H., Ohmori, K., Ikeuchi, M. and Ohmori, M., 2006. The role of a gene cluster for trehalose metabolism in dehydration tolerance of the filamentous cyanobacterium *Anabaena* sp. PCC 7120. Microbiology, 152(4), pp.979-987.

Hirai, M., Yamakawa, R., Nishio, J., Yamaji, T., Kashino, Y., Koike, H. and Satoh, K., 2004. Deactivation of photosynthetic activities is triggered by loss of a small amount of water in a desiccation-tolerant cyanobacterium, *Nostoc commune*. Plant and cell physiology, 45(7), pp.872-878.

Holzinger, A., Kaplan, F., Blaas, K., Zechmann, B., Komsic-Buchmann, K. and Becker, B., 2014. Transcriptomics of desiccation tolerance in the streptophyte green alga *Klebsormidium* reveal a land plant-like defense reaction. PloS one, 9(10), p.e110630.

Hottiger, T., De Virgilio, C., Hall, M. N., Boller, T. & Wiemken, A.(1994).The role of trehalose synthesis for the acquisition of thermo-tolerance in yeast. II. Physiological concentrations of trehaloseincrease the thermal stability of proteinsin vitro.Eur J Biochem219,187–193.

Hyatt, D., Chen, G.L., LoCascio, P.F., Land, M.L., Larimer, F.W. and Hauser, L.J., 2010. Prodigal: prokaryotic gene recognition and translation initiation site identification. BMC bioinformatics, 11(1), pp.1-11.

Imlay, J.A., 2003. Pathways of oxidative damage. Annual Reviews in Microbiology, 57(1), pp.395-418.

Jain, C., Rodriguez-R, L.M., Phillippy, A.M., Konstantinidis, K.T. and Aluru, S., 2018. High throughput ANI analysis of 90K prokaryotic genomes reveals clear species boundaries. Nature communications, 9(1), p.5114.

Johannes Alneberg, Brynjar Smári Bjarnason, Ino de Bruijn, Melanie Schirmer, Joshua Quick, Umer Z Ijaz, Leo Lahti, Nicholas J Loman, Anders F Andersson & Christopher Quince. 2014. Binning metagenomic contigs by coverage and composition. Nature Methods, doi: 10.1038/nmeth.3103

Jungblut, A.D. and Vincent, W.F., 2017. Cyanobacteria in polar and alpine ecosystems. Psychrophiles: from biodiversity to biotechnology, pp.181-206.

Kanehisa, M., Sato, Y., and Morishima, K. (2016) BlastKOALA and GhostKOALA: KEGG tools for functional characterization of genome and metagenome sequences. J. Mol. Biol. 428, 726-731.

Kaplan, A. and Reinhold, L., 1999. CO2 concentrating mechanisms in photosynthetic microorganisms. Annual review of plant biology, 50(1), pp.539-570.

Karsten, U., Herburger, K. and Holzinger, A., 2014. Dehydration, temperature, and light tolerance in members of the aeroterrestrial green algal genus *Interfilum* (Streptophyta) from biogeographically different temperate soils. Journal of Phycology, 50(5), pp.804-816.

Katoh, H., Asthana, R.K. and Ohmori, M., 2004. Gene expression in the cyanobacterium *Anabaena* sp. PCC7120 under desiccation. Microbial ecology, 47, pp.164-174.

Katoh, H., Furukawa, J., Tomita-Yokotani, K. and Nishi, Y., 2012. Isolation and purification of an axenic diazotrophic drought-tolerant cyanobacterium, *Nostoc commune*, from natural cyanobacterial crusts and its utilization for field research on soils polluted with radioisotopes. Biochimica et Biophysica Acta (BBA)-Bioenergetics, 1817(8), pp.1499-1505.

Kerfeld, C.A., Melnicki, M.R., Sutter, M. and Dominguez-Martin, M.A., 2017. Structure, function and evolution of the cyanobacterial orange carotenoid protein and its homologs. New Phytologist, 215(3), pp.937-951.

Kirchhoff, H., Li, M. and Puthiyaveetil, S., 2017. Sublocalization of cytochrome b6f complexes in photosynthetic membranes. Trends in plant science, 22(7), pp.574-582.

Kirilovsky, D. and Kerfeld, C.A., 2012. The orange carotenoid protein in photoprotection of photosystem II in cyanobacteria. Biochimica et Biophysica Acta (BBA)-Bioenergetics, 1817(1), pp.158-166.

Kirsch, F., Klähn, S. and Hagemann, M., 2019. Salt-regulated accumulation of the compatible solutes sucrose and glucosylglycerol in cyanobacteria and its biotechnological potential. Frontiers in microbiology, 10, p.2139.

Kolmogorov, M., Bickhart, D.M., Behsaz, B., Gurevich, A., Rayko, M., Shin, S.B., Kuhn, K., Yuan, J., Polevikov, E., Smith, T.P. and Pevzner, P.A., 2020. metaFlye: scalable long-read metagenome assembly using repeat graphs. Nature Methods, 17(11), pp.1103-1110.

Kolodny, N.H., Bauer, D., Bryce, K., Klucevsek, K., Lane, A., Medeiros, L., Mercer, W., Moin, S., Park, D., Petersen, J. and Wright, J., 2006. Effect of nitrogen source on cyanophycin synthesis in Synechocystis sp. strain PCC 6308. Journal of bacteriology, 188(3), pp.934-940.

Komárek J. 2013. Cyanoprokaryota. Part 3: Heterocytous genera. In: Büdel B, Gärtner G, Krienitz L, Schagerl M, eds. Freshwater Flora of Central Europe. Berlin: Springer.).

Lan, S., Wu, L., Zhang, D., Hu, C. and Liu, Y., 2010. Effects of drought and salt stresses on man-made cyanobacterial crusts. European Journal of Soil Biology, 46(6), pp.381-386.

Letunic I and Bork P (2020) SMART: recent updates, new developments and status in 2020. Nucleic Acids Res; doi:10.1093/nar/gkaa937

Li H. and Durbin R. (2009) Fast and accurate short read alignment with Burrows-Wheeler Transform. Bioinformatics, 25:1754-60. [PMID: 19451168]

Li, H., Handsaker, B., Wysoker, A., Fennell, T., Ruan, J., Homer, N., Marth, G., Abecasis, G., Durbin, R. and 1000 Genome Project Data Processing Subgroup, 2009. The sequence alignment/map format and SAMtools. bioinformatics, 25(16), pp.2078-2079.

Li, X., Ding, M., Wang, M., Yang, S., Ma, X., Hu, J., Song, F., Wang, L. and Liang, W., 2022. Proteome profiling reveals changes in energy metabolism, transport and antioxidation during drought stress in Nostoc flagelliforme. *BMC Plant Biology*, *22*(1), p.162.

Liu, Y., Jeraldo, P., Herbert, W., McDonough, S., Eckloff, B., Schulze-Makuch, D., De Vera, J.P., Cockell, C., Leya, T., Baqué, M. and Jen, J., 2022. Whole genome sequencing of cyanobacterium *Nostoc* sp. CCCryo 231-06 using microfluidic single cell technology. Iscience, 25(5), p.104291.

Niederberger, T.D., Sohm, J.A., Tirindelli, J., Gunderson, T., Capone, D.G., Carpenter, E.J. and Cary, S.C., 2012. Diverse and highly active diazotrophic assemblages inhabit ephemerally wetted soils of the Antarctic Dry Valleys. FEMS microbiology ecology, 82(2), pp.376-390.

Maeda, S.I., Price, G.D., Badger, M.R., Enomoto, C. and Omata, T., 2000. Bicarbonate binding activity of the CmpA protein of the cyanobacterium *Synechococcus* sp. strain PCC 7942 involved in active transport of bicarbonate. Journal of Biological Chemistry, 275(27), pp.20551-20555.

Makhalanyane, T.P., Valverde, A., Velázquez, D., Gunnigle, E., Van Goethem, M.W., Quesada, A. and Cowan, D.A., 2015. Ecology and biogeochemistry of cyanobacteria in soils, permafrost, aquatic and cryptic polar habitats. Biodiversity and Conservation, 24, pp.819-840.

Martinez, A. and Kolter, R., 1997. Protection of DNA during oxidative stress by the nonspecific DNA-binding protein Dps. Journal of bacteriology, 179(16), pp.5188-5194.

Meetam, M., Keren, N., Ohad, I. and Pakrasi, H.B., 1999. The PsbY protein is not essential for oxygenic photosynthesis in the cyanobacterium *Synechocystis* sp. PCC 6803. Plant physiology, 121(4), pp.1267-1272.

Melnicki MR, Leverenz RL, Sutter M, López-Igual R, Wilson A, Paw-lowski EG, Perreau F, Kirilovsky D, Kerfeld CA (2016) Structure, diversity, and evolution of a new family of soluble carotenoid-binding proteins in cyanobacteria. Mol Plant 9:1379–1394

Mohamed, A., Eriksson, J., Osiewacz, H.D. and Jansson, C., 1993. Differential expression of the psbA genes in the cyanobacterium *Synechocystis* 6803. Molecular and General Genetics MGG, 238, pp.161-168.

Morgan-Kiss, R.M., Priscu, J.C., Pocock, T., Gudynaite-Savitch, L. and Huner, N.P., 2006. Adaptation and acclimation of photosynthetic microorganisms to permanently cold environments. Microbiology and molecular biology reviews, 70(1), pp.222-252.

Mullineaux, C.W. and Emlyn-Jones, D., 2005. State transitions: an example of acclimation to low-light stress. Journal of experimental botany, 56(411), pp.389-393.

O'Leary, N.A., Wright, M.W., Brister, J.R., Ciufo, S., Haddad, D., McVeigh, R., Rajput, B., Robbertse, B., Smith-White, B., Ako-Adjei, D. and Astashyn, A., 2016. Reference sequence (RefSeq) database at NCBI: current status, taxonomic expansion, and functional annotation. Nucleic acids research, 44(D1), pp.D733-D745.

Ohad, I., Berg, A., Berkowicz, S.M., Kaplan, A. and Keren, N., 2011. Photoinactivation of photosystem II: is there more than one way to skin a cat?. Physiologia Plantarum, 142(1), pp.79-86.

Olson, J.A. and Krinsky, N.I., 1995. Introduction: the colorful, fascinating world of the carotenoids: important physiologic modulators. The FASEB Journal, 9(15), pp.1547-1550.

Orakov, A., Fullam, A., Coelho, L.P., Khedkar, S., Szklarczyk, D., Mende, D.R., Schmidt, T.S. and Bork, P., 2021. GUNC: detection of chimerism and contamination in prokaryotic genomes. Genome biology, 22(1), pp.1-19.

Parks DH, et al. 2018. A standardized bacterial taxonomy based on genome phylogeny substantially revises the tree of life. Nature Biotechnology, http://dx.doi.org/10.1038/nbt.4229

Parks DH, Imelfort M, Skennerton CT, Hugenholtz P, Tyson GW. 2014. Assessing the quality of microbial genomes recovered from isolates, single cells, and metagenomes. Genome Research, 25: 1043-1055.

Pearce, D.A., 2012. Extremophiles in Antarctica: life at low temperatures (pp. 87-118). Springer Vienna.

Petr Danecek, James K Bonfield, Jennifer Liddle, John Marshall, Valeriu Ohan, Martin O Pollard, Andrew Whitwham, Thomas Keane, Shane A McCarthy, Robert M Davies, Heng Li GigaScience, Volume 10, Issue 2, February 2021, giab008, https://doi.org/10.1093/gigascience/giab008

Pointing, S., Belnap, J. 2012. Microbial colonization and controls in dryland systems. Nature ReviewsMicrobiology 10:551–562 https://doi.org/https://doi.org/10.1038/nrmicro2831

G.D. Price, D. Sultemeyer, B. Klughammer, M. Ludwig, M.R. Badger, The func-tioning of the CO2concentrating mechanism in several cyanobacterial strains: areview of general physiological characteristics, genes, proteins, and recent advances, Can. J. Bot. 76 (1998) 973–1001

Pointing, S.B., Chan, Y., Lacap, D.C., Lau, M.C., Jurgens, J.A. and Farrell, R.L., 2009. Highly specialized microbial diversity in hyper-arid polar desert. Proceedings of the National Academy of Sciences, 106(47), pp.19964-19969.

Potts, M., 2001. Desiccation tolerance: a simple process?. Trends in microbiology, 9(11), pp.553-559.

Potts, M., 1994. Desiccation tolerance of prokaryotes. Microbiological reviews, 58(4), pp.755-805.

Pruitt, K.D., Tatusova, T. and Maglott, D.R., 2007. NCBI reference sequences (RefSeq): a curated non-redundant sequence database of genomes, transcripts and proteins. Nucleic acids research, 35(suppl_1), pp.D61-D65.

Pushkareva, E., Pessi, I.S., Namsaraev, Z., Mano, M.J., Elster, J. and Wilmotte, A., 2018. Cyanobacteria inhabiting biological soil crusts of a polar desert: Sør Rondane Mountains, Antarctica. Systematic and applied microbiology, 41(4), pp.363-373.

Qiu, B. and Gao, K., 2001. Photosynthetic characteristics of the terrestrial blue-green alga, *Nostoc flagelliforme*. European Journal of Phycology, 36(2), pp.147-156.

Quesada, A. and Vincent, W.F., 1997. Strategies of adaptation by Antarctic cyanobacteria to ultraviolet radiation. European Journal of Phycology, 32(4), pp.335-342.

R Core Team (2021) R: A Language and Environment for Statistical Computing. R Foundation for Statistical Computing, Vienna.https://www.R-project.org

Raymond, J.A., Janech, M.G., and Mangiagalli, M. (2021) Ice-binding proteins associated with an Antarctic cyanobacterium, *Nostoc* sp. HG1. Appl Environ Microbiol 87: e02499–e02420.

Rodriguez, J. Rivas, M.G. Guerrero, M. Losada, Nitrogen-fixing cyanobacterium with a high phycoerythrin content, Appl. Environ. Microbiol. 55 (1989) 758–760.

Rodriguez-Caballero, E., Belnap, J., Büdel, B., Crutzen, P.J., Andreae, M.O., Pöschl, U. and Weber, B., 2018. Dryland photoautotrophic soil surface communities endangered by global change. Nature Geoscience, 11(3), pp.185-189.

Rossi, F. and De Philippis, R., 2015. Role of cyanobacterial exopolysaccharides in phototrophic biofilms and in complex microbial mats. Life, 5(2), pp.1218-1238.

Roure, B., Rodriguez-Ezpeleta, N. and Philippe, H., 2007. SCaFoS: a tool for selection, concatenation and fusion of sequences for phylogenomics. BMC Evolutionary Biology, 7(1), pp.1-12.

Saary, Paul, Alex L. Mitchell, and Robert D. Finn. “Estimating the quality of eukaryotic genomes recovered from metagenomic analysis with EukCC.” Genome biology 21.1 (2020): 1-21.

Sayers, E.W., Cavanaugh, M., Clark, K., Pruitt, K.D., Schoch, C.L., Sherry, S.T. and Karsch-Mizrachi, I., 2022. GenBank. Nucleic acids research, 50(D1), p.D161.

Scheer, H. and Zhao, K.H., 2008. Biliprotein maturation: the chromophore attachment. Molecular microbiology, 68(2), pp.263-276.

Schuurmans, R.M., van Alphen, P., Schuurmans, J.M., Matthijs, H.C. and Hellingwerf, K.J., 2015. Comparison of the photosynthetic yield of cyanobacteria and green algae: different methods give different answers. PloS one, 10(9), p.e0139061.

Seemann, T., 2014. Prokka: rapid prokaryotic genome annotation. Bioinformatics, 30(14), pp.2068-2069.

Sherman, D.M., Tucker, D. and Sherman, L.A., 2000. Heterocyst development and localization of cyanophycin in N2-fixing cultures of *Anabaena* sp. PCC 7120 (Cyanobacteria). Journal of Phycology, 36(5), pp.932-941.

Sen, S., Rai, S., Yadav, S., Agrawal, C., Rai, R., Chatterjee, A. and Rai, L.C., 2017. Dehydration and rehydration-induced temporal changes in cytosolic and membrane proteome of the nitrogen fixing cyanobacterium Anabaena sp. PCC 7120. Algal research, 27, pp.244-258.

Shih, P.M., Wu, D., Latifi, A., Axen, S.D., Fewer, D.P., Talla, E., Calteau, A., Cai, F., Tandeau de Marsac, N., Rippka, R. and Herdman, M., 2013. Improving the coverage of the cyanobacterial phylum using diversity-driven genome sequencing. Proceedings of the National Academy of Sciences, 110(3), pp.1053-1058.

Shimura, Y., Hirose, Y., Misawa, N., Osana, Y., Katoh, H., Yamaguchi, H. and Kawachi, M., 2015. Comparison of the terrestrial cyanobacterium *Leptolyngbya* sp. NIES-2104 and the freshwater *Leptolyngbya boryana* PCC 6306 genomes. DNA Research, 22(6), pp.403-412.

Sicora, C.I., Ho, F.M., Salminen, T., Styring, S. and Aro, E.M., 2009. Transcription of a "silent" cyanobacterial psbA gene is induced by microaerobic conditions. *Biochimica et Biophysica Acta (BBA)-Bioenergetics*, *1787*(2), pp.105-112.

Simão, F.A., Waterhouse, R.M., Ioannidis, P., Kriventseva, E.V. and Zdobnov, E.M., 2015. BUSCO: assessing genome assembly and annotation completeness with single-copy orthologs. Bioinformatics, 31(19), pp.3210-3212

Sinetova, M.A. and Los, D.A., 2016. New insights in cyanobacterial cold stress responses: Genes, sensors, and molecular triggers. Biochimica et Biophysica Acta (BBA)-General Subjects, 1860(11), pp.2391-2403.

Soule, T., Gao, Q., Stout, V. and Garcia-Pichel, F., 2013. The global response of Nostoc punctiforme ATCC 29133 to UVA stress, assessed in a temporal DNA microarray study. *Photochemistry and photobiology*, *89*(2), pp.415-423.

Summerfield, T.C., Toepel, J. and Sherman, L.A., 2008. Low-oxygen induction of normally cryptic *psbA* genes in cyanobacteria. Biochemistry, 47(49), pp.12939-12941.

Stamatakis, A., Hoover, P. and Rougemont, J., 2008. A rapid bootstrap algorithm for the RAxML web servers. Systematic biology, 57(5), pp.758-771.

Stothard P, Wishart DS (2005) Circular genome visualization and exploration using CGView. Bioinformatics 21:537-539.

Tamaru, Y., Takani, Y., Yoshida, T. and Sakamoto, T., 2005. Crucial role of extracellular polysaccharides in desiccation and freezing tolerance in the terrestrial cyanobacterium *Nostoc commune*. Applied and Environmental Microbiology, 71(11), pp.7327-7333.

Taton, A., Grubisic, S., Ertz, D., Hodgson, D. A., Piccardi, R., Biondi, N., Tredici, M. R., Mainini, M., Losi, D., Marinelli, F., &Wilmotte, A. (2006). Polyphasic study of Antarctic cyanobacterial strains. Journal of Phycology, 42(6), 1257-1270.

Thoisen, C., Hansen, B.W. and Nielsen, S.L., 2017. A simple and fast method for extraction and quantification of cryptophyte phycoerythrin. MethodsX, 4, pp.209-213.

Vézina, S. and Vincent, W.F., 1997. Arctic cyanobacteria and limnological properties of their environment: Bylot Island, Northwest Territories, Canada (73 N, 80 W). Polar Biology, 17(6), pp.523-534.

Wada, N., Sakamoto, T. and Matsugo, S., 2013. Multiple roles of photosynthetic and sunscreen pigments in cyanobacteria focusing on the oxidative stress. Metabolites, 3(2), pp.463-483.

Walker, B.J., Abeel, T., Shea, T., Priest, M., Abouelliel, A., Sakthikumar, S., Cuomo, C.A., Zeng, Q., Wortman, J., Young, S.K. and Earl, A.M., 2014. Pilon: an integrated tool for comprehensive microbial variant detection and genome assembly improvement. PloS one, 9(11), p.e112963.

Wang, M.H., Cordell, H.J. and Van Steen, K., 2019, April. Statistical methods for genome-wide association studies. In Seminars in cancer biology (Vol. 55, pp. 53-60). Academic Press.

Wang, L., Lei, X., Yang, J., Wang, S., Liu, Y. and Liang, W., 2018. Comparative transcriptome analysis reveals that photosynthesis contributes to drought tolerance of *Nostoc flagelliforme* (Nostocales, Cyanobacteria). Phycologia, 57(1), pp.113-120.963

Warren, M.J., Smith, A.G., Frankenberg-Dinkel, N. and Terry, M.J., 2009. Synthesis and role of bilins in photosynthetic organisms. Tetrapyrroles: Birth, life and death, pp.208-220.

Watzer, B. and Forchhammer, K., 2018. Cyanophycin synthesis optimizes nitrogen utilization in the unicellular cyanobacterium Synechocystis sp. strain PCC 6803. Applied and Environmental Microbiology, 84(20), pp.e01298-18.

Weber, B., Belnap, J., Büdel, B., Antoninka, A.J., Barger, N.N., Chaudhary, V.B., Darrouzet-Nardi, A., Eldridge, D.J., Faist, A.M., Ferrenberg, S. and Havrilla, C.A., 2022. What is a biocrust? A refined, contemporary definition for a broadening research community. *Biological Reviews*, *97*(5), pp.1768-1785.

Wickham, H., Chang, W. and Wickham, M.H., 2016. Package 'ggplot2'. Create elegant data visualisations using the grammar of graphics. Version, 2(1), pp.1-189.

Wood, D.E., Lu, J. and Langmead, B., 2019. Improved metagenomic analysis with Kraken 2. Genome biology, 20(1), pp.1-13.

Xu, H.F., Dai, G.Z., Bai, Y., Shang, J.L., Zheng, B., Ye, D.M., Shi, H., Kaplan, A. and Qiu, B.S., 2022. Coevolution of tandemly repeated hlips and RpaB-like transcriptional factor confers desiccation tolerance to subaerial Nostoc species. Proceedings of the National Academy of Sciences, 119(42), p.e2211244119.

Yadav, R.K., Tripathi, K., Varghese, E. and Abraham, G., 2021. Physiological and proteomic studies of the cyanobacterium Anabaena sp. acclimated to desiccation stress. Current Microbiology, 78(6), pp.2429-2439.

Yoshimura, H., Okamoto, S., Tsumuraya, Y. and Ohmori, M., 2007. Group 3 sigma factor gene, sigJ, a key regulator of desiccation tolerance, regulates the synthesis of extracellular polysaccharide in cyanobacterium *Anabaena* sp. strain PCC 7120. DNA research, 14(1), pp.13-24.

Zhang, P., Allahverdiyeva, Y., Eisenhut, M. and Aro, E.M., 2009. Flavodiiron proteins in oxygenic photosynthetic organisms: photoprotection of photosystem II by Flv2 and Flv4 in *Synechocystis* sp. PCC 6803. PLoS One, 4(4), p.e5331.

Zhang, Z.C., Wang, K., Hao, F.H., Shang, J.L., Tang, H.R. and Qiu, B.S., 2021. New types of ATP-grasp ligase are associated with the novel pathway for complicated mycosporine-like amino acid production in desiccation-tolerant cyanobacteria. Environmental Microbiology, 23(11), pp.6420-6432.

Ziegler, K., Diener, A., Herpin, C., Richter, R., Deutzmann, R. and Lockau, W., 1998. Molecular characterization of cyanophycin synthetase, the enzyme catalyzing the biosynthesis of the cyanobacterial reserve material multi-L-arginyl-poly-L-aspartate (cyanophycin). European journal of biochemistry, 254(1), pp.154-159.

CHAPTER 5

GENERAL DISCUSSION

This Ph.D. thesis aimed at using a multidisciplinary approach to underpin the main microbial distribution patterns across the ice-free nunataks and valleys of the western Sør Rondane Mountains, the main abiotic stressors that drive their communities, by characterizing putative keystone taxa that have a fundamental role within these communities, and, ultimately, to unveil which adaptation mechanisms are adopted by cyanobacteria to face the extreme abiotic conditions, such as desiccation. Below, follows a general discussion of the results.

5.1 INTRODUCTION

Despite the preeminent importance of microbial communities in the Antarctic, our understanding of their evolutionary characteristics and ecologic role is still at a rudimentary stage. The need for this information has heightened with the increasing level of human activities and climate change impacts, such as the growing risks of heatwaves events (Bergstrom, Woehler et al. 2018, Robinson et al. 2020). Antarctic microbial communities are thus threatened to change, and in some regions such as the Antarctic Peninsula, initial communities' shifts have already been observed (Andriuzzi et al. 2018, Cannone et al. 2022, Robinson et al. 2018). Nonetheless, we still lack the fundamental knowledge to assess the current biodiversity and uniqueness of microbial communities of several understudied Antarctic ice-free areas, necessary to model the future changes expected within these ecosystems.

The distribution of species, diversity-levels, structuring factors and the adaptation mechanisms of the microbiota inhabiting such extreme but vulnerable environments, are advancing fields in molecular ecology. Yet, impaired efforts have been dedicated to different regions of the Antarctic ice-free areas, leading to well characterized microbial communities of the Antarctic Peninsula and the McMurdo Dry Valleys in Victoria Land, and understudied microbial communities of e.g. the Sør Rondane Mountains in Dronning Maud Land. Moreover, specific surveys of (mainly) cyanobacteria and micro-eukaryotes carried out in terrestrial habitats

remain limited. This is surprisingly especially for cyanobacteria, the 'ecosystem engineers' of these oligotrophic soils, given their important role in the carbon and nitrogen cycles (Belnap et al. 2003, Lee et al. 2016, Chrismas et al. 2018, Ortiz et al. 2020, Van Goethem et al. 2017). Antarctic microbial surveys often suffer of understudied or misidentified micro-eukaryotic and cyanobacteria taxa. This is, at least in part, due to the fact that the study of species distribution cannot overlook the concept of species itself, which is a key challenge in microbial ecology. Bacterial and micro-eukaryotic "species" are typically defined coarsely (i.e. 97 %, 97.5 % or 99 % similarity of 16S or 18S rRNA genes, resulting in distinct taxonomic resolutions, often above the species level; Hanson et al. 2012). Apart from these issues, cyanobacteria have a further particular characteristic: they have traditionally been studied in botany and taxonomically classified analogously to algae and plants. This, in addition to the difficulties in correctly classify cyanobacteria because of similar morphologies, have led to frequent misidentifications of the species encountered in environmental samples. While these taxonomic issues may seem far out and only important to cyanobacterial taxonomists, they prove to be a much larger problem when investigating the ecological role of these organisms. The use of general kingdom-wide primer sets that target relatively conserved genes, such as the ribosomal gene 16S, intensify the problem since it does not have sufficient resolution in cyanobacterial taxonomic group, similarly to the 18S rRNA for specific groups of the micro-eukaryotic lineages (i.e. diatoms). Targeting single groups, finer taxonomic scale can be assessed for i.e. cyanobacterial communities (see Pessi et al. 2018 and Pushkareva et al. 2018). However, such fine taxonomic scale surveys remain very limited in the terrestrial Antarctic ice-free areas, which hampers our general understanding about the ecology of i.e. such ecosystem engineers. Not only understanding the abiotic conditions favouring specific microorganisms' dispersal both at global and local scales is critical, but also it is the characterization of the adaptation mechanisms that they are able to employ in order to face the extreme abiotic forcing. Cyanobacteria are one of the most diverse bacterial groups inhabiting the terrestrial ice-free areas of the Antarctic. Previous studies focusing their attention on their main physiological response investigated their EPS and compatible compounds production (i.e. trehalose and sucrose), their photosynthetic activity and their pigment content

(e.g. the photoprotective carotenoids). The physiological response, however, can only give a partial answer about their adaptative strategies to face the extreme Antarctic environments. Linking physiological and omics techniques is therefore fundamental to fill the gap between the ecophysiology and the genetic adaptative response to abiotic stressors, overall enhancing our knowledge regarding their ecological role in cold deserts.

With this Ph.D. thesis, the above described issues were addressed by focusing on two distinct datasets. The first dataset comprised amplicon sequences of bacteria, cyanobacteria and micro-eukaryotes from nearly 100 samples collected in the western Sør Rondane Mountains (**Chapters 2** and **3**). Here, we observed that microbial assemblages varied across substrate types, such as gneiss, granite, marble and moraines of different valleys. Keystone taxa were identified, such as *Nostoc* sp. (Cyanobacteriota) in granite and gneiss samples, *Aliterella* sp. (Cyanobacteriota) in marble samples and Solirubrobacterales phylotypes (Actinomycetota) in moraine samples (**Chapter 2**). Also, comparisons with previous studies revealed that earlier assessments of the Antarctic largely underestimated cyanobacterial diversity (**Chapter 3**). The second dataset encompass the ecophysiological and transcriptomic response of a pair of *Nostoc* sp. strains belonging to the same species, but originating from two contrasting Antarctic habitats: terrestrial and freshwater (**Chapter 4**). Here we highlighted that both strains employ different strategies to cope with desiccation. For instance, the terrestrial strain responded by up-regulating a higher number of genes under desiccation compared to the freshwater strain, which however responded faster to rehydration by e.g. fastly restoring its chlorophyll *a* production. None strain seemed to be however very drought resistant, since the photosynthetic apparatus as well as other metabolic functions did not become immediately inactive under desiccation and did not reactivate immediately upon rehydration. These results also highlight the importance of studying non-model organisms to understand the ecologic role of cold desert adapted organisms.

5.2 METHODOLOGICAL CONSIDERATIONS

With the current development and improvement of omics tools in microbial ecology, the microbial surveys have increased even in the remote and extreme Antarctic ice-free areas. The use of metabarcoding specifically for characterizing the diversity and community structure of cyanobacteria has been less frequently employed in comparison to bacteria, although its application increased within the last several years (i.e. Taton et al. 2003, 2006a and 2006b, Pessi et al. 2016 and 2018), with only a few surveys focusing on the terrestrial instead of lacustrine Antarctic ice-free areas (e.g. Pushkareva et al. 2018). Metabarcoding studies have provided a more accurate and robust overview of cyanobacterial communities compared to exclusive traditional morphology-based studies (Li et al. 2019, MacKeigan et al. 2022). Therefore, the significance of the 16S rRNA cannot be underrated and serves as a valuable tool for cyanobacterial identification (Lefler et al. 2023). These studies generally entrusted their classification to SILVA (Quast et al. 2013) or Greengenes (DeSantis et al. 2006) databases, which also contain cyanobacterial sequences. However, they neither sufficiently nor accurately curate the class Cyanobacteria. For instance, SILVA database uses Genome Taxonomy Database (GTDB; Parks et al. 2021) to help guide its nomenclature which often encompass outdated or invalid taxonomic affiliations. For example, the class “Cyanobacteriia” replace the currently validated “Cyanophyceae” one, the order “Cyanobacteriales” is in place of several validly described orders of Cyanobacteria, many valid families are not present, such as Gomantiellaceae, or some genus are placed in wrong families, as in the case of *Cyanothece*, whose “species” names belong to two different families, such as Microcystaceae or Thermosynechococcaceae, depending on the strain name. These databases are not curated by incorporating the frequent changes in cyanobacterial taxonomy with the newly described and revised taxa, which poses a true issue when attempting to properly assign taxonomy and understanding their significance in the environment. A newly released and constantly curated cyanobacterial 16S rRNA sequences database was conceived to circumnavigate these problems, the CyanoSeq database (https://zenodo.org/record/7569105; Lefler et al. 2022). In **Chapter 2**, the taxonomy of the microbial sequences was assigned via the SILVA database, including the cyanobacterial sequences. The use of this database impacted, at

least in part, the accuracy of the cyanobacterial taxonomy assignation. However, the use such database resulted as a good compromise when investigating both the bacterial and micro-eukaryotic communities structures. Also, the use of general bacterial primers targeting the V1-V3 16S rRNA gene was not ideal to underpin the detailed diversity characterizing the cyanobacterial communities of the investigated samples. In order to overcome these issues, the cyanobacteria-specific primers developed by Nübel et al. (1997) targeting the V3–V4 region of the 16S rRNA gene were used on a separated survey focusing only on cyanobacterial communities (**Chapter 3**) inhabiting the same regions of **Chapter 2** and the CyanoSeq database was employed for the taxonomic assignation of cyanobacterial-only sequences. The taxonomy of these sequences was first assigned through the Greengenes database. Comparisons showed that the use of the CyanoSeq database allowed the taxonomic identification at the order level for 78 % of the encountered cyanobacterial OTUs (1211 out of 1551) compared to the classification at the class level for the 68 % of the designated cyanobacterial OTUs (1237 out of 1824). Thus, the use of this new database improves the taxonomic identification of the OTUs, linking it to the current cyanobacterial taxonomic system that has evolved quite a lot recently (Strunecký et al. 2022), via continuous updates (Lefler et al. 2023). Nonetheless, phylogenetic reconstructions based on a single gene remain problematic, for instance, because of the result from gene trees rather than species trees, overlooking the possibility of horizontal transfer extensively documented in prokaryotic rRNA operons (Ueda et al. 1999, Yap et al. 1999, Marěs 2017). These horizontal transfers can amount up to 10.95 % of some genomes (Lin et al. 2010) conferring to cyanobacterial genomes a high plasticity. Because phylotypes of a same cyanobacterial species are defined as having the same genotype, the question about which gene (or genes) has to be used in order to characterize their taxonomy is appropriate. In light of all these considerations, genomics prevails as being the most promising framework for revising and defining the taxonomic classification of cyanobacteria. However, there is a need for broader genome sequencing efforts especially of Antarctic cyanobacteria, that are currently limited to a handful of strains in public databases, such as *P. priestleyi* ULC007 (Lara et a. 2017), *Leptolyngbya* sp. BC1307 Chrismas et al. 2018, *Synechococcus* sp. SynAce01 (Tang et al. 2019), *Nostoc* sp. SO-36

(Effendi et al. 2022) and *Nostoc* sp. CCCryo 231-06 (Liu et al. 2022). Other 9 low-/medium-quality genomes obtained by a metagenome-like assembling approach of non-axenic strains are also available (Cornet et al. 2018). Genome-resolved metagenomics is a well-established approach to increase our knowledge in microbial diversity and their ecological preferences, as it overlooks the above mentioned issues associated with taxonomic identification from a single gene and the problems that arise with the culturing process. Some interesting results were recently provided by a metagenomics survey characterizing novel lineages of early-branching Cyanobacteria of the order Gleobacterales from Antarctica (Pessi et al. 2023).

Overall, increasing the genomic effort of Antarctic cyanobacteria may help providing a more complete picture of the Cyanobacteriota phylum and therefore gaining knowledge in their molecular biology and ecology. Being cyanobacterial taxa often neglected compared to other bacterial phyla in genomic databases, sequences especially from extreme environments may bring to light answers to meaningful questions also regarding their ecology. This knowledge in addition to the ecophysiologic measurements is essential to fill the gap of our understanding regarding how cyanobacteria could adapt to polar environments, exploring the basis of cold, high-irradiance, desiccation and oligotrophic adaptation (Richards 2015, Jungblut 2022).

5.3 ADAPTATION MECHANISMS OF CYANOBACTERIA TO ICE-FREE AREAS CONDITIONS

Photoautotrophic organisms face extreme conditions in the Antarctic ice-free areas including permanently low temperatures, freezing-thaw events during summer, general low nutrient concentrations and high irradiance over half of the year. Cyanobacteria are excellent to withstand these conditions and adaptation mechanisms associated with photophysiology protection, osmotic balance and reduction of metabolism play an important role in overcoming challenges created by the abiotic stressors. Although they are able to thrive to sub-zero temperatures, to date psychrophile phylotypes (organisms with optimal growth temperatures of ≤ 15 °C, not surviving temperatures exceeding 18 °- 20 °C; Morita 1975) have not yet been described. These organisms are therefore considered photopsychrotolerant, tolerating and surviving a broad

range of temperatures (5 ° - 40 °C). The low temperatures in their natural environment lower their photosynthetic ability by impeding the use of energy excess resulting from the high irradiance (Ort 2001). This often leads them to a photoprotection state that prevent them to damage their photosystem with consequent slowing down of their growth and metabolic activity.

Adaptation of photoautotrophs to a polar environment must compensate for the potential energy imbalances experienced by living in a low temperature environment. Thus, non-model biological species from seemingly inhospitable Antarctic ecosystems need to be studied to understand the mechanisms allowing these organisms to adapt to life under these extreme conditions (Kennicutt et al. 2014 and 2015, Xavier et al. 2016, Grossman 2021). A goal of this Ph.D. thesis was to illustrate how non-model, polar, freshwater and terrestrial photosynthetic species of cyanobacteria would provide evidence of their actual plasticity. Genome-resolved metagenomics was therefore applied in **Chapter 4** to two non-axenic cyanobacterial strains from the cyanobacterial culture collection BCCM (https://bccm.belspo.be/) belonging to the same species (ANI > 95 %) of *Nostoc* sp. isolated from two contrasted habitats of the Antarctic ice-free areas: ULC180 from a BSC of a granitic outcrop in the Sør Rondane Mountains and ULC008 from a benthic mat of a lake in Larsemann Hills (East Antarctica). Although cyanobacteria often dominate their habitats in the cryosphere, they are not the only organism inhabiting these environments. Instead, they are often part of diverse microbial communities, where they interact with other cyanobacteria, bacteria and eukaryotes (e.g. Chapter 2 and 3, Tytgat et al. 2016, Jungblut and Vincent 2017). Also, some bacteria such as Bacteroidota and Pseudomonadota are known to feed on the cyanobacterial EPS and osmolytes (Stuart et al. 2016, Lee et al. 2014, Peeters et al. 2012). Overall, culturing them in complete axenic conditions is challenging, and this is why ULC008 and ULC180 were cultured in non-axenic conditions. Nonetheless, both genomes showed very little contamination (0.44 %, see Table 4.1) and only small contigs of other bacterial genomes were retrieved during the assembly, which have been further discarded. The impact of not using axenic cultures for this study is therefore negligible. Both *Nostoc* sp. strains showed a variety of genetic and physiologic adaptations to desiccation, highlighting their potential to overcome to such abiotic stressor. Among the two genomes, and in contrast with other

comparative genomics surveys from temperate *Nostoc* sp. (e.g. Khani-Juyabad et al. 2022, Prabha et al. 2016), our terrestrial strain was characterized by a smaller genome compared to the freshwater one. Indeed, other *Nostoc* terrestrial genomes are characterized by 8-10 Mbp and freshwater ones by 6-7 Mbp (Khani-Juyabad et al. 2022) whilst both the *Nostoc* sp. investigated in Chapter 4 had a relatively similar genome size (terrestrial: 5.7 Mbp vs. freshwater: 6.3 Mbp). The higher genome size is often linked to an increased metabolic diversity which enable them to produce different enzymes. It was showed that in terrestrial environments, the harsh conditions require the expression of diverse enzymes for the growth and survival of Antarctic bacteria in order to exploit the scarce nutrients (Dsouza et al. 2015). Therefore, it is not yet very clear why in the studied cyanobacteria this difference was not observed. Nonetheless, the transcriptomics response to desiccation was similar to other drought-tolerant organisms, showing a higher number of up-regulated genes compared to the freshwater strain (Wang et al. 2018, Rajeev et al. 2013, Khani-Juyabad 2022). Surveys investigating a higher number of strains from contrasted environments such as the investigated ones should be carried out in order to determine whether this difference would not be detected in other Antarctic cyanobacterial strains.

Desiccation tolerance has been extensively studied in terrestrial drought-resistant *Nostoc* sp. strains from temperate environments (e.g. Yoshimura et al. 2007, Wang et al. 2018, Khani-Juyabad et al. 2022) and only a few surveys investigated desiccation response in freshwater cyanobacteria, limiting their focus almost exclusively to the model drought-sensitive *Anabaena* (*Nostoc*) 7120 sp. strains (e.g. Katoh et al. 2004, Higo et al. 2006 and 2007, Sen et al. 2017). Adaptation mechanisms to cold resistance, UVR resistance, high irradiance and osmotic stress are often characterized by similar ecophysiologic and genetic response (Jungblut 2022) and investigating the adaptation mechanisms developed by organisms living within the natural environments compared to only cultures enabled to observe mechanisms that were not shown in laboratory (i.e. faster recover in photosynthetic activity of *Microcoleus vaginatus* after rehydration in natural crusts compared to culture). A quick response of photosynthesis to rehydration was also observed in field from a natural well-developed BSC in the Sør Rondane Mountains. Photosynthetic active radiation, temperature and effective quantum yield were

monitored during a whole sunny day on a BSC from the Utsteinen ridge (Fig. 5.1). Photosynthetic activity followed the irradiance pattern even at temperatures below zero, suggesting that liquid water was available within the BSC already with the small increase in temperature due to the increase in irradiance. Overall, differences exist between 'natural' crust and strains from cultures and further investigations should therefore take into consideration to combine *in situ* with laboratory experiments.

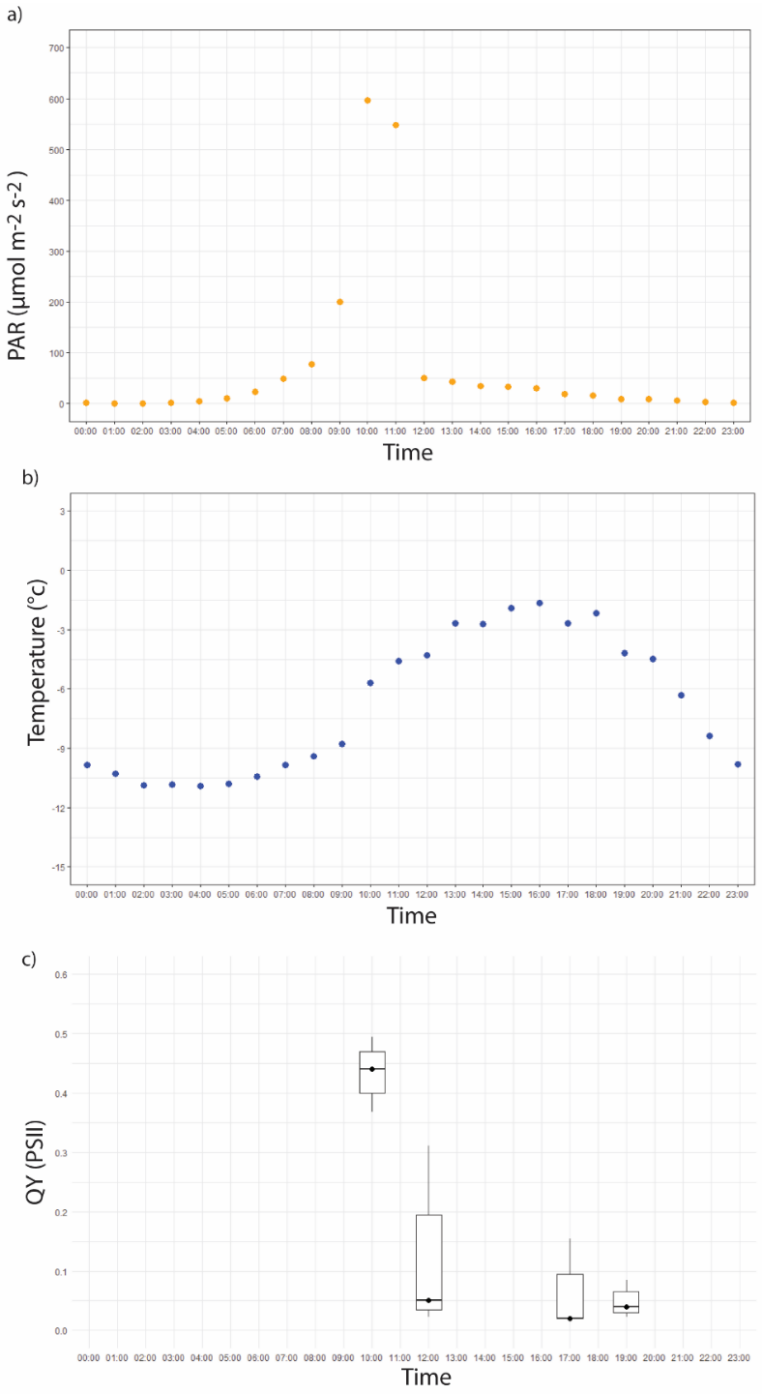

Fig. 5.1 (a) PAR, (b) surface temperature and (c) boxplots of effective quantum yield (QY) of photosystem II (PSII) *measured on a developed BSC on Utsteinen ridge (Sør Rondane Mountains) over a complete day with clear sky. n=3.*

5.4 FINAL CONCLUSIONS AND FUTURE PERSPECTIVES

5.4.1 MICROBIAL COMMUNITIES STRUCTURE AND COMPOSITION IN THE SØR RONDANE MOUNTAINS

Chapter 2 and Chapter 3 included only a relatively small, yet understudied, ice-free area of the Antarctic continent. Nonetheless, big differences among the studied communities were encountered, even at very small scales (few meters). Different substrates are characterized by a different microtopography, microstructure and elemental composition, apart from the typical geochemical properties that are often measured. Microbiology survey should therefore be combined with geologic ones. In the presented studies, granitic soils were expected to host the most diverse microbial communities because of its intrinsic features of being a hard kind of substrate characterized by crevices and cavities favouring micro-habitats that could enhance microbial communities. This was also observed by Tytgat et al. (2016), Obbels et al. (2016) and Pushkareva et al. (2018), who showed that bacterial, cyanobacterial and micro-eukaryotic communities were more diverse in granitic soils of SRM. Because of the granitic micro-structures, but also because of the low rock porosity, also liquid water is probably more retained on the surface compared to other bedrock types such as marble. Indeed, in Chapter 2 and 3 it was showed that marble soils were particularly dry and not surprisingly hosted wide communities of unicellular cyanobacteria belonging to the Chroococcidiopsaceae. Phylotypes of this family are known to be particularly drough-tolerant, being *Chroococcidiopsis* and *Alitarella* among the most abundant cyanobacterial genus colonizing endoliths from arid deserts (Meslier and DiRuggiero 2019, Ertekin et al. 2021, Archer et al. 2017, Jung et al. 2019) and having survived even two years in outer space (Napoli et al. 2022). As expected (e.g. Pointing et al. 2009), also a higher abundance of Actinomycetota phylotypes was encountered within the most arid and oligotrophic soils of our surveys, such as the moraines of Dry Valley and Austkampane. Future studies should therefore be carried on similar substrates and verify whether the differences in microbial communities among substrate types are also observed within other ice-free areas. Indeed, specifications about the bedrock type in microbial surveys from Antarctic edaphic environments are very scarce. Some studies observed that K, P, Ca, from rock weathering are important limiting trace metals for the microbial communities, including cyanobacteria (i.e. Woods et al. 2008). This latter study

highlighted that elemental composition of the substrate may be an even more important diversity driver than soil moisture content. Geologic surveys should therefore be combined more often with microbial ones. Also, more metadata on microclimate, numbers of days during which temperatures are above the freezing level and number of hours within a day in which the communities receive direct sunlight should also be investigated as potential structuring factors. Broader sampling designs should be carried on to verify cyanobacterial and other key taxa distribution across terrestrial habitats within the whole continent, to better understand their ecologic role. In order to improve the lower taxonomic resolution of the whole microbiome inhabiting ice-free areas, shotgun metagenomics might be preferred over amplicon sequencing or the use of more specific primers. Another underestimated factor in Antarctic surveys is biotic filtering. Indeed, underpinning the nature of interactions within specific communities should be increasingly addressed in order to better understand the food webs complexes that exist in specific niches.

Overall, a better understanding of the substrates and microclimatic conditions of the sampled microbial communities, addressing broader general surveys with the use of either specific primers to detect lower taxonomic levels or shotgun metagenomics as well as the biotic interactions among microorganisms with the use of co-occurrence network analysis is recommended for future microbial surveys.

5.4.2 CYANOBACTERIAL ADAPTATION MECHANISMS TO DESICCATION

In Chapter 4 of this thesis, two strains of the *Nostoc* genus were used to understand their adaptation mechanisms to cope with desiccation. Surprisingly, the terrestrial strain showed a smaller genome compared to the freshwater strain, which is in contrast to the existing literature (e.g. Khani-Juyabad et al. 2022, Prabha et al. 2016). Nonetheless, and as expected, the terrestrial strain showed a higher expression of genes and a more performant photosynthetic apparatus under desiccation compared to the freshwater strain. Drought-resistant phylotypes of this genus have been intensively investigated. Nonetheless, most of the studies focused on very drought resistant terrestrial model strains mostly originating from temperate habitats. In Chapter 4, the used strains were cultivated in laboratory conditions for over a decade and may therefore have accumulated genetic modifications. However, the two strains behaved coherently to our hypothesis, and overall both strains showed mechanisms

to thrive to, at least short-term, desiccation conditions. Further studies should however focus on more and diversified strains of cyanobacteria, also using different taxa. Employing multidisciplinary studies, although time consuming, is the only way to really understand the ecophysiological and genetic adaptation of single strains. Also, the use of non-model organisms as well as field experiments should be carried out in order to increase our knowledge regarding their response in 'natural' environments. Available genomic data is also lacking for Cyanobacteriota compared to other bacteria phyla, hence an increased effort in genomics and comparative genomics of understudied groups of cyanobacteria is desirable.

I. CHAPTER 2 – SUPPLEMENTARY MATERIALS

I.I SUPPLEMENTARY FIGURES OF CHAPTER 2

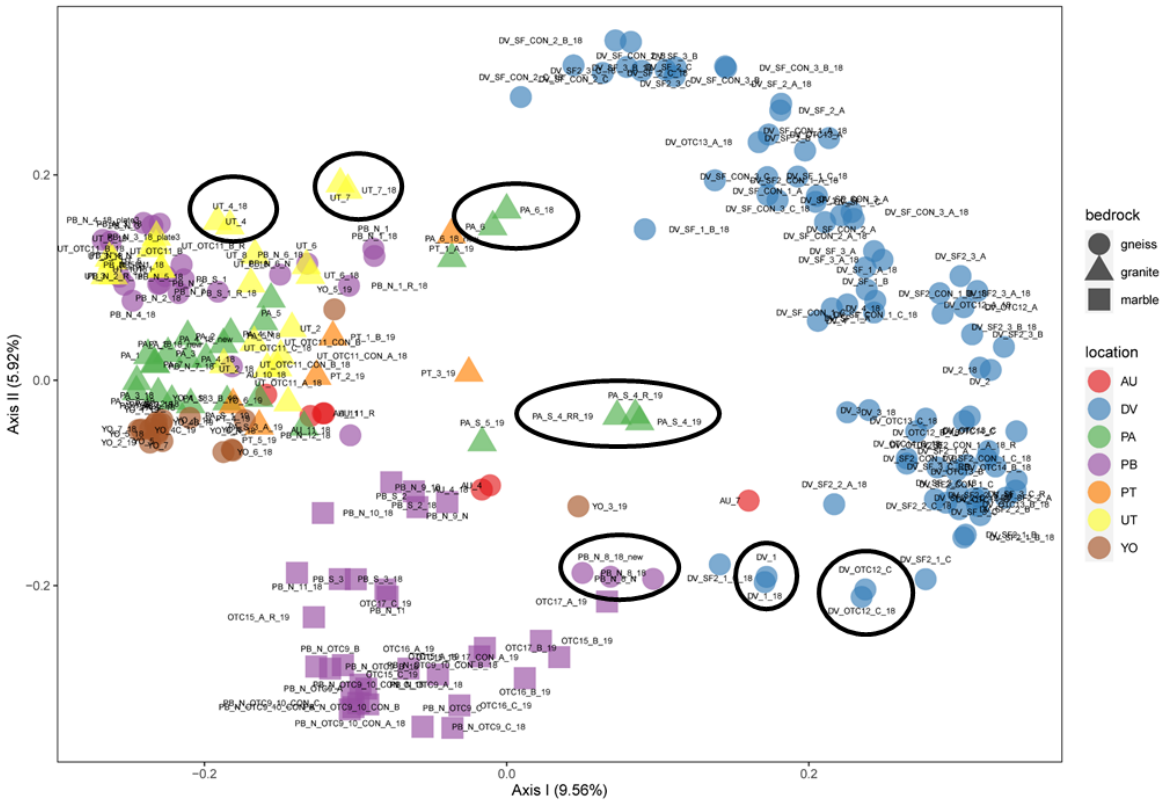

Fig. S2.1 PCoA of bacterial ASV table representing replicates *(encircled in black).*

Fig. S2.2 PCoA of eukaryotic ASV table representing replicates *(encircled in black).*

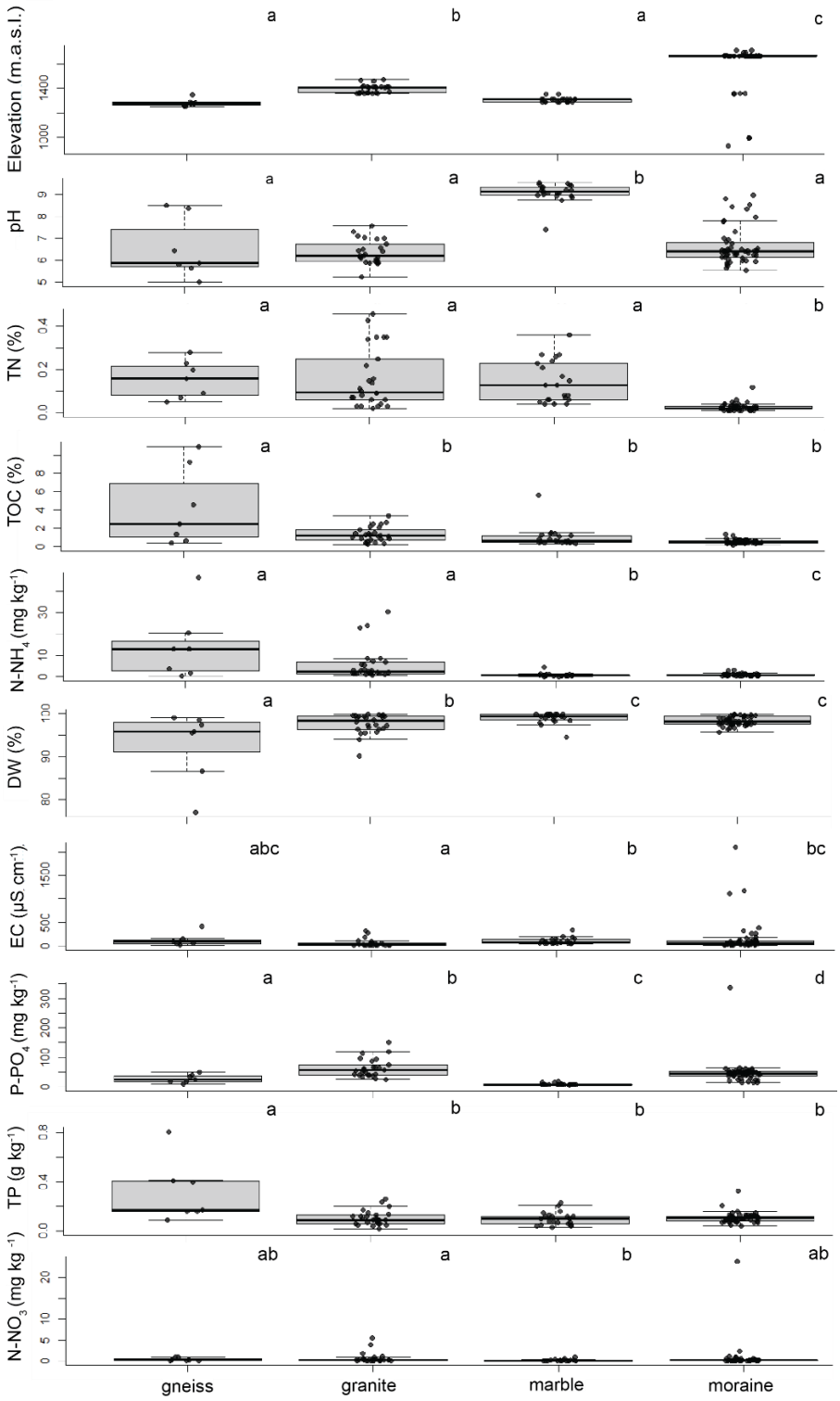

Fig. S2.3 Elevation and geochemical characterization of the soil ecosystems (four substrate types: gneiss, granite, marble and moraine). *Boxplots followed by different letters are significantly different (Kruskal-Wallis rank sum test, p < 0.05). Bars represent standard error.*

Fig. S2.4 Correlogram showing Pearson's correlation coefficients of all geochemical transformed variables. *EC: electrical conductivity; TOC: total organic carbon; DW: dry weight; TN: total nitrogen; TP: total phosphorus.*

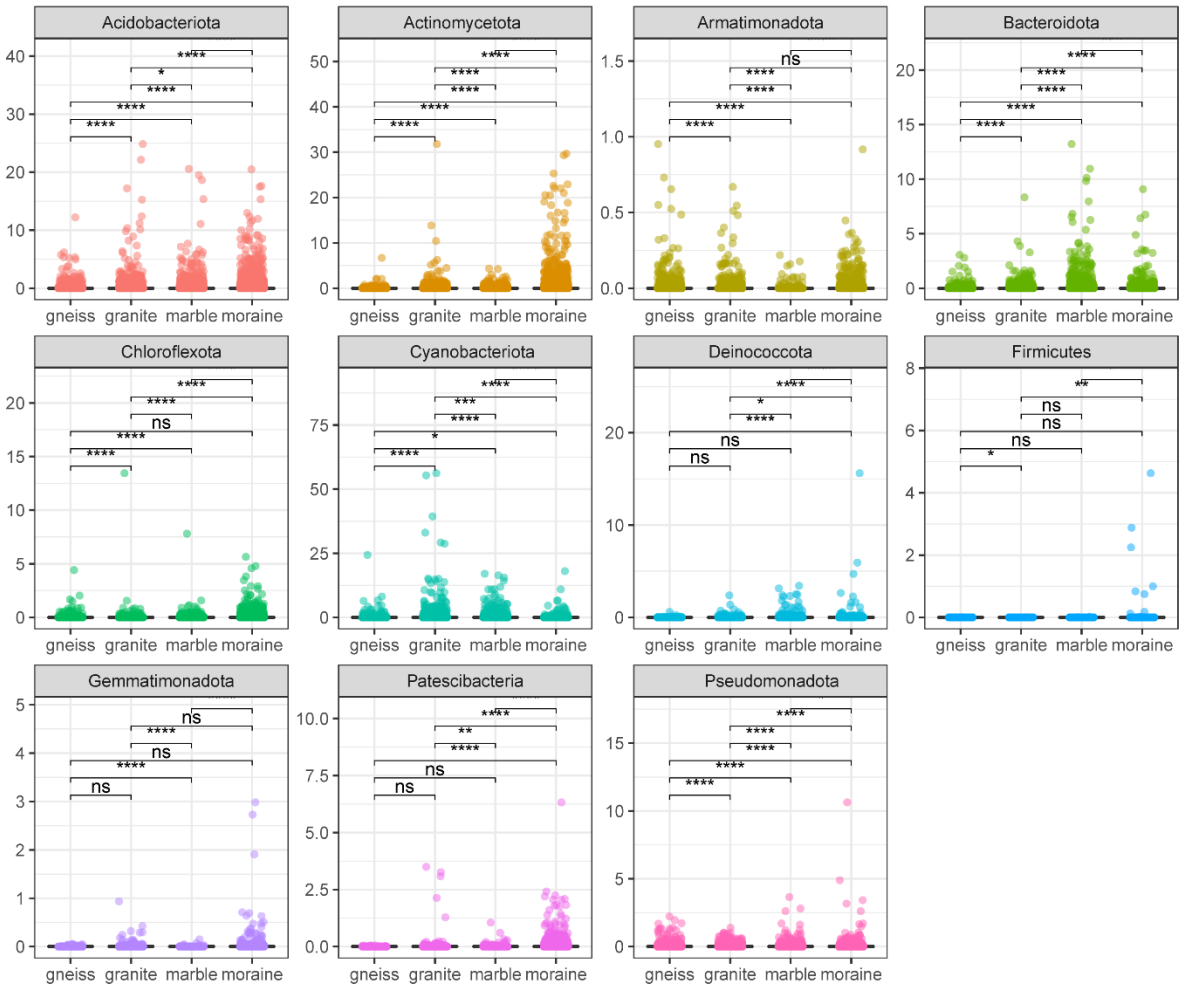

Fig. S2.5 Boxplot of relative abundances of bacterial phyla in the different kinds of substrate. *Colors represent different phyla. Asterisks represent the significance of the p-value of the pairwise Wilcoxon test after mean comparison by the Kruskal Wallis test. Asteriks represent p-values: * = p < 0.05; ** = p < 0.01; *** = p < 0.001; ns = to p > 0.05.*

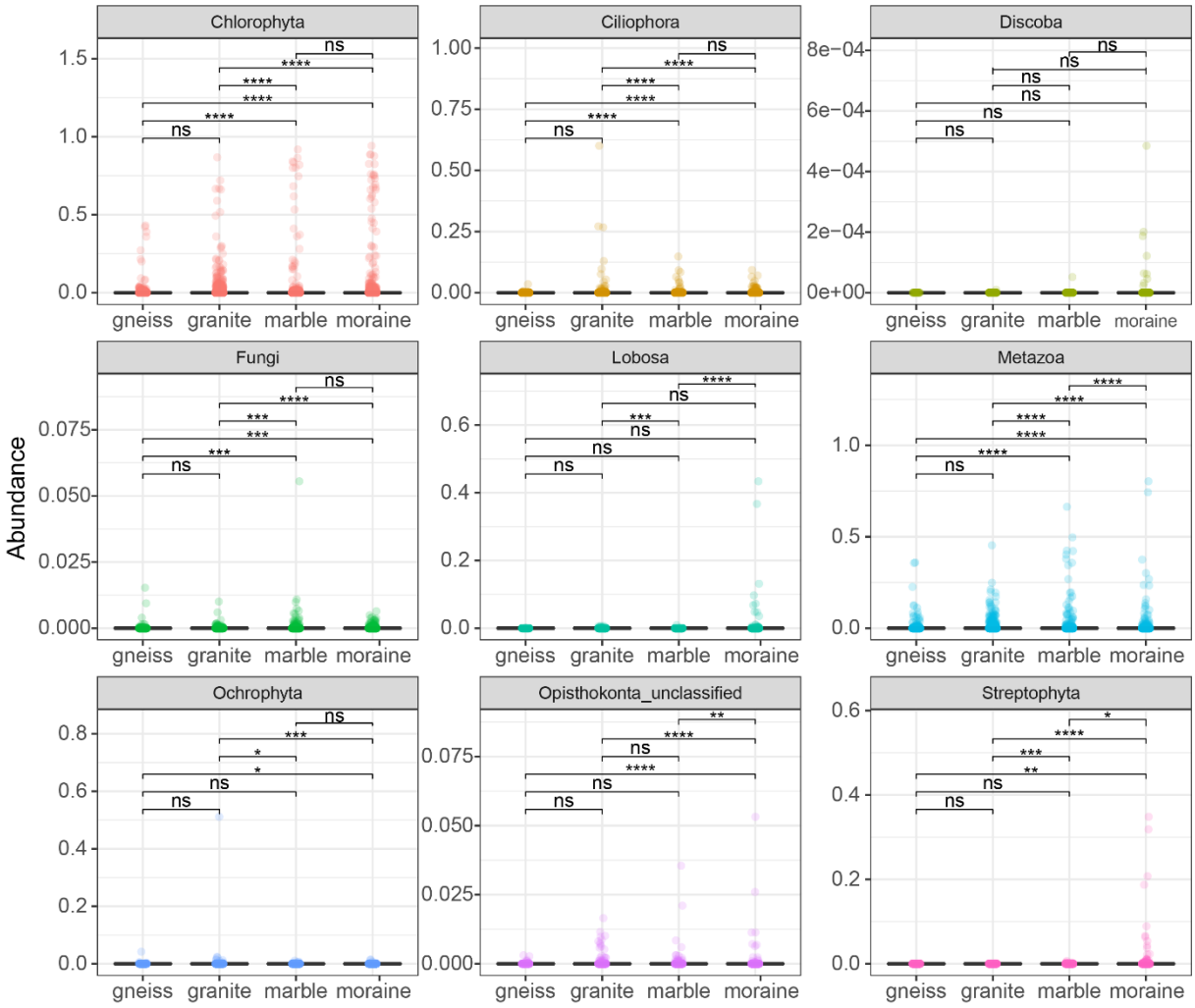

Fig. S2.6 Boxplot of relative abundances of eukaryotic phyla in the different kinds of substrate. *Colors represent different phyla. Asteriscs represent the significance of the p-value ($p < 0.05$) of the pairwise Wilcoxon test after mean comparison by the Kruskal Wallis test. ns correspond to $p > 0.05$. Asteriks represent p-values: * = $p < 0.05$; ** = $p < 0.01$; *** = $p < 0.001$; ns = to $p > 0.05$.*

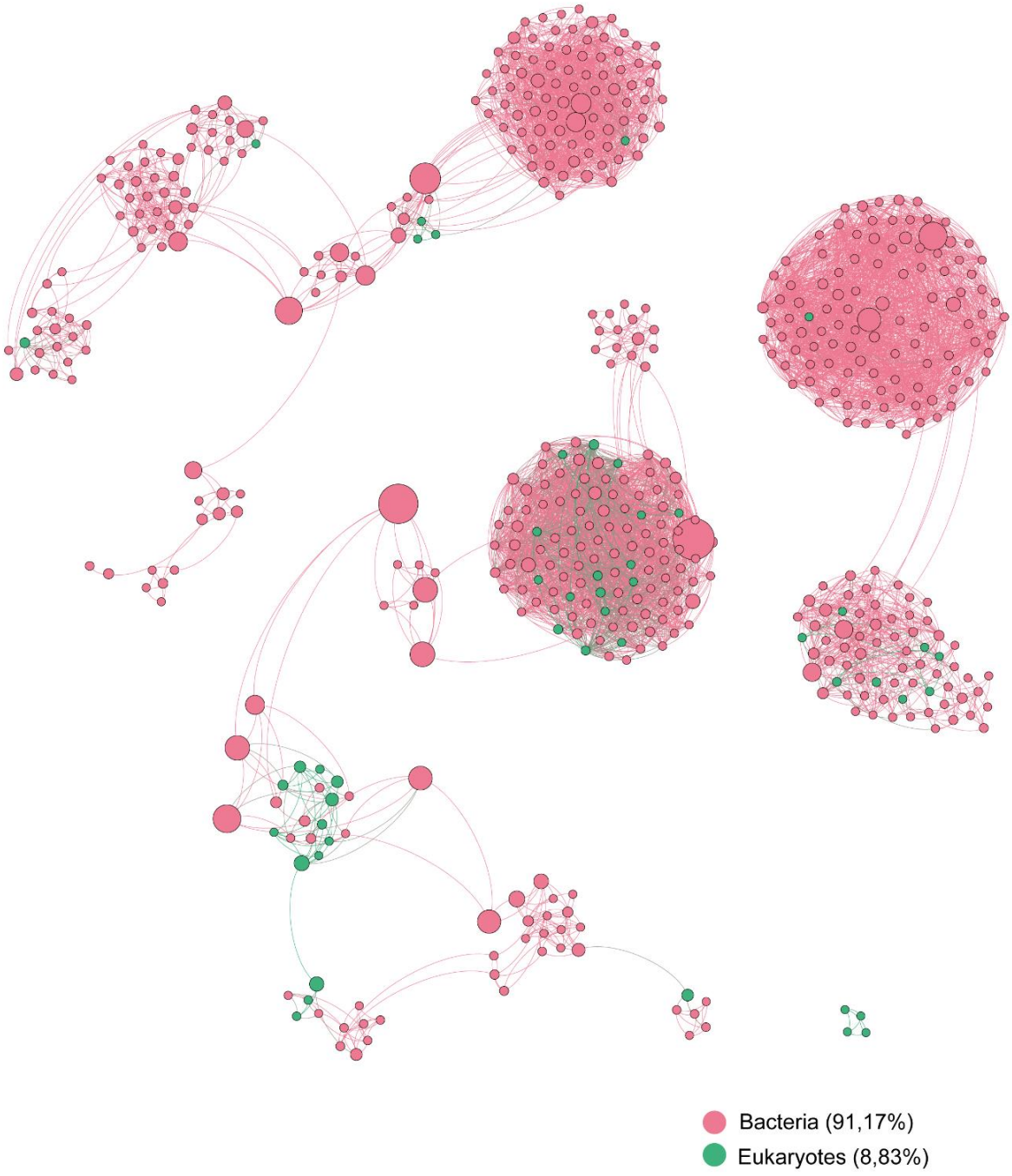

Fig. S2.7 Co-occurrence network analysis based on bacterial and eukaryotic ASVs across all sampling sites, *colored by Kingdom (red: bacterial ASVs; green: eukaryotic ASVs). Size of nodes corresponds to the betweenness centrality degree.*

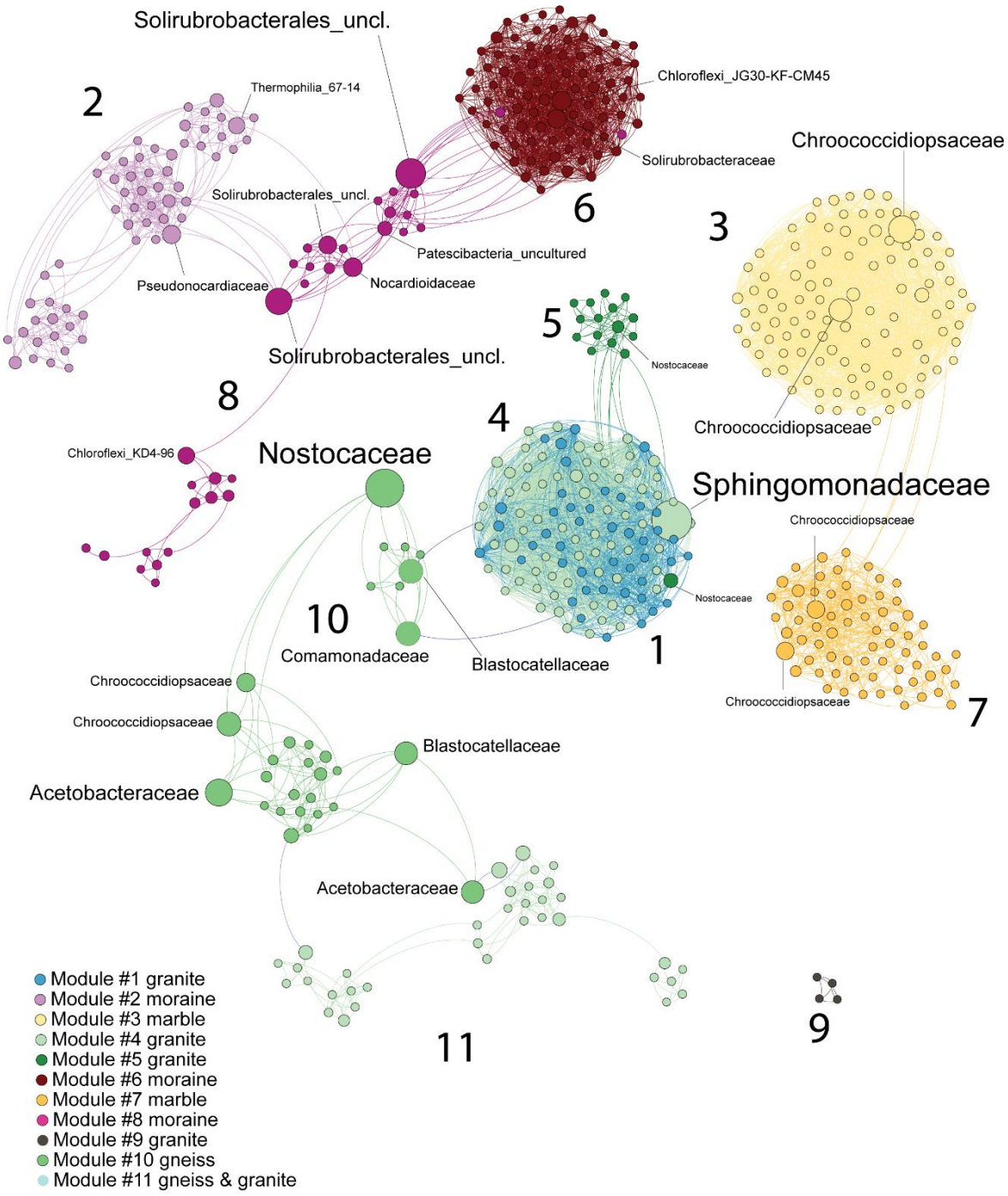

Fig. S2.8 Co-occurrence network analysis based on bacterial and eukaryotic ASVs across all sampling sites*, colored by Modules (see legend). Size of nodes and label corresponds to the betweenness centrality degree.*

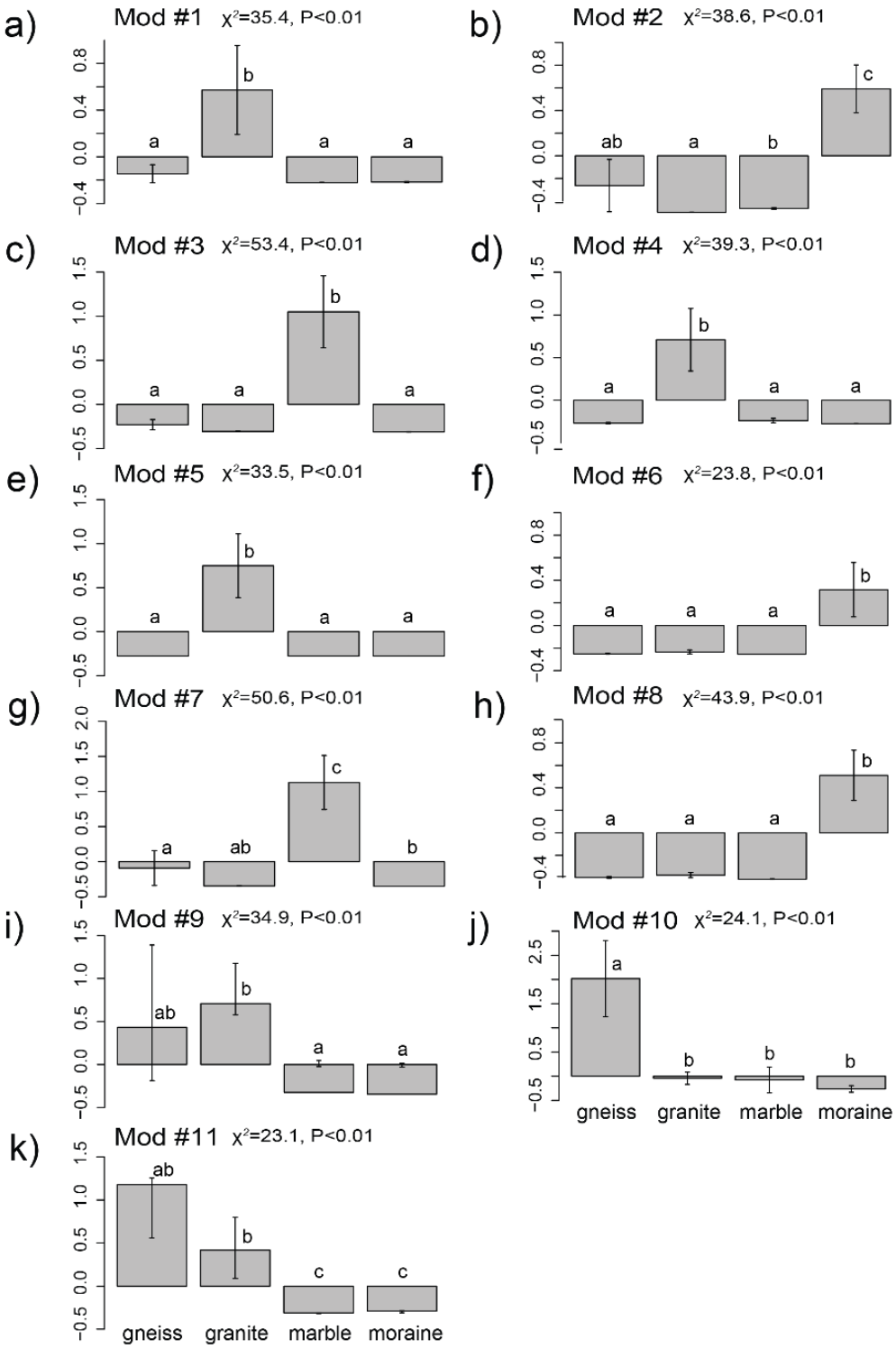

Fig. S2.9 Mean values (±SE) for the relative abundance (Z-score) of modules #1–11 across four different substrate types. *Different letters in this panel indicate significant differences among substrate types. χ^2 and P-value are from Kruskas-Wallis rank sum test.*

I.II SUPPLEMENTARY TABLES OF CHAPTER 2

Table S2.1. Environmental data.

Sample	Latitude	Longitude	Substrate	Substrate detail	pH	EC ($\mu S\ cm^{-1}$)	TOC (%)	N-NH_4 ($mg\ kg^{-1}$)	N-NO_3 ($mg\ kg^{-1}$)	Dry weight (%)	P-PO_4 ($mg\ kg^{-1}$)	TN (%)	TP (%)	Elevation (m a.s.l.)	# 16S reads	#18S reads
AU_2018_11	-71.661156	25.150839	moraine	(Mo)_Amp	7.77	164.6	0.61	3.034	23.99	99.81	337.269	0.12	0.33	930	79153	48216
AU_2018_4	-71.67534	25.136383	moraine	(Mo)_Amp	8.34	112.7	0.92	1.143	0.213	99.56	18.631	0.01	0.16	996	32443	NA
AU_2018_8	-71.67574	25.139032	moraine	(Mo)_Amp	8.2	165.6	0.81	0.536	80.518	99.38	15.965	0.02	0.12	994	NA	19445
AU_2018_7	-71.67593	25.136465	moraine	(Mo)_Amp	7.01	1112	0.68	0.742	0.421	99.65	25.596	0.01	0.21	995	118695	13805
DV_2018_1	-72.115875	23.157526	moraine	(Mo)_Sch_D_Gbh_To	7.96	2110	0.76	0.591	0.607	99.65	21.138	0.03	0.08	1714	28411	85993
DV_2018_2	-72.11599	23.157045	moraine	(Mo)_Sch_D_Gbh_To	6.36	119.5	0.46	1.645	0.133	99.55	16.177	0.02	0.08	1712	98841	1375
DV_2018_3	-72.11476	23.163443	moraine	(Mo)_Sch_D_Gbh_To	6.33	260	0.74	1.31	0.077	99.51	28.958	0.02	0.07	1694	134443	NA
DV_2018_4	-72.11468	23.163328	moraine	(Mo)_Sch_D_Gbh_To	6.44	78.9	0.49	1.085	0.021	99.64	24.585	0.03	0.07	1694	53267	NA
DV_OTC12_2018_A	-72.11223	23.184898	moraine	(Mo)_Sch_D_Gbh_To	6.14	47.6	0.49	0.637	0.125	99.92	44.325	0.01	0.07	1666	45965	9917
DV_OTC12_2018_B	-72.11223	23.184898	moraine	(Mo)_Sch_D_Gbh_To	6.29	140	0.3	0.922	0.135	99.87	40.959	0.01	0.09	1666	50727	19343
DV_OTC12_2018_C	-72.11223	23.184898	moraine	(Mo)_Sch_D_Gbh_To	7.31	1175	0.45	1.245	0.989	99.73	42.879	0.04	0.09	1666	63362	60322
DV_OTC13_2018_A	-72.11219	23.184841	moraine	(Mo)_Sch_D_Gbh_To	6.1	41.5	0.39	0.855	0.091	99.91	52.72	0.02	0.13	1667	54683	127788
DV_OTC13_2018_B	-72.11219	23.184841	moraine	(Mo)_Sch_D_Gbh_To	6.78	57.2	0.7	1.342	0.202	99.88	43.947	0.02	0.1	1667	40174	128774
DV_OTC13_2018_C	-72.11219	23.184841	moraine	(Mo)_Sch_D_Gbh_To	6.56	50.8	0.64	1.047	0.082	99.91	37.159	0.01	0.07	1667	32797	25292
DV_OTC14_2018_B	-72.11219	23.184841	moraine	(Mo)_Sch_D_Gbh_To	6.5	264	0.4	0.927	0.646	99.89	41.475	0.06	0.15	1667	30670	117064

Sample	Latitude	Longitude	Substrate	Substrate detail	pH	EC ($\mu S\ cm^{-1}$)	TOC (%)	N-NH_4 ($mg\ kg^{-1}$)	N-NO_3 ($mg\ kg^{-1}$)	Dry weight (%)	P-PO_4 ($mg\ kg^{-1}$)	TN (%)	TP (%)	Elevation (m a.s.l.)	# 16S reads	#18S reads
DV_OTC14_2018_C	-72.11219	23.184841	moraine	(Mo)_Sch_D_Gbh_To	6.46	46.9	0.3	1.275	0.211	99.92	43.192	0.05	0.15	1667	44296	101652
DV_SF_2018_1_A	-72.11258	23.18555	moraine	(Mo)_Sch_D_Gbh_To	6.06	382	0.6	0.986	0.272	99.84	46.216	0.03	0.12	1667	44638	NA
DV_SF_2018_1_B	-72.11258	23.18555	moraine	(Mo)_Sch_D_Gbh_To	6.45	59.2	0.34	0.802	0.143	99.74	37.011	0.02	0.09	1667	73228	45577
DV_SF_2018_1_C	-72.11258	23.18555	moraine	(Mo)_Sch_D_Gbh_To	6.4	52.7	0.57	1.101	0.026	99.82	37.628	0.03	0.07	1667	72354	54217
DV_SF_2018_2_A	-72.11258	23.18555	moraine	(Mo)_Sch_D_Gbh_To	6.22	34.7	0.38	0.94	0.102	99.87	47.913	0.02	0.11	1667	162952	NA
DV_SF_2018_2_B	-72.11258	23.18555	moraine	(Mo)_Sch_D_Gbh_To	6.34	30.8	0.38	1.011	0.177	99.9	53.034	0.02	0.13	1667	26318	15084
DV_SF_2018_2_C	-72.11258	23.18555	moraine	(Mo)_Sch_D_Gbh_To	5.98	40.8	0.52	1.041	0.918	99.86	57.324	0.03	0.13	1667	66432	NA
DV_SF_2018_3_A	-72.11258	23.18555	moraine	(Mo)_Sch_D_Gbh_To	6.43	95	0.47	0.836	0.088	99.89	46.376	0.03	0.12	1667	33494	NA
DV_SF_2018_3_B	-72.11258	23.18555	moraine	(Mo)_Sch_D_Gbh_To	5.94	328	0.19	0.946	0.157	99.88	50.124	0.03	0.13	1667	31021	NA
DV_SF_2018_3_C	-72.11258	23.18555	moraine	(Mo)_Sch_D_Gbh_To	6.49	62.7	0.49	1.217	0.046	99.63	37.329	0.02	0.08	1667	154035	49349
DV_SF_2018_CON_1_A	-72.11262	23.185282	moraine	(Mo)_Sch_D_Gbh_To	6.26	22.6	0.6	1.192	0.169	99.47	54.103	0.02	0.13	1668	33026	47456
DV_SF_2018_CON_1_B	-72.11262	23.185282	moraine	(Mo)_Sch_D_Gbh_To	6.09	341	0.34	0.657	0.097	99.42	39.202	0.02	0.11	1668	NA	15693
DV_SF_2018_CON_1_C	-72.11262	23.185282	moraine	(Mo)_Sch_D_Gbh_To	6.24	33.7	0.38	0.377	0.092	99.34	40.899	0.01	0.1	1668	36168	8002
DV_SF_2018_CON_2_A	-72.11278	23.185186	moraine	(Mo)_Sch_D_Gbh_To	5.75	125.6	0.85	0.259	0.031	99.84	61.912	0.03	0.12	1668	49707	28584
DV_SF_2018_CON_2_B	-72.11278	23.185186	moraine	(Mo)_Sch_D_Gbh_To	5.64	16.6	0.36	0.851	0.041	99.12	52.525	0.02	0.12	1668	104192	19851
DV_SF_2018_CON_2_C	-72.11278	23.185186	moraine	(Mo)_Sch_D_Gbh_To	5.55	38.9	0.35	0.631	0.031	98.91	62.933	0.03	0.12	1668	66614	68553

Sample	Latitude	Longitude	Substrate	Substrate detail	pH	EC (µS cm^{-1})	TOC (%)	N-NH_4 (mg kg^{-1})	N-NO_3 (mg kg^{-1})	Dry weight (%)	P-PO_4 (mg kg^{-1})	TN (%)	TP (%)	Elevation (m a.s.l.)	# 16S reads	#18S reads
DV_SF_2018_CON_3_A	-72.11271	23.184937	moraine	(Mo)_Sch_D_Gbh_To	6.14	37.4	0.38	0.477	0.634	99.72	53.264	0.02	0.09	1668	16321	43271
DV_SF_2018_CON_3_B	-72.11271	23.184937	moraine	(Mo)_Sch_D_Gbh_To	5.81	22.3	0.3	0.504	0.232	99.19	63.504	0.02	0.12	1668	29065	40965
DV_SF_2018_CON_3_C	-72.11271	23.184937	moraine	(Mo)_Sch_D_Gbh_To	5.88	16.9	0.43	0.733	0.056	99.19	42.924	0.02	0.12	1668	29400	NA
DV_SF2_2018_1_A	-72.11214	23.185244	moraine	(Mo)_Sch_D_Gbh_To	6.44	26.4	0.44	1.234	0.066	99.34	44.511	0.01	0.05	1666	77807	13801
DV_SF2_2018_1_B	-72.11214	23.185244	moraine	(Mo)_Sch_D_Gbh_To	6.95	39.2	0.44	1.167	0.112	99.25	51.044	0.02	0.08	1666	115279	81302
DV_SF2_2018_1_C	-72.11214	23.185244	moraine	(Mo)_Sch_D_Gbh_To	7.8	74.9	0.57	2.735	0.619	99.89	55.622	0.04	0.12	1666	105677	27177
DV_SF2_2018_2_A	-72.112114	23.185379	moraine	(Mo)_Sch_D_Gbh_To	6.41	29	0.73	1.082	0.081	99.52	48.976	0.02	0.11	1666	50966	106464
DV_SF2_2018_2_B	-72.112114	23.185379	moraine	(Mo)_Sch_D_Gbh_To	6.51	32.8	0.58	0.636	0.076	99.87	50.217	0.03	0.11	1666	59901	17667
DV_SF2_2018_2_C	-72.112114	23.185379	moraine	(Mo)_Sch_D_Gbh_To	6.59	100.4	0.53	0.831	0.549	99.88	42.732	0.04	0.1	1666	72295	NA
DV_SF2_2018_3_A	-72.112114	23.185379	moraine	(Mo)_Sch_D_Gbh_To	5.91	19.3	0.48	0.663	0.051	99.88	62.873	0.02	0.13	1666	53201	44627
DV_SF2_2018_3_B	-72.112114	23.185379	moraine	(Mo)_Sch_D_Gbh_To	6.29	108.7	0.43	0.482	0.188	99.81	51.853	0.02	0.1	1666	151156	119697
DV_SF2_2018_3_C	-72.112114	23.185379	moraine	(Mo)_Sch_D_Gbh_To	5.98	18.2	0.46	0.889	0.076	99.75	53.056	0.01	0.12	1666	126795	39826
DV_SF2_2018_CON_1_A	-72.11206	23.184668	moraine	(Mo)_Sch_D_Gbh_To	6.23	21.1	0.49	0.327	0.101	99.65	55.756	0.01	0.1	1667	20881	42126
DV_SF2_2018_CON_1_B	-72.11206	23.184668	moraine	(Mo)_Sch_D_Gbh_To	6.36	64.9	0.63	0.518	0.086	99.72	48.878	0.01	0.09	1667	56442	26676
DV_SF2_2018_CON_1_C	-72.11206	23.184668	moraine	(Mo)_Sch_D_Gbh_To	6.85	185.5	0.67	0.558	0.091	99.68	56.133	0.02	0.12	1667	43438	69557
PB_N_OTC15_16_17_2019_CON_A	-71.84423	22.831173	marble	(M)	9.09	208.1	0.48	0.926	0.27	99.95	6.899	0.04	0.03	1310	6074	NA

Sample	Latitude	Longitude	Substrate	Substrate detail	pH	EC ($\mu S\ cm^{-1}$)	TOC (%)	N-NH_4 ($mg\ kg^{-1}$)	N-NO_3 ($mg\ kg^{-1}$)	Dry weight (%)	P-PO_4 ($mg\ kg^{-1}$)	TN (%)	TP (%)	Elevation (m a.s.l.)	# 16S reads	#18S reads
PB_N_OTC15_2019_A	-71.84423	22.831173	marble	(M)	9.31	68.2	0.34	0.816	0.06	99.92	6.636	0.13	0.08	1310	42613	35953
PB_N_OTC15_2019_B	-71.84423	22.831173	marble	(M)	9.21	58.2	0.5	0.292	0.05	99.78	6.686	0.06	0.07	1310	10504	98432
PB_N_OTC15_2019_C	-71.84423	22.831173	marble	(M)	9.34	60.2	0.46	0.096	0.031	99.85	6.537	0.13	0.08	1310	23842	NA
PB_N_OTC16_2019_A	-71.84423	22.831173	marble	(M)	9.22	62.9	0.69	0.786	0.121	99.81	6.571	0.07	0.05	1310	43381	63102
PB_N_OTC16_2019_B	-71.84423	22.831173	marble	(M)	9.13	65.4	0.47	0.105	0.26	99.95	6.666	0.05	0.05	1310	12665	62095
PB_N_OTC16_2019_C	-71.84423	22.831173	marble	(M)	9.08	90.7	0.6	0.286	0.827	99.89	6.445	0.06	0.06	1310	8694	83367
PB_N_OTC17_2019_A	-71.84423	22.831173	marble	(M)	8.73	72.5	0.59	1.081	0.025	99.74	7.534	0.08	0.13	1310	6270	85397
PB_N_OTC17_2019_B	-71.84423	22.831173	marble	(M)	8.93	57.6	0.38	0.997	0.022	99.91	6.749	0.06	0.04	1310	18596	13355
PB_N_OTC17_2019_C	-71.84423	22.831173	marble	(M)	8.88	66.4	0.69	1.354	0.015	99.74	6.906	0.08	0.07	1310	427	NA
PA4_2018_1	-72.00135	22.999208	granite	(Gr)	6.12	22.9	0.76	2.753	0.088	99.75	48.568	0.06	0.12	1409	37553	64886
PA4_2018_2	-72.00131	22.999477	granite	(Gr)	6.06	19.4	0.88	0.989	0.089	99.82	55.398	0.08	0.09	1410	52255	65644
PA4_2018_3	-72.00144	22.999647	granite	(Gr)	6.41	22.4	1.46	3.359	0.389	99.45	57.074	0.09	0.13	1410	96637	91044
PA4_2018_4	-72.00144	22.999647	granite	(Gr)	6.58	20.7	1.05	2.004	0.223	99.36	61.305	0.03	0.05	1410	37361	39331
PA4_2018_5	-72.00149	23.000029	granite	(Gr)	6.21	21.1	0.43	1.379	0.111	99.45	67.494	0.14	0.1	1411	47827	45814
PA4_2018_6	-72.00143	23.000105	granite	(Gr)	6.22	15.4	1.13	1.464	0.116	99.25	40.294	0.03	0.06	1412	61407	90664
PA4_2018_7	-72.00139	23.000048	granite	(Gr)	6.45	47.4	1.54	8.585	0.108	99.74	55.434	0.1	0.05	1412	37221	96722
PA6_2019_1	-72.010506	22.989674	granite	(Gr)	7.31	62.1	0.78	2.017	0.898	99.41	86.474	0.06	0.09	1412	33007	NA
PA6_2019_2	-72.01036	22.991528	granite	(Gr)	7.04	193.4	1.47	1.859	0.289	98.25	73.589	0.07	0.07	1416	5397	112914
PA6_2019_4	-72.010056	22.993479	granite	(Gr)	6.97	24.8	0.31	7.283	0.312	99.75	114.824	0.02	0.09	1416	91806	97871
PA6_2019_5	-72.01002	22.993422	granite	(Gr)	7.57	65.6	0.32	8.557	1.053	99.85	95.352	0.03	0.06	1416	46842	221282
PA6_2019_6	-72.0101	22.993536	granite	(Gr)	6.52	108.8	3.4	24.04	5.464	99.35	119.427	0.46	0.02	1417	8795	24800

Sample	Latitude	Longitude	Substrate	Substrate detail	pH	EC ($\mu S\ cm^{-1}$)	TOC (%)	N-NH_4 ($mg\ kg^{-1}$)	N-NO_3 ($mg\ kg^{-1}$)	Dry weight (%)	P-PO_4 ($mg\ kg^{-1}$)	TN (%)	TP (%)	Elevation (m a.s.l.)	# 16S reads	#18S reads
PB_N_2018_1	-71.84361	22.838146	gneiss	(Gbg)	5.88	414.2	9.23	20.526	0.04	98.25	38.751	0.23	0.4	1256	86362	270390
PB_N_2018_10	-71.84405	22.834051	marble	(Gbg)	9.09	149.7	1.48	0.89	0.506	99.74	7.968	0.27	0.21	1287	134	71300
PB_N_2018_11	-71.84405	22.834051	marble	(Gbg)	8.98	56.5	0.79	0.437	0.036	99.68	8.81	0.15	0.12	1287	106411	74000
PB_N_2018_12	-71.84414	22.833708	gneiss	(Gbg)	8.51	62.2	0.45	0.404	0.828	99.75	9.592	0.05	0.09	1290	40	34500
PB_N_2018_3	-71.84353	22.838034	gneiss	(Gbg)	5.01	163.1	10.95	46.657	0.136	98.21	48.899	0.28	0.17	1255	58605	15081
PB_N_2018_6	-71.84395	22.835169	gneiss	(Gbg)	5.63	91.7	4.6	12.926	0.036	99.15	34.056	0.2	0.41	1279	48899	74851
PB_N_2018_7	-71.843895	22.835245	gneiss	(Gbg)	5.82	49.2	2.52	13.117	0.131	99.22	18.639	0.16	0.16	1277	52543	39805
PB_N_2018_8	-71.84399	22.834904	gneiss	(Gbg)	8.38	89.4	0.68	3.906	0.964	99.02	23.818	0.07	0.81	1282	139319	47148
PB_N_2018_9	-71.84405	22.834051	marble	(M)	7.4	336	5.62	4.553	0.351	99.45	18.515	0.36	0.23	1287	31911	82615
PB_N_OTC9_10_CON_A	-71.84405	22.834051	marble	(M)	9.42	117.9	1.19	0.321	0.035	99.91	6.918	0.24	0.12	1287	31565	47675
PB_N_OTC9_10_CON_B	-71.84405	22.834051	marble	(M)	9.17	73.6	0.58	0.59	0.06	99.95	7.173	0.27	0.16	1287	32512	119600
PB_N_OTC9_10_CON_C	-71.84405	22.834051	marble	(M)	9.45	117.3	1.14	0.282	0.05	99.78	7.104	0.21	0.1	1287	50091	39996
PB_N_OTC9_A_18	-71.84405	22.834051	marble	(M)	9.46	160.4	1.3	0.761	0.062	99.91	8.042	0.23	0.15	1287	25218	6032
PB_N_OTC9_B	-71.84405	22.834051	marble	(M)	9.49	185.5	1.49	0.392	0.151	99.78	8.109	0.17	0.12	1287	45852	48553
PB_N_OTC9_C_18	-71.84405	22.834051	marble	(M)	9.55	142.6	1.56	0.748	0.045	99.82	9.184	0.26	0.12	1287	15260	81208
PB_S_2018_1	-71.8797	22.746996	gneiss	(Gbh)	6.45	17.6	1.41	1.648	0.088	99.27	17.073	0.09	0.16	1349	71864	78606
PB_S_2018_2	-71.87994	22.746687	marble	(M)	9.01	63.7	0.53	0.299	0.173	99.35	14.094	0.04	0.1	1354	23529	108313
PB_S_2018_3	-71.88009	22.74659	marble	(M)	8.94	50.7	0.78	0.333	0.09	99.41	14.28	0.04	0.04	1357	43623	294308
PT_2019_1_A	-72.007385	22.832005	granite	(Gr)	6.11	28.8	0.15	2.204	0.387	99.45	52.049	0.05	0.11	1469	NA	154275
PT_2019_2	-72.007385	22.832005	granite	(Gr)	6.13	70.4	1.28	2.444	3.837	99.57	60.359	0.11	0.14	1469	845	404670
PT_2019_3	-72.007416	22.831738	granite	(Gr)	7.11	31.8	0.45	3.258	0.428	99.47	42.777	0.04	0.06	1472	5459	84779
PT_2019_5	-72.00757	22.833204	granite	(Gr)	7.01	14.9	0.25	0.721	0.28	99.9	36.502	0.03	0.07	1460	16428	13779
UT_2018_1	-71.9456	23.345005	granite	(Gr)	5.89	21.1	2.46	7.048	0.303	99.55	64.229	0.15	0.11	1362	27478	30572

Sample	Latitude	Longitude	Substrate	Substrate detail	pH	EC (µS cm^{-1})	TOC (%)	N-NH_4 (mg kg^{-1})	N-NO_3 (mg kg^{-1})	Dry weight (%)	P-PO_4 (mg kg^{-1})	TN (%)	TP (%)	Elevation (m a.s.l.)	# 16S reads	#18S reads
UT_2018_2	-71.94543	23.345041	granite	(Gr)	6.28	20.9	1.83	2.835	0.077	99.28	26.373	0.16	0.15	1358	102793	NA
UT_2018_3	-71.94559	23.345139	granite	(Gr)	5.24	30.1	2.15	5.929	0.084	99.36	151.121	0.22	0.12	1361	80256	107111
UT_2018_4	-71.94573	23.345177	granite	(Gr)	6.1	15.6	1.24	1.483	0.086	99.62	34.375	0.35	0.09	1364	49357	91872
UT_2018_6	-71.94626	23.3456	granite	(Gr)	5.95	30.3	1.1	1.607	0.076	99.75	39.742	0.25	0.12	1372	32239	43205
UT_2018_7	-71.94624	23.345734	granite	(Gr)	5.87	14.2	0.59	1.151	0.146	99.81	40.212	0.07	0.04	1370	95682	59959
UT_OTC11_2018_A	-71.945465	23.344967	granite	(Gr)	5.92	58.1	2.49	2.059	0.091	99.72	23.943	0.35	0.17	1359	107	36767
UT_OTC11_2018_CON_B	-71.945465	23.344967	granite	(Gr)	6.73	36.6	0.89	1.334	0.115	99.89	43.154	0.09	0.09	1359	29017	69947
UT_OTC2_2018_CON_1_A	-71.946075	23.345505	granite	(Gr)	5.83	329.1	2.67	30.354	0.497	99.25	96.667	0.34	0.24	1369	65588	42987
UT_OTC2_2018_CON_1_B	-71.946075	23.345505	granite	(Gr)	5.9	89.8	1.31	5.449	0.082	99.12	66.263	0.35	0.26	1369	45595	42684
UT_OTC2_2018_CON_1_C	-71.946075	23.345505	granite	(Gr)	5.97	273.1	2.13	22.79	1.773	99.72	50.768	0.43	0.2	1369	69907	55313
YO_2019_3	-72.08115	23.793186	moraine	(Mo)_Sch_To	8.81	90.5	0.54	0.256	0.236	99.81	22.712	0.04	0.09	1361	10252	16922
YO_2018_5	-72.081375	23.793673	moraine	(Mo)_Sch_To	8.45	110.8	1.19	0.627	0.197	99.74	15.318	0.05	0.1	1360	43198	88956
YO_2019_6	-72.08344	23.790731	moraine	(Mo)_Sch_To	8.96	93.7	0.57	0.286	2.38	99.65	27.897	0.02	0.08	1357	15497	120712
YO_2018_6	-72.08111	23.793453	moraine	(Mo)_Sch_To	8.53	60.2	1.38	0.407	0.296	99.82	16.151	0.03	0.04	1360	76449	54595

AU: Austkampane; DV: Dry Valley; PB_N: Perlebandet North; PB_S: Perlebandet South; PA4: Pingvinane 4th nunatak; PA6: Pingvinane 6th nunatak; PT: Petrellnuten; UT: Utsteinen; YO: Yûboku Valley. (Mo)_Amp: Moraine with orthopyroxene amphibolite; (Mo)_Sch_D_Gbh_To: Moraine with amphibole schist, diorite and quartz, biotite-hornblende gneiss and metatonalite; (M): Marble and skarns; (Gbg): Sillimanite-garnet-biotite gneiss, partly containing cordierite; (Gr): Granite and pegmatite; (Gbh): Biotite-hornblende gneiss and hornblende gneiss containing garnet in places; (Mo)_Sch_To: Moraine with amphibole schist and metatonalite. EC: electric conductivity; TOC: total carbon; TN: total nitrogen; TP: total phosphorus.

Table S2.2. 18S Mock community

Species ID	Species name	mock (% cell count)
M01_1352	*Ulnaria ulna*	4.28
M02_1343	*Ulnaria ulna*	
M03_494	*Ulnaria ulna*	
M04_1180	*Fragilaria crotonensis*	5.38
M05_1163	*Fragilaria crotonensis*	15.28
M06_1164	*Fragilaria crotonensis*	
M07_512	*Fragilaria nanana*	3.06
M08_1176	*Asterionella formosa*	13.08
M09_679	*Tabellaria flocculosa*	7.58
M10_499	*Aulacoseira granulata*	3.91
M11_1170	*Aulacoseira subarctica*	35.09
M12_1175	*Nitzschia palea*	7.58
M13_1770	*Staurodesmus sp.*	0.12
M14_1771	*Chlorella vulgaris*	0.86
M15_1772	*Peridinium sp.*	0.12
M16_1773	*Cosmarium reniforme*	0.24
M17_1774	*Desmodesmus sp.*	1.22
M18_1775	*Scenedesmus sp.*	0.12
M19_1776	*Mallomonas sp.*	0.24
M20_1777	*Tetrahymena pyriformis*	1.71
M21_1778	*Dinobryon sp.*	0.12

Table S2.3. Kruskal-Wallis rank sum test showing the effect of substrate type on environmental parameters.

	df	χ2	P
pH	3	49.861	<0.001
TOC	3	25.983	<0.001
$N\text{-}NO_3$	3	9.9442	<0.05
$N\text{-}NH_4$	3	51.778	<0.001
TN	3	63.1	<0.001
$P\text{-}PO_4$	3	59.322	<0.001
TP	3	12.324	<0.05
DW	3	23.604	<0.001
EC	3	14.945	<0.05

EC: Electric conductivity; TOC: Total carbon; TN: Total nitrogen; TP: Total phosphorus

Table S2.4. Relative influence of environmental, spatial and substrate type variables on bacterial communities using a dbRDA and a forward, stepwise variable selection.

Environmental variables	Adj. R2	F	df	P
Elevation	0.07	8.26	1	0.002
pH	0.12	6.24	1	0.002
TN	0.14	3.14	1	0.002
Conductivity	0.15	2.58	1	0.002
TP	0.17	2.21	1	0.002
NH4	0.17	1.86	1	0.002
NO3	0.18	1.51	1	0.014
Dry weight	0.18	1.51	1	0.01
TOC	0.19	1.58	1	0.01
All	0.19	NA	NA	NA

PCNM	Adj. R2	F	df	P
PCNM3	0.07	0.09	1	0.002
PCNM4	0.09	0.10	1	0.002
PCNM1	0.10	0.09	1	0.002
PCNM2	0.10	0.10	1	0.002
All	0.11	NA	NA	NA

Substrate type	Adj. R2	F	df	P
moraine	0.08	9.54	1	0.002
marble	0.13	6.52	1	0.002
gneiss	0.14	2.17	1	0.002
All	0.14	NA	NA	NA

Table S2.5. Relative influence of environmental, spatial and substrate type variables on eukaryotic communities using a dbRDA and a forward, stepwise variable selection.

Environmental variables	Adj. R2	F	df	P
pH	0.06	7.32	1	0.002
Elevation	0.13	7.94	1	0.002
TN	0.16	4.50	1	0.002
Conductivity	0.17	2.57	1	0.002
TP	0.18	2.02	1	0.004
TOC	0.19	2.00	1	0.002
N_NO3	0.20	1.99	1	0.004
N_NH4	0.21	1.52	1	0.028
All	0.21	NA	NA	NA

PCNM	Adj. R2	F	df	P
PCNM3	0.05	6.25	1.00	0.00
PCNM4	0.08	3.51	1.00	0.00
PCNM1	0.09	2.65	1.00	0.00
All	0.10	2.21	1.00	0.00

Substrate type	Adj. R2	F	df	P
moraine	0.08	8.77	1.00	0.00
marble	0.14	8.41	1.00	0.00
granite	0.16	3.03	1.00	0.00
All	0.16	NA	1.00	NA

Table S2.4. Bacterial Phylum taxonomic assignment of the ASVs with cumulative abundance calculated for each substrate type.

Granite			Gneiss		
Phylum	**n. reads**	**% reads**	**Phylum**	**n. reads**	**% reads**
Cyanobacteriota	238856	31.97%	Acidobacteriota	92844	35.64%
Acidobacteriota	204719	27.40%	Cyanobacteriota	52823	20.28%
Actinobacteriota	123943	16.59%	Actinobacteriota	31466	12.08%
Bacteroidota	62056	8.31%	Pseudomonadota	28660	11.00%
Pseudomonadota	32563	4.36%	Bacteroidota	25496	9.79%
Abditibacteriota	26897	3.60%	Chloroflexota	11279	4.33%
Bacteria_unclassified	24335	3.26%	Armatimonadota	6520	2.50%
Chloroflexota	11120	1.49%	Abditibacteriota	4824	1.85%
Deinococcota	6592	0.88%	Bacteria_unclassified	2728	1.05%
Patescibacteria	6093	0.82%	Planctomycetota	1785	0.69%
Armatimonadota	4114	0.55%	Deinococcota	1164	0.45%
Planctomycetota	2840	0.38%	Gemmatimonadota	368	0.14%
Gemmatimonadota	1584	0.21%	Patescibacteria	203	0.08%
Myxococcota	792	0.11%	Bdellovibrionota	77	0.03%
unknown_unclassified	475	0.06%	unknown_unclassified	71	0.03%
Verrucomicrobiota	54	0.01%	Myxococcota	69	0.03%
Bdellovibrionota	45	0.01%	Verrucomicrobiota	53	0.02%
WPS-2	25	0.00%	WPS-2	51	0.02%
Sumerlaeota	5	0.00%	Nitrospirota	30	0.01%
Bacillota	2	0.00%	SAR324_clade(Marine_group_B)	8	0.00%
			Bacillota	4	0.00%
			Elusimicrobiota	3	0.00%
			Sumerlaeota	2	0.00%

Marble			Moraine		
Phylum	**n. reads**	**% reads**	**Phylum**	**n. reads**	**% reads**
Cyanobacteriota	115789	32.54%	Actinobacteriota	920322	49.13%
Acidobacteriota	103679	29.14%	Acidobacteriota	576097	30.75%
Bacteroidota	55915	15.71%	Chloroflexota	100324	5.36%
Actinobacteriota	31358	8.81%	Bacteroidota	64721	3.45%
Pseudomonadota	14742	4.14%	Cyanobacteriota	54147	2.89%
Deinococcota	10948	3.08%	Patescibacteria	48464	2.59%
Abditibacteriota	8186	2.30%	Pseudomonadota	25947	1.39%
Chloroflexota	6185	1.74%	Abditibacteriota	25012	1.34%
Bacteria_unclassified	5899	1.66%	Bacteria_unclassified	21774	1.16%
Planctomycetota	1284	0.36%	Deinococcota	11303	0.60%
Patescibacteria	840	0.24%	Gemmatimonadota	9486	0.51%
Armatimonadota	589	0.17%	Armatimonadota	8693	0.46%
Myxococcota	140	0.04%	Planctomycetota	4150	0.22%

Marble			Moraine		
Phylum	**n. reads**	**% reads**	**Phylum**	**n. reads**	**% reads**
unknown_unclassified	117	0.03%	Bacillota	1450	0.08%
Gemmatimonadota	67	0.02%	Verrucomicrobiota	495	0.03%
Bdellovibrionota	66	0.02%	unknown_unclassified	393	0.02%
SAR324_clade(Marine_group_B)	13	0.00%	Nitrospirota	212	0.01%
Verrucomicrobiota	11	0.00%	Myxococcota	153	0.01%
Bacillota	6	0.00%	Bdellovibrionota	121	0.01%
WPS-2	4	0.00%	Sumerlaeota	44	0.00%
		0.00%	SAR324_clade(Marine_group_B)	35	0.00%
		0.00%	WPS-2	35	0.00%
		0.00%	Desulfobacterota	13	0.00%
		0.00%	Dependentiae	8	0.00%

***Table S2.5**. Bacterial Family taxonomic assignment of the ASVs with cumulative abundance calculated for each substrate type.*

Granite			Gneiss		
Family	n. reads	% reads	Family	n. reads	% reads
Blastocatellaceae	202488	27.10%	Blastocatellaceae	80105	30.75%
Nostocaceae	150339	20.12%	Chroococcidiopsaceae	45003	17.27%
Chroococcidiopsaceae	32603	4.36%	Acetobacteraceae	19566	7.51%
Solirubrobacteraceae	31525	4.22%	Pseudonocardiaceae	16532	6.35%
Phormidiaceae	31150	4.17%	Acidobacteriaceae_(Subgroup_1)	9930	3.81%
Chitinophagaceae	27480	3.68%	Chitinophagaceae	9796	3.76%
Abditibacteriaceae	26897	3.60%	Ktedonobacteraceae	7926	3.04%
Bacteria_unclassified	24335	3.26%	Armatimonadales_fa	6464	2.48%
Pseudonocardiaceae	23244	3.11%	Hymenobacteraceae	6258	2.40%
Acetobacteraceae	17819	2.39%	Spirosomaceae	5992	2.30%
Nocardioidaceae	14312	1.92%	Abditibacteriaceae	4824	1.85%
Hymenobacteraceae	12109	1.62%	Phormidiaceae	3892	1.49%
Spirosomaceae	11196	1.50%	Sphingomonadaceae	2758	1.06%
Cyanobacteriia_unclassified	9595	1.28%	Bacteria_unclassified	2728	1.05%
Propionibacteriaceae	8601	1.15%	Sphingobacteriaceae	2692	1.03%
Actinobacteria_unclassified	8189	1.10%	Beijerinckiaceae	2397	0.92%
Leptolyngbyaceae	7824	1.05%	Nocardioidaceae	1930	0.74%
Solirubrobacterales_unclassified	7723	1.03%	Solirubrobacteraceae	1850	0.71%
Cyanobacteriales_unclassified	5677	0.76%	Cyanobacteriales_unclassified	1844	0.71%
Deinococcaceae	5423	0.73%	Caulobacteraceae	1701	0.65%
Sphingomonadaceae	5270	0.71%	WD2101_soil_group	1500	0.58%
Frankiales_unclassified	4951	0.66%	Frankiales_unclassified	1366	0.52%
Nocardiaceae	4580	0.61%	Nakamurellaceae	1282	0.49%
Chloroflexales_unclassified	4199	0.56%	Actinobacteria_unclassified	1242	0.48%
Sphingobacteriaceae	4145	0.55%	Nostocaceae	1200	0.46%
Armatimonadales_fa	4025	0.54%	Pyrinomonadaceae	1014	0.39%
67-14	3962	0.53%	AKIW781	1001	0.38%
LWQ8	3372	0.45%	Propionibacteriaceae	898	0.34%
Nakamurellaceae	3151	0.42%	uncultured	851	0.33%
uncultured	2796	0.37%	Deinococcaceae	808	0.31%
Flavobacteriaceae	2752	0.37%	Solirubrobacterales_unclassified	777	0.30%
AKIW781	2606	0.35%	Solibacteraceae	700	0.27%
Frankiaceae	2368	0.32%	Intrasporangiaceae	606	0.23%
Intrasporangiaceae	1960	0.26%	JG30-KF-CM45	579	0.22%
WD2101_soil_group	1847	0.25%	67-14	551	0.21%
uncultured_fa	1728	0.23%	Bryobacteraceae	531	0.20%
Phormidesmiaceae	1657	0.22%	Micromonosporaceae	508	0.19%
Gemmatimonadaceae	1584	0.21%	C0119_fa	487	0.19%
Cytophagales_unclassified	1579	0.21%	Ilumatobacteraceae	446	0.17%
Beijerinckiaceae	1504	0.20%	Comamonadaceae	439	0.17%

Granite			Gneiss		
Family	n. reads	% reads	Family	n. reads	% reads
JG30-KF-CM45	1420	0.19%	Nocardiaceae	406	0.16%
Iamiaceae	1415	0.19%	Frankiaceae	403	0.15%
Comamonadaceae	1248	0.17%	Cyanobacteriia_unclassified	380	0.15%
Proteobacteria_unclassified	1246	0.17%	Leptolyngbyaceae	374	0.14%
Kineosporiaceae	1213	0.16%	Iamiaceae	367	0.14%
Trueperaceae	1165	0.16%	Trueperaceae	356	0.14%
Chloroflexaceae	1159	0.16%	Thermoleophilaceae	349	0.13%
Cytophagaceae	969	0.13%	Caldilineaceae	340	0.13%
Caulobacteraceae	954	0.13%	Alphaproteobacteria_unclassified	336	0.13%
Oxalobacteraceae	788	0.11%	Thermobaculaceae	330	0.13%
Dermacoccaceae	699	0.09%	Gemmatimonadaceae	325	0.12%
Micromonosporaceae	696	0.09%	Proteobacteria_unclassified	262	0.10%
Tepidisphaeraceae	682	0.09%	Acidobacteriae_unclassified	248	0.10%
Xanthomonadaceae	648	0.09%	Bacteroidia_unclassified	242	0.09%
Micrococcaceae	638	0.09%	Blastocatellia_unclassified	237	0.09%
Acidobacteriaceae_(Subgroup_1)	602	0.08%	Rubrobacteriaceae	231	0.09%
Burkholderiaceae	588	0.08%	Thermoleophilia_unclassified	230	0.09%
Xanthobacteraceae	570	0.08%	Burkholderiales_unclassified	198	0.08%
Rhodobacteraceae	561	0.08%	KD4-96_fa	190	0.07%
Roseiflexaceae	533	0.07%	Burkholderiaceae	188	0.07%
Solibacteraceae	495	0.07%	Xanthobacteraceae	186	0.07%
unknown_unclassified	475	0.06%	Cytophagales_unclassified	167	0.06%
Acidimicrobiia_unclassified	462	0.06%	Actinobacteriota_unclassified	135	0.05%
Rubrobacteriaceae	457	0.06%	Tepidisphaeraceae	130	0.05%
Polyangiaceae	430	0.06%	Phormidesmiaceae	123	0.05%
Saccharimonadales_fa	418	0.06%	Rhizobiaceae	112	0.04%
Blastocatellia_unclassified	399	0.05%	Chitinophagales_unclassified	108	0.04%
Burkholderiales_unclassified	385	0.05%	Acidimicrobiia_unclassified	107	0.04%
Bacteroidia_unclassified	374	0.05%	Kineosporiaceae	104	0.04%
RBG-13-54-9_fa	365	0.05%	Gaiellaceae	99	0.04%
Rhodothermaceae	326	0.04%	Microtrichales_unclassified	87	0.03%
Saccharimonadales_unclassified	313	0.04%	Rhodobacteraceae	87	0.03%
env.OPS_17	310	0.04%	Micrococcaceae	86	0.03%
Pyrinomonadaceae	291	0.04%	LWQ8	83	0.03%
Bryobacteraceae	289	0.04%	TK10_fa	78	0.03%
Actinobacteriota_unclassified	288	0.04%	Silvanigrellaceae	71	0.03%
Thermoleophilia_unclassified	285	0.04%	unknown_unclassified	71	0.03%
C0119_fa	270	0.04%	Gemmataceae	70	0.03%
Geodermatophilaceae	240	0.03%	Herpetosiphonaceae	64	0.02%
Parcubacteria_fa	221	0.03%	Parcubacteria_fa	59	0.02%
Caldilineaceae	180	0.02%	Rhodothermaceae	59	0.02%
Alphaproteobacteria_unclassified	169	0.02%	SC-I-84	56	0.02%
Microtrichales_unclassified	140	0.02%	WPS-2_fa	51	0.02%

Granite			Gneiss		
Family	n. reads	% reads	Family	n. reads	% reads
Cyclobacteriaceae	136	0.02%	Ktedonobacteria_unclassified	48	0.02%
Ktedonobacteraceae	131	0.02%	Tepidisphaerales_unclassified	48	0.02%
Ilumatobacteraceae	129	0.02%	Chthoniobacteraceae	47	0.02%
Isosphaeraceae	121	0.02%	Armatimonadales_unclassified	46	0.02%
Microscillaceae	117	0.02%	Chloroflexia_unclassified	44	0.02%
Rickettsiaceae	113	0.02%	Micrococcales_unclassified	44	0.02%
Rhizobiaceae	107	0.01%	Longimicrobiaceae	43	0.02%
Gemmataceae	98	0.01%	Rhizobiales_unclassified	43	0.02%
Geminicoccaceae	88	0.01%	AKYG1722	41	0.02%
Tepidisphaerales_unclassified	88	0.01%	Cytophagaceae	40	0.02%
Rhizobiales_unclassified	85	0.01%	Oxalobacteraceae	39	0.01%
Thermoleophilaceae	83	0.01%	Xanthomonadaceae	39	0.01%
Nannocystaceae	80	0.01%	Geodermatophilaceae	38	0.01%
Nitrosomonadaceae	80	0.01%	A21b	37	0.01%
IMCC26256_fa	73	0.01%	Ardenticatenaceae	35	0.01%
Herpetosiphonaceae	71	0.01%	Saccharimonadales_fa	33	0.01%
Rickettsiales_fa	70	0.01%	Cyclobacteriaceae	32	0.01%
Haliangiaceae	68	0.01%	Geminicoccaceae	31	0.01%
Polyangiales_unclassified	65	0.01%	Microbacteriaceae	30	0.01%
Armatimonadales_unclassified	60	0.01%	Nitrospiraceae	30	0.01%
KD4-96_fa	58	0.01%	Roseiflexaceae	30	0.01%
Micropepsaceae	54	0.01%	RBG-13-54-9_fa	29	0.01%
Patescibacteria_unclassified	54	0.01%	uncultured_fa	28	0.01%
Rhodanobacteraceae	52	0.01%	Vicinamibacterales_unclassified	27	0.01%
11-24_fa	49	0.01%	Vicinamibacteraceae	25	0.01%
BIrii41	46	0.01%	JG30-KF-CM66_fa	23	0.01%
Streptomycetaceae	46	0.01%	Kapabacteriales_fa	23	0.01%
Chitinophagales_unclassified	43	0.01%	Acidobacteriota_unclassified	22	0.01%
Phaselicystidaceae	43	0.01%	Sutterellaceae	22	0.01%
Sporichthyaceae	40	0.01%	Flavobacteriaceae	20	0.01%
Corynebacteriales_unclassified	38	0.01%	Phycisphaeraceae	20	0.01%
Microbacteriaceae	37	0.00%	Polyangiaceae	20	0.01%
TK10_fa	37	0.00%	BIrii41	19	0.01%
Berkelbacteria_fa	35	0.00%	Isosphaeraceae	17	0.01%
Flavobacteriales_unclassified	33	0.00%	Devosiaceae	16	0.01%
JG30-KF-CM66_fa	33	0.00%	Microscillaceae	16	0.01%
Micrococcales_unclassified	30	0.00%	TRA3-20	16	0.01%
Acidobacteriae_unclassified	29	0.00%	Propionibacteriales_unclassified	15	0.01%
Chthoniobacteraceae	28	0.00%	Haliangiaceae	14	0.01%
Polyangia_unclassified	27	0.00%	IMCC26256_fa	14	0.01%
WPS-2_fa	25	0.00%	Anaerolineae_unclassified	13	0.00%
Saccharimonadaceae	21	0.00%	Chloroflexi_unclassified	13	0.00%
AKYG1722	20	0.00%	Euzebyaceae	9	0.00%

Granite			Gneiss		
Family	n. reads	% reads	Family	n. reads	% reads
Bdellovibrionaceae	20	0.00%	Gammaproteobacteria_unclassified	9	0.00%
SC-I-84	20	0.00%	SJA-28_fa	9	0.00%
Paracaedibacteraceae	18	0.00%	Chthonomonadaceae	8	0.00%
Propionibacteriales_unclassified	18	0.00%	SAR324_clade(Marine_group_B)_fa	8	0.00%
Caedibacteraceae	17	0.00%	B1-7BS	7	0.00%
Microtrichales_fa	17	0.00%	Saccharimonadales_unclassified	7	0.00%
Silvanigrellaceae	17	0.00%	Sericytochromatia_fa	7	0.00%
mle1-27_fa	15	0.00%	Acidothermaceae	6	0.00%
Bacteroidota_unclassified	14	0.00%	Oligoflexaceae	6	0.00%
Chthonomonadaceae	14	0.00%	P2-11E_fa	6	0.00%
Weeksellaceae	14	0.00%	Verrucomicrobiaceae	6	0.00%
Acidothermaceae	13	0.00%	Polyangiales_unclassified	5	0.00%
Chloroflexi_unclassified	13	0.00%	Bacteroidaceae	4	0.00%
Gammaproteobacteria_unclassified	12	0.00%	Corynebacteriales_unclassified	4	0.00%
Vicinamibacterales_unclassified	12	0.00%	Myxococcaceae	4	0.00%
Opitutaceae	11	0.00%	Polyangia_unclassified	4	0.00%
Vampirovibrionales_fa	11	0.00%	Rickettsiaceae	4	0.00%
Chloroflexia_unclassified	10	0.00%	Caedibacteraceae	3	0.00%
Verrucomicrobiae_unclassified	10	0.00%	Lineage_IIa_fa	3	0.00%
A21b	9	0.00%	Phaselicystidaceae	3	0.00%
A4b	9	0.00%	Firmicutes_unclassified	2	0.00%
Acidobacteriota_unclassified	9	0.00%	Gitt-GS-136_fa	2	0.00%
Myxococcaceae	9	0.00%	Porphyromonadaceae	2	0.00%
Sandaracinaceae	9	0.00%	Sphingobacteriales_unclassified	2	0.00%
0319-6G20_fa	8	0.00%	Streptococcaceae	2	0.00%
Gaiellales_unclassified	8	0.00%	Subgroup_7_fa	2	0.00%
Gallionellaceae	8	0.00%	Sumerlaeaceae	2	0.00%
Armatimonadota_unclassified	7	0.00%	Weeksellaceae	2	0.00%
Devosiaceae	7	0.00%	Gaiellales_unclassified	1	0.00%
Rhizobiales_Incertae_Sedis	7	0.00%			
B12-WMSP1_fa	6	0.00%			
Corynebacteriaceae	6	0.00%			
Kapabacteriales_fa	6	0.00%			
Sumerlaeaceae	5	0.00%			
Sutterellaceae	5	0.00%			
TSBb06_fa	5	0.00%			
Deinococci_unclassified	4	0.00%			
Phycisphaeraceae	4	0.00%			
Candidatus_Kaiserbacteria_fa	3	0.00%			
Legionellaceae	3	0.00%			
Verrucomicrobiales_unclassified	3	0.00%			
Acetobacterales_unclassified	2	0.00%			
Cellulomonadaceae	2	0.00%			

Chthoniobacterales_unclassified	2	0.00%
Clostridiaceae	2	0.00%
TRA3-20	2	0.00%
Vicinamibacteraceae	2	0.00%

Marble			Moraine		
Family	**n. reads**	**% reads**	**Family**	**n. reads**	**% reads**
Chroococcidiopsaceae	110552	31.07%	Blastocatellaceae	564050	30.11%
Blastocatellaceae	99209	27.88%	Pseudonocardiaceae	336533	17.96%
Spirosomaceae	44303	12.45%	Solirubrobacteraceae	140967	7.52%
Trueperaceae	10889	3.06%	Solirubrobacterales_unclassified	116762	6.23%
Acetobacteraceae	8231	2.31%	Nocardioidaceae	70467	3.76%
Abditibacteriaceae	8186	2.30%	Actinobacteria_unclassified	67362	3.60%
Euzebyaceae	6325	1.78%	JG30-KF-CM45	65097	3.47%
Bacteria_unclassified	5899	1.66%	Chitinophagaceae	45146	2.41%
Pseudonocardiaceae	4952	1.39%	uncultured_fa	36217	1.93%
Hymenobacteraceae	3567	1.00%	Frankiales_unclassified	31541	1.68%
AKIW781	3364	0.95%	Leptolyngbyaceae	27878	1.49%
Cyanobacteriales_unclassified	3359	0.94%	Abditibacteriaceae	25012	1.34%
Solirubrobacterales_unclassified	2510	0.71%	uncultured	22714	1.21%
Chitinophagaceae	2475	0.70%	Bacteria_unclassified	21774	1.16%
Nocardioidaceae	2417	0.68%	Thermoleophilia_unclassified	19516	1.04%
uncultured	2386	0.67%	67-14	17434	0.93%
67-14	2299	0.65%	Chroococcidiopsaceae	16371	0.87%
Solirubrobacteraceae	2190	0.62%	Acidimicrobiia_unclassified	13027	0.70%
Pyrinomonadaceae	2123	0.60%	Propionibacteriaceae	12770	0.68%
Thermoleophilia_unclassified	2001	0.56%	Ilumatobacteraceae	12043	0.64%
Actinobacteria_unclassified	1712	0.48%	Gemmatimonadaceae	9308	0.50%
Cytophagaceae	1534	0.43%	Acetobacteraceae	8967	0.48%
Rhodobacteraceae	1531	0.43%	Armatimonadales_fa	8471	0.45%
Blastocatellia_unclassified	1438	0.40%	Intrasporangiaceae	8214	0.44%
Rhizobiaceae	1373	0.39%	KD4-96_fa	7680	0.41%
Cyanobacteriia_unclassified	1360	0.38%	Pyrinomonadaceae	7373	0.39%
JG30-KF-CM45	1243	0.35%	Frankiaceae	6870	0.37%
WD2101_soil_group	1099	0.31%	Cyanobacteriia_unclassified	6690	0.36%
Frankiales_unclassified	1025	0.29%	Rubrobacteriaceae	6558	0.35%
Caulobacteraceae	993	0.28%	Sphingobacteriaceae	6060	0.32%
Beijerinckiaceae	848	0.24%	Trueperaceae	6017	0.32%
Propionibacteriaceae	794	0.22%	B12-WMSP1_fa	5863	0.31%
Bryobacteraceae	652	0.18%	LWQ8	5647	0.30%
Frankiaceae	645	0.18%	Deinococcaceae	5277	0.28%
Sphingomonadaceae	639	0.18%	AKIW781	5169	0.28%
Microscillaceae	615	0.17%	Nocardiaceae	4887	0.26%
Armatimonadales_fa	557	0.16%	Thermoleophilaceae	4695	0.25%
Thermoleophilaceae	542	0.15%	Saccharimonadales_unclassified	4676	0.25%
uncultured_fa	510	0.14%	Micrococcaceae	4654	0.25%

Marble			Moraine		
Family	n. reads	% reads	Family	n. reads	% reads
AKYG1722	500	0.14%	Iamiaceae	4608	0.25%
Ilumatobacteraceae	485	0.14%	Hymenobacteraceae	4391	0.23%
Cytophagales_unclassified	448	0.13%	IMCC26256_fa	4356	0.23%
MWH-CFBk5	444	0.12%	Spirosomaceae	3708	0.20%
Rhodothermaceae	434	0.12%	C0119_fa	3664	0.20%
Intrasporangiaceae	423	0.12%	Comamonadaceae	3377	0.18%
Micrococcaceae	399	0.11%	Sphingomonadaceae	3358	0.18%
Gaiellaceae	345	0.10%	Thermobaculaceae	3139	0.17%
KD4-96_fa	336	0.09%	Micrococcales_unclassified	2877	0.15%
Proteobacteria_unclassified	323	0.09%	Beijerinckiaceae	2846	0.15%
Sphingobacteriaceae	321	0.09%	WD2101_soil_group	2839	0.15%
Leptolyngbyaceae	320	0.09%	Actinobacteriota_unclassified	2617	0.14%
Saccharimonadales_unclassified	300	0.08%	Blastocatellia_unclassified	2315	0.12%
Microtrichales_unclassified	262	0.07%	Euzebyaceae	1919	0.10%
Rubrobacteriaceae	234	0.07%	Flavobacteriaceae	1835	0.10%
Acidobacteriae_unclassified	215	0.06%	Parcubacteria_fa	1823	0.10%
Caldilineaceae	205	0.06%	Caldilineaceae	1673	0.09%
Cyclobacteriaceae	194	0.05%	Phormidiaceae	1449	0.08%
Nostocaceae	192	0.05%	Planococcaceae	1418	0.08%
Acidimicrobiia_unclassified	190	0.05%	Microtrichales_unclassified	1393	0.07%
Thermobaculaceae	189	0.05%	Gitt-GS-136_fa	1392	0.07%
Iamiaceae	157	0.04%	A4b	1315	0.07%
Chitinophagales_unclassified	143	0.04%	Rhodobacteraceae	1299	0.07%
Xanthomonadaceae	128	0.04%	Chloroflexaceae	1294	0.07%
Gemmataceae	120	0.03%	Kineosporiaceae	1212	0.06%
LWQ8	120	0.03%	AKYG1722	1038	0.06%
unknown_unclassified	117	0.03%	Cytophagales_unclassified	1006	0.05%
Gaiellales_unclassified	105	0.03%	Nostocaceae	976	0.05%
Actinobacteriota_unclassified	99	0.03%	SJA-28_fa	972	0.05%
Chloroflexi_unclassified	95	0.03%	Gaiellaceae	931	0.05%
Comamonadaceae	91	0.03%	Nakamurellaceae	872	0.05%
Sutterellaceae	90	0.03%	Chloroflexia_unclassified	849	0.05%
Micromonosporaceae	89	0.03%	Solibacteraceae	847	0.05%
BIrii41	74	0.02%	Xanthomonadaceae	811	0.04%
Herpetosiphonaceae	72	0.02%	Saccharimonadales_fa	762	0.04%
Kineosporiaceae	70	0.02%	TK10_fa	678	0.04%
Gemmatimonadaceae	67	0.02%	Sutterellaceae	644	0.03%
Xanthomonadales_unclassified	67	0.02%	Pseudanabaenaceae	640	0.03%
Bdellovibrionaceae	66	0.02%	Gemmataceae	627	0.03%
Sporichthyaceae	62	0.02%	Bryobacteraceae	561	0.03%
TK10_fa	59	0.02%	Cyclobacteriaceae	515	0.03%
Alphaproteobacteria_unclassified	52	0.01%	Caulobacteraceae	511	0.03%
IMCC26256_fa	51	0.01%	Oxalobacteraceae	511	0.03%

Marble			Moraine		
Family	n. reads	% reads	Family	n. reads	% reads
Bacteroidia_unclassified	50	0.01%	B10-SB3A_fa	488	0.03%
C0119_fa	46	0.01%	Chthoniobacteraceae	476	0.03%
Devosiaceae	43	0.01%	Propionibacteriales_unclassified	463	0.02%
Vicinamibacteraceae	39	0.01%	Micromonosporaceae	435	0.02%
Deinococcaceae	34	0.01%	Sporichthyaceae	431	0.02%
Isosphaeraceae	33	0.01%	Nitrosomonadaceae	407	0.02%
Unknown_Family	33	0.01%	Acidobacteriae_fa	403	0.02%
Armatimonadales_unclassified	29	0.01%	unknown_unclassified	393	0.02%
Gitt-GS-136_fa	29	0.01%	Microbacteriaceae	362	0.02%
Polyangiaceae	26	0.01%	Corynebacteriales_unclassified	358	0.02%
Rhizobiales_unclassified	23	0.01%	Xanthobacteraceae	339	0.02%
JG30-KF-CM66_fa	18	0.01%	Rhizobiales_unclassified	325	0.02%
Ardenticatenaceae	17	0.00%	Rhodanobacteraceae	290	0.02%
Saccharimonadales_fa	16	0.00%	JG30-KF-CM66_fa	284	0.02%
Deinococci_unclassified	14	0.00%	Microscillaceae	273	0.01%
Oxalobacteraceae	14	0.00%	Bacteroidia_unclassified	256	0.01%
SC-I-84	14	0.00%	Ktedonobacteraceae	253	0.01%
Haliangiaceae	13	0.00%	Rhodothermaceae	247	0.01%
Parcubacteria_fa	13	0.00%	Proteobacteria_unclassified	240	0.01%
Planctomycetes_unclassified	13	0.00%	Gaiellales_unclassified	235	0.01%
SAR324_clade(Marine_group_B)_fa	13	0.00%	Vicinamibacteraceae	234	0.01%
Micrococcales_unclassified	12	0.00%	Tepidisphaeraceae	232	0.01%
Phaselicystidaceae	12	0.00%	Nitrospiraceae	212	0.01%
Tepidisphaeraceae	12	0.00%	Pirellulaceae	183	0.01%
0319-7L14_fa	11	0.00%	Rhizobiales_Incertae_Sedis	170	0.01%
Bacteroidota_unclassified	11	0.00%	Streptomycetaceae	169	0.01%
Chthoniobacteraceae	11	0.00%	Burkholderiales_unclassified	162	0.01%
Deinococcales_unclassified	11	0.00%	Longimicrobiaceae	157	0.01%
TRA3-20	11	0.00%	Isosphaeraceae	152	0.01%
Chloroflexia_unclassified	10	0.00%	Chloroflexi_unclassified	148	0.01%
Porphyromonadaceae	9	0.00%	MB-A2-108_fa	141	0.01%
Burkholderiales_unclassified	8	0.00%	Herpetosiphonaceae	118	0.01%
NS9_marine_group	7	0.00%	Gammaproteobacteria_unclassified	117	0.01%
Xanthobacteraceae	7	0.00%	Patescibacteria_unclassified	112	0.01%
Bacillaceae	6	0.00%	Kapabacteriales_fa	107	0.01%
Polyangiales_unclassified	6	0.00%	Geminicoccaceae	96	0.01%
Pseudanabaenaceae	6	0.00%	TRA3-20	93	0.00%
B1-7BS	5	0.00%	Chitinophagales_unclassified	92	0.00%
Geminicoccaceae	5	0.00%	Bdellovibrionaceae	91	0.00%
Myxococcaceae	4	0.00%	Geodermatophilaceae	88	0.00%
Rickettsiaceae	4	0.00%	Sericytochromatia_fa	75	0.00%
Rickettsiales_fa	4	0.00%	0319-7L14_fa	66	0.00%
Tepidisphaerales_unclassified	4	0.00%	Burkholderiaceae	66	0.00%

Marble			Moraine		
Family	n. reads	% reads	Family	n. reads	% reads
WPS-2_fa	4	0.00%	vadinHA49_fa	66	0.00%
Acidobacteriaceae_(Subgroup_1)	3	0.00%	Acidimicrobiaceae	61	0.00%
Burkholderiaceae	3	0.00%	Acidobacteriae_unclassified	60	0.00%
Gaiellales_fa	3	0.00%	Berkelbacteria_fa	56	0.00%
mle1-27_fa	3	0.00%	Subgroup_7_fa	54	0.00%
Nitrosomonadaceae	3	0.00%	Alphaproteobacteria_unclassified	53	0.00%
Phycisphaerae_unclassified	3	0.00%	Armatimonadales_unclassified	52	0.00%
Diplorickettsiaceae	2	0.00%	Microtrichaceae	51	0.00%
Parcubacteria_unclassified	2	0.00%	Rhizobiaceae	51	0.00%
Propionibacteriales_unclassified	2	0.00%	Diplorickettsiaceae	47	0.00%
Sandaracinaceae	2	0.00%	Anaerolineaceae	46	0.00%
Thermomicrobiales_unclassified	2	0.00%	Sumerlaeaceae	44	0.00%

***Table S2.6**. Eukaryotic Phylum taxonomic assignment of the ASVs with cumulative abundance calculated for each substrate type.*

Granite			Gneiss		
Phylum	n. reads	% reads	Phylum	n. reads	% reads
Chlorophyta	1395307	61.20%	Chlorophyta	483408	63.18%
Metazoa	555705	24.38%	Metazoa	242798	31.74%
Ciliophora	252995	11.10%	Cercozoa	21618	2.83%
Ochrophyta	29245	1.28%	Ciliophora	6260	0.82%
Cercozoa	22814	1.00%	Eukaryota_unclassified	6043	0.79%
Opisthokonta_unclassified	10671	0.47%	Fungi	2683	0.35%
Lobosa	5238	0.23%	Opisthokonta_unclassified	1858	0.24%
Fungi	3915	0.17%	Lobosa	200	0.03%
Eukaryota_unclassified	3529	0.15%	Ochrophyta	74	0.01%
Streptophyta	333	0.01%	Pseudofungi	69	0.01%
Dinoflagellata	27	0.00%	Streptophyta	55	0.01%
Opalozoa	9	0.00%	Opalozoa	9	0.00%
Marble			**Moraine**		
Phylum	n. reads	% reads	Phylum	n. reads	% reads
Chlorophyta	1005651	46.34%	Chlorophyta	1988246	66.73%
Metazoa	718026	33.08%	Cercozoa	409745	13.75%
Cercozoa	310928	14.33%	Metazoa	261472	8.78%
Ciliophora	84106	3.88%	Lobosa	121032	4.06%
Eukaryota_unclassified	19443	0.90%	Ciliophora	74857	2.51%
Fungi	16745	0.77%	Eukaryota_unclassified	51478	1.73%
Opisthokonta_unclassified	7294	0.34%	Streptophyta	32053	1.08%
Ochrophyta	2768	0.13%	Fungi	7700	0.26%
Streptophyta	2016	0.09%	Apicomplexa	6694	0.22%
Lobosa	1522	0.07%	Opisthokonta_unclassified	5614	0.19%

Marble			Moraine		
Phylum	**n. reads**	**% reads**	**Phylum**	**n. reads**	**% reads**
Archaeplastida_unclassified	1089	0.05%	Centroheliozoa	4724	0.16%
Dinoflagellata	467	0.02%	Ochrophyta	4410	0.15%
Apicomplexa	163	0.01%	Dinoflagellata	3697	0.12%
Opalozoa	150	0.01%	Cryptophyta	3539	0.12%
Discoba	7	0.00%	Conosa	3155	0.11%
			Opalozoa	474	0.02%
			Pseudofungi	318	0.01%
			Discoba	141	0.00%

Table S2.7. Eukaryotic Family taxonomic assignment of the ASVs with cumulative abundance calculated for each substrate type.

Granite			Gneiss		
Family	**n. reads**	**% reads**	**Family**	**n. reads**	**% reads**
Microthamniales_X	947963	41.58%	Microthamniales_X	305363	39.91%
Prasiolales_X	378942	16.62%	Prasiolales_X	143485	18.75%
Rotifera_XX	304706	13.37%	Rotifera_XX	127867	16.71%
Tardigrada_XX	165459	7.26%	Tardigrada_XX	88690	11.59%
Nassulida	126306	5.54%	Metazoa_unclassified	26241	3.43%
Chilodonellidae	98401	4.32%	Watanabea-Clade_X	20989	2.74%
Metazoa_unclassified	68112	2.99%	Cercozoa_unclassified	8703	1.14%
Watanabea-Clade_X	38133	1.67%	Eukaryota_unclassified	6043	0.79%
Xanthophyceae_XX	29245	1.28%	Sandonidae	5960	0.78%
Chlamydomonadales_X	23154	1.02%	Rhogostoma-lineage	5673	0.74%
Collembola	16814	0.74%	Trebouxiophyceae_unclassified	5631	0.74%
Oxytrichidae	16389	0.72%	Chlorophyta_unclassified	4891	0.64%
Rhogostoma-lineage	13747	0.60%	Oxytrichidae	2620	0.34%
Opisthokonta_unclassified	10671	0.47%	Chilodonellidae	2520	0.33%
Sessilida	4940	0.22%	Chlamydomonadales_X	2497	0.33%
Cercozoa_unclassified	4335	0.19%	Opisthokonta_unclassified	1858	0.24%
Endostelium-lineage	3967	0.17%	Tremellomycetes	1394	0.18%
Trebouxiophyceae_unclassified	3728	0.16%	Colpodida	774	0.10%
Eukaryota_unclassified	3529	0.15%	Cercomonadidae	669	0.09%
Sandonidae	3422	0.15%	Pezizomycotina_unclassified	667	0.09%
Pleurostomatida	2775	0.12%	Glissomonadida_unclassified	574	0.08%
Tokophryidae	2601	0.11%	Chlamydomonadales_unclassified	333	0.04%
Chytridiomycetes	2243	0.10%	Dothideomycetes	220	0.03%
Ulotrichales_X	1991	0.09%	Coccomyxaceae	219	0.03%
LOS7N/I-lineage	1236	0.05%	Chytridiomycetes	206	0.03%
Cercomonadidae	1052	0.05%	Endostelium-lineage	153	0.02%
Pezizomycotina_unclassified	970	0.04%	Platyophryida	137	0.02%
Ciliophora_unclassified	788	0.03%	Fungi_unclassified	104	0.01%

Granite			Gneiss		
Family	n. reads	% reads	Family	n. reads	% reads
Chlorophyta_unclassified	702	0.03%	Ciliophora_unclassified	80	0.01%
Ulvophyceae_unclassified	689	0.03%	Xanthophyceae_XX	74	0.01%
Arachnida	528	0.02%	Oomycota_X_unclassified	69	0.01%
Embryophyceae_XX	333	0.01%	Pleurostomatida	64	0.01%
Colpodida	306	0.01%	Embryophyceae_XX	55	0.01%
Tremellomycetes	252	0.01%	Lecanoromycetes	54	0.01%
Platyophryida	210	0.01%	Dileptidae	41	0.01%
Halteriidae	201	0.01%	Allapsidae	39	0.01%
Dothideomycetes	158	0.01%	LOS7N/I-lineage	39	0.01%
Glissomonadida_unclassified	142	0.01%	Cystobasidiomycetes	24	0.00%
Fungi_unclassified	110	0.00%	Tokophryidae	17	0.00%
Annelida_XX	86	0.00%	Sordariomycetes	14	0.00%
Lecanoromycetes	86	0.00%	MAST-12C_X	9	0.00%
Cryomonadida_unclassified	77	0.00%	Arcellinida-A3	8	0.00%
Saccharomycetales	50	0.00%	Nassulida	4	0.00%
Tubulinea_unclassified	35	0.00%	Litostomatea_unclassified	3	0.00%
Glissomonadida_X	34	0.00%			
Taphrinomycetes	30	0.00%			
Tetrahymenida	27	0.00%			
Dinophyceae_unclassified	23	0.00%			
Litostomatea_XX	19	0.00%			
Rhodomelaceae	18	0.00%			
Colpodea_X_unclassified	12	0.00%			
Evaginogenida	12	0.00%			
Sordariomycetes	11	0.00%			
MAST-12C_X	9	0.00%			
OLIGO2	8	0.00%			

Marble			Moraine		
Family	n. reads	% reads	Family	n. reads	% reads
Microthamniales_X	916175	42.21%	Microthamniales_X	172969	58.06%
Rotifera_XX	462990	21.33%	Sandonidae	260396	8.74%
Tardigrada_XX	208567	9.61%	Rotifera_XX	128598	4.32%
Rhogostoma-lineage	188226	8.67%	Metazoa_unclassified	116861	3.92%
Sandonidae	114553	5.28%	LOS7N/I-lineage	111234	3.73%
Chilodonellidae	73592	3.39%	Rhogostoma-lineage	108817	3.65%
Prasiolales_X	71511	3.29%	Chlamydomonadales_X	108198	3.63%
Metazoa_unclassified	45579	2.10%	Prasiolales_X	95817	3.22%
Eukaryota_unclassified	19443	0.90%	Chilodonellidae	52336	1.76%
Watanabea-Clade_X	10117	0.47%	Eukaryota_unclassified	51478	1.73%
Chytridiomycetes	7445	0.34%	Embryophyceae_XX	32053	1.08%
Opisthokonta_unclassified	7294	0.34%	Chlorellales_X	29345	0.98%
Cercomonadidae	5504	0.25%	Cercozoa_unclassified	23995	0.81%

Marble			Moraine		
Family	n. reads	% reads	Family	n. reads	% reads
Pezizomycotina_unclassified	3560	0.16%	Watanabea-Clade_X	15895	0.53%
Pleurostomatida	3022	0.14%	Trachelocercidae	8939	0.30%
Fungi_unclassified	2881	0.13%	Allapsidae	8869	0.30%
Colpodida	2831	0.13%	Endostelium-lineage	8712	0.29%
Tremellomycetes	2647	0.12%	Annelida_XX	8698	0.29%
Trebouxiophyceae_unclassified	2455	0.11%	Trebouxiophyceae_unclassified	7570	0.25%
Chlorophyta_unclassified	2400	0.11%	Alphamonaceae	6481	0.22%
Oxytrichidae	2348	0.11%	Tardigrada_XX	5775	0.19%
Polar-centric-Mediophyceae	2176	0.10%	Opisthokonta_unclassified	5614	0.19%
Embryophyceae_XX	2016	0.09%	Centroheliozoa_X_unclassified	4724	0.16%
Chlamydomonadales_X	1623	0.07%	Cryptomonadales_X	3539	0.12%
Pyramimonadales_XX	1346	0.06%	Polar-centric-Mediophyceae	3165	0.11%
Arcellinida-A3	1293	0.06%	Evaginogenida	2752	0.09%
Archaeplastida_unclassified	1089	0.05%	Litostomatea_XX	2742	0.09%
Litostomatea_XX	1043	0.05%	Cercomonadidae	2625	0.09%
Allapsidae	702	0.03%	Platyophryida	2597	0.09%
Xanthophyceae_XX	592	0.03%	Glissomonadida_unclassified	2386	0.08%
Spirotrichea_unclassified	566	0.03%	Pezizomycotina_unclassified	2330	0.08%
Glissomonadida_unclassified	555	0.03%	Acramoebidae	1922	0.06%
Novel-clade-2	484	0.02%	Dino-Group-I-Clade-1	1695	0.06%
Cryomonadida_unclassified	427	0.02%	Ciliophora_unclassified	1601	0.05%
Cercozoa_unclassified	406	0.02%	Filosa-Sarcomonadea_unclassified	1461	0.05%
Ciliophora_unclassified	396	0.02%	Oxytrichidae	1335	0.04%
Dinophyceae_unclassified	376	0.02%	Xanthophyceae_XX	1187	0.04%
Annelida_XX	368	0.02%	Colpodida	1182	0.04%
Dileptidae	299	0.01%	Enoplea_X	1133	0.04%
Insecta	295	0.01%	Fungi_unclassified	1094	0.04%
Maxillopoda	227	0.01%	Dothideomycetes	1086	0.04%
LOS7N/I-lineage	167	0.01%	Tremellomycetes	1064	0.04%
MAST-12C_X	150	0.01%	Dinophyceae_unclassified	907	0.03%
Lecanoromycetes	101	0.00%	Ulotrichales_X	795	0.03%
Dino-Group-I-Clade-1	86	0.00%	Heterocapsaceae	667	0.02%
Colpodellida_unclassified	82	0.00%	Variosea_XX	665	0.02%
Gregarinidae	81	0.00%	Chytridiomycetes	616	0.02%
Eurotiomycetes	67	0.00%	Taphrinomycetes	615	0.02%
Endostelium-lineage	62	0.00%	Arcellinida-A3	575	0.02%
Filosa-Thecofilosea_unclassified	56	0.00%	Strombidinopsidae	562	0.02%
Exobasidiomycetes	39	0.00%	Chlorophyta_unclassified	492	0.02%
Chlamydomonadales_unclassified	24	0.00%	Tubulinea_unclassified	480	0.02%
Spongomonadidae	15	0.00%	Lecanoromycetes	461	0.02%
Tetrahymenida	9	0.00%	Nassulida	444	0.01%
Vahlkampfiidae	7	0.00%	Ceratiaceae	428	0.01%

Marble			Moraine		
Family	n. reads	% reads	Family	n. reads	% reads
Heterocapsaceae	5	0.00%	Schizoplasmodiids	414	0.01%
Pezizomycotina_X	5	0.00%	Pseudodendromonadales_X	402	0.01%
			Glissomonadida_X	354	0.01%
			Cercomonadida_unclassified	330	0.01%
			Archosauria	311	0.01%
			Saccharomycetales	234	0.01%
			Limnofilidae	230	0.01%
			Oomycota_XX	212	0.01%
			Chlamydomonadales_unclassified	185	0.01%
			Flamella-lineage	149	0.01%

Table S2.8. Number of reads and ASVs in each module, with percentages relative to the whole network dataset, identified with the network analysis.

	n. reads	% of reads	n. ASVs	% of ASVs	n. bac ASVs	% bac ASVs	n. euk ASV	% euk ASVs	n. bac reads	n. euk reads
M1	225416	11.01%	44	7.77%	37	84.09%	7	15.91%	62446	162970
M2	403884	19.74%	60	10.60%	58	96.67%	2	3.33%	350142	53742
M3	112933	5.52%	107	18.90%	106	99.07%	1	0.93%	110336	2597
M4	89470	4.37%	71	12.54%	62	87.32%	9	12.68%	51445	38025
M5	8291	0.41%	16	2.83%	16	100.00%	0	0.00%	8291	0
M6	188358	9.21%	84	14.84%	83	98.81%	1	1.19%	185188	3170
M7	81559	3.99%	72	12.72%	64	88.89%	8	11.11%	51398	30161
M8	177059	8.65%	38	6.71%	35	92.11%	3	7.89%	46924	690
M9	278904	13.63%	4	0.71%	0	0.00%	4	100.00%	0	278904
M10	431806	21.10%	34	6.01%	23	67.65%	11	32.35%	29466	402340
M11	48510	2.37%	36	6.36%	32	88.89%	4	11.11%	402340	9593

Table S2.9. Family taxonomic assignment of the ASV with cumulative abundance calculated for each module (M).

M1				M2				M3			
Family	**n ASVs**	**n reads**	**Abund.**	**Family**	**n ASVs**	**n reads**	**Abund.**	**Family**	**n ASVs**	**n reads**	**Abund.**
Nassulida	2	126197	55.98%	Pseudonocardiaceae	26	255313	63.21%	Chroococcidiopsaceae	25	57095	50.56%
Rotifera_XX	2	34578	15.34%	Sandonidae	2	53742	13.31%	Blastocatellaceae	16	25513	22.59%
Nostocaceae	14	28075	12.45%	Blastocatellaceae	8	43995	10.89%	Spirosomaceae	5	7077	6.27%
Phormidiaceae	6	23977	10.64%	Solirubrobacterales_uncl.	4	23784	5.89%	Euzebyaceae	7	4380	3.88%
Cyanobacteriales_uncl.	1	3629	1.61%	67-14	2	6544	1.62%	Trueperaceae	12	3935	3.48%
Solirubrobacteraceae	2	1350	0.60%	Nocardioidaceae	4	6127	1.52%	Abditibacteriaceae	6	2747	2.43%
Chytridiomycetes	1	920	0.41%	Actinobacteria_uncl.	3	2844	0.70%	Opisthokonta_uncl.	1	2597	2.30%
Cytophagales_uncl.	1	913	0.41%	Thermoleophilaceae	1	2810	0.70%	Pseudonocardiaceae	2	1387	1.23%
Chroococcidiopsaceae	2	904	0.40%	Thermobaculaceae	1	2679	0.66%	Hymenobacteraceae	3	960	0.85%
Sandonidae	1	793	0.35%	Rubrobacteriaceae	1	1816	0.45%	AKIW781	2	931	0.82%
Cyanobacteriia_uncl.	3	773	0.34%	KD4-96_fa	2	1536	0.38%	Cyanobacteriales_uncl.	4	827	0.73%
Sphingomonadaceae	2	625	0.28%	Euzebyaceae	2	1106	0.27%	Bacteria_uncl.	5	759	0.67%
Cytophagaceae	1	554	0.25%	Thermoleophilia_uncl.	1	779	0.19%	Thermoleophilia_uncl.	2	662	0.59%
Spirosomaceae	1	525	0.23%	JG30-KF-CM45	1	380	0.09%	uncultured	1	455	0.40%
Chilodonellidae	1	482	0.21%	Iamiaceae	1	216	0.05%	Actinobacteria_uncl.	1	441	0.39%
Acetobacteraceae	2	453	0.20%	Frankiales_uncl.	1	213	0.05%	Pyrinomonadaceae	2	425	0.38%
Nocardioidaceae	1	400	0.18%					Blastocatellia_uncl.	2	421	0.37%
Flavobacteriaceae	1	268	0.12%					Acetobacteraceae	3	413	0.37%
								MWH-CFBk5	1	389	0.34%
								Microscillaceae	1	338	0.30%
								Nocardioidaceae	1	299	0.26%
								AKYG1722	1	295	0.26%
								Intrasporangiaceae	1	156	0.14%
								JG30-KF-CM45	1	153	0.14%
								Cyanobacteriia_uncl.	1	150	0.13%
								Solirubrobacteraceae	1	128	0.11%

M4				M5				M6			
Family	**n ASVs**	**n reads**	**Abund.**	**Family**	**n ASVs**	**n reads**	**Abund.**	**Family**	**n ASVs**	**n reads**	**Abund.**
Nostocaceae	25	33368	37.30%	Nostocaceae	7	4277	51.59%	Solirubrobacteraceae	11	62479	33.17%
Watanabea-Clade_X	1	12779	14.28%	Phormidesmiaceae	2	1399	16.87%	JG30-KF-CM45	14	28309	15.03%
Rotifera_XX	1	9781	10.93%	Chroococcidiopsaceae	2	1083	13.06%	Actinobacteria_uncl.	3	19813	10.52%
Sessilida	1	4765	5.33%	Spirosomaceae	1	720	8.68%	Frankiales_uncl.	4	14741	7.83%
Prasiolales_X	2	4241	4.74%	Acetobacteraceae	2	468	5.64%	uncultured_fa	3	13818	7.34%
Leptolyngbyaceae	5	3438	3.84%	Cyanobacteriia_uncl.	1	267	3.22%	Solirubrobacterales_uncl.	12	12005	6.37%
Opisthokonta_uncl.	1	3424	3.83%	Bacteria_uncl.	1	77	0.93%	Bacteria_uncl.	5	4953	2.63%
Solirubrobacteraceae	4	3035	3.39%					Blastocatellaceae	2	4347	2.31%
Blastocatellaceae	8	2967	3.32%					Gemmatimonadaceae	2	4313	2.29%
Cyanobacteriia_uncl.	3	1825	2.04%					Thermoleophilia_uncl.	9	3731	1.98%
Tardigrada_XX	1	1544	1.73%					Sandonidae	1	3170	1.68%
Rhogostoma-lineage	2	1491	1.67%					Nocardioidaceae	2	3005	1.60%
Chroococcidiopsaceae	2	968	1.08%					uncultured	2	2636	1.40%
Acetobacteraceae	2	877	0.98%					Intrasporangiaceae	3	2439	1.29%
Sphingomonadaceae	2	863	0.96%					B12-WMSP1_fa	2	1718	0.91%
Bacteria_uncl.	2	815	0.91%					Acidimicrobiia_uncl.	1	1635	0.87%
Spirosomaceae	3	698	0.78%					Micrococcales_uncl.	2	1326	0.70%
Chloroflexales_uncl.	1	682	0.76%					IMCC26256_fa	1	1276	0.68%
Chloroflexaceae	1	612	0.68%					Chitinophagaceae	1	1130	0.60%
Frankiales_uncl.	1	519	0.58%					Frankiaceae	1	453	0.24%
Actinobacteria_uncl.	1	326	0.36%					Armatimonadales_fa	1	410	0.22%
Pseudonocardiaceae	1	270	0.30%					Propionibacteriaceae	1	401	0.21%
Chitinophagaceae	1	182	0.20%					Nocardiaceae	1	250	0.13%

M7				M8				M9			
Family	**n ASVs**	**n reads**	**Abund.**	**Family**	**n ASVs**	**n reads**	**Abund.**	**Family**	**n ASVs**	**n reads**	**Abund.**
Spirosomaceae	17	31516	38.64%	Sandonidae	3	95632	54.01%	Prasiolales_X	2	152513	54.68%
Chroococcidiopsaceae	25	12044	14.77%	Solirubrobacterales_uncl.	7	27213	15.37%	Microthamniales_X	2	126391	45.32%
Rhogostoma-lineage	1	9415	11.54%	Blastocatellaceae	9	20334	11.48%				
Chytridiomycetes	1	7198	8.83%	Nocardioidaceae	2	7440	4.20%				
Cercomonadidae	1	5408	6.63%	uncultured_fa	1	4926	2.78%				
Sandonidae	2	3975	4.87%	JG30-KF-CM45	1	4457	2.52%				
Blastocatellaceae	7	3076	3.77%	Ilumatobacteraceae	1	4372	2.47%				
Opisthokonta_uncl.	1	3037	3.72%	Propionibacteriaceae	4	4294	2.43%				
Cytophagaceae	1	1065	1.31%	Solirubrobacteraceae	3	3392	1.92%				
Hymenobacteraceae	1	778	0.95%	Chitinophagaceae	1	1889	1.07%				
Acetobacteraceae	1	752	0.92%	67-14	1	1402	0.79%				
Tardigrada_XX	1	626	0.77%	KD4-96_fa	2	900	0.51%				
Colpodida	1	502	0.62%	Acidimicrobiia_uncl.	1	353	0.20%				
Thermoleophilaceae	1	496	0.61%	Saccharimonadales_fa	1	259	0.15%				
Cyanobacteriales_uncl.	2	471	0.58%	LWQ8	1	196	0.11%				
AKIW781	1	411	0.50%								
Trueperaceae	1	223	0.27%								
Pyrinomonadaceae	1	136	0.17%								
Solirubrobacterales_uncl.	2	132	0.16%								
67-14	2	107	0.13%								
Thermoleophilia_uncl.	1	106	0.13%								
Gaiellaceae	1	85	0.10%								

M10				M11			
Family	**n ASVs**	**n reads**	**Abund.**	**Family**	**n ASVs**	**n reads**	**Abund.**
Microthamniales_X	7	322569	74.70%	Blastocatellaceae	9	24112	49.71%
Rotifera_XX	1	40036	9.27%	Chlorophyta_uncl.	1	4399	9.07%
Watanabea-Clade_X	3	39735	9.20%	Chlamydomonadales_X	2	3256	6.71%

M10				M11			
Family	**n ASVs**	**n reads**	**Abund.**	**Family**	**n ASVs**	**n reads**	**Abund.**
Chroococcidiopsaceae	4	17513	4.06%	Bacteria_uncl.	3	2329	4.80%
Acetobacteraceae	8	5108	1.18%	Acetobacteraceae	3	1963	4.05%
Blastocatellaceae	4	4601	1.07%	Eukaryota_uncl.	1	1938	4.00%
Spirosomaceae	2	995	0.23%	67-14	1	1709	3.52%
Gemmatimonadaceae	1	358	0.08%	Acidobacteriaceae_(Subgroup_1)	1	1585	3.27%
Comamonadaceae	1	269	0.06%	Hymenobacteraceae	3	1248	2.57%
Nostocaceae	1	239	0.06%	Deinococcaceae	1	1101	2.27%
uncultured	1	216	0.05%	Caulobacteraceae	1	932	1.92%
Hymenobacteraceae	1	167	0.04%	Beijerinckiaceae	2	790	1.63%
				Frankiaceae	1	592	1.22%
				Sphingobacteriaceae	1	522	1.08%
				Chitinophagaceae	1	466	0.96%
				Propionibacteriaceae	1	439	0.90%
				Nakamurellaceae	1	309	0.64%
				Abditibacteriaceae	1	299	0.62%
				Armatimonadales_fa	1	264	0.54%
				Solirubrobacteraceae	1	257	0.53%

Table S2.10. Phylum taxonomic assignment of the ASV with cumulative abundance calculated for each module (M).

M1				M2				M3			
Phylum	**n. ASVs**	**n. reads**	**Abund.**	**Phylum**	**n. ASVs**	**n. reads**	**Abund.**	**Phylum**	**n. ASVs**	**n. reads**	**Abund.**
Ciliophora	3	126679	56.20%	Actinobacteriota	46	301552	74.66%	Cyanobacteriota	30	58072	51.42%
Cyanobacteriota	26	57358	25.45%	Cercozoa	2	53742	13.31%	Acidobacteriota	20	26359	23.34%
Metazoa	2	34578	15.34%	Acidobacteriota	8	43995	10.89%	Bacteroidota	11	9219	8.16%
Bacteroidota	4	2260	1.00%	Chloroflexota	4	4595	1.14%	Actinobacteriota	15	7453	6.60%
Actinobacteriota	3	1750	0.78%					Deinococcota	12	3935	3.48%
Pseudomonadota	4	1078	0.48%					Abditibacteriota	6	2747	2.43%
Fungi	1	920	0.41%					Opisthokonta_uncl.	1	2597	2.30%
Cercozoa	1	793	0.35%					Chloroflexota	4	1379	1.22%
								Bacteria_uncl.	5	759	0.67%
M4				**M5**				**M6**			
Phylum	**n. ASVs**	**n. reads**	**Abund.**	**Phylum**	**n. ASVs**	**n. reads**	**Abund.**	**Phylum**	**n. ASVs**	**n. reads**	**Abund.**
Cyanobacteriota	35	39599	44.26%	Cyanobacteriota	12	7026	84.74%	Actinobacteriota	53	126190	66.99%
Chlorophyta	3	17020	19.02%	Bacteroidota	1	720	8.68%	Chloroflexota	16	30027	15.94%
Metazoa	2	11325	12.66%	Pseudomonadota	2	468	5.64%	Patescibacteria	3	13818	7.34%
Ciliophora	1	4765	5.33%	Bacteria_uncl.	1	77	0.93%	Bacteria_uncl.	5	4953	2.63%
Actinobacteriota	7	4150	4.64%					Acidobacteriota	2	4347	2.31%
Opisthokonta_uncl.	1	3424	3.83%					Gemmatimonadota	2	4313	2.29%
Acidobacteriota	8	2967	3.32%					Cercozoa	1	3170	1.68%
Pseudomonadota	4	1740	1.94%					Bacteroidota	1	1130	0.60%
Cercozoa	2	1491	1.67%					Armatimonadota	1	410	0.22%
Chloroflexota	2	1294	1.45%								
Bacteroidota	4	880	0.98%								
Bacteria_uncl.	2	815	0.91%								

M7				M8				M9			
Phylum	**n. ASVs**	**n. reads**	**Abund.**	**Phylum**	**n. ASVs**	**n. reads**	**Abund.**	**Phylum**	**n. ASVs**	**n. reads**	**Abund.**
Bacteroidota	19	33359	40.90%	Cercozoa	3	95632	54.01%	Chlorophyta	4	278904	100.00%
Cercozoa	4	18798	23.05%	Actinobacteriota	19	48466	27.37%				
Cyanobacteriota	27	12515	15.34%	Acidobacteriota	9	20334	11.48%				
Fungi	1	7198	8.83%	Patescibacteria	3	5381	3.04%				
Acidobacteriota	8	3212	3.94%	Chloroflexota	3	5357	3.03%				
Opisthokonta_uncl.	1	3037	3.72%	Bacteroidota	1	1889	1.07%				
Actinobacteriota	7	926	1.14%								
Pseudomonadota	1	752	0.92%								
Metazoa	1	626	0.77%								
Ciliophora	1	502	0.62%								
Chloroflexota	1	411	0.50%								
Deinococcota	1	223	0.27%								

M10				M11			
Phylum	**n. ASVs**	**n. reads**	**Abund.**	**Phylum**	**n. ASVs**	**n. reads**	**Abund.**
Chlorophyta	10	362304	83.90%	Acidobacteriota	10	25697	52.97%
Metazoa	1	40036	9.27%	Chlorophyta	3	7655	15.78%
Cyanobacteriota	5	17752	4.11%	Pseudomonadota	6	3685	7.60%
Pseudomonadota	9	5377	1.25%	Actinobacteriota	5	3306	6.82%
Acidobacteriota	4	4601	1.07%	Bacteria_uncl.	3	2329	4.80%
Bacteroidota	4	1378	0.32%	Bacteroidota	5	2236	4.61%
Gemmatimonadota	1	358	0.08%	Eukaryota_uncl.	1	1938	4.00%
				Deinococcota	1	1101	2.27%
				Abditibacteriota	1	299	0.62%
				Armatimonadota	1	264	0.54%

Table S2.11. Results of the Pearson moment correlation between the cumulative abundances of the ASVs in each module (M) and environmental variables. *Only correlations with p<0.01 are highlighted in bold, after correction for multiple hypothesis testing.*

Modules	Factor	r2	df	*adj. p*	Modules	Factor	r2	df	*adj. p*
M1	Cond.	-0.22	83	0.0432	M8	**pH**	-0.32	83	0.0034
M2	**Cond.**	0.28	83	0.0085		TOC	-0.32	83	0.0032
	TOC	-0.24	83	0.0287		**PO_4^{3-}**	-0.33	83	0.0021
	TN	-0.43	83	5.01E-05	M9	$N\text{-}NH_4^+$	0.46	83	1.01E-05
M3	**pH**	0.51	83	6.83E-07		$P\text{-}PO_4^{3-}$	0.26	83	0.0184
	$N\text{-}NH_4^+$	-.026	83	0.0168	M10	**TOC**	0.56	83	2.77E-08
	$N\text{-}NO_3^-$	-0.27	83	0.0464		**$N\text{-}NH_4^+$**	0.35	83	0.0012
	TN	-0.28	83	0.0005		**DW**	-0.26	83	0.016
	$P\text{-}PO_4^{3-}$	0.68	83	8.55E-05		TN	-0.25	83	0.0227
M4	**Cond.**	-0.26	83	0.0168		TP	-0.24	83	0.0260
M5	**TN**	0.26	83	0.0183	M11	**pH**	-0.30	83	0.0048
M6	**pH**	-0.26	83	0.0157		**TOC**	0.44	83	2.70E-05
	Cond.	-0.26	83	0.0184		**$N\text{-}NH_4^+$**	0.46	83	8.06E-06
	TOC	-0.21	83	0.0489		**DW**	-0.30	83	0.0055
	TN	-0.27	83	0.0144		**TN**	0.38	83	0.0003
M7	**pH**	0.52	83	4.40E-07		TP	0.25	83	0.0203
	$N\text{-}NH_4^+$	-0.25	83	0.0226					
	$P\text{-}PO_4^{3-}$	-0.46	83	1.13E-05					

Table S2.12. Results of the Spearman rank correlation between the cumulative abundance of the ASVs in each module (M) and environmental variables. *Only correlations with p<0.01 are reported, after applying the holm correction for multiple hypothesis testing.*

Modules	Factor	Rho, ρ	*adj. p*	Modules	Factor	Rho, ρ	*adj. p*
M1	Cond.	-0.32	0.0025	M7	pH	0.57	1.43E-08
	TOC	0.41	0.0001		$P\text{-}PO_4^{3-}$	-0.60	1.75E-09
	$N\text{-}NH_4^+$	0.33	0.0018	M8	pH	-0.41	9.16E-05
	TN	0.32	0.0031		TOC	-0.53	2.39E-07
M2	TOC	-0.39	0.0002		TN	-0.68	1.17E-12
	$N\text{-}NH_4^+$	-0.34	0.0017		$P\text{-}PO_4^{3-}$	0.32	0.0023
	DW	0.31	0.0037	M9	$N\text{-}NH_4^+$	0.46	1.23E-05
	TN	-0.50	9.75E-07		TN	0.31	0.0040
M3	pH	0.63	1.12E-10		$P\text{-}PO_4^{3-}$	0.36	0.0008
	DW	0.32	0.0025	M10	pH	-0.32	0.0031
	TN	0.39	0.0002		TOC	0.54	8.45E-08
	$P\text{-}PO_4^{3-}$	-0.59	3.31E-09		$N\text{-}NH_4^+$	0.49	1.93E-06
	TN	0.30	0.0049		DW	-0.45	1.66E-05
	PO4	0.30	0.0048		TN	0.37	0.00051
M4	Cond.	-0.38	0.0004	M11	pH	-0.30	0.0048
	$N\text{-}NH_4^+$	0.35	0.0010		TOC	0.44	2.70E-05
	TN	0.31	0.0029		$N\text{-}NH_4^+$	0.46	8.06E-06
M5	Cond.	-0.35	0.0009		DW	-0.30	0.0055
	$N\text{-}NH_4^+$	0.32	0.0025		TN	0.38	0.0003
	TN	0.01	0.006		TP	0.25	0.0204
M6	pH	-0.53	2.09E-07				
	TOC	-0.37	0.0006				
	$P\text{-}PO_4^{3-}$	0.32	0.0031				

Table S2.13. Results of the Random Forests (RF) approach to the identification of the environmental explanatory variables for the distribution of each module across the sampled substrate types. *The environmental variables are reported in ranking order. Thresh. var. - number of variables that passed the Important Variable threshold; interpr. var. - number of variables identified as important in interpreting the module (M) distribution. Interpretation variables are marked in bold.*

			Environmental variable importance ranking in Random Forests interpretation								
Modules	**thresh. var.**	**interp. var.**	**1**	**2**	**3**	**4**	**5**	**6**	**7**	**8**	**9**
M1	4	3	**Cond.**	**DW**	**TOC**	$N\text{-}NH_4^+$					
M2	9	4	**TN**	**pH**	**Cond.**	**$N\text{-}NH_4^+$**	TOC	$P\text{-}PO_4^{3-}$	$N\text{-}NO_3^-$	DW	TP
M3	8	3	**pH**	**$P\text{-}PO_4^{3-}$**	**TN**	TP	TOC	Cond.	$N\text{-}NH_4^+$	DW	
M4	6	5	**Cond.**	**$N\text{-}NO_3^-$**	**TN**	$N\text{-}NH_4^+$	pH	TOC			
M5	9	3	**TN**	**$N\text{-}NH_4^+$**	**Cond.**	TOC	DW	TP	$P\text{-}PO_4^{3-}$	pH	$N\text{-}NO_3^-$
M6	8	4	**Cond.**	**pH**	**TN**	**TOC**	$P\text{-}PO_4^{3-}$	TP	$N\text{-}NH_4^+$	$N\text{-}NO_3^-$	
M7	8	5	**$P\text{-}PO_4^{3-}$**	**pH**	**Cond.**	**$N\text{-}NH_4^+$**	**TN**	TOC	TP	$N\text{-}NO_3^-$	
M8	6	4	**TN**	**pH**	**TOC**	**TP**	$N\text{-}NH_4^+$	$P\text{-}PO_4^{3-}$			
M9	6	1	**$N\text{-}NH_4^+$**	pH	DW	TN	$P\text{-}PO_4^{3-}$	TOC			
M10	7	2	**TOC**	**$P\text{-}PO_4^{3-}$**	$N\text{-}NH_4^+$	TN	pH	TP			
M11	8	3	**$N\text{-}NH_4^+$**	**pH**	**TP**	TOC	TN	Cond.	DW	$P\text{-}PO_4^{3-}$	

Table S2.14. Table reporting the environmental variables selected using the different techniques (scatterplot inspection, Spearman rank correlation, Pearson moment correlation, Random Forests) and the selected variable plotted in Figure 6 for each module (M). *In the RF column the bold variables are those selected by the model.*

	M1				M2				M3				M4			
Var. ranking	Scatter	Pearson	Spearman	RF	Scatter	Pearson	Spearman	RF	Scatter	Pearson	Spearman	RF	Scatter	Pearson	Spearman	RF
1	**Cond.**	**Cond.**	**Cond.**	**Cond.**	**TN**	Cond.	TOC	**TN**	**pH**	**pH**	**pH**	**pH**	**Cond.**	**Cond.**	**Cond.**	**Cond.**
2			TOC	DW		TOC	$N\text{-}NH_4^+$	**pH**	$N\text{-}NH_4^+$	$N\text{-}NH_4^+$	DW	**$P\text{-}PO_4^{3-}$**			$N\text{-}NH_4^+$	$N\text{-}NO_3^-$
3			$N\text{-}NH_4^+$	TOC		**TN**	DW	**Cond.**	$N\text{-}NO_3^-$	$N\text{-}NO_3^-$	**TN**	**TN**			TN	TN
4			TN	$N\text{-}NH_4^+$			**TN**	$N\text{-}NH_4^+$	**TN**	**TN**	**$P\text{-}PO_4^{3-}$**	TP				$N\text{-}NH_4^+$
5								TOC	DW	**$P\text{-}PO_4^{3-}$**		TOC				pH
6								$P\text{-}PO_4^{3-}$	**$P\text{-}PO_4^{3-}$**			Cond.				TOC
7								$N\text{-}NO_3^-$				$N\text{-}NH_4^+$				
8								DW				DW				
9								TP								
Selected var.	Cond.				TN				pH, TN, $P\text{-}PO_4^{3-}$				Cond.			
	M5				M6				M7				M8			
Var. ranking	Scatter	Pearson	Spearman	RF	Scatter	Pearson	Spearman	RF	Scatter	Pearson	Spearman	RF	Scatter	Pearson	Spearman	RF
1	Cond.	**TN**	Cond.	**TN**	**pH**	**pH**	**pH**	Cond.	**pH**	**pH**	**pH**	**$P\text{-}PO_4^{3-}$**	**pH**	**pH**	**pH**	**TN**
2	$N\text{-}NO_3^-$		$N\text{-}NH_4^+$	**$N\text{-}NH_4^+$**	Cond.	Cond.	**TOC**	**pH**	TOC	$N\text{-}NH_4^+$	**$P\text{-}PO_4^{3-}$**	**pH**	Cond.	**TOC**	**TOC**	**pH**
3	**TN**		**TN**	**Cond.**	**TOC**	**TOC**	**TN**	**TN**	TN	**$P\text{-}PO_4^{3-}$**		**Cond.**	**TOC**	**TN**	**TN**	**TOC**
4				TOC	$N\text{-}NO_3^-$		$P\text{-}PO_4^{3-}$	**TOC**	**$P\text{-}PO_4^{3-}$**			**$N\text{-}NH_4^+$**	$N\text{-}NH_4^+$		$P\text{-}PO_4^{3-}$	**TP**
5				DW	**TN**			$P\text{-}PO_4^{3-}$				**TN**	**TN**			$N\text{-}NH_4^+$
6				TP				TP				TOC				$P\text{-}PO_4^{3-}$
7				$P\text{-}PO_4^{3-}$				$N\text{-}NH_4^+$				TP				
8				pH				$N\text{-}NO_3^-$				$N\text{-}NO_3^-$				
Selected var.	TN				pH, TOC, TN				pH, $P\text{-}PO_4^{3-}$				pH, TOC, TN			

	M9				M10				M11			
Var. ranking	Scatter	Pearson	Spearman	RF	Scatter	Pearson	Spearman	RF	Scatter	Pearson	Spearman	RF
1	**$N\text{-}NH_4^+$**	**$N\text{-}NH_4^+$**	**$N\text{-}NH_4^+$**	**$N\text{-}NH_4^+$**	**TOC**	**TOC**	pH	**TOC**	**$N\text{-}NH_4^+$**	pH	pH	**$N\text{-}NH_4^+$**
2		$P\text{-}PO_4^{3-}$	TN	pH	TN	$N\text{-}NH_4^+$	**TOC**	**$P\text{-}PO_4^{3-}$**		**TOC**	**TOC**	pH
3			$P\text{-}PO_4^{3-}$	DW	TP	DW	$N\text{-}NH_4^+$	$N\text{-}NH_4^+$		**$N\text{-}NH_4^+$**	**$N\text{-}NH_4^+$**	TP
4				TN		**TN**	DW	TN		DW	DW	TOC
5				$P\text{-}PO_4^{3-}$		TP	TN	pH		TN	TN	TN
6				TOC				TP		TP	TP	Cond.
7								Cond.				DW
												$P\text{-}PO_4^{3-}$
Selected var.	$N\text{-}NH_4^+$				TOC				$N\text{-}NH_4^+$			

Table S2.15. Keystone taxa candidates' topology parameters (betweenness centrality and vertex degree) per module. Module 9 was not included because of its low node number.

	Id	Kingdom	Phylum	Class	Family	Genus	Betweenness centrality	vertex degree
	ASV_896	Bacteria	Bacteroidota	Bacteroidia	Cytophagales_unclassified	Cytophagales_unclassified	786.444105	27
	ASV_2043	Bacteria	Pseudomonadota	Alphaproteobacteria	Acetobacteraceae	Acidiphilium	786.444105	27
M1	ASV_1162	Bacteria	Bacteroidota	Bacteroidia	Spirosomaceae	Spirosoma	502.564893	39
	ASV_370	Eukaryota	Fungi	Chytridiomycota	Chytridiomycetes	Chytridiomycetes_unclassified	418.361635	50
	ASV_705	Bacteria	Actinobacteriota	Thermoleophilia	Solirubrobacteraceae	Solirubrobacteraceae_uncl.	418.361635	50
	ASV_1634	Bacteria	Actinobacteriota	Actinobacteria	Nocardioidaceae	Kribbella	418.361635	50
M2	ASV_123	Bacteria	Actinobacteriota	Actinobacteria	Pseudonocardiaceae	Crossiella	2917.799535	22
	ASV_92	Bacteria	Actinobacteriota	Thermoleophilia	67-14	67-14_ge	2396.116041	8
	ASV_221	Bacteria	Cyanobacteriota	Cyanobacteriia	Chroococcidiopsaceae	Aliterella	5438.213756	10
M3	ASV_183	Bacteria	Cyanobacteriota	Cyanobacteriia	Chroococcidiopsaceae	Aliterella	4142.854019	41
	ASV_293	Bacteria	Deinococcota	Deinococci	Trueperaceae	Truepera	592.953118	68
	ASV_300	Bacteria	Actinobacteriota	Actinobacteria	Euzebyaceae	uncultured	720.380285	68
	ASV_865	Bacteria	Pseudomonadota	Alphaproteobacteria	Sphingomonadaceae	Polymorphobacter	9121.593414	14
M4	ASV_419	Bacteria	Cyanobacteriota	Cyanobacteriia	Nostocaceae	Nostocaceae_unclassified	351.416438	66
	ASV_218	Bacteria	Cyanobacteriota	Cyanobacteriia	Nostocaceae	Nostocaceae_unclassified	351.416438	66
M5	ASV_400	Bacteria	Cyanobacteriota	Cyanobacteriia	Nostocaceae	Nostocaceae_unclassified	1729.069272	11
	ASV_776	Bacteria	Cyanobacteriota	Cyanobacteriia	Nostocaceae	Nostocaceae_unclassified	1088.324112	15
	ASV_156	Bacteria	Chloroflexota	Chloroflexia	JG30-KF-CM45	JG30-KF-CM45_ge	3239.797823	16
M6	ASV_5	Bacteria	Actinobacteriota	Thermoleophilia	Solirubrobacteraceae	Solirubrobacteraceae_uncl.	3032.724051	15
	ASV_306	Bacteria	Actinobacteriota	Thermoleophilia	Solirubrobacteraceae	Solirubrobacteraceae_uncl.	470.025382	54
	ASV_1163	Bacteria	Cyanobacteriota	Cyanobacteriia	Chroococcidiopsaceae	Chroococcidiopsaceae_uncl.	2738.475742	27
	ASV_523	Bacteria	Cyanobacteriota	Cyanobacteriia	Chroococcidiopsaceae	uncultured	2738.475742	27
M7	ASV_91	Bacteria	Bacteroidota	Bacteroidia	Spirosomaceae	Spirosoma	1101.852178	22
	ASV_2795	Bacteria	Cyanobacteriota	Cyanobacteriia	Chroococcidiopsaceae	Chroococcidiopsaceae_uncl.	654.766362	28
	ASV_2142	Bacteria	Cyanobacteriota	Cyanobacteriia	Chroococcidiopsaceae	uncultured	558.370211	27

	Id	Kingdom	Phylum	Class	Family	Genus	Betweenness centrality	vertex degree
M8	ASV_20	Bacteria	Actinobacteriota	Thermoleophilia	Solirubrobacterales_unclassified	Solirubrobacteraceae_uncl.	6184.945817	16
	ASV_73	Bacteria	Patescibacteria	uncultured	uncultured_fa	uncultured_ge	1809.283696	14
	ASV_1328	Bacteria	Cyanobacteriota	Cyanobacteriia	Nostocaceae	Nostoc_PCC-73102	8556	7
	ASV_245	Bacteria	Acidobacteriota	Blastocatellia	Blastocatellaceae	Blastocatella	4534.083333	8
M10	ASV_1433	Bacteria	Pseudomonadota	Gammaproteobacteria	Comamonadaceae	Rhizobacter	4534.083333	8
	ASV_129	Eukaryota	Chlorophyta	Trebouxiophyceae	Microthamniales_X	Trebouxia_jamesii	1896.735441	10
	ASV_70	Eukaryota	Chlorophyta	Trebouxiophyceae	Microthamniales_X	Trebouxia_jamesii	1282.315171	13
	ASV_68	Eukaryota	Chlorophyta	Trebouxiophyceae	Microthamniales_X	Trebouxia_jamesii	900.838217	12
	ASV_1011	Bacteria	Actinobacteriota	Actinobacteria	Frankiaceae	Jatrophihabitans	2120.63113	6
	ASV_115	Eukaryota	Chlorophyta	Chlorophyta_unclassified	Chlorophyta_unclassified	Chlorophyta_unclassified	1696.519161	4
M11	ASV_191	Bacteria	Acidobacteriota	Blastocatellia	Blastocatellaceae	Blastocatella	1802.592833	8
	ASV_193	Bacteria	Acidobacteriota	Blastocatellia	Blastocatellaceae	Blastocatella	1319.347179	7
	ASV_594	Bacteria	Deinococcota	Deinococci	Deinococcaceae	Deinococcus	580.033951	12
	ASV_87	Bacteria	Acidobacteriota	Blastocatellia	Blastocatellaceae	Blastocatella	580.033951	12

I.III SUPPLEMENTARY RESULTS

Environmental variables

Elevation data and the main physicochemical parameters of the investigated soils are summarized in Fig. S2.3 and Table S2.1. Samples were grouped by their bedrock substrate type (granite, gneiss, marble and moraine). Moraine soils were taken from sites with different altitudes: Dry Valley was the highest site (~ 1600 m), Yûboku Valley was lower (~ 1300 m) and Austkampane (~ 900 m) was the lowest site among all sampled sites. pH values were highest in marble soils (median 9.17), whilst all the other bedrock substrate types were on average more acidic (median 6.36). The exceptional alkalinity of marble is due to the characteristic salt accumulation in such bedrock. Different amounts of total organic carbon (TOC) were measured, ranging from 0.19% (in moraine soils) to 10.95% (in gneiss soils), and TOC was the highest in soils with developed biocrusts (lichens or moss dominated). A reverse trend was observed for dry weight, with lowest values recorded in gneiss soils (77.04 - 99.05 %) and highest in moraine (95.64 - 99.8 %) and marble (94.48 - 99.93 %), whilst granite (88.91 - 99.87 %) had intermediate values. Total N values were particularly low in moraine soils, with an average of 0.01 % compared to the other soils which had average values comprised between 0.08 and 0.15 %. Highest values of N-NH_4^+ were recorded in gneiss (46 mg kg^{-1}) and granite (30mg kg^{-1}) whereas the lowest values were observed in moraine (0.5 mg kg^{-1}) and marble (0.7 mg kg^{-1}). Conductivity did not show strong differences across the sampled sites, though very high values were found in two samples of the Dry Valley and in one of Austkampane (> 1000 µS cm^{-1}). P-PO_4^{3-} values were significantly different in all bedrock substrate types, being highest in granitic (65.3 ± 31; min: 26.4; max: 151.1 mg kg^{-1}) and lowest in marble soils (8.6 ± 3.3; min: 6.5; max: 18.5mg kg^{-1}), although a very high value (337 mg kg^{-1}) was found in a moraine sample from Austkampane that was characterized by an algal community. This latter sample also showed the highest N-NO_3^- concentration (24 mg kg^{-1}), that was, on average, below 1 mg kg^{-1} in all other samples. Total P was significantly higher in gneiss bedrock bedrock compared to the other bedrock kinds of substratetypes.

II. CHAPTER 3 - SUPPLEMENTARY MATERIALS

II.I SUPPLEMENTARY FIGURES OF CHAPTER 3

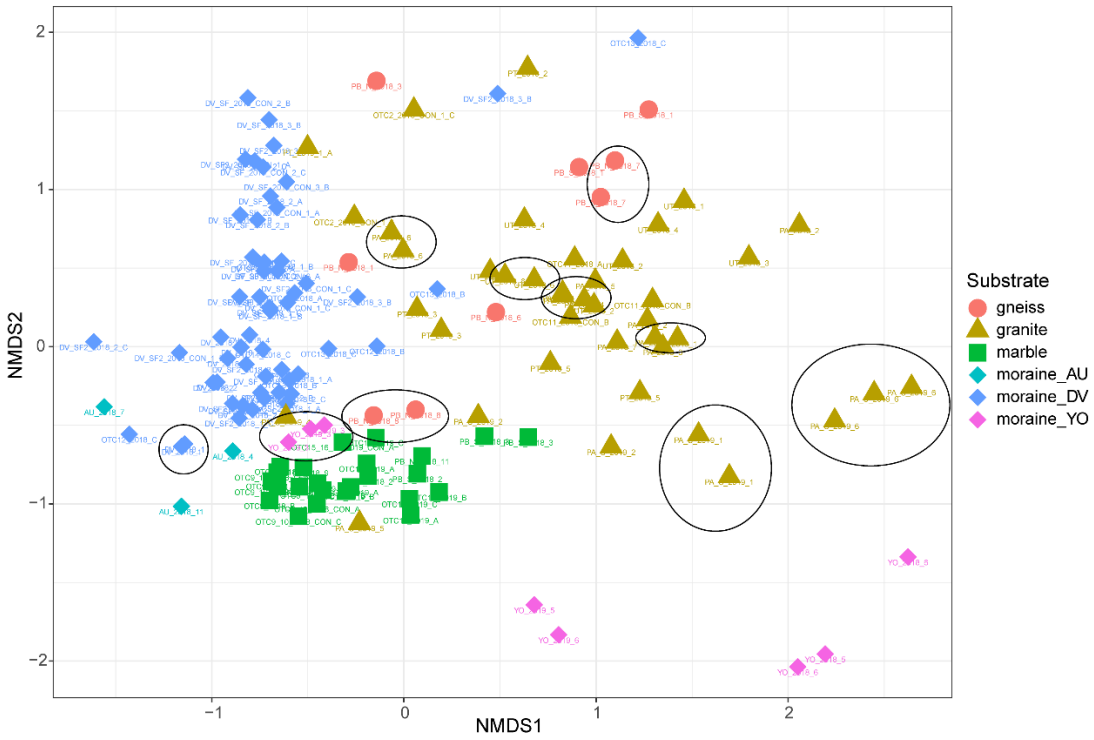

Fig. S3.1 Non-metric multidimensional scaling (nMDS) plot of 100 samples of bacterial and cyanobacterial communities representing all sequenced samples including replicates *(encircled in black). Circles represent gneiss, triangles granite, squares marble and diamonds moraine samples. Colors are according to the different kinds of substrate. Moraine_DV: moraine substrates of Dry Valley samples; moraine_YO: moraine substrates of Yûboku samples.*

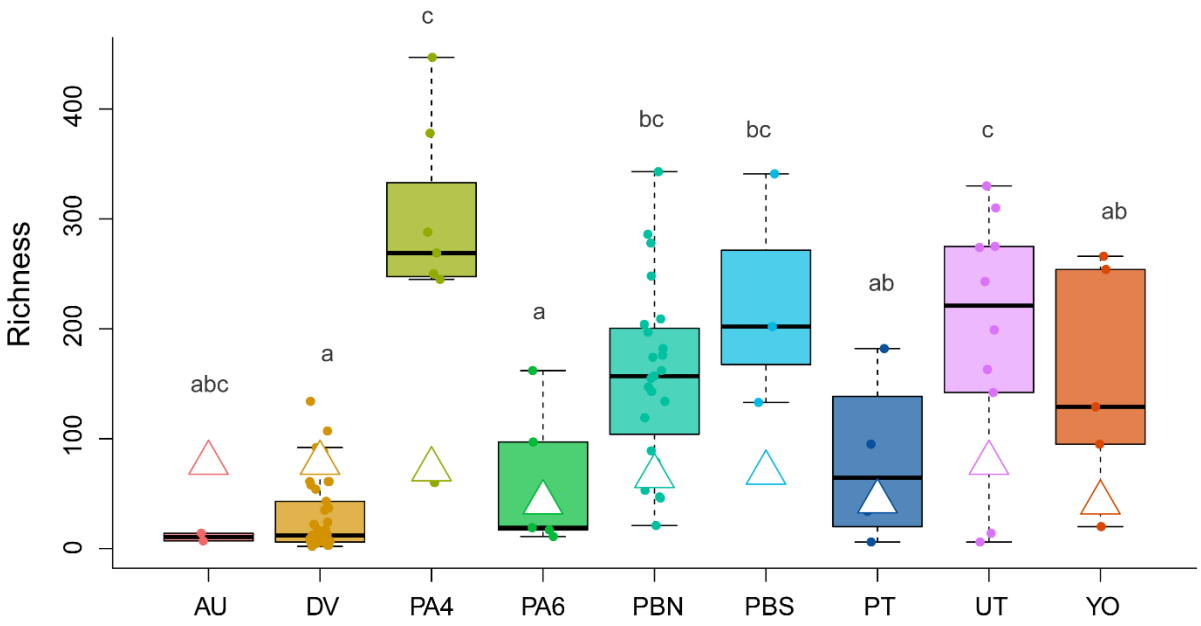

Fig. S3.2 Boxplots of cyanobacterial richness per sampled site. *Triangles represent evenness; circles data points. DV = moraines of Dry Valley; PA4 = granitic Pingvinane 4th nunatak; PA6 = granitic Pingvinane 6th nunatak; PBN = Perlebandet N nunatak; PBS = Perlebandet S nunatak; PT = granitic Petrellnuten nunatak; UT = granitic Utsteinen ridge; YO = moraines of Yûboku Valley. Letters correspond tot he significant differences tested via Kruskas Wallis test.*

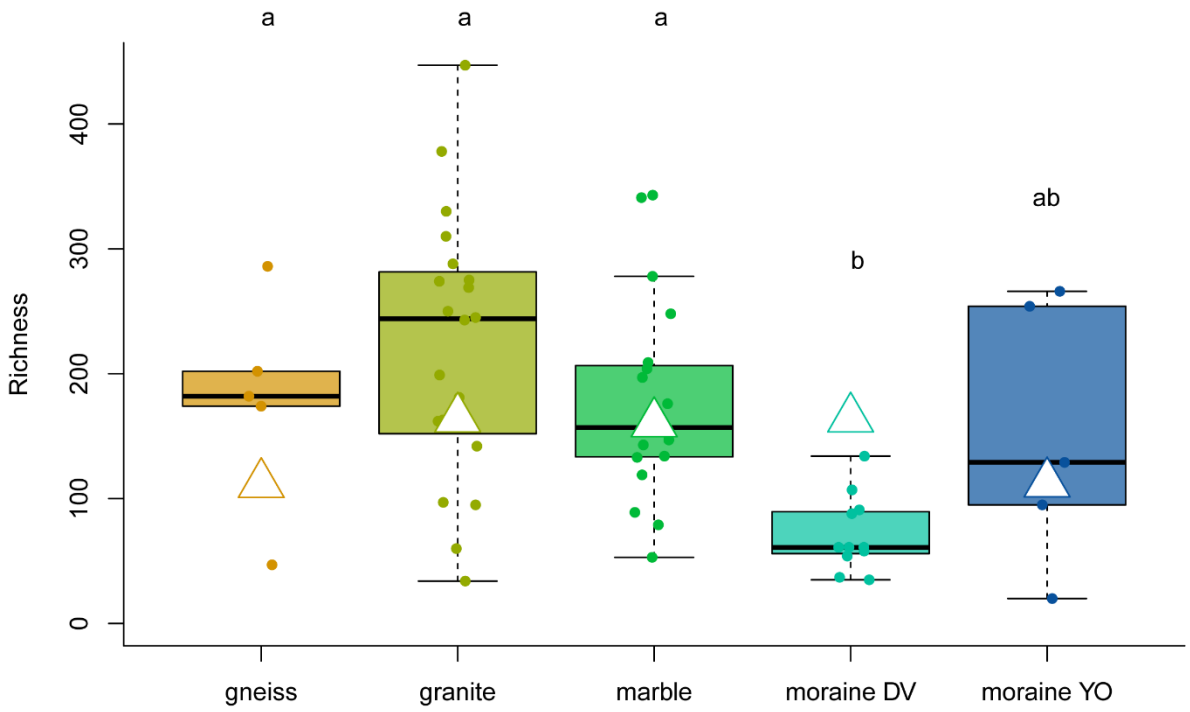

Fig. S3.3 Boxplots of cyanobacterial richness per substrate type. *Triangles represent evenness; circles data points. Letters correspond tot he significant differences tested via Kruskas Wallis test.*

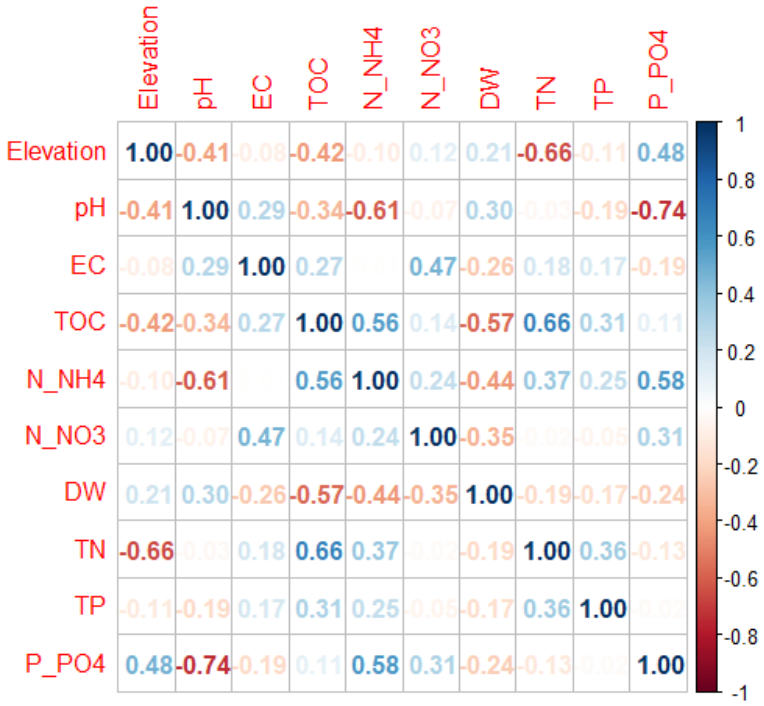

Fig. S3.4 Correlogram showing Pearson's correlation coefficients of all geochemical transformed variables. *TOC: total organic carbon; N_NH4: N-NH_4^+; N_NO3: N-NO_3^-; DW: dry weight; TN: total nitrogen; TP: total phosphorus; P_PO4: P-PO_4^{3-}.*

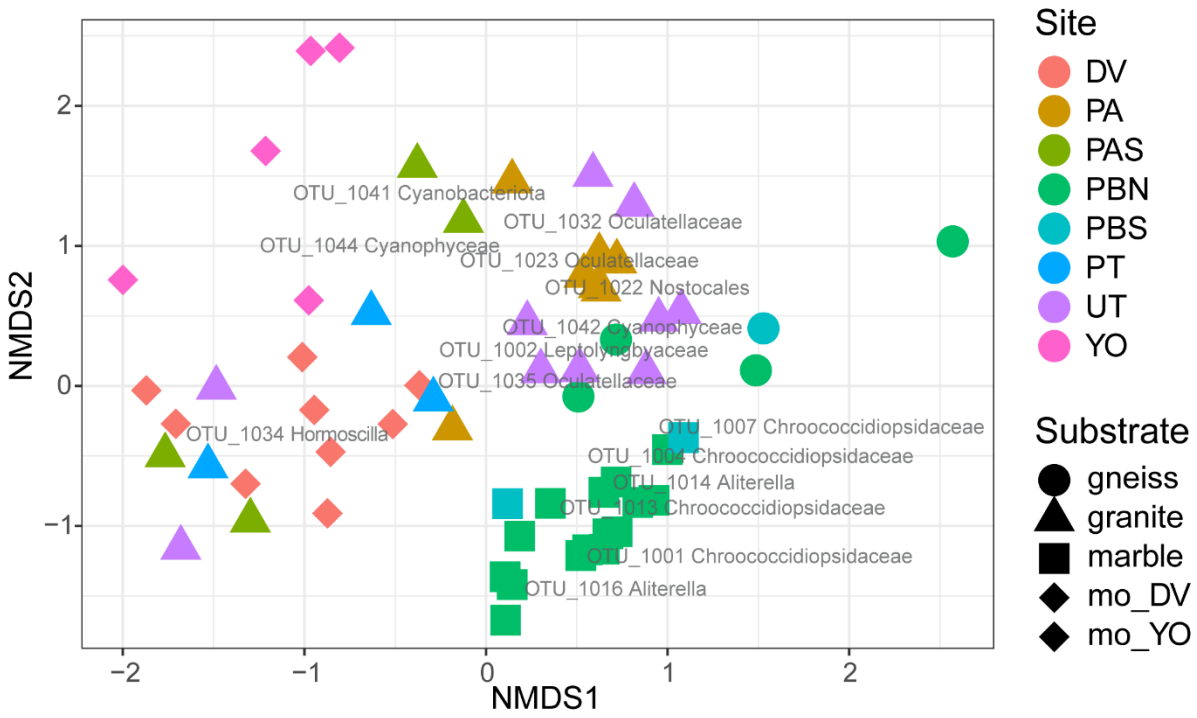

Fig. S3.5 Non-metric multidimensional scaling (nMDS) plot of 60 samples of cyanobacterial communities with the top 20 OTUs plotted. *Circles represent gneiss, triangles granite, squares marble and diamonds moraine samples. Colors are according to the different kinds of substrate. Moraine_DV: moraine substrates of Dry Valley samples; moraine_YO: moraine substrates of Yûboku samples.*

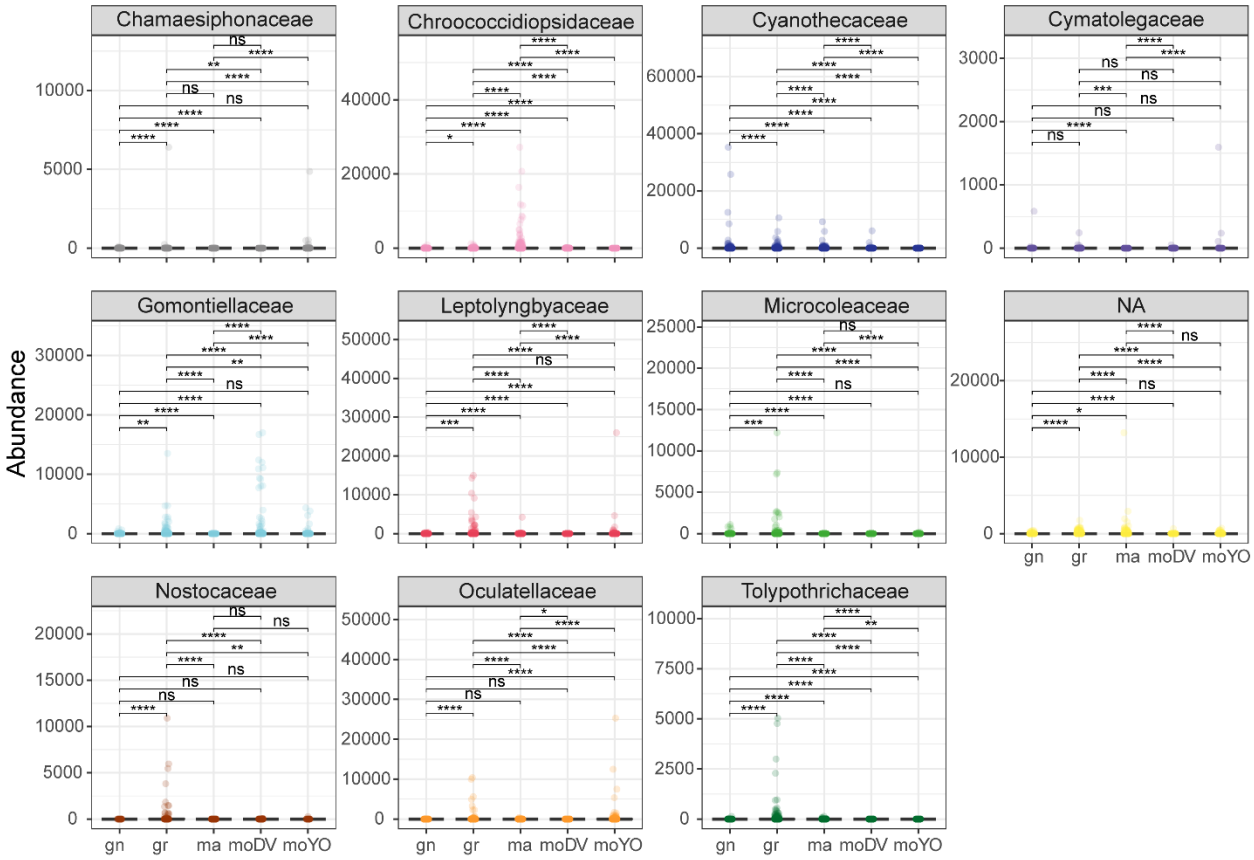

Fig. S3.6 Boxplot representing the abundances of Cyanobacteriota families in the different substrate types. *Colors represent different families. Asterisks represent the significance of the p-value of the pairwise Wilcoxon test after mean comparison by the Kruskal Wallis test. Asteriks represent p-values: * = p< 0.05; ** = p<0.01; *** = p<0.001; ns = to p>0.05. gn= gneiss; gr = granite; ma = marble; moDV = moraines of Dry Valley; moYO = moraines of Yûboku Valley.*

II.II SUPPLEMENTARY TABLES OF CHAPTER 3

Table S3.1. Environmental data

Sample	Latitude	Longitude	Substrate	Substrate detail	pH	EC ($\mu S\ cm^{-1}$)	TOC (%)	N-NH_4 ($mg\ kg^{-1}$)	N-NO_3 ($mg\ kg^{-1}$)	DW (%)	P-PO_4 ($mg\ kg^{-1}$)	TN (%)	TP (%)	Elevation (m a.s.l.)	# cyano reads	# tot reads
AU_2018_11	-71.661156	25.150839	mo_AU	(Mo)_Amp	7.77	164.6	0.61	3.034	23.99	99.81	337.269	0.12	0.33	930	149	20517
AU_2018_4	-71.67534	25.136383	mo_AU	(Mo)_Amp	8.34	112.7	0.92	1.143	0.213	99.56	18.631	0.01	0.16	996	32	9662
AU_2018_7	-71.67593	25.136465	mo_AU	(Mo)_Amp	7.01	1112	0.68	0.742	0.421	99.65	25.596	0.01	0.21	995	1	944
DV_2018_1	-72.115875	23.157526	mo_DV	(Mo)_Sch_D_Gbh_To	7.96	2110	0.76	0.591	0.607	99.65	21.138	0.03	0.08	1714	23	24206
DV_2018_2	-72.11599	23.157045	mo_DV	(Mo)_Sch_D_Gbh_To	6.36	119.5	0.46	1.645	0.133	99.55	16.177	0.02	0.08	1712	83	55191
DV_2018_3	-72.11476	23.163443	mo_DV	(Mo)_Sch_D_Gbh_To	6.33	260	0.74	1.31	0.077	99.51	28.958	0.02	0.07	1694	6	14588
DV_2018_4	-72.11468	23.163328	mo_DV	(Mo)_Sch_D_Gbh_To	6.44	78.9	0.49	1.085	0.021	99.64	24.585	0.03	0.07	1694	11	29976
DV_OTC12_2018_A	-72.11223	23.184898	mo_DV	(Mo)_Sch_D_Gbh_To	6.14	47.6	0.49	0.637	0.125	99.92	44.325	0.01	0.07	1666	38	4899
DV_OTC12_2018_B	-72.11223	23.184898	mo_DV	(Mo)_Sch_D_Gbh_To	6.29	140	0.3	0.922	0.135	99.87	40.959	0.01	0.09	1666	22307	27307
DV_OTC12_2018_C	-72.11223	23.184898	mo_DV	(Mo)_Sch_D_Gbh_To	7.31	1175	0.45	1.245	0.989	99.73	42.879	0.04	0.09	1666	0	736
DV_OTC13_2018_A	-72.11219	23.184841	mo_DV	(Mo)_Sch_D_Gbh_To	6.1	41.5	0.39	0.855	0.091	99.91	52.72	0.02	0.13	1667	9	29162
DV_OTC13_2018_B	-72.11219	23.184841	mo_DV	(Mo)_Sch_D_Gbh_To	6.78	57.2	0.7	1.342	0.202	99.88	43.947	0.02	0.1	1667	21534	49240
DV_OTC13_2018_C	-72.11219	23.184841	mo_DV	(Mo)_Sch_D_Gbh_To	6.56	50.8	0.64	1.047	0.082	99.91	37.159	0.01	0.07	1667	43001	46208
DV_OTC14_2018_B	-72.11219	23.184841	mo_DV	(Mo)_Sch_D_Gbh_To	6.5	264	0.4	0.927	0.646	99.89	41.475	0.06	0.15	1667	4511	31911
DV_OTC14_2018_C	-72.11219	23.184841	mo_DV	(Mo)_Sch_D_Gbh_To	6.46	46.9	0.3	1.275	0.211	99.92	43.192	0.05	0.15	1667	4071	59525
DV_SF_2018_1_A	-72.11258	23.18555	mo_DV	(Mo)_Sch_D_Gbh_To	6.06	382	0.6	0.986	0.272	99.84	46.216	0.03	0.12	1667	14	8004

Sample	Latitude	Longitude	Substrate	Substrate detail	pH	EC ($\mu S\ cm^{-1}$)	TOC (%)	N-NH_4 ($mg\ kg^{-1}$)	N-NO_3 ($mg\ kg^{-1}$)	DW (%)	P-PO_4 ($mg\ kg^{-1}$)	TN (%)	TP (%)	Elevation (m a.s.l.)	# cyano reads	# tot reads
DV_SF_2018_1_B	-72.11258	23.18555	mo_DV	(Mo)_Sch_D_Gbh_To	6.45	59.2	0.34	0.802	0.143	99.74	37.011	0.02	0.09	1667	29	34955
DV_SF_2018_1_C	-72.11258	23.18555	mo_DV	(Mo)_Sch_D_Gbh_To	6.4	52.7	0.57	1.101	0.026	99.82	37.628	0.03	0.07	1667	19	33372
DV_SF_2018_2_A	-72.11258	23.18555	mo_DV	(Mo)_Sch_D_Gbh_To	6.22	34.7	0.38	0.94	0.102	99.87	47.913	0.02	0.11	1667	8	9120
DV_SF_2018_2_B	-72.11258	23.18555	mo_DV	(Mo)_Sch_D_Gbh_To	6.34	30.8	0.38	1.011	0.177	99.9	53.034	0.02	0.13	1667	6	15625
DV_SF_2018_2_C	-72.11258	23.18555	mo_DV	(Mo)_Sch_D_Gbh_To	5.98	40.8	0.52	1.041	0.918	99.86	57.324	0.03	0.13	1667	6	18855
DV_SF_2018_3_A	-72.11258	23.18555	mo_DV	(Mo)_Sch_D_Gbh_To	6.43	95	0.47	0.836	0.088	99.89	46.376	0.03	0.12	1667	6	14683
DV_SF_2018_3_B	-72.11258	23.18555	mo_DV	(Mo)_Sch_D_Gbh_To	5.94	328	0.19	0.946	0.157	99.88	50.124	0.03	0.13	1667	147	2156
DV_SF_2018_3_C	-72.11258	23.18555	mo_DV	(Mo)_Sch_D_Gbh_To	6.49	62.7	0.49	1.217	0.046	99.63	37.329	0.02	0.08	1667	945	32680
DV_SF_2018_CON_1_A	-72.11262	23.185282	mo_DV	(Mo)_Sch_D_Gbh_To	6.26	22.6	0.6	1.192	0.169	99.47	54.103	0.02	0.13	1668	29	4536
DV_SF_2018_CON_1_C	-72.11262	23.185282	mo_DV	(Mo)_Sch_D_Gbh_To	6.24	33.7	0.38	0.377	0.092	99.34	40.899	0.01	0.1	1668	248	5413
DV_SF_2018_CON_2_A	-72.11278	23.185186	mo_DV	(Mo)_Sch_D_Gbh_To	5.75	125.6	0.85	0.259	0.031	99.84	61.912	0.03	0.12	1668	35	10466
DV_SF_2018_CON_2_B	-72.11278	23.185186	mo_DV	(Mo)_Sch_D_Gbh_To	5.64	16.6	0.36	0.851	0.041	99.12	52.525	0.02	0.12	1668	16	3205
DV_SF_2018_CON_2_C	-72.11278	23.185186	mo_DV	(Mo)_Sch_D_Gbh_To	5.55	38.9	0.35	0.631	0.031	98.91	62.933	0.03	0.12	1668	53	40199
DV_SF_2018_CON_3_A	-72.11271	23.184937	mo_DV	(Mo)_Sch_D_Gbh_To	6.14	37.4	0.38	0.477	0.634	99.72	53.264	0.02	0.09	1668	37	23005
DV_SF_2018_CON_3_B	-72.11271	23.184937	mo_DV	(Mo)_Sch_D_Gbh_To	5.81	22.3	0.3	0.504	0.232	99.19	63.504	0.02	0.12	1668	26	9622
DV_SF_2018_CON_3_C	-72.11271	23.184937	mo_DV	(Mo)_Sch_D_Gbh_To	5.88	16.9	0.43	0.733	0.056	99.19	42.924	0.02	0.12	1668	3	24815
DV_SF2_2018_1_B	-72.11214	23.185244	mo_DV	(Mo)_Sch_D_Gbh_To	6.95	39.2	0.44	1.167	0.112	99.25	51.044	0.02	0.08	1666	13140	26432
DV_SF2_2018_1_C	-72.11214	23.185244	mo_DV	(Mo)_Sch_D_Gbh_To	7.8	74.9	0.57	2.735	0.619	99.89	55.622	0.04	0.12	1666	10236	14997

Sample	Latitude	Longitude	Substrate	Substrate detail	pH	EC ($\mu S\ cm^{-1}$)	TOC (%)	N-NH_4 ($mg\ kg^{-1}$)	N-NO_3 ($mg\ kg^{-1}$)	DW (%)	P-PO_4 ($mg\ kg^{-1}$)	TN (%)	TP (%)	Elevation (m a.s.l.)	# cyano reads	# tot reads
DV_SF2_2018_2_A	-72.112114	23.185379	mo_DV	(Mo)_Sch_D_Gbh_To	6.41	29	0.73	1.082	0.081	99.52	48.976	0.02	0.11	1666	1489	12583
DV_SF2_2018_2_B	-72.112114	23.185379	mo_DV	(Mo)_Sch_D_Gbh_To	6.51	32.8	0.58	0.636	0.076	99.87	50.217	0.03	0.11	1666	330	12481
DV_SF2_2018_2_C	-72.112114	23.185379	mo_DV	(Mo)_Sch_D_Gbh_To	6.59	100.4	0.53	0.831	0.549	99.88	42.732	0.04	0.1	1666	11698	36065
DV_SF2_2018_3_A	-72.112114	23.185379	mo_DV	(Mo)_Sch_D_Gbh_To	5.91	19.3	0.48	0.663	0.051	99.88	62.873	0.02	0.13	1666	119	23390
DV_SF2_2018_3_B	-72.112114	23.185379	mo_DV	(Mo)_Sch_D_Gbh_To	6.29	108.7	0.43	0.482	0.188	99.81	51.853	0.02	0.1	1666	5543	6054
DV_SF2_2018_3_C	-72.112114	23.185379	mo_DV	(Mo)_Sch_D_Gbh_To	5.98	18.2	0.46	0.889	0.076	99.75	53.056	0.01	0.12	1666	392	19974
DV_SF2_2018_CON_1_A	-72.11206	23.184668	mo_DV	(Mo)_Sch_D_Gbh_To	6.23	21.1	0.49	0.327	0.101	99.65	55.756	0.01	0.1	1667	5	1956
DV_SF2_2018_CON_1_B	-72.11206	23.184668	mo_DV	(Mo)_Sch_D_Gbh_To	6.36	64.9	0.63	0.518	0.086	99.72	48.878	0.01	0.09	1667	1	7637
DV_SF2_2018_CON_1_C	-72.11206	23.184668	mo_DV	(Mo)_Sch_D_Gbh_To	6.85	185.5	0.67	0.558	0.091	99.68	56.133	0.02	0.12	1667	26087	36980
PA_2018_1	-72.00135	22.999208	granite	(Gr)	6.12	22.9	0.76	2.753	0.088	99.75	48.568	0.06	0.12	1409	40462	40511
PA_2018_2	-72.00131	22.999477	granite	(Gr)	6.06	19.4	0.88	0.989	0.089	99.82	55.398	0.08	0.09	1410	41651	41828
PA_2018_3	-72.00144	22.999647	granite	(Gr)	6.41	22.4	1.46	3.359	0.389	99.45	57.074	0.09	0.13	1410	5670	5728
PA_2018_4	-72.00144	22.999647	granite	(Gr)	6.58	20.7	1.05	2.004	0.223	99.36	61.305	0.03	0.05	1410	34686	35579
PA_2018_5	-72.00149	23.000029	granite	(Gr)	6.21	21.1	0.43	1.379	0.111	99.45	67.494	0.14	0.1	1411	30093	31217
PA_2018_6	-72.00143	23.000105	granite	(Gr)	6.22	15.4	1.13	1.464	0.116	99.25	40.294	0.03	0.06	1412	1976	14798
PA_2018_7	-72.00139	23.000048	granite	(Gr)	6.45	47.4	1.54	8.585	0.108	99.74	55.434	0.1	0.05	1412	27926	28057
PA_S_2019_1	-72.010506	22.989674	granite	(Gr)	7.31	62.1	0.78	2.017	0.898	99.41	86.474	0.06	0.09	1412	16567	16590
PA_S_2019_2	-72.01036	22.991528	granite	(Gr)	7.04	193.4	1.47	1.859	0.289	98.25	73.589	0.07	0.07	1416	37390	37629
PA_S_2019_4	-72.010056	22.993479	granite	(Gr)	6.97	24.8	0.31	7.283	0.312	99.75	114.824	0.02	0.09	1416	130	16464
PA_S_2019_5	-72.01002	22.993422	granite	(Gr)	7.57	65.6	0.32	8.557	1.053	99.85	95.352	0.03	0.06	1416	30093	1165

Sample	Latitude	Longitude	Substrate	Substrate detail	pH	EC ($\mu S\ cm^{-1}$)	TOC (%)	N-NH_4 ($mg\ kg^{-1}$)	N-NO_3 ($mg\ kg^{-1}$)	DW (%)	P-PO_4 ($mg\ kg^{-1}$)	TN (%)	TP (%)	Elevation (m a.s.l.)	# cyano reads	# tot reads
PA_S_2019_6	-72.0101	22.993536	granite	(Gr)	6.52	108.8	3.4	24.04	5.464	99.35	119.427	0.46	0.02	1417	1976	80
PB_N_2018_1	-71.84361	22.838146	gneiss	(Gbg)	5.88	414.2	9.23	20.526	0.04	98.25	38.751	0.23	0.4	1256	127	13700
PB_N_2018_3	-71.84353	22.838034	gneiss	(Gbg)	5.01	163.1	10.95	46.657	0.136	98.21	48.899	0.28	0.17	1255	10452	17146
PB_N_2018_6	-71.84395	22.835169	gneiss	(Gbg)	5.63	91.7	4.6	12.926	0.036	99.15	34.056	0.2	0.41	1279	6783	15393
PB_N_2018_7	-71.843895	22.835245	gneiss	(Gbg)	5.82	49.2	2.52	13.117	0.131	99.22	18.639	0.16	0.16	1277	38447	38498
PB_N_2018_8	-71.84399	22.834904	gneiss	(Gbg)	8.38	89.4	0.68	3.906	0.964	99.02	23.818	0.07	0.81	1282	21575	24966
PB_N_2018_9	-71.84405	22.834051	marble	(M)	7.4	336	5.62	4.553	0.351	99.45	18.515	0.36	0.23	1287	6552	21039
PB_N_2018_10	-71.84405	22.834051	marble	(Gbg)	9.09	149.7	1.48	0.89	0.506	99.74	7.968	0.27	0.21	1287	26148	38821
PB_N_2018_11	-71.84405	22.834051	marble	(Gbg)	8.98	56.5	0.79	0.437	0.036	99.68	8.81	0.15	0.12	1287	27061	33139
PB_N_OTC9_10_CON_A	-71.84405	22.834051	marble	(M)	9.42	117.9	1.19	0.321	0.035	99.91	6.918	0.24	0.12	1287	40462	48470
PB_N_OTC9_10_CON_B	-71.84405	22.834051	marble	(M)	9.17	73.6	0.58	0.59	0.06	99.95	7.173	0.27	0.16	1287	11449	15690
PB_N_OTC9_10_CON_C	-71.84405	22.834051	marble	(M)	9.45	117.3	1.14	0.282	0.05	99.78	7.104	0.21	0.1	1287	12013	15480
PB_N_OTC9_A_18	-71.84405	22.834051	marble	(M)	9.46	160.4	1.3	0.761	0.062	99.91	8.042	0.23	0.15	1287	6537	15288
PB_N_OTC9_B	-71.84405	22.834051	marble	(M)	9.49	185.5	1.49	0.392	0.151	99.78	8.109	0.17	0.12	1287	2496	4345
PB_N_OTC9_C_18	-71.84405	22.834051	marble	(M)	9.55	142.6	1.56	0.748	0.045	99.82	9.184	0.26	0.12	1287	423	2634
PB_N_OTC15_16_17_2019_CON_A	-71.84423	22.831173	marble	(M)	9.09	208.1	0.48	0.926	0.27	99.95	6.899	0.04	0.03	1310	9751	19338
PB_N_OTC15_2019_A	-71.84423	22.831173	marble	(M)	9.31	68.2	0.34	0.816	0.06	99.92	6.636	0.13	0.08	1310	24981	27625

Sample	Latitude	Longitude	Substrate	Substrate detail	pH	EC ($\mu S\ cm^{-1}$)	TOC (%)	N-NH_4 ($mg\ kg^{-1}$)	N-NO_3 ($mg\ kg^{-1}$)	DW (%)	P-PO_4 ($mg\ kg^{-1}$)	TN (%)	TP (%)	Elevation (m a.s.l.)	# cyano reads	# tot reads
PB_N_OTC15_2019_B	-71.84423	22.831173	marble	(M)	9.21	58.2	0.5	0.292	0.05	99.78	6.686	0.06	0.07	1310	34837	53099
PB_N_OTC15_2019_C	-71.84423	22.831173	marble	(M)	9.34	60.2	0.46	0.096	0.031	99.85	6.537	0.13	0.08	1310	11841	12622
PB_N_OTC16_2019_A	-71.84423	22.831173	marble	(M)	9.22	62.9	0.69	0.786	0.121	99.81	6.571	0.07	0.05	1310	10620	10994
PB_N_OTC16_2019_C	-71.84423	22.831173	marble	(M)	9.08	90.7	0.6	0.286	0.827	99.89	6.445	0.06	0.06	1310	22569	29041
PB_N_OTC17_2019_A	-71.84423	22.831173	marble	(M)	8.73	72.5	0.59	1.081	0.025	99.74	7.534	0.08	0.13	1310	10339	13873
PB_N_OTC17_2019_B	-71.84423	22.831173	marble	(M)	8.93	57.6	0.38	0.997	0.022	99.91	6.749	0.06	0.04	1310	20583	21820
PB_N_OTC17_2019_C	-71.84423	22.831173	marble	(M)	8.88	66.4	0.69	1.354	0.015	99.74	6.906	0.08	0.07	1310	4575	6851
PB_S_2018_1	-71.8797	22.746996	gneiss	(Gbh)	6.45	17.6	1.41	1.648	0.088	99.27	17.073	0.09	0.16	1349	45349	47539
PB_S_2018_2	-71.87994	22.746687	marble	(M)	9.01	63.7	0.53	0.299	0.173	99.35	14.094	0.04	0.1	1354	4602	27841
PB_S_2018_3	-71.88009	22.74659	marble	(M)	8.94	50.7	0.78	0.333	0.09	99.41	14.28	0.04	0.04	1357	32825	33169
PT_2019_1_A	-72.007385	22.832005	granite	(Gr)	6.11	28.8	0.15	2.204	0.387	99.45	52.049	0.05	0.11	1469	22	5298
PT_2019_2	-72.007385	22.832005	granite	(Gr)	6.13	70.4	1.28	2.444	3.837	99.57	60.359	0.11	0.14	1469	3643	3657
PT_2019_3	-72.007416	22.831738	granite	(Gr)	7.11	31.8	0.45	3.258	0.428	99.47	42.777	0.04	0.06	1472	4894	11359
PT_2019_5	-72.00757	22.833204	granite	(Gr)	7.01	14.9	0.25	0.721	0.28	99.9	36.502	0.03	0.07	1460	37395	37804
UT_2018_1	-71.9456	23.345005	granite	(Gr)	5.89	21.1	2.46	7.048	0.303	99.55	64.229	0.15	0.11	1362	5974	7152
UT_2018_2	-71.94543	23.345041	granite	(Gr)	6.28	20.9	1.83	2.835	0.077	99.28	26.373	0.16	0.15	1358	26079	26268
UT_2018_3	-71.94559	23.345139	granite	(Gr)	5.24	30.1	2.15	5.929	0.084	99.36	151.121	0.22	0.12	1361	20527	20805
UT_2018_4	-71.94573	23.345177	granite	(Gr)	6.1	15.6	1.24	1.483	0.086	99.62	34.375	0.35	0.09	1364	24770	29865
UT_2018_6	-71.94626	23.3456	granite	(Gr)	5.95	30.3	1.1	1.607	0.076	99.75	39.742	0.25	0.12	1372	18334	19425
UT_2018_7	-71.94624	23.345734	granite	(Gr)	5.87	14.2	0.59	1.151	0.146	99.81	40.212	0.07	0.04	1370	10240	13813
UT_OTC11_2018_A	-71.945465	23.344967	granite	(Gr)	5.92	58.1	2.49	2.059	0.091	99.72	23.943	0.35	0.17	1359	10189	11384

Sample	Latitude	Longitude	Substrate	Substrate detail	pH	EC ($\mu S\ cm^{-1}$)	TOC (%)	N-NH_4 ($mg\ kg^{-1}$)	N-NO_3 ($mg\ kg^{-1}$)	DW (%)	P-PO_4 ($mg\ kg^{-1}$)	TN (%)	TP (%)	Elevation (m a.s.l.)	# cyano reads	# tot reads
UT_OTC11_2018_CON_B	-71.945465	23.344967	granite	(Gr)	6.73	36.6	0.89	1.334	0.115	99.89	43.154	0.09	0.09	1359	25763	26367
UT_OTC2_2018_CON_1_A	-71.946075	23.345505	granite	(Gr)	5.83	329.1	2.67	30.354	0.497	99.25	96.667	0.34	0.24	1369	18	18174
UT_OTC2_2018_CON_1_C	-71.946075	23.345505	granite	(Gr)	5.97	273.1	2.13	22.79	1.773	99.72	50.768	0.43	0.2	1369	9	2323
YO_2018_5	-72.081375	23.793673	mo_YO	(Mo)_Sch_To	8.45	110.8	1.19	0.627	0.197	99.74	15.318	0.05	0.1	1360	56457	56459
YO_2018_6	-72.08111	23.793453	mo_YO	(Mo)_Sch_To	8.53	60.2	1.38	0.407	0.296	99.82	16.151	0.03	0.04	1360	27272	27288
YO_2019_3	-72.08115	23.793186	mo_YO	(Mo)_Sch_To	8.81	90.5	0.54	0.256	0.236	99.81	22.712	0.04	0.09	1361	18073	35188
YO_2019_5	-72.08344	23.790731	mo_YO	(Mo)_Sch_To	8.03	4750	2.47	1.04	290	98.25	20.732	0.09	0.07	1357	29306	39478
YO_2019_6	-72.08344	23.790731	mo_YO	(Mo)_Sch_To	8.96	93.7	0.57	0.286	2.38	99.65	27.897	0.02	0.08	1357	6978	9075

AU: Austkampane; DV: Dry Valley; PB_N: Perlebandet North (I nunatak); PB_S: Perlebandet South (III nunatak); PA: Pingvinane North (III nunatak); PA_S: Pingvinane South (VI nunatak); PT: Petrellnuten; UT: Utsteinen; YO: Yûboku Valley.
Mo_DV: moraines of Dry Valley; mo_YO: moraines of Yûboku Valley.
(Mo)_Amp: Moraine with orthopyroxene amphibolite; (Mo)_Sch_D_Gbh_To: Moraine with amphibole schist, diorite and quartz, biotite-hornblende gneiss and metatonalite; (M): Marble and skarns; (Gbg): Sillimanite-garnet-biotite gneiss, partly containing cordierite; (Gr): Granite and pegmatite; (Gbh): Biotite-hornblende gneiss and hornblende gneiss containing garnet in places; (Mo)_Sch_To: Moraine with amphibole schist and metatonalite.
EC: electric conductivity; TOC: total carbon; DW: dry weight; TN: total nitrogen; TP: total phosphorus.

Table S3.1. Summary of the geochemical parameters *(mean ± sd)**.***

	marble	granite	gneiss	moraine_DV	moraine_YO	moraine_AU
pH	9.09 ± 0.46	6.37 ± 0.54	6.20 ± 1.17	6.33 ± 0.47	8.56 ± 0.36	8.05 ± 0.40
EC ($\mu S\ cm^{-1}$)	109.9 ± 71.5	61.5 ± 80.6	137.5 ± 144.1	137.7 ± 340.3	1021 ± 2084	138.7 ± 36.7
TOC (%)	1.06 ± 1.14	1.28 ± 0.85	4.89 ± 4.3	0.49 ± 0.15	8.56 ± 0.79	0.77 ± 0.22
N-NO^-_3 ($mg\ kg^{-1}$)	0.15 ± 0.20	0.67 ± 1.25	0.23 ± 0.36	0.20 ± 0.22	58.6 ± 129.3	12.1 ± 16.8
N–NH^+_4 ($mg\ kg^{-1}$)	0.81 ± 0.94	5.75 ± 7.80	16.7 ± 16.3	0.92 ± 0.43	0.52 ± 0.32	2.09 ± 1.34
P–PO^{3-}_4 ($mg\ kg^{-1}$)	8.55 ± 3.24	63.0 ± 30.9	30.2 ± 12.5	46.4 ± 11.2	20.6 ± 5.13	178.0 ± 225.3
Dry weight (%)	99.77 ± 0.18	99.53 ± 0.33	98.85 ± 0.49	99.69 ± 0.26	99.45 ± 0.68	99.69 ± 0.18
TN (%)	0.15 ± 0.10	0.15 ± 0.13	0.17 ± 0.08	0.02 ± 0.01	0.05 ± 0.03	0.07 ± 0.08
TP (%)	0.10 ± 0.05	0.10 ± 0.05	0.35 ± 0.25	0.10 ± 0.24	0.08 ± 0.44	0.03 ± 0.12

Table S3.3. Mock community taxonomy details. *In house mock community OTU table composed by BCCM strains.*

Strain name	#OTU ID	Control reads	Total reads	ULC093	ULC100	ULC112	ULC166	ULC420	ULC469	Taxonomy
ULC337	OTU_1	0	2089	3	3	7	2	4	34750	g__Synechococcus_unclassified
ULC720	OTU_21	0	2479	37970	0	4	0	1	3	g__Phormidium(100);s__pseudopriestleyi
ULC489	OTU_18	0	2551	1	40870	2	0	1	1	p__Cyanobacteria_unclassified
ULC133	OTU_14	0	2106	4	1	7	1	14090	3	g__Nostoc(99);g__Nostoc_unclassified
ULC682	OTU_11	0	2234	2	0	84230	2	0	0	g__Phormidium(100);s__priestleyi
ULC48	OTU_13	0	2167	1	1	2	23550	0	0	g__Phormidium_unclassified
ULC91	OTU_49	0	72	1	0	0	0	253	0	o__JG30-KF-CM45_unclassified

Table S3.4. Kruskal-Wallis rank sum test showing the effect of substrate type on environmental parameters.

	df	χ2	P
pH	4	44.841	<0.001
TOC	4	17.693	<0.05
N-NO_3	4	12.617	<0.05
P-PO_4	3	46.136	<0.001
N-NH_4	4	36.576	<0.001
TN	4	25.693	<0.001
TP	4	13.887	<0.001
DW	4	21.477	<0.001
EC	4	23.886	<0.001

EC: Electric conductivity; TOC: Total carbon; TN: Total nitrogen; TP: Total phosphorus

Table S3.5. Family taxonomic assignment of the OTUs with cumulative abundance calculated for each substrate type. *When the genus was unclassified, the higher taxonomic assignation was indicated: "_p": Phylum; "_c": Class; "_o ": Order.*

All substrates			Granite			Gneiss		
Family	**n. reads**	**% reads**	**Family**	**n. reads**	**% reads**	**Family**	**n. reads**	**% reads**
Chroococcidiopsidaceae	250920	21.402%	Leptolyngbyaceae	97090	22.871%	Cyanothecaceae	107478	87.571%
Gomontiellaceae	227516	19.405%	Gomontiellaceae	56669	13.349%	Microcoleaceae	3605	2.937%
Cyanothecaceae	210719	17.973%	Cyanothecaceae	53546	12.614%	Gomontiellaceae	2756	2.246%
Leptolyngbyaceae	142134	12.123%	Microcoleaceae	48631	11.456%	Chroococcidiopsidaceae	2069	1.686%
Oculatellaceae	117629	10.033%	Oculatellaceae	45822	10.794%	Leptolyngbyaceae	1886	1.537%
Cyanophyceae_c	56158	4.790%	Nostocaceae	37042	8.726%	Cyanophyceae_c	1449	1.181%
Microcoleaceae	52868	4.509%	Tolypothrichaceae	25488	6.004%	Cyanobacteriota_p	1174	0.957%
Nostocaceae	37920	3.234%	Nostocales_o	20624	4.858%	Cymatolegaceae	625	0.509%
Tolypothrichaceae	26189	2.234%	Cyanophyceae_c	19196	4.522%	Gomontiellales_o	598	0.487%
Nostocales_o	20757	1.770%	Chroococcidiopsidaceae	10261	2.417%	Chamaesiphonaceae	433	0.353%
Chamaesiphonaceae	13842	1.181%	Chamaesiphonaceae	6795	1.601%	Tolypothrichaceae	235	0.191%
Cyanobacteriota_p	8473	0.723%	Gomontiellales	1664	0.392%	Oculatellaceae	205	0.167%
Gomontiellales_o	3183	0.271%	Cyanobacteriota_p	774	0.182%	Stigonemataceae	172	0.140%
Cymatolegaceae	3020	0.258%	Cymatolegaceae	372	0.088%	Nostocales_o	40	0.033%
Nodosilineales_o	285	0.024%	Nodosilineales_o	285	0.067%	Nostocaceae	6	0.005%
Leptolyngbyales_o	266	0.023%	Oscillatoriales_o	168	0.040%	Prochlorococcaceae	1	0.001%
Stigonemataceae	184	0.016%	Leptolyngbyales_o	48	0.011%	Wilmottiaceae	1	0.001%
Oscillatoriales_o	169	0.014%	Stigonemataceae	11	0.003%			
Pseudanabaenaceae	52	0.004%	Rivulariaceae	7	0.002%			
Prochlorococcaceae	41	0.003%	Chroococcaceae	6	0.001%			
Rivulariaceae	28	0.002%	Aphanizomenonaceae	5	0.001%			
Pleurocapsaceae	20	0.002%	Prochlorococcaceae	3	0.001%			
Microcystaceae	19	0.002%	Microcystaceae	1	0.000%			
Aphanizomenonaceae	12	0.001%						

Nodosilineaceae	10	0.001%
Wilmottiaceae	9	0.001%
Chroococcaceae	6	0.001%
Oscillatoriaceae	3	0.000%

Marble			Moraine Dry Valley			Moraine Yûboku Valley		
Family	**n. reads**	**% reads**	**Family**	**n. reads**	**% reads**	**Family**	**n. reads**	**% reads**
Chroococcidiopsidaceae	236757	73.833%	Gomontiellaceae	152575	91.769%	Oculatellaceae	70462	51.028%
Cyanothecaceae	39606	12.351%	Cyanothecaceae	9773	5.878%	Leptolyngbyaceae	37391	27.078%
Cyanophyceae_c	30613	9.547%	Chroococcidiopsidaceae	1816	1.092%	Gomontiellaceae	15456	11.193%
Cyanobacteriota_p	6509	2.030%	Gomontiellales	825	0.496%	Chamaesiphonaceae	6572	4.759%
Leptolyngbyaceae	5418	1.690%	Nostocaceae	543	0.327%	Cyanophyceae_c	4857	3.517%
Oculatellaceae	1005	0.313%	Leptolyngbyaceae	335	0.201%	Cymatolegaceae	1954	1.415%
Tolypothrichaceae	458	0.143%	Oculatellaceae	132	0.079%	Microcoleaceae	410	0.297%
Nostocales_o	78	0.024%	Cymatolegaceae	69	0.042%	Cyanothecaceae	309	0.224%
Gomontiellaceae	60	0.019%	Microcoleaceae	52	0.031%	Nostocaceae	283	0.205%
Nostocaceae	44	0.014%	Cyanophyceae_c	43	0.026%	Leptolyngbyales	216	0.156%
Chamaesiphonaceae	32	0.010%	Prochlorococcaceae	19	0.011%	Gomontiellales_o	93	0.067%
Microcoleaceae	23	0.007%	Nostocales_o	14	0.008%	Pseudanabaenaceae	36	0.026%
Rivulariaceae	21	0.007%	Microcystaceae	13	0.008%	Cyanobacteriota_p	14	0.010%
Pseudanabaenaceae	16	0.005%	Pleurocapsaceae	13	0.008%	Chroococcidiopsidaceae	12	0.009%
Prochlorococcaceae	10	0.003%	Chamaesiphonaceae	10	0.006%	Prochlorococcaceae	8	0.006%
Wilmottiaceae	4	0.001%	Nodosilineaceae	10	0.006%	Pleurocapsaceae	6	0.004%
Aphanizomenonaceae	3	0.001%	Tolypothrichaceae	6	0.004%	Microcystaceae	4	0.003%
Gomontiellales_o	3	0.001%	Wilmottiaceae	4	0.002%	Aphanizomenonaceae	1	0.001%
Microcystaceae	1	0.000%	Aphanizomenonaceae	2	0.001%	Oscillatoriaceae	1	0.001%
Oscillatoriaceae	1	0.000%	Cyanobacteriota_p	2	0.001%	Tolypothrichaceae	1	0.001%
Pleurocapsaceae	1	0.000%	Leptolyngbyales_o	2	0.001%			
Stigonemataceae	1	0.000%	Oscillatoriaceae	1	0.001%			
			Oscillatoriales_o	1	0.001%			

Moraine Austkampane		
Family	**n. reads**	**% reads**
Microcoleaceae	147	81.215%
Leptolyngbyaceae	14	7.735%
Cyanothecaceae_c	7	3.867%
Chroococcidiopsidaceae	5	2.762%
Oculatellaceae	3	1.657%
Nostocaceae	2	1.105%
Aphanizomenonaceae	1	0.552%
Nostocales_o	1	0.552%
Tolypothrichaceae	1	0.552%

Table S3.6. Genus taxonomic assignment of the OTUs with cumulative abundance calculated for each substrate type. *When the genus was unclassified, the higher taxonomic assignation was indicated: "_p": Phylum; "_c": Class; "_o ": Order; "_f": Family.*

All substrate types			Granite			Gneis		
Family	**# reads**	**% reads**	**Family**	**# reads**	**% reads**	**Family**	**# reads**	**% reads**
Aliterella	214579	18.302%	*Phormidesmis*	60149	14.169%	*Cyanothece*	107478	87.571%
Cyanothece	210719	17.973%	*Cyanothece*	53546	12.614%	*Tychonema*	2899	2.362%
Hormoscilla	176804	15.080%	*Hormoscilla*	36913	8.695%	*Hormoscilla*	2349	1.914%
Phormidesmis	68519	5.844%	*Nostoc*	36837	8.678%	*Aliterella*	1970	1.605%
Timaviella	59661	5.089%	Microcoleaceae_f	34084	8.029%	Cyanophyceae_c	1449	1.181%
Cyanophyceae_c	56158	4.790%	*Heteroleibleinia*	33714	7.942%	Cyanobacteriota_p	1174	0.957%
Oculatellaceae_f	55134	4.703%	*Timaviella*	28168	6.635%	*Phormidesmis*	856	0.697%
Crinalium	42386	3.615%	Nostocales_o	20624	4.858%	*Heteroleibleinia*	820	0.668%
Nostoc	37712	3.217%	Cyanophyceae_c	19196	4.522%	*Microcoleus*	643	0.524%
Heteroleibleinia	34607	2.952%	*Toxopsis*	18547	4.369%	*Cymatolege*	625	0.509%
Microcoleaceae	34458	2.939%	Oculatellaceae_f	17529	4.129%	Gomontiellales_o	598	0.487%

All substrate types			Granite			Gneis		
Family	**# reads**	**% reads**	**Family**	**# reads**	**% reads**	**Family**	**# reads**	**% reads**
Leptolyngbyaceae_f	36157	3.084%	*Crinalium*	13878	3.269%	*Chamaesiphon*	433	0.353%
Chroococcidiopsidaceae_f	22564	1.925%	*Tychonema*	11743	2.766%	Gomontiellaceae_f	373	0.304%
Nostocales_o	20757	1.770%	*Aliterella*	8859	2.087%	*Timaviella*	203	0.165%
Toxopsis	18727	1.597%	*Chamaesiphon*	6795	1.601%	*Stenomitos*	198	0.161%
Tychonema	14778	1.260%	Tolypothrichaceae_f	6767	1.594%	*Stigonema*	172	0.140%
Chamaesiphon	13842	1.181%	Gomontiellaceae_f	5878	1.385%	*Toxopsis*	168	0.137%
Chroococcidiopsidaceae_f	13387	1.142%	*Microcoleus*	2804	0.661%	Chroococcidiopsidaceae_f	94	0.077%
Cyanobacteriota_p	8473	0.723%	Leptolyngbyaceae_f	1764	0.416%	Microcoleaceae_f	63	0.051%
Gomontiellaceae_f	8326	0.710%	Gomontiellales_o	1664	0.392%	Tolypothrichaceae_f	63	0.051%
Tolypothrichaceae_f	7284	0.621%	*Stenomitos*	1408	0.332%	Nostocales_o	40	0.033%
Microcoleus	3626	0.309%	Chroococcidiopsidaceae_f	1285	0.303%	*Crinalium*	34	0.028%
Gomontiellales_o	3183	0.271%	Cyanobacteriota_p	774	0.182%	Leptolyngbyaceae_f	12	0.010%
Cymatolege	3020	0.258%	*Cymatolege*	372	0.088%	*Nostoc*	6	0.005%
Shackletoniella	1739	0.148%	Nodosilineales_o	285	0.067%	*Sorospora*	5	0.004%
Stenomitos	1624	0.139%	Nostocaceae_f	205	0.048%	*Dactylothamnos*	4	0.003%
Oculatellaceae_f	1092	0.093%	*Dactylothamnos*	174	0.041%	*Anagnostidinema*	1	0.001%
Apatinema	1041	0.089%	Oscillatoriales_o	168	0.040%	Oculatellaceae_f	1	0.001%
Nodosilineales_o	285	0.024%	Oculatellaceae_f	124	0.029%	Prochlorococcaceae_f	1	0.001%
Compactococcus	268	0.023%	*Sorospora*	117	0.028%	*Shackletoniella*	1	0.001%
Leptolyngbyales_o	266	0.023%	Leptolyngbyales_f	65	0.015%			
Nostocaceae_f	208	0.018%	*Myxacorys*	25	0.006%			
Stigonema	184	0.016%	*Speos*	13	0.003%			
Dactylothamnos	178	0.015%	*Stigonema*	11	0.003%			
Oscillatoriales_o	169	0.014%	*Macrochaete*	7	0.002%			
Speos	149	0.013%	*Inacoccus*	6	0.001%			
Sorospora	122	0.010%	*Dolichospermum*	5	0.001%			

All substrate types			Granite		
Family	**# reads**	**% reads**	**Family**	**# reads**	**% reads**
Pseudanabaenaceae_f	47	0.004%	Prochlorococcaceae_f	3	0.001%
Prochlorococcaceae_f	41	0.003%	*Microcystis*	1	0.000%
Macrochaete	28	0.002%	*Shackletoniella*	1	0.000%
Myxacorys	25	0.002%			
Dermocarpella	20	0.002%			
Microcystis	19	0.002%			
Dolichospermum	12	0.001%			
Plectolyngbya	12	0.001%			
Nodosilinea	10	0.001%			
Anagnostidinema	9	0.001%			
Inacoccus	6	0.001%			
Limnospira	6	0.001%			
Pseudanabaena	5	0.000%			
Drouetiella	3	0.000%			
Laspinema	3	0.000%			

Marble			Moraine Dry Valley			Moraine Yûboku Valley		
Family	**# reads**	**% reads**	**Family**	**# reads**	**% reads**	**Family**	**# reads**	**% reads**
Aliterella	201940	62.976%	*Hormoscilla*	123214	74.109%	Oculatellaceae_f	36661	26.549%
Cyanothece	39606	12.351%	*Crinalium*	27896	16.779%	Leptolyngbyaceae_f	33928	24.570%
Chroococcidiopsidaceae_f	34549	10.774%	*Cyanothece*	9773	5.878%	*Timaviella*	31100	22.522%
Cyanophyceae_c	30613	9.547%	*Aliterella*	1794	1.079%	*Hormoscilla*	14281	10.342%
Cyanobacteriota_p	6509	2.030%	Gomontiellaceae_f	1465	0.881%	*Chamaesiphon*	6572	4.759%
Phormidesmis	5190	1.619%	Gomontiellales_o	825	0.496%	Cyanophyceae_c	4857	3.517%
Oculatellaceae_f	932	0.291%	*Nostoc*	541	0.325%	*Phormidesmis*	2304	1.669%
Tolypothrichaceae_f	450	0.140%	Leptolyngbyaceae_f	277	0.167%	*Cymatolege*	1954	1.415%
Compactococcus	268	0.084%	*Timaviella*	119	0.072%	*Shackletoniella*	1733	1.255%

Marble			Moraine Dry Valley			Moraine Yûboku Valley		
Family	**# reads**	**% reads**	**Family**	**# reads**	**% reads**	**Family**	**# reads**	**% reads**
Leptolyngbyaceae_f	158	0.049%	*Cymatolege*	69	0.042%	*Apatinema*	1005	0.728%
Nostocales_o	78	0.024%	Microcoleaceae_f	46	0.028%	Oculatellaceae_f	968	0.701%
Timaviella	71	0.022%	Cyanophyceae_c	43	0.026%	Gomontiellaceae_f	606	0.439%
Heteroleibleinia	56	0.017%	*Apatinema*	35	0.021%	*Crinalium*	569	0.412%
Hormoscilla	47	0.015%	Chroococcidiopsidaceae_f	22	0.013%	*Cyanothece*	309	0.224%
Nostoc	44	0.014%	Prochlorococcaceae_f	19	0.011%	*Nostoc*	282	0.204%
Chamaesiphon	32	0.010%	Nostocales_o	14	0.008%	Microcoleaceae_f	229	0.166%
Macrochaete	21	0.007%	*Dermocarpella*	13	0.008%	Leptolyngbyales_o	216	0.156%
Pseudanabaenaceae_f	16	0.005%	*Microcystis*	13	0.008%	*Speos*	136	0.098%
Stenomitos	13	0.004%	*Heteroleibleinia*	11	0.007%	*Tychonema*	127	0.092%
Microcoleaceae_f	12	0.004%	*Phormidesmis*	11	0.007%	Gomontiellales_o	93	0.067%
Prochlorococcaceae_f	10	0.003%	*Chamaesiphon*	10	0.006%	*Microcoleus*	54	0.039%
Crinalium	9	0.003%	*Nodosilinea*	10	0.006%	Pseudanabaenaceae_f	31	0.022%
Toxopsis	8	0.002%	Oculatellaceae_f	9	0.005%	Cyanobacteriota_p	14	0.010%
Tychonema	6	0.002%	*Anagnostidinema*	4	0.002%	*Aliterella*	12	0.009%
Microcoleus	5	0.002%	*Drouetiella*	3	0.002%	*Plectolyngbya*	12	0.009%
Anagnostidinema	4	0.001%	*Microcoleus*	3	0.002%	Prochlorococcaceae_f	8	0.006%
Gomontiellaceae_f	4	0.001%	*Tolypothrichaceae*	3	0.002%	*Dermocarpella*	6	0.004%
Dolichospermum	3	0.001%	*Toxopsis*	3	0.002%	*Pseudanabaena*	5	0.004%
Gomontiellales_o	3	0.001%	*Tychonema*	3	0.002%	*Microcystis*	4	0.003%
Shackletoniella	2	0.001%	Cyanobacteriot_p	2	0.001%	*Heteroleibleinia*	3	0.002%
Apatinema	1	0.000%	*Dolichospermum*	2	0.001%	*Stenomitos*	3	0.002%
Dermocarpella	1	0.000%	Leptolyngbyales_o	2	0.001%	*Dolichospermum*	1	0.001%
Laspinema	1	0.000%	Nostocaceae_f	2	0.001%	*Laspinema*	1	0.001%
Microcystis	1	0.000%	*Laspinema*	1	0.001%	Nostocaceae_f	1	0.001%
Stigonema	1	0.000%	Oscillatoriales_o	1	0.001%	*Toxopsis*	1	0.001%
			Shackletoniella	1	0.001%			

Moraine Austkampane		
Family	**# reads**	**% reads**
Microcoleus	117	64.641%
Microcoleaceae	24	13.260%
Phormidesmis	9	4.972%
Cyanothece	7	3.867%
Limnospira	6	3.315%
Aliterella	4	2.210%
Heteroleibleinia	3	1.657%
Nostoc	2	1.105%
Oculatellaceae_f	2	1.105%
Chroococcidiopsidaceae_f	1	0.552%
Dolichospermum	1	0.552%
Leptolyngbyaceae_f	1	0.552%
Nostocales_o	1	0.552%
Shackletoniella	1	0.552%
Stenomitos	1	0.552%
Tolypothrichaceae	1	0.552%

Table S3.7 Indicator species analysis results per substrate type. *Mo_YO = moraines of Yûboku Valley; mo_AU = moraines of Austkampane.*

	OTU	stat.	p-value		taxonomy
granite	OTU_921	0.716	0.019	*	k__Bacteria; p__Cyanobacteriota; c__Cyanophyceae; o__Nostocales; f__NA; g__NA
	OTU_521	0.694	0.018	*	k__Bacteria; p__Cyanobacteriota; c__Cyanophyceae; o__Nostocales; f__Tolypothrichaceae; g__Toxopsis
	OTU_289	0.675	0.022	*	k__Bacteria; p__Cyanobacteriota; c__Cyanophyceae; o__Nostocales; f__NA; g__NA
	OTU_2849	0.663	0.019	*	k__Bacteria; p__Cyanobacteriota; c__Cyanophyceae; o__Oculatellales; f__Oculatellaceae; g__Timaviella
	OTU_633	0.663	0.021	*	k__Bacteria; p__Cyanobacteriota; c__Cyanophyceae; o__Nostocales; f__NA; g__NA
	OTU_1297	0.657	0.022	*	k__Bacteria; p__Cyanobacteriota; c__Cyanophyceae; o__Nostocales; f__NA; g__NA
	OTU_661	0.65	0.017	*	k__Bacteria; p__Cyanobacteriota; c__Cyanophyceae; o__Nostocales; f__Tolypothrichaceae; g__Toxopsis
	OTU_2151	0.642	0.03	*	k__Bacteria; p__Cyanobacteriota; c__Cyanophyceae; o__NA; f__NA; g__NA
	OTU_4154	0.637	0.02	*	k__Bacteria; p__Cyanobacteriota; c__Cyanophyceae; o__Oculatellales; f__Oculatellaceae; g__Timaviella
	OTU_951	0.633	0.023	*	k__Bacteria; p__Cyanobacteriota; c__Cyanophyceae; o__Oculatellales; f__Oculatellaceae; g__Timaviella
	OTU_974	0.632	0.022	*	k__Bacteria; p__Cyanobacteriota; c__Cyanophyceae; o__Nostocales; f__NA; g__NA
	OTU_4085	0.632	0.024	*	k__Bacteria; p__Cyanobacteriota; c__Cyanophyceae; o__Nostocales; f__Nostocaceae; g__NA
	OTU_279	0.63	0.026	*	k__Bacteria; p__Cyanobacteriota; c__Cyanophyceae; o__Nostocales; f__NA; g__NA
	OTU_2175	0.627	0.022	*	k__Bacteria; p__Cyanobacteriota; c__Cyanophyceae; o__Nostocales; f__NA; g__NA
	OTU_2890	0.62	0.017	*	k__Bacteria; p__Cyanobacteriota; c__Cyanophyceae; o__Nostocales; f__NA; g__NA
	OTU_317	0.62	0.026	*	k__Bacteria; p__Cyanobacteriota; c__Cyanophyceae; o__NA; f__NA; g__NA
	OTU_1190	0.603	0.024	*	k__Bacteria; p__Cyanobacteriota; c__Cyanophyceae; o__Nostocales; f__NA; g__NA
	OTU_2399	0.601	0.029	*	k__Bacteria; p__Cyanobacteriota; c__Cyanophyceae; o__Nostocales; f__NA; g__NA
	OTU_3373	0.599	0.036	*	k__Bacteria; p__Cyanobacteriota; c__Cyanophyceae; o__Nostocales; f__NA; g__NA
	OTU_1171	0.588	0.037	*	k__Bacteria; p__Cyanobacteriota; c__Cyanophyceae; o__Oscillatoriales; f__Microcoleaceae; g__NA
	OTU_3793	0.588	0.039	*	k__Bacteria; p__Cyanobacteriota; c__Cyanophyceae; o__Oscillatoriales; f__Microcoleaceae; g__NA
	OTU_2833	0.575	0.047	*	k__Bacteria; p__Cyanobacteriota; c__Cyanophyceae; o__Oculatellales; f__Oculatellaceae; g__Timaviella
	OTU_1892	0.568	0.048	*	k__Bacteria; p__Cyanobacteriota; c__Cyanophyceae; o__Nostocales; f__Tolypothrichaceae; g__Toxopsis
marble	OTU_1987	0.632	0.009	**	k__Bacteria; p__Cyanobacteriota; c__Cyanophyceae; o__Chroococcidiopsidales; f__Chroococcidiopsidaceae; g__Aliterella
	OTU_1048	0.614	0.024	*	k__Bacteria; p__Cyanobacteriota; c__Cyanophyceae; o__Chroococcidiopsidales; f__Chroococcidiopsidaceae; g__Aliterella
	OTU_1178	0.598	0.03	*	k__Bacteria; p__Cyanobacteriota; c__Cyanophyceae; o__Chroococcidiopsidales; f__Chroococcidiopsidaceae; g__Aliterella
	OTU_1708	0.592	0.05	*	k__Bacteria; p__Cyanobacteriota; c__Cyanophyceae; o__Chroococcidiopsidales; f__Chroococcidiopsidaceae; g__Aliterella

	OTU	stat.	p-value		taxonomy
gneiss	OTU_20	0.696	0.006	**	k__Bacteria; p__Cyanobacteriota; c__Cyanophyceae; o__Gomontiellales; f__Chamaesiphonaceae; g__Chamaesiphon
	OTU_127	0.682	0.011	*	k__Bacteria; p__Cyanobacteriota; c__Cyanophyceae; o__NA; f__NA; g__NA
	OTU_1014	0.681	0.011	*	k__Bacteria; p__Cyanobacteriota; c__Cyanophyceae; o__Chroococcidiopsidales; f__Chroococcidiopsidaceae; g__Aliterella
	OTU_2693	0.572	0.042	*	k__Bacteria; p__Cyanobacteriota; c__Cyanophyceae; o__Gomontiellales; f__Cyanothecaceae; g__Cyanothece
	OTU_2691	0.568	0.05	*	k__Bacteria; p__Cyanobacteriota; c__Cyanophyceae; o__NA; f__NA; g__NA
mo_YO	OTU_439	0.96	0.001	***	k__Bacteria; p__Cyanobacteriota; c__Cyanophyceae; o__Gomontiellales; f__Chamaesiphonaceae; g__Chamaesiphon
	OTU_919	0.894	0.001	***	k__Bacteria; p__Cyanobacteriota; c__Cyanophyceae; o__Leptolyngbyales; f__Leptolyngbyaceae; g__Leptolyngbyaceae_XXXXXX
	OTU_1443	0.882	0.004	**	k__Bacteria; p__Cyanobacteriota; c__Cyanophyceae; o__Leptolyngbyales; f__Leptolyngbyaceae; g__Leptolyngbyaceae_XXXXXX
	OTU_56	0.874	0.002	**	k__Bacteria; p__Cyanobacteriota; c__Cyanophyceae; o__Leptolyngbyales; f__Leptolyngbyaceae; g__Phormidesmis
	OTU_3500	0.856	0.003	**	k__Bacteria; p__Cyanobacteriota; c__Cyanophyceae; o__Gomontiellales; f__Chamaesiphonaceae; g__Chamaesiphon
	OTU_79	0.824	0.003	**	k__Bacteria; p__Cyanobacteriota; c__Cyanophyceae; o__Gomontiellales; f__Chamaesiphonaceae; g__Chamaesiphon
	OTU_3096	0.784	0.008	**	k__Bacteria; p__Cyanobacteriota; c__Cyanophyceae; o__Oscillatoriales; f__Microcoleaceae; g__Tychonema
	OTU_1225	0.775	0.001	***	k__Bacteria; p__Cyanobacteriota; c__Cyanophyceae; o__NA; f__NA; g__NA
	OTU_1311	0.775	0.001	***	k__Bacteria; p__Cyanobacteriota; c__Cyanophyceae; o__Oculatellales; f__Oculatellaceae; g__Timaviella
	OTU_1315	0.775	0.001	***	k__Bacteria; p__Cyanobacteriota; c__Cyanophyceae; o__Oculatellales; f__Oculatellaceae; g__Timaviella
	OTU_1328	0.775	0.001	***	k__Bacteria; p__Cyanobacteriota; c__Cyanophyceae; o__Oculatellales; f__Oculatellaceae; g__Timaviella
	OTU_1543	0.775	0.001	***	k__Bacteria; p__Cyanobacteriota; c__Cyanophyceae; o__Oculatellales; f__Oculatellaceae; g__Timaviella
	OTU_1677	0.775	0.001	***	k__Bacteria; p__Cyanobacteriota; c__Cyanophyceae; o__NA; f__NA; g__NA
	OTU_1684	0.775	0.001	***	k__Bacteria; p__Cyanobacteriota; c__Cyanophyceae; o__Oculatellales; f__Oculatellaceae; g__Timaviella
	OTU_1711	0.775	0.001	***	k__Bacteria; p__Cyanobacteriota; c__Cyanophyceae; o__Leptolyngbyales; f__Leptolyngbyaceae; g__Leptolyngbyaceae_XXXXXX
	OTU_183	0.775	0.001	***	k__Bacteria; p__Cyanobacteriota; c__Cyanophyceae; o__Leptolyngbyales; f__Leptolyngbyaceae; g__Phormidesmis
	OTU_1850	0.775	0.001	***	k__Bacteria; p__Cyanobacteriota; c__Cyanophyceae; o__Leptolyngbyales; f__Leptolyngbyaceae; g__Leptolyngbyaceae_XXXXXX
	OTU_1914	0.775	0.001	***	k__Bacteria; p__Cyanobacteriota; c__Cyanophyceae; o__Leptolyngbyales; f__Leptolyngbyaceae; g__Leptolyngbyaceae_XXXXXX
	OTU_204	0.775	0.001	***	k__Bacteria; p__Cyanobacteriota; c__Cyanophyceae; o__Leptolyngbyales; f__Leptolyngbyaceae; g__Speos
	OTU_217	0.775	0.001	***	k__Bacteria; p__Cyanobacteriota; c__Cyanophyceae; o__NA; f__NA; g__NA
	OTU_2369	0.775	0.001	***	k__Bacteria; p__Cyanobacteriota; c__Cyanophyceae; o__Oculatellales; f__Oculatellaceae; g__Timaviella
	OTU_2767	0.775	0.001	***	k__Bacteria; p__Cyanobacteriota; c__Cyanophyceae; o__Leptolyngbyales; f__Leptolyngbyaceae; g__Leptolyngbyaceae_XXXXXX
	OTU_3000	0.775	0.001	***	k__Bacteria; p__Cyanobacteriota; c__Cyanophyceae; o__Oculatellales; f__Oculatellaceae; g__Timaviella

	OTU	stat.	p-value		taxonomy
mo_YO	OTU_3795	0.775	0.001	***	k__Bacteria; p__Cyanobacteriota; c__Cyanophyceae; o__Oculatellales; f__Oculatellaceae; g__Timaviella
	OTU_3842	0.775	0.001	***	k__Bacteria; p__Cyanobacteriota; c__Cyanophyceae; o__Leptolyngbyales; f__Leptolyngbyaceae; g__Phormidesmis
	OTU_3859	0.775	0.001	***	k__Bacteria; p__Cyanobacteriota; c__Cyanophyceae; o__Leptolyngbyales; f__Leptolyngbyaceae; g__Leptolyngbyaceae_XXXXXX
	OTU_4200	0.775	0.001	***	k__Bacteria; p__Cyanobacteriota; c__Cyanophyceae; o__Leptolyngbyales; f__Leptolyngbyaceae; g__Leptolyngbyaceae_XXXXXX
	OTU_4274	0.775	0.001	***	k__Bacteria; p__Cyanobacteriota; c__Cyanophyceae; o__NA; f__NA; g__NA
	OTU_4345	0.775	0.001	***	k__Bacteria; p__Cyanobacteriota; c__Cyanophyceae; o__Oculatellales; f__Oculatellaceae; g__Timaviella
	OTU_4348	0.775	0.001	***	k__Bacteria; p__Cyanobacteriota; c__Cyanophyceae; o__NA; f__NA; g__NA
	OTU_612	0.775	0.001	***	k__Bacteria; p__Cyanobacteriota; c__Cyanophyceae; o__NA; f__NA; g__NA
	OTU_772	0.775	0.001	***	k__Bacteria; p__Cyanobacteriota; c__Cyanophyceae; o__Oculatellales; f__Oculatellaceae; g__Timaviella
	OTU_805	0.775	0.001	***	k__Bacteria; p__Cyanobacteriota; c__Cyanophyceae; o__Leptolyngbyales; f__Leptolyngbyaceae; g__NA
	OTU_964	0.775	0.001	***	k__Bacteria; p__Cyanobacteriota; c__Cyanophyceae; o__Leptolyngbyales; f__Leptolyngbyaceae; g__Leptolyngbyaceae_XXXXXX
	OTU_196	0.767	0.003	**	k__Bacteria; p__Cyanobacteriota; c__Cyanophyceae; o__NA; f__NA; g__NA
	OTU_1272	0.767	0.001	***	k__Bacteria; p__Cyanobacteriota; c__Cyanophyceae; o__NA; f__NA; g__NA
	OTU_563	0.765	0.002	**	k__Bacteria; p__Cyanobacteriota; c__Cyanophyceae; o__Oculatellales; f__Oculatellaceae; g__Timaviella
	OTU_1255	0.765	0.002	**	k__Bacteria; p__Cyanobacteriota; c__Cyanophyceae; o__Leptolyngbyales; f__Leptolyngbyaceae; g__NA
	OTU_3129	0.764	0.001	***	k__Bacteria; p__Cyanobacteriota; c__Cyanophyceae; o__NA; f__NA; g__NA
	OTU_3014	0.762	0.003	**	k__Bacteria; p__Cyanobacteriota; c__Cyanophyceae; o__NA; f__NA; g__NA
	OTU_790	0.762	0.001	***	k__Bacteria; p__Cyanobacteriota; c__Cyanophyceae; o__NA; f__NA; g__NA
	OTU_3740	0.761	0.001	***	k__Bacteria; p__Cyanobacteriota; c__Cyanophyceae; o__Oculatellales; f__Oculatellaceae; g__Timaviella
	OTU_493	0.76	0.001	***	k__Bacteria; p__Cyanobacteriota; c__Cyanophyceae; o__Leptolyngbyales; f__Leptolyngbyaceae; g__Leptolyngbyaceae_XXXXXX
	OTU_1864	0.758	0.003	**	k__Bacteria; p__Cyanobacteriota; c__Cyanophyceae; o__Leptolyngbyales; f__NA; g__NA
	OTU_611	0.755	0.003	**	k__Bacteria; p__Cyanobacteriota; c__Cyanophyceae; o__Oculatellales; f__Oculatellaceae; g__Timaviella
	OTU_1546	0.755	0.003	**	k__Bacteria; p__Cyanobacteriota; c__Cyanophyceae; o__Oculatellales; f__Oculatellaceae; g__Timaviella
	OTU_280	0.753	0.003	**	k__Bacteria; p__Cyanobacteriota; c__Cyanophyceae; o__Oculatellales; f__Oculatellaceae; g__Timaviella
	OTU_192	0.753	0.016	*	k__Bacteria; p__Cyanobacteriota; c__Cyanophyceae; o__Oscillatoriales; f__Microcoleaceae; g__NA
	OTU_942	0.749	0.001	***	k__Bacteria; p__Cyanobacteriota; c__Cyanophyceae; o__Oculatellales; f__Oculatellaceae; g__Oculatellaceae_XX
	OTU_237	0.741	0.003	**	k__Bacteria; p__Cyanobacteriota; c__Cyanophyceae; o__Oculatellales; f__Oculatellaceae; g__Timaviella
	OTU_1263	0.716	0.003	**	k__Bacteria; p__Cyanobacteriota; c__Cyanophyceae; o__NA; f__NA; g__NA

	OTU	stat.	p-value		taxonomy
mo_YO	OTU_96	0.705	0.003	**	k__Bacteria; p__Cyanobacteriota; c__Cyanophyceae; o__Oculatellales; f__Oculatellaceae; g__Timaviella
	OTU_2696	0.699	0.008	**	k__Bacteria; p__Cyanobacteriota; c__Cyanophyceae; o__Oculatellales; f__Oculatellaceae; g__Timaviella
	OTU_1002	0.632	0.044	*	k__Bacteria; p__Cyanobacteriota; c__Cyanophyceae; o__Leptolyngbyales; f__Leptolyngbyaceae; g__Leptolyngbyaceae_XXXXXX
	OTU_1009	0.632	0.038	*	k__Bacteria; p__Cyanobacteriota; c__Cyanophyceae; o__NA; f__NA; g__NA
	OTU_1024	0.632	0.038	*	k__Bacteria; p__Cyanobacteriota; c__Cyanophyceae; o__Oculatellales; f__Oculatellaceae; g__Timaviella
	OTU_1029	0.632	0.038	*	k__Bacteria; p__Cyanobacteriota; c__Cyanophyceae; o__Oculatellales; f__Oculatellaceae; g__Timaviella
	OTU_1035	0.632	0.038	*	k__Bacteria; p__Cyanobacteriota; c__Cyanophyceae; o__Oculatellales; f__Oculatellaceae; g__Oculatellaceae_XX
	OTU_1085	0.632	0.038	*	k__Bacteria; p__Cyanobacteriota; c__Cyanophyceae; o__NA; f__NA; g__NA
	OTU_1097	0.632	0.038	*	k__Bacteria; p__Cyanobacteriota; c__Cyanophyceae; o__Oculatellales; f__Oculatellaceae; g__Oculatellaceae_XX
	OTU_1106	0.632	0.042	*	k__Bacteria; p__Cyanobacteriota; c__NA; o__NA; f__NA; g__NA
	OTU_1187	0.632	0.038	*	k__Bacteria; p__Cyanobacteriota; c__Cyanophyceae; o__Oculatellales; f__Oculatellaceae; g__Timaviella
	OTU_1228	0.632	0.042	*	k__Bacteria; p__Cyanobacteriota; c__Cyanophyceae; o__NA; f__NA; g__NA
	OTU_1291	0.632	0.04	*	k__Bacteria; p__Cyanobacteriota; c__Cyanophyceae; o__NA; f__NA; g__NA
	OTU_1314	0.632	0.038	*	k__Bacteria; p__Cyanobacteriota; c__Cyanophyceae; o__Oculatellales; f__Oculatellaceae; g__Oculatellaceae_XX
	OTU_1415	0.632	0.04	*	k__Bacteria; p__Cyanobacteriota; c__Cyanophyceae; o__Oculatellales; f__Oculatellaceae; g__Timaviella
	OTU_1453	0.632	0.038	*	k__Bacteria; p__Cyanobacteriota; c__Cyanophyceae; o__Oculatellales; f__Oculatellaceae; g__Timaviella
	OTU_1457	0.632	0.038	*	k__Bacteria; p__Cyanobacteriota; c__Cyanophyceae; o__Leptolyngbyales; f__Leptolyngbyaceae; g__Leptolyngbyaceae_XXXXXX
	OTU_1471	0.632	0.038	*	k__Bacteria; p__Cyanobacteriota; c__Cyanophyceae; o__Oculatellales; f__Oculatellaceae; g__Timaviella
	OTU_1481	0.632	0.038	*	k__Bacteria; p__Cyanobacteriota; c__Cyanophyceae; o__Oculatellales; f__Oculatellaceae; g__Oculatellaceae_XX
	OTU_1491	0.632	0.038	*	k__Bacteria; p__Cyanobacteriota; c__Cyanophyceae; o__NA; f__NA; g__NA
	OTU_1510	0.632	0.038	*	k__Bacteria; p__Cyanobacteriota; c__Cyanophyceae; o__Oculatellales; f__Oculatellaceae; g__Timaviella
	OTU_1544	0.632	0.038	*	k__Bacteria; p__Cyanobacteriota; c__Cyanophyceae; o__Oculatellales; f__Oculatellaceae; g__Timaviella
	OTU_1581	0.632	0.038	*	k__Bacteria; p__Cyanobacteriota; c__Cyanophyceae; o__Oculatellales; f__Oculatellaceae; g__Oculatellaceae_XX
	OTU_1654	0.632	0.038	*	k__Bacteria; p__Cyanobacteriota; c__Cyanophyceae; o__Gomontiellales; f__Chamaesiphonaceae; g__Chamaesiphon
	OTU_1669	0.632	0.038	*	k__Bacteria; p__Cyanobacteriota; c__Cyanophyceae; o__Oculatellales; f__Oculatellaceae; g__Timaviella
	OTU_1675	0.632	0.038	*	k__Bacteria; p__Cyanobacteriota; c__Cyanophyceae; o__Oculatellales; f__Oculatellaceae; g__Timaviella
	OTU_1738	0.632	0.038	*	k__Bacteria; p__Cyanobacteriota; c__Cyanophyceae; o__Oculatellales; f__Oculatellaceae; g__Timaviella
	OTU_1759	0.632	0.038	*	k__Bacteria; p__Cyanobacteriota; c__Cyanophyceae; o__Oculatellales; f__Oculatellaceae; g__Oculatellaceae_XX

	OTU	stat.	p-value		taxonomy
mo_YO	OTU_1772	0.632	0.042	*	k__Bacteria; p__Cyanobacteriota; c__Cyanophyceae; o__Oculatellales; f__Oculatellaceae; g__Timaviella
	OTU_1777	0.632	0.038	*	k__Bacteria; p__Cyanobacteriota; c__Cyanophyceae; o__Oculatellales; f__Oculatellaceae; g__Timaviella
	OTU_1889	0.632	0.038	*	k__Bacteria; p__Cyanobacteriota; c__Cyanophyceae; o__Oculatellales; f__Oculatellaceae; g__Timaviella
	OTU_1894	0.632	0.038	*	k__Bacteria; p__Cyanobacteriota; c__Cyanophyceae; o__Oculatellales; f__Oculatellaceae; g__Oculatellaceae_XX
	OTU_1986	0.632	0.038	*	k__Bacteria; p__Cyanobacteriota; c__Cyanophyceae; o__Oculatellales; f__Oculatellaceae; g__Timaviella
	OTU_2036	0.632	0.038	*	k__Bacteria; p__Cyanobacteriota; c__Cyanophyceae; o__Oculatellales; f__Oculatellaceae; g__Oculatellaceae_XX
	OTU_2040	0.632	0.034	*	k__Bacteria; p__Cyanobacteriota; c__Cyanophyceae; o__Leptolyngbyales; f__Leptolyngbyaceae; g__Leptolyngbyaceae_XXXXXX
	OTU_2043	0.632	0.042	*	k__Bacteria; p__Cyanobacteriota; c__Cyanophyceae; o__Leptolyngbyales; f__Leptolyngbyaceae; g__Leptolyngbyaceae_XXXXXX
	OTU_2044	0.632	0.038	*	k__Bacteria; p__Cyanobacteriota; c__Cyanophyceae; o__NA; f__NA; g__NA
	OTU_2061	0.632	0.038	*	k__Bacteria; p__Cyanobacteriota; c__Cyanophyceae; o__NA; f__NA; g__NA
	OTU_2063	0.632	0.04	*	k__Bacteria; p__Cyanobacteriota; c__Cyanophyceae; o__Leptolyngbyales; f__Leptolyngbyaceae; g__Leptolyngbyaceae_XXXXXX
	OTU_2087	0.632	0.038	*	k__Bacteria; p__Cyanobacteriota; c__Cyanophyceae; o__Oculatellales; f__Oculatellaceae; g__Timaviella
	OTU_2098	0.632	0.038	*	k__Bacteria; p__Cyanobacteriota; c__Cyanophyceae; o__Oculatellales; f__Oculatellaceae; g__Timaviella
	OTU_2110	0.632	0.038	*	k__Bacteria; p__Cyanobacteriota; c__Cyanophyceae; o__Oculatellales; f__Oculatellaceae; g__Timaviella
	OTU_2122	0.632	0.038	*	k__Bacteria; p__Cyanobacteriota; c__Cyanophyceae; o__Oculatellales; f__Oculatellaceae; g__Oculatellaceae_XX
	OTU_2125	0.632	0.038	*	k__Bacteria; p__Cyanobacteriota; c__Cyanophyceae; o__Oculatellales; f__Oculatellaceae; g__Timaviella
	OTU_2148	0.632	0.038	*	k__Bacteria; p__Cyanobacteriota; c__Cyanophyceae; o__Oculatellales; f__Oculatellaceae; g__Oculatellaceae_XX
	OTU_2156	0.632	0.038	*	k__Bacteria; p__Cyanobacteriota; c__Cyanophyceae; o__Oculatellales; f__Oculatellaceae; g__Oculatellaceae_XX
	OTU_2195	0.632	0.033	*	k__Bacteria; p__Cyanobacteriota; c__Cyanophyceae; o__Oculatellales; f__Oculatellaceae; g__Oculatellaceae_XX
	OTU_2217	0.632	0.038	*	k__Bacteria; p__Cyanobacteriota; c__Cyanophyceae; o__Leptolyngbyales; f__Leptolyngbyaceae; g__Leptolyngbyaceae_XXXXXX
	OTU_2218	0.632	0.038	*	k__Bacteria; p__Cyanobacteriota; c__Cyanophyceae; o__Oculatellales; f__Oculatellaceae; g__Timaviella
	OTU_2224	0.632	0.042	*	k__Bacteria; p__Cyanobacteriota; c__Cyanophyceae; o__NA; f__NA; g__NA
	OTU_2245	0.632	0.042	*	k__Bacteria; p__Cyanobacteriota; c__Cyanophyceae; o__Leptolyngbyales; f__Leptolyngbyaceae; g__Phormidesmis
	OTU_2315	0.632	0.038	*	k__Bacteria; p__Cyanobacteriota; c__Cyanophyceae; o__Oculatellales; f__Oculatellaceae; g__Timaviella
	OTU_2353	0.632	0.038	*	k__Bacteria; p__Cyanobacteriota; c__Cyanophyceae; o__Oculatellales; f__Oculatellaceae; g__Oculatellaceae_XX
	OTU_2374	0.632	0.042	*	k__Bacteria; p__Cyanobacteriota; c__NA; o__NA; f__NA; g__NA
	OTU_2398	0.632	0.042	*	k__Bacteria; p__Cyanobacteriota; c__Cyanophyceae; o__NA; f__NA; g__NA
	OTU_2410	0.632	0.038	*	k__Bacteria; p__Cyanobacteriota; c__Cyanophyceae; o__Oculatellales; f__Oculatellaceae; g__Timaviella

	OTU	stat.	p-value		taxonomy
mo_YO	OTU_2420	0.632	0.038	*	k__Bacteria; p__Cyanobacteriota; c__Cyanophyceae; o__Oculatellales; f__Oculatellaceae; g__NA
	OTU_2427	0.632	0.038	*	k__Bacteria; p__Cyanobacteriota; c__Cyanophyceae; o__Oculatellales; f__Oculatellaceae; g__Timaviella
	OTU_2431	0.632	0.038	*	k__Bacteria; p__Cyanobacteriota; c__Cyanophyceae; o__Oculatellales; f__Oculatellaceae; g__Oculatellaceae_XX
	OTU_2443	0.632	0.038	*	k__Bacteria; p__Cyanobacteriota; c__Cyanophyceae; o__Oculatellales; f__Oculatellaceae; g__NA
	OTU_2458	0.632	0.033	*	k__Bacteria; p__Cyanobacteriota; c__Cyanophyceae; o__Oculatellales; f__Oculatellaceae; g__Oculatellaceae_XX
	OTU_2554	0.632	0.038	*	k__Bacteria; p__Cyanobacteriota; c__Cyanophyceae; o__NA; f__NA; g__NA
	OTU_2578	0.632	0.042	*	k__Bacteria; p__Cyanobacteriota; c__Cyanophyceae; o__Leptolyngbyales; f__Leptolyngbyaceae; g__Leptolyngbyaceae_XXXXXX
	OTU_2604	0.632	0.038	*	k__Bacteria; p__Cyanobacteriota; c__Cyanophyceae; o__Oculatellales; f__Oculatellaceae; g__Timaviella
	OTU_2626	0.632	0.04	*	k__Bacteria; p__Cyanobacteriota; c__Cyanophyceae; o__Oculatellales; f__Oculatellaceae; g__Oculatellaceae_XX
	OTU_2661	0.632	0.038	*	k__Bacteria; p__Cyanobacteriota; c__Cyanophyceae; o__Leptolyngbyales; f__Leptolyngbyaceae; g__NA
	OTU_2662	0.632	0.038	*	k__Bacteria; p__Cyanobacteriota; c__Cyanophyceae; o__Oculatellales; f__Oculatellaceae; g__Timaviella
	OTU_2664	0.632	0.038	*	k__Bacteria; p__Cyanobacteriota; c__Cyanophyceae; o__NA; f__NA; g__NA
	OTU_2667	0.632	0.038	*	k__Bacteria; p__Cyanobacteriota; c__Cyanophyceae; o__Oculatellales; f__Oculatellaceae; g__Timaviella
	OTU_277	0.632	0.038	*	k__Bacteria; p__Cyanobacteriota; c__Cyanophyceae; o__Pseudanabaenales; f__Pseudanabaenaceae; g__Pseudanabaenaceae_X
	OTU_2794	0.632	0.042	*	k__Bacteria; p__Cyanobacteriota; c__Cyanophyceae; o__Leptolyngbyales; f__Leptolyngbyaceae; g__Phormidesmis
	OTU_2911	0.632	0.038	*	k__Bacteria; p__Cyanobacteriota; c__Cyanophyceae; o__NA; f__NA; g__NA
	OTU_2953	0.632	0.04	*	k__Bacteria; p__Cyanobacteriota; c__Cyanophyceae; o__Leptolyngbyales; f__Leptolyngbyaceae; g__Leptolyngbyaceae_XXXXXX
	OTU_3010	0.632	0.038	*	k__Bacteria; p__Cyanobacteriota; c__Cyanophyceae; o__NA; f__NA; g__NA
	OTU_3020	0.632	0.038	*	k__Bacteria; p__Cyanobacteriota; c__Cyanophyceae; o__Oculatellales; f__Oculatellaceae; g__Timaviella
	OTU_304	0.632	0.038	*	k__Bacteria; p__Cyanobacteriota; c__Cyanophyceae; o__Oculatellales; f__Oculatellaceae; g__Timaviella
	OTU_3070	0.632	0.038	*	k__Bacteria; p__Cyanobacteriota; c__Cyanophyceae; o__Oculatellales; f__Oculatellaceae; g__Oculatellaceae_XX
	OTU_3072	0.632	0.038	*	k__Bacteria; p__Cyanobacteriota; c__Cyanophyceae; o__Leptolyngbyales; f__Leptolyngbyaceae; g__Leptolyngbyaceae_XXXXXX
	OTU_3081	0.632	0.038	*	k__Bacteria; p__Cyanobacteriota; c__Cyanophyceae; o__NA; f__NA; g__NA
	OTU_3095	0.632	0.038	*	k__Bacteria; p__Cyanobacteriota; c__Cyanophyceae; o__NA; f__NA; g__NA
	OTU_3145	0.632	0.038	*	k__Bacteria; p__Cyanobacteriota; c__Cyanophyceae; o__Oculatellales; f__Oculatellaceae; g__Timaviella
	OTU_3172	0.632	0.038	*	k__Bacteria; p__Cyanobacteriota; c__Cyanophyceae; o__NA; f__NA; g__NA
	OTU_3225	0.632	0.038	*	k__Bacteria; p__Cyanobacteriota; c__Cyanophyceae; o__Oculatellales; f__Oculatellaceae; g__Oculatellaceae_XX
	OTU_3275	0.632	0.038	*	k__Bacteria; p__Cyanobacteriota; c__Cyanophyceae; o__Oculatellales; f__Oculatellaceae; g__Oculatellaceae_XX

	OTU	stat.	p-value		taxonomy
mo_YO	OTU_3334	0.632	0.042	*	k__Bacteria; p__Cyanobacteriota; c__Cyanophyceae; o__NA; f__NA; g__NA
	OTU_3339	0.632	0.038	*	k__Bacteria; p__Cyanobacteriota; c__Cyanophyceae; o__Oculatellales; f__Oculatellaceae; g__Timaviella
	OTU_3341	0.632	0.042	*	k__Bacteria; p__Cyanobacteriota; c__Cyanophyceae; o__Leptolyngbyales; f__NA; g__NA
	OTU_3368	0.632	0.038	*	k__Bacteria; p__Cyanobacteriota; c__Cyanophyceae; o__NA; f__NA; g__NA
	OTU_3375	0.632	0.038	*	k__Bacteria; p__Cyanobacteriota; c__Cyanophyceae; o__NA; f__NA; g__NA
	OTU_3398	0.632	0.038	*	k__Bacteria; p__Cyanobacteriota; c__Cyanophyceae; o__Oculatellales; f__Oculatellaceae; g__Timaviella
	OTU_3451	0.632	0.038	*	k__Bacteria; p__Cyanobacteriota; c__Cyanophyceae; o__Oculatellales; f__Oculatellaceae; g__Oculatellaceae_XX
	OTU_3496	0.632	0.038	*	k__Bacteria; p__Cyanobacteriota; c__Cyanophyceae; o__Oculatellales; f__Oculatellaceae; g__Oculatellaceae_XX
	OTU_3498	0.632	0.033	*	k__Bacteria; p__Cyanobacteriota; c__Cyanophyceae; o__Oculatellales; f__Oculatellaceae; g__Oculatellaceae_XX
	OTU_352	0.632	0.038	*	k__Bacteria; p__Cyanobacteriota; c__Cyanophyceae; o__Oculatellales; f__Oculatellaceae; g__Timaviella
	OTU_353	0.632	0.038	*	k__Bacteria; p__Cyanobacteriota; c__Cyanophyceae; o__Oculatellales; f__Oculatellaceae; g__Oculatellaceae_XX
	OTU_3559	0.632	0.038	*	k__Bacteria; p__Cyanobacteriota; c__Cyanophyceae; o__Oculatellales; f__Oculatellaceae; g__Timaviella
	OTU_3590	0.632	0.04	*	k__Bacteria; p__Cyanobacteriota; c__Cyanophyceae; o__NA; f__NA; g__NA
	OTU_3611	0.632	0.042	*	k__Bacteria; p__Cyanobacteriota; c__Cyanophyceae; o__NA; f__NA; g__NA
	OTU_363	0.632	0.038	*	k__Bacteria; p__Cyanobacteriota; c__Cyanophyceae; o__Oculatellales; f__Oculatellaceae; g__Oculatellaceae_XX
	OTU_3701	0.632	0.042	*	k__Bacteria; p__Cyanobacteriota; c__Cyanophyceae; o__Leptolyngbyales; f__Leptolyngbyaceae; g__Leptolyngbyaceae_XXXXXX
	OTU_3739	0.632	0.038	*	k__Bacteria; p__Cyanobacteriota; c__Cyanophyceae; o__Oculatellales; f__Oculatellaceae; g__Timaviella
	OTU_3762	0.632	0.038	*	k__Bacteria; p__Cyanobacteriota; c__Cyanophyceae; o__Oculatellales; f__Oculatellaceae; g__Timaviella
	OTU_3768	0.632	0.038	*	k__Bacteria; p__Cyanobacteriota; c__Cyanophyceae; o__Oculatellales; f__Oculatellaceae; g__Oculatellaceae_XX
	OTU_3841	0.632	0.038	*	k__Bacteria; p__Cyanobacteriota; c__Cyanophyceae; o__Oculatellales; f__Oculatellaceae; g__Timaviella
	OTU_3843	0.632	0.047	*	k__Bacteria; p__Cyanobacteriota; c__Cyanophyceae; o__Leptolyngbyales; f__Leptolyngbyaceae; g__Leptolyngbyaceae_XXXXXX
	OTU_3868	0.632	0.038	*	k__Bacteria; p__Cyanobacteriota; c__Cyanophyceae; o__NA; f__NA; g__NA
	OTU_3870	0.632	0.042	*	k__Bacteria; p__Cyanobacteriota; c__Cyanophyceae; o__NA; f__NA; g__NA
	OTU_3932	0.632	0.038	*	k__Bacteria; p__Cyanobacteriota; c__Cyanophyceae; o__Oculatellales; f__Oculatellaceae; g__Timaviella
	OTU_3968	0.632	0.038	*	k__Bacteria; p__Cyanobacteriota; c__Cyanophyceae; o__Oculatellales; f__Oculatellaceae; g__Oculatellaceae_XX
	OTU_3970	0.632	0.04	*	k__Bacteria; p__Cyanobacteriota; c__Cyanophyceae; o__NA; f__NA; g__NA
	OTU_4021	0.632	0.038	*	k__Bacteria; p__Cyanobacteriota; c__Cyanophyceae; o__Oculatellales; f__Oculatellaceae; g__Oculatellaceae_XX
	OTU_4086	0.632	0.028	*	k__Bacteria; p__Cyanobacteriota; c__Cyanophyceae; o__Oculatellales; f__Oculatellaceae; g__Timaviella

	OTU	stat.	p-value		taxonomy
mo_YO	OTU_4089	0.632	0.042	*	k__Bacteria; p__Cyanobacteriota; c__Cyanophyceae; o__Oculatellales; f__Oculatellaceae; g__Timaviella
	OTU_409	0.632	0.038	*	k__Bacteria; p__Cyanobacteriota; c__Cyanophyceae; o__Oculatellales; f__Oculatellaceae; g__Timaviella
	OTU_4143	0.632	0.04	*	k__Bacteria; p__Cyanobacteriota; c__Cyanophyceae; o__NA; f__NA; g__NA
	OTU_4164	0.632	0.038	*	k__Bacteria; p__Cyanobacteriota; c__Cyanophyceae; o__Oculatellales; f__Oculatellaceae; g__Shackletoniella
	OTU_4186	0.632	0.038	*	k__Bacteria; p__Cyanobacteriota; c__Cyanophyceae; o__Oculatellales; f__Oculatellaceae; g__Timaviella
	OTU_4197	0.632	0.047	*	k__Bacteria; p__Cyanobacteriota; c__Cyanophyceae; o__Leptolyngbyales; f__Leptolyngbyaceae; g__Leptolyngbyaceae_XXXXXX
	OTU_4264	0.632	0.033	*	k__Bacteria; p__Cyanobacteriota; c__Cyanophyceae; o__Oculatellales; f__Oculatellaceae; g__Shackletoniella
	OTU_4298	0.632	0.038	*	k__Bacteria; p__Cyanobacteriota; c__Cyanophyceae; o__NA; f__NA; g__NA
	OTU_502	0.632	0.038	*	k__Bacteria; p__Cyanobacteriota; c__Cyanophyceae; o__Oculatellales; f__Oculatellaceae; g__Timaviella
	OTU_580	0.632	0.038	*	k__Bacteria; p__Cyanobacteriota; c__Cyanophyceae; o__Oculatellales; f__Oculatellaceae; g__Oculatellaceae_XX
	OTU_592	0.632	0.042	*	k__Bacteria; p__Cyanobacteriota; c__Cyanophyceae; o__Leptolyngbyales; f__Leptolyngbyaceae; g__Leptolyngbyaceae_XXXXXX
	OTU_608	0.632	0.038	*	k__Bacteria; p__Cyanobacteriota; c__Cyanophyceae; o__Oculatellales; f__Oculatellaceae; g__NA
	OTU_622	0.632	0.041	*	k__Bacteria; p__Cyanobacteriota; c__Cyanophyceae; o__Leptolyngbyales; f__Leptolyngbyaceae; g__Leptolyngbyaceae_XXXXXX
	OTU_651	0.632	0.038	*	k__Bacteria; p__Cyanobacteriota; c__Cyanophyceae; o__NA; f__NA; g__NA
	OTU_668	0.632	0.038	*	k__Bacteria; p__Cyanobacteriota; c__Cyanophyceae; o__NA; f__NA; g__NA
	OTU_697	0.632	0.038	*	k__Bacteria; p__Cyanobacteriota; c__Cyanophyceae; o__NA; f__NA; g__NA
	OTU_726	0.632	0.042	*	k__Bacteria; p__Cyanobacteriota; c__Cyanophyceae; o__Leptolyngbyales; f__Leptolyngbyaceae; g__Speos
	OTU_740	0.632	0.042	*	k__Bacteria; p__Cyanobacteriota; c__Cyanophyceae; o__NA; f__NA; g__NA
	OTU_758	0.632	0.038	*	k__Bacteria; p__Cyanobacteriota; c__Cyanophyceae; o__Oculatellales; f__Oculatellaceae; g__Timaviella
	OTU_769	0.632	0.038	*	k__Bacteria; p__Cyanobacteriota; c__Cyanophyceae; o__Gomontiellales; f__Chamaesiphonaceae; g__Chamaesiphon
	OTU_841	0.632	0.038	*	k__Bacteria; p__Cyanobacteriota; c__Cyanophyceae; o__Leptolyngbyales; f__NA; g__NA
	OTU_852	0.632	0.044	*	k__Bacteria; p__Cyanobacteriota; c__Cyanophyceae; o__Leptolyngbyales; f__Leptolyngbyaceae; g__Leptolyngbyaceae_XXXXXX
	OTU_865	0.632	0.033	*	k__Bacteria; p__Cyanobacteriota; c__Cyanophyceae; o__Oculatellales; f__Oculatellaceae; g__Oculatellaceae_XX
	OTU_870	0.632	0.038	*	k__Bacteria; p__Cyanobacteriota; c__Cyanophyceae; o__NA; f__NA; g__NA
	OTU_888	0.632	0.044	*	k__Bacteria; p__Cyanobacteriota; c__Cyanophyceae; o__Leptolyngbyales; f__Leptolyngbyaceae; g__Leptolyngbyaceae_XXXXXX
	OTU_965	0.632	0.038	*	k__Bacteria; p__Cyanobacteriota; c__Cyanophyceae; o__Oculatellales; f__Oculatellaceae; g__Oculatellaceae_XX
	OTU_977	0.632	0.04	*	k__Bacteria; p__Cyanobacteriota; c__Cyanophyceae; o__Leptolyngbyales; f__Leptolyngbyaceae; g__Leptolyngbyaceae_XXXXXX
	OTU_997	0.632	0.038	*	k__Bacteria; p__Cyanobacteriota; c__Cyanophyceae; o__Oculatellales; f__Oculatellaceae; g__Oculatellaceae_XX

	OTU	stat.	p-value		taxonomy
mo_YO	OTU_4237	0.621	0.042	*	k__Bacteria; p__Cyanobacteriota; c__Cyanophyceae; o__Oculatellales; f__Oculatellaceae; g__Oculatellaceae_XX
	OTU_295	0.618	0.04	*	k__Bacteria; p__Cyanobacteriota; c__Cyanophyceae; o__Leptolyngbyales; f__Leptolyngbyaceae; g__Leptolyngbyaceae_XXXXXX
	OTU_724	0.617	0.05	*	k__Bacteria; p__Cyanobacteriota; c__Cyanophyceae; o__Oculatellales; f__Oculatellaceae; g__Oculatellaceae_XX
	OTU_703	0.617	0.04	*	k__Bacteria; p__Cyanobacteriota; c__Cyanophyceae; o__Oculatellales; f__Oculatellaceae; g__Shackletoniella
	OTU_557	0.616	0.05	*	k__Bacteria; p__Cyanobacteriota; c__Cyanophyceae; o__Oculatellales; f__Oculatellaceae; g__Timaviella
	OTU_1381	0.612	0.05	*	k__Bacteria; p__Cyanobacteriota; c__Cyanophyceae; o__NA; f__NA; g__NA
	OTU_2572	0.608	0.05	*	k__Bacteria; p__Cyanobacteriota; c__Cyanophyceae; o__NA; f__NA; g__NA
	OTU_1455	0.608	0.041	*	k__Bacteria; p__Cyanobacteriota; c__Cyanophyceae; o__Oculatellales; f__Oculatellaceae; g__Timaviella
	OTU_1692	0.606	0.048	*	k__Bacteria; p__Cyanobacteriota; c__Cyanophyceae; o__Leptolyngbyales; f__Leptolyngbyaceae; g__Leptolyngbyaceae_XXXXXX
mo_AU	OTU_2702	0.707	0.019	*	k__Bacteria; p__Cyanobacteriota; c__Cyanophyceae; o__Oscillatoriales; f__Microcoleaceae; g__Limnospira
	OTU_2974	0.611	0.041	*	k__Bacteria; p__Cyanobacteriota; c__Cyanophyceae; o__Oscillatoriales; f__Microcoleaceae; g__Microcoleus
	OTU_74	0.584	0.04	*	k__Bacteria; p__Cyanobacteriota; c__Cyanophyceae; o__Nostocales; f__Aphanizomenonaceae; g__Dolichospermum

Table S3.8. Relative influence of physicochemical, spatial and bedrock type variables on bacterial communities using a dbRDA and a forward, stepwise variable selection.

Environmental variables	Adj. R2	F	df	P	
pH		0.13	10.5	1	0.002
TN		0.18	5.34	1	0.002
$N\text{-}NO_3^-$		0.22	3.98	1	0.002
EC		0.24	2.42	1	0.002
All		0.26	NA	NA	NA
PCNM	Adj. R2	F	df	P	
PCNM1		0.13	10.6	1	0.002
PCNM3		0.18	5.12	1	0.002
PCNM2		0.22	4.02	1	0.002
PCNM10		0.25	3.72	1	0.002
PCNM4		0.27	2.55	1	0.002
PCNM8		0.30	2.62	1	0.002
PCNM9		0.31	2.30	1	0.002
All		0.32	NA	NA	NA
Bedrock type	Adj. R2	F	df	P	
marble		0.18	15.4	1	0.002
mo_YO		0.25	6.96	1	0.002
mo_DV		0.29	4.66	1	0.002
granite		0.31	3.20	1	0.002
All		0.31	NA	NA	NA

III. CHAPTER 4 - SUPPLEMENTARY MATERIALS

III.I SUPPLEMENTARY FIGURES OF CHAPTER 4

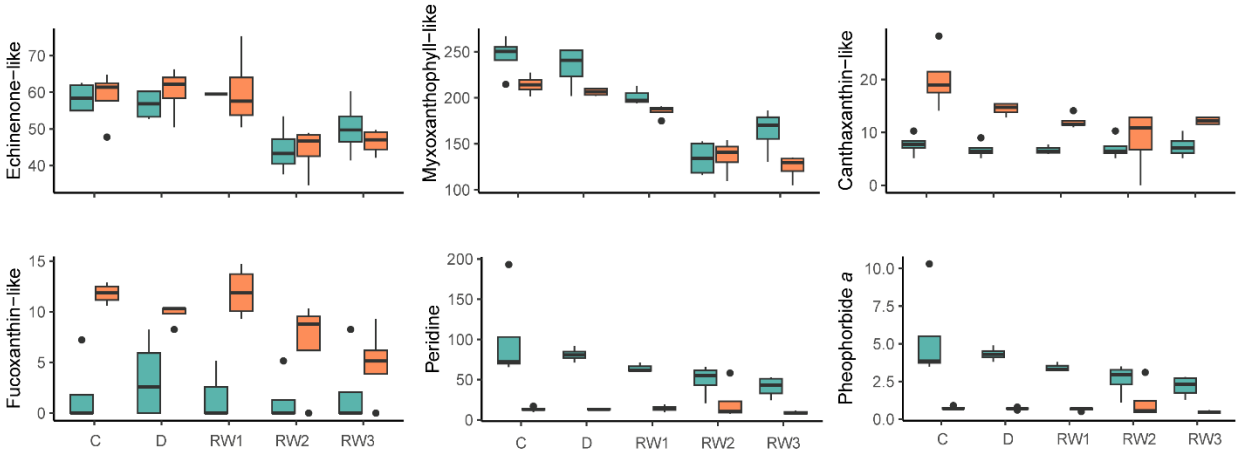

Fig. S4.1 Boxplots of the complete list of pigments detected (in µg L^{-1}) *of the of terrestrial Nostoc sp. ULC180 (in orange) and aquatic Nostoc sp. ULC008 (in blue) per treatment measured via HPLC.*

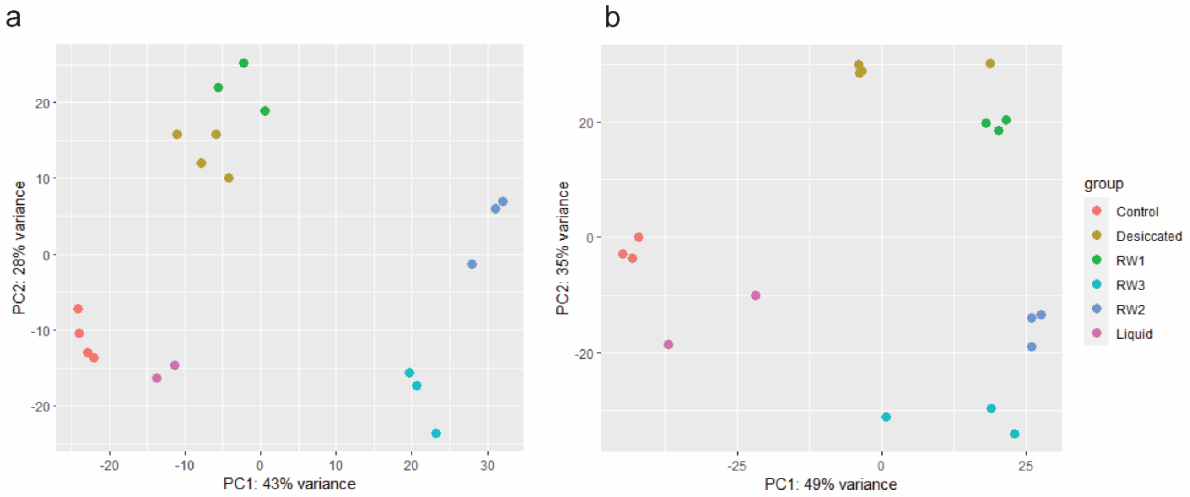

Fig. S4.2 Principal Component Analysis of transcriptomics results of the different treatments per strain *(ULC180 on the left; ULC008 on the right), including the "test" samples from liquid culture medium. C=control, D=desiccation, RW1=10 min after re-wetting, RW2=24h after re-wetting, RW3=72h after re-wetting.*

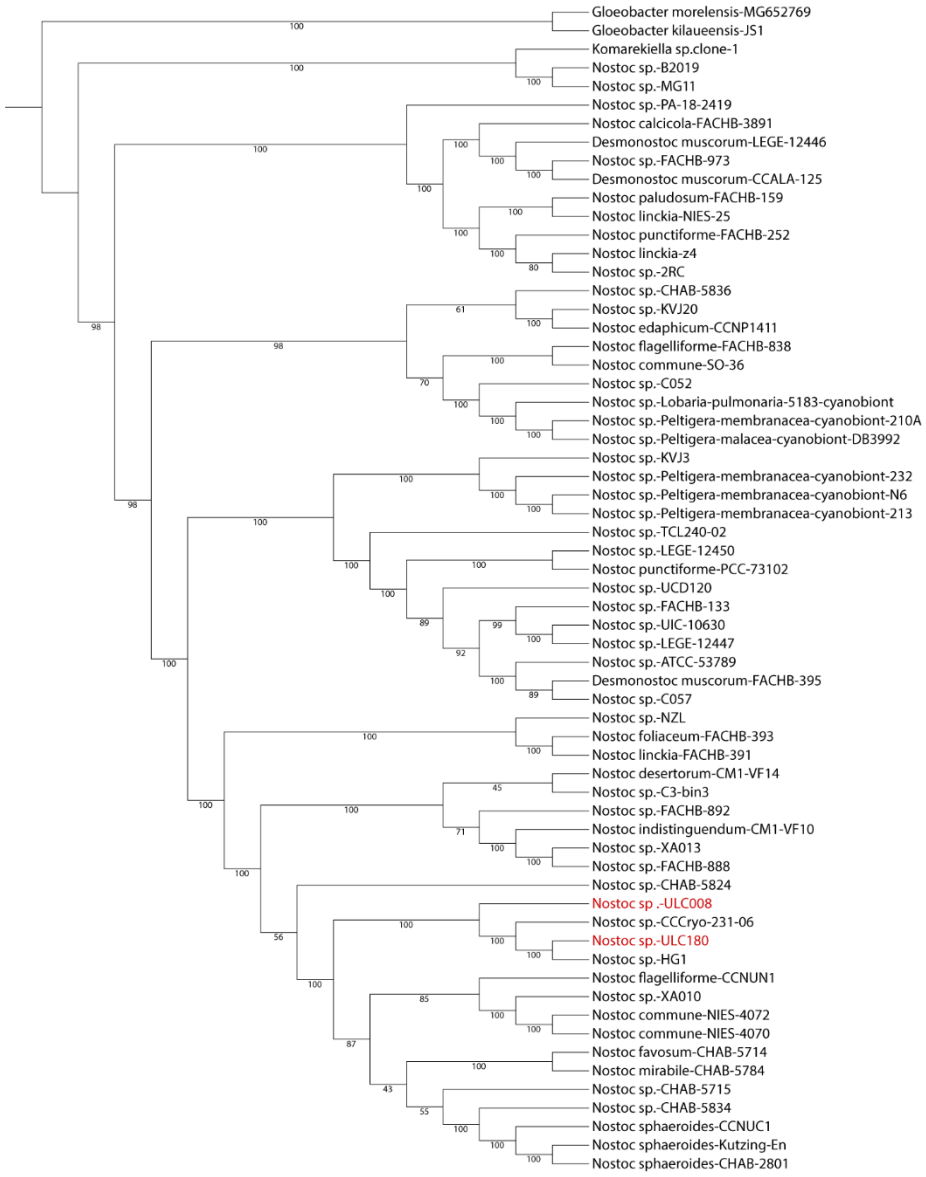

Fig. S4.3* Concensus jackknife phylogenomic tree *of all (63) the cyanobacterial genomes belonging to the Nostocaceae family downloaded from RefSeq. *100 x 100 000 concatenation of genes were produced with SCaFoS and the corresponding trees computed with RAxML under the models PROTGAMMALGF. ULC008 and ULC180 highlighted in red, forming a cluster with other two terrestrial Antarctic genomes: Nostoc sp. HG1 (GCA_014324315.1) and Nostoc sp. CCCryo 231-06 (GCA_023522315.1).*

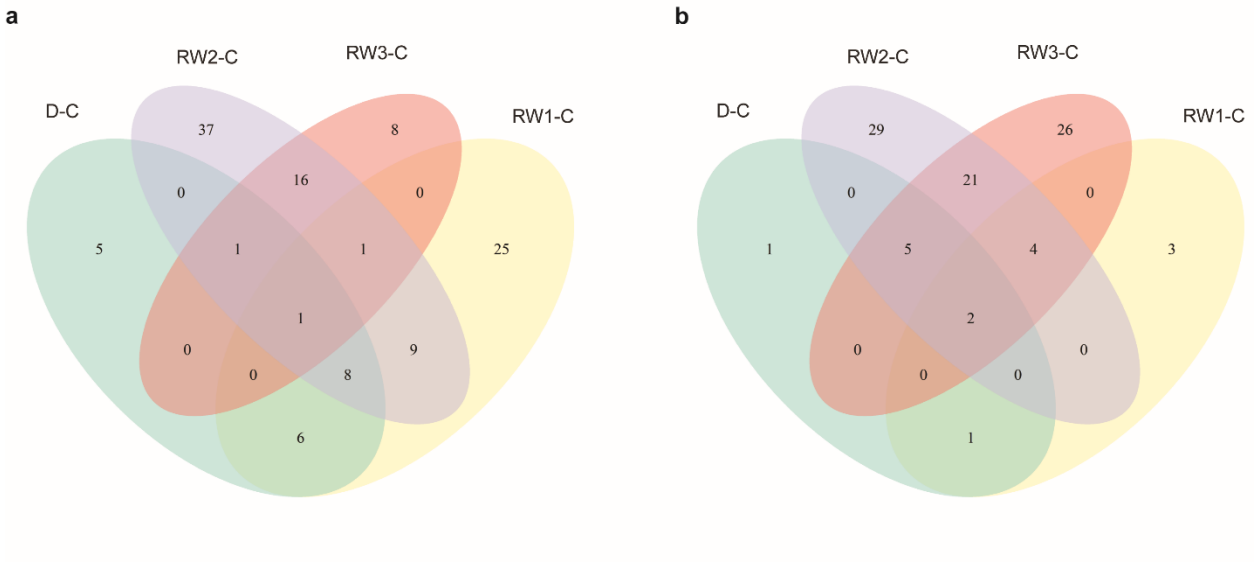

Fig. S4.4 Venn diagram of the shared up-regulated (a) and down-regulated (b) DEGs of treatments with comparison to control of the freshwater Nostoc sp. ULC008.

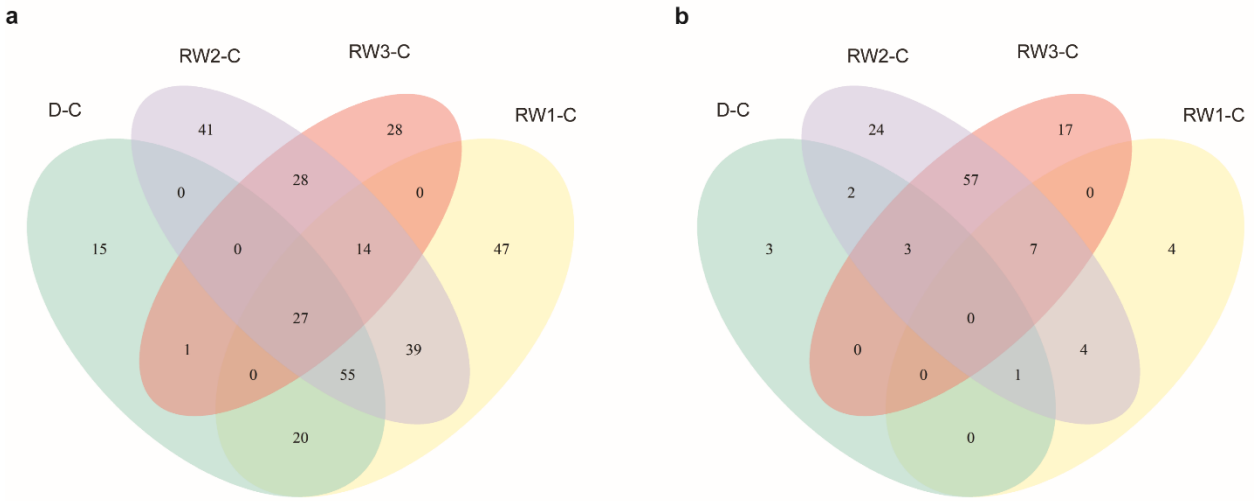

Fig. S4.5 Venn diagram of the shared up-regulated (a) and down-regulated (b) DEGs of treatments with comparison to control of the terrestrial Nostoc sp. ULC180.

III.II SUPPLEMENTARY TABLES OF CHAPTER 4

(see Table on the next page)

***Table S4.1. Ecophysiological parameters mean ± sd of each strain (freshwater Nostoc sp. ULC008 and terrestrial Nostoc sp. ULC0180)**: effective quantum yield (QY, a.u.), pigments concentration (µg L^{-1}) and osmolytes concentration (mg mL^{-1}) per treatment (C = control; D = desiccated; RW1 = after 10 min of rewetting; RW2 = after 24h of rewetting; RW3 = after 72h of rewetting). Only pigments giving yields are shown: echin = echinenone; myxo = myxoxanthophyll; canth= canthaxanthin; fuco = fucoxanthin; chlide a = chlorophyllide a; phide a = pheophorbide a; perid = peridinine; chl a = chlorophyll a; b-car = β-carotene.*

Strain	Treatments	Photosynthesis	Pigments												Osmolytes	
		QY	echin-like	myxo-like	canth-like	fuco-like	chlide *a*	phide *a*	perid	myxo	cantha	echin	chl *a*	b-car	trehalose	sucrose
180	C	0.580 ± 0.058	58.8 ± 7.54	214 ± 10.7	20.1 ± 5.90	11.8 ± 1.02	177 ± 46.1	0.73 ± 0.13	13.2 ± 2.95	280 ± 16.8	110 ± 3.23	504 ± 230	5365 ± 326	598 ± 26.9	31.4 ± 10.9	181 ± 35.6
	D	0.034 ± 0.049	60.2 ± 6.87	206 ± 4.42	14.4 ± 1.23	9.80 ± 1.03	169 ± 34.8	0.70 ± 0.08	13.1 ± 1.53	274 ± 6.66	104 ± 2.77	592 ± 13.8	5415 ± 247	573 ± 14.6	103 ± 23.7	124 ± 5.79
	RW1	0.295 ± 0.148	60.2 ± 10.8	185 ± 7.17	12.0 ± 1.40	11.9 ± 2.56	143 ± 58.5	0.68 ± 0.13	14.1 ± 3.90	250 ± 18.3	103 ± 5.23	572 ± 30.4	4809 ± 449	513 ± 17.8	110 ± 23.4	396 ± 200
	RW2	0.262 ± 0.087	44.2 ± 6.60	136 ± 19.1	8.66 ± 6.05	6.96 ± 4.72	206 ± 93.0	1.15 ± 1.30	21.6 ± 24.4	154 ± 29.7	91.7 ± 19.7	507 ± 22.3	4040 ± 816	532 ± 97.0	154 ± 88.7	568 ± 256
	RW3	0.332 ± 0.204	46.5 ± 3.49	125 ± 13.9	12.2 ± 0.74	4.89 ± 3.80	24.9 ± 5.98	0.48 ± 0.10	8.90 ± 1.79	142 ± 17.9	107 ± 9.68	411 ± 23.1	4526 ± 383	407 ± 34.0	137 ± 111	643 ± 139
008	C	0.497 ± 0.081	58.5 ± 4.14	246 ± 22.1	7.69 ± 2.09	1.80 ± 3.61	349 ± 173	5.38 ± 3.29	101 ± 61.6	342 ± 26.9	69.6 ± 3.97	567 ± 4.19	5661 ± 240	772 ± 8.46	104 ± 61.4	352 ± 12.6
	D	0.019 ± 0.032	56.7 ± 4.14	234 ± 23.7	6.73 ± 1.62	3.35 ± 4.07	570 ± 51.3	4.32 ± 0.46	81.1 ± 8.57	321 ± 9.66	71.8 ± 2.77	602 ± 9.77	4955 ± 59.6	811 ± 26.0	119 ± 41.6	719 ± 209
	RW1	0.226 ± 0.140	59.5 ± 0	201 ± 10.2	6.67 ± 0.92	1.72 ± 2.97	332 ± 41.9	3.43 ± 0.32	64.4 ± 6.02	266 ± 12.9	70.5 ± 7.14	571 ± 11.0	4916 ± 525	692 ± 8.04	210 ± 80.3	823 ± 125
	RW2	0.274 ± 0.100	44.4 ± 6.76	134 ± 19.4	7.05 ± 2.22	1.29 ± 2.58	248 ± 89.3	2.62 ± 1.07	49.2 ± 20.0	161 ± 49.0	70.8 ± 17.6	508 ± 66.6	4383 ± 404	647 ± 79.3	258 ± 193	1305 ± 297
	RW3	0.240 ± 0.097	50.3 ± 7.81	164 ± 24.3	7.37 ± 2.19	2.06 ± 4.12	112 ± 34.6	2.17 ± 0.71	40.8 ± 13.3	186 ± 36.3	75.3 ± 8.47	430 ± 39.1	5679 ± 888	569 ± 50.5	513 ± 229	1580 ± 397

Table S4.2. One-way ANOVA or non-parametric Kruskas-Wallis p-values of effective quantum yield (QY), pigments concentration and osmolytes concentration on treatments (n > 4). *Only significantly different pigments were shown: chlide a = chlorophyllide a; chl a = chlorophyll a; myxo = myxoxanthophyll; echin = echinenone; b-car = β-carotene.*

	Photosynthesis	**Pigments**					**Osmolytes**	
	QY	chlide *a*	chl *a*	myxo	echin	b-car	trehalose	sucrose
ULC180	< 0.0001	0.00324	0.00543	0.00310	0.03089	0.00057	ns	0.00363
ULC008	< 0.0001	0.00018	0.01290	< 0.0001	0.01125	< 0.0001	0.03936	0.00012

Table S4.3 DEGs of treatments vs. control annotated via COG/KEGG/Pfam. *Only DEGs whose | LFC | > 2 and p-values < 0.01 are shown: + represents up-regulated DEGs; - represents down-regulated DEGs.*

				D-C		**RW1-C**		**RW2-C**		**RW3-C**		**RW2-D**		**RW3-D**	
Category	**ID**	**Protein**	**Gene**	**008**	**180**	**008**	**180**	**008**	**180**	**008**	**180**	**008**	**180**	**008**	**180**
Amino acid transport and metabolism	COG0140	Phosphoribosyl-ATP pyrophosphohydrolase	HisI2		+										
	COG0134	Indole-3-glycerol phosphate synthase	TrpC		+										
	COG0683	ABC-type branched-chain amino acid transport system, periplasmic component	LivK									-	-		-
	COG0119	Isopropylmalate/homocitrate/ citramalate synthases	LeuA										-		-

				D-C		RW1-C		RW2-C		RW3-C		RW2-D		RW3-D	
Category	**ID**	**Protein**	**Gene**	**008**	**180**	**008**	**180**	**008**	**180**	**008**	**180**	**008**	**180**	**008**	**180**
Amino acid transport and metabolism	COG1104	Cysteine sulfinate desulfinase/cysteine desulfurase or related enzyme	IscS, NFS1												-
Carbohydrate transport and metabolism	COG2133	Glucose/arabinose dehydrogenase, beta-propeller fold	YliI		+										
	K01236	maltooligosyltrehalose trehalohydrolase	TreZ		+	+	+	+	+						-
	K06044	(1->4)-alpha-D-glucan 1-alpha-D-glucosylmutase	TreY			+	+		+						
	K05343	Maltose alpha-D-glucosyltransferase / alpha-amylase	Tres		+			+				+			
	K00695	Sucrose synthase	SusA						+						
	K01187	Alpha-glucosidase	MalZ			+		+	+						
	COG0363	6-phosphogluconolactonase/Glucosamine-6-phosphate isomerase/deaminase	NagB	+	+										
	COG1523	Pullulanase/glycogen debranching enzyme	PulA	+											
	COG4668	Mannitol/fructose-specific phosphotransferase system, IIA domain	MtlA2									+			
	COG1850	Ribulose 1,5-bisphosphate carboxylase, large subunit, or a RuBisCO-like protein	RbcL												-
	COG0366	Glycosidase/amylase (phosphorylase)	AmyA												-

				D-C		RW1-C		RW2-C		RW3-C		RW2-D		RW3-D	
Category	**ID**	**Protein**	**Gene**	**008**	**180**	**008**	**180**	**008**	**180**	**008**	**180**	**008**	**180**	**008**	**180**
Cell motility	COG1215	Glycosyltransferase, catalytic subunit of cellulose synthase and poly-beta-1,6-N-acetylglucosamine synthase	BcsA		+								-		-
	COG2804	Type II secretory pathway ATPase GspE/PulE or T4P pilus assembly pathway ATPase PilB	PulE or PilB									-			
	COG2805	Tfp pilus assembly protein PilT, pilus retraction ATPase	PilT											-	
Cell wall/membrane/envelope biogenesis	COG1136	ABC-type lipoprotein export system, ATPase component	LolD		+										
	COG0489	Uncharacterized protein involved in exopolysaccharide biosynthesis	GumC		+										
	COG0463	Glycosyltransferase involved in cell wall bisynthesis	WcaA		+								-		-
	COG0451	Nucleoside-diphosphate-sugar epimerase	WcaG									+			-
	COG0438	Glycosyltransferase involved in cell wall bisynthesis	RfaB		+										
	COG0562	UDP-galactopyranose mutase	Glf		+										
	COG0668	Small-conductance mechanosensitive channel	MscS		+										
	COG4775	Outer membrane protein assembly factor	BamA										+		
	COG1210	UTP-glucose-1-phosphate uridylyltransferase	GalU										-		-

				D-C		RW1-C		RW2-C		RW3-C		RW2-D		RW3-D	
Category	**ID**	**Protein**	**Gene**	**008**	**180**	**008**	**180**	**008**	**180**	**008**	**180**	**008**	**180**	**008**	**180**
Coenzyme transport and metabolism	COG0157	Nicotinate-nucleotide pyrophosphorylase	NadC		-										
	COG0476	Molybdopterin or thiamine biosynthesis adenylyltransferase	ThiF		+										-
	COG5759	Mg-protoporphyrin IX monomethyl ester cyclase	Ycf59		+										
	COG0596	BchE, aerobic 2-succinyl-6-hydroxy-2,4-cyclohexadiene-1-carboxylate synthase MenH and related esterases, alpha/beta hydrolase fold	MenH		+										
	COG0596	Pimeloyl-ACP methyl ester carboxylesterase	MhpC		+										
	COG0321	Lipoate-protein ligase B	LipB												+
	COG0276	Protoheme ferro-lyase (ferrochelatase)	HemH												+
	COG0001	Glutamate-1-semialdehyde aminotransferase	HemL												-
Defense mechanisms	COG0841	Multidrug efflux pump subunit	AcrB	+	+										
	COG0845	Multidrug efflux pump subunit AcrA (membrane-fusion protein)	AcrA									+		+	+
	COG2367	Beta-lactamase class A	PenP									+			
	COG1566	Multidrug resistance efflux pump EmrA (EmrA) (PDB:4TKO)	EmrA		+										

				D-C		RW1-C		RW2-C		RW3-C		RW2-D		RW3-D	
Category	**ID**	**Protein**	**Gene**	**008**	**180**	**008**	**180**	**008**	**180**	**008**	**180**	**008**	**180**	**008**	**180**
Defense mechanisms	COG0534	Na+-driven multidrug efflux pump	NorM	+											
	COG0693	Protein/nucleotide deglycase, PfpI/YajL/DJ-1 family (repair of methylglyoxal-glycated proteins and nucleic acids)	YajL		+										
Energy production and conversion	COG0426	Flavorubredoxin	NorV	-	-										
	COG0247	Fe-S oxidoreductase	GlpC		-										
	COG5772	Cyanobacterial/chloroplast membrane protein	Tic21									+			
	K02689	Photosystem I P700 chlorophyll a apoprotein A1	PsaA												-
	K02690	Photosystem I P700 chlorophyll a apoprotein A2	PsaB												-
	K02691	Photosystem I subunit VII	PsaC						-		-		-		
	K02693	Photosystem I subunit IV	PsaE										-		
	K02694	Photosystem I subunit III	PsaF						-		-		-		-
	K02696	Photosystem I subunit VIII	PsaI						-		-		-		-
	K02699	Photosystem I subunit IX	PsaJ										+		-
	K02698	photosystem I subunit X	PsaK										-		-
	K02699	Photosystem I subunit XI	PsaL						-		-		-		-
	K02700	Photosystem I subunit XII	PsaM												-
	COG5716	Photosystem II reaction center D1	PsbA2		+										
	COG5716	Photosystem II reaction center D1	PsbA1						-		-		-		-
	COG5729	Photosystem II reaction center Mn-stabilizing protein	PsbO												-

				D-C		RW1-C		RW2-C		RW3-C		RW2-D		RW3-D	
Category	**ID**	**Protein**	**Gene**	**008**	**180**	**008**	**180**	**008**	**180**	**008**	**180**	**008**	**180**	**008**	**180**
Energy production and conversion	COG5717	Photosystem II reaction center chlorophyll a-binding protein CP47	PsbB												-
	K02092	Allophycocyanin alpha subunit	ApcA					-	-		-	-	-		-
	K02093	Allophycocyanin beta subunit	ApcB						-		-	-	-		-
	K02094	Phycobilisome core linker protein	ApcC						-		-		-		-
	K02096	Phycobilisome core-membrane linker protein	ApcE						-		-				
	K02097	Phycobilisome core component	ApcF												-
	K02284	Phycocyanin alpha chain	CpcA										-		-
	K02285	Phycocyanin beta chain	CpcB						-		-		-		-
	K02286	Phycocyanin-associated rod linker protein	CpcC					-	-		-	-	-		-
	K02286	Phycocyanin-associated rod linker protein	CpcC2					-	-		-		-		
	K02288	Phycocyanobilin lyase subunit alpha	CpcE						-		-	-	-	-	-
	COG5743	Photosystem I light harvesting complex protein, LHCA5/LHCA6/HLI5/Ycf17 family	LHCA5		+										
	COG0401	Membrane potential modulator PMP3/YqaE, plasma membrane proteolipid 3 (PMP3)/Esi3/RCI2/UPF0057 family	YqaE		+										
	K03542	Photosystem II 22kDa protein	PsbS		+										

				D-C		RW1-C		RW2-C		RW3-C		RW2-D		RW3-D	
Category	**ID**	**Protein**	**Gene**	**008**	**180**	**008**	**180**	**008**	**180**	**008**	**180**	**008**	**180**	**008**	**180**
Energy production and conversion	COG2811	Archaeal/vacuolar-type H+-ATPase subunit H	NtpH		+										
	COG0243	Anaerobic selenocysteine-containing dehydrogenase	BisC		+										
	COG4221	NADP-dependent 3-hydroxy acid dehydrogenase YdfG	YdfG												
	COG1008	NADH:ubiquinone oxidoreductase subunit 4 (chain M)	NuoM										-		-
	K02636	Cytochrome b6f complex	PetC	-			+							+	
	K02641	ferredoxin--NADP+ reductase	PetH				-				-	-	-		-
	K02635	cytochrome b6	PetB				+		+		+				
	K02639	ferredoxin	PetF								-				-
	COG3312	FoF1-type ATP synthase assembly protein I	AtpI										-		
	COG1902	2,4-dienoyl-CoA reductase or related NADH-dependent reductase, Old Yellow Enzyme (OYE) family	FadH												+
Function unknown	COG2823	Osmotically-inducible protein OsmY, contains BON domain	OsmY		+										
	COG3861	Stress response protein YsnF	YsnF	+	+										
	COG4804	Predicted nuclease of restriction endonuclease-like (RecB) superfamily, DUF1016 family	YhcG		+										
	COG1950	Uncharacterized membrane protein YvlD, DUF360 family			+										
	COG1808	Uncharacterized membrane protein			+										

				D-C		RW1-C		RW2-C		RW3-C		RW2-D		RW3-D	
Category	**ID**	**Protein**	**Gene**	**008**	**180**	**008**	**180**	**008**	**180**	**008**	**180**	**008**	**180**	**008**	**180**
Function unknown	COG1649	Uncharacterized lipoprotein YddW, UPF0748 family	YddW		+										
	COG4244	Uncharacterized membrane protein			+										
	COG2323	Uncharacterized membrane protein YcaP, DUF421 family	YcaP		+										-
	COG1295	Uncharacterized membrane protein, BrkB/YihY/UPF0761 family (not an RNase)	BrkB		+										-
	COG5637	Uncharacterized protein, contains SRPBCC domain (PDB:3GGN)			+										
	COG2261	Uncharacterized membrane protein YeaQ/YmgE, transglycosylase-associated protein family (YeaQ)	YeaQ	+	+										-
	COG3431	Uncharacterized membrane protein, DUF373 family		-	+										
	COG1357	Uncharacterized protein YjbI, contains pentapeptide repeats	YjbI	+											
General function prediction only	COG3247	Acid resistance membrane protein HdeD, DUF308 family			+										
	COG4636	Endonuclease, Uma2 family (restriction endonuclease fold)	HdeF		+										
	COG3608	Predicted deacylase	Uma2	+	+										-

				D-C		RW1-C		RW2-C		RW3-C		RW2-D		RW3-D	
Category	**ID**	**Protein**	**Gene**	**008**	**180**	**008**	**180**	**008**	**180**	**008**	**180**	**008**	**180**	**008**	**180**
General function prediction only	COG4804	Predicted nuclease of restriction endonuclease-like (RecB) superfamily, DUF1016 family	YchG		+										
	COG3631	Ketosteroid isomerase-related protein	YesE		+										
	COG0312	Predicted Zn-dependent protease or its inactivated homolog	TldD	+											
	COG1032	Radical SAM superfamily enzyme YgiQ, UPF0313 family	YgiQ	+										-	
	K10094	nickel transport protein	CbiK									-		-	
	COG5266	Uncharacterized protein, contains GH25 family domain													
Inorganic ion transport and metabolism	COG0004	Ammonia channel protein	AmtB										-		-
	K11950	Bicarbonate transport system substrate-binding protein	CmpA	-	-			-	-	-	-				
	K11951	Bicarbonate transport system permease protein	CmpB_1					-	-	-	-				
	K11951	Bicarbonate transport system permease protein	CmpB_2		+										
	K11952	Bicarbonate transport system ATP-binding protein	CmpC			-	-	-	-	-					
	K11953	Bicarbonate transport system ATP-binding protein	CmpD					-	-	-	-				
	COG3025	Inorganic triphosphatase YgiF, contains CYTH and CHAD domains	PPPi		+										

				D-C		RW1-C		RW2-C		RW3-C		RW2-D		RW3-D	
Category	**ID**	**Protein**	**Gene**	**008**	**180**	**008**	**180**	**008**	**180**	**008**	**180**	**008**	**180**	**008**	**180**
Inorganic ion transport and metabolism	K06886	Hemoglobin	GlbN		+										
	COG4572	Cation transport regulator	ChaB		+										
	COG0730	Sulfite exporter TauE/SafE/YfcA and related permeases, UPF0721 family	TauE		+										
	COG2710	Nitrogenase molybdenum-iron protein, alpha and beta chains	NifD		+										-
	K02591	Nitrogenase molybdenum-iron protein beta chain	NifK	+	+										-
	K02592	Nitrogenase molybdenum-iron protein NifN	NifE												-
	K02587	Nitrogenase molybdenum-cofactor synthesis protein NifE	NifN												-
	K02596	Nitrogen fixation protein	NifX												-
	K00367	Ferredoxin-nitrate reductase	NarB										-		-
	K00366	Ferredoxin-nitrite reductase	NirA									-	-	-	-
	COG1055	Na+/H+ antiporter NhaD or related arsenite permease	ArsB		+										
	COG0025	NhaP-type Na+/H+ or K+/H+ antiporter (NhaP) (PDB:4CZB)	NhaP		+										
	COG0783	DNA-binding ferritin-like protein (oxidative damage protectant)	Dps	-	+				+		+				
	COG0659	Sulfate permease or related transporter, MFS superfamily	SUL1									-			
Intracellular trafficking, secretion, and vesicular transport	COG2911	Autotransporter translocation and assembly protein TamB (TamB) (PDB:5VTG)	TamB		+										
	COG0848	Biopolymer transport protein ExbD	ExbD		+										

				D-C		RW1-C		RW2-C		RW3-C		RW2-D		RW3-D	
Category	**ID**	**Protein**	**Gene**	**008**	**180**	**008**	**180**	**008**	**180**	**008**	**180**	**008**	**180**	**008**	**180**
Lipid transport and metabolism	COG2230	Cyclopropane fatty-acyl-phospholipid synthase and related methyltransferases	Cfa		+										
	K09836	beta-carotene/zeaxanthin 4-ketolase	CrtW		+		+								
	K02292	beta-carotene ketolase (CrtO type)	CrtO		+						+				
	COG0204	1-acyl-sn-glycerol-3-phosphate acyltransferase	PlsC		+										
	PF09150.13	Orange carotenoid protein, N-terminal	OCP		+										
	COG1502	Phosphatidylserine/phosphatidylglycerophosphate/cardiolipin synthase or related enzyme	Cls		+										
	COG1028	NAD(P)-dependent dehydrogenase, short-chain alcohol dehydrogenase family	FabG		+						+	+			
	COG0331	Malonyl CoA-acyl carrier protein transacylase	FabD										-		-
	COG0248	Exopolyphosphatase/pppGpp-phosphohydrolase	GppA									+			
Mobilome: prophages, transposons	COG1943	REP element-mobilizing transposase RayT	RAYT											+	
Posttranslational modification, protein turnover, chaperones	COG0705	Membrane-associated serine protease, rhomboid family	GlpG		-										
	COG0459	Chaperonin GroEL (HSP60 family)	GroEL		-										

				D-C		RW1-C		RW2-C		RW3-C		RW2-D		RW3-D	
Category	**ID**	**Protein**	**Gene**	**008**	**180**	**008**	**180**	**008**	**180**	**008**	**180**	**008**	**180**	**008**	**180**
Posttranslational modification, protein turnover, chaperones	COG0234	Co-chaperonin GroES (HSP10)	GroES		+								+		+
	COG0443	Molecular chaperone DnaK (HSP70)	DnaK										+		+
	COG2239	Mg/Co/Ni transporter MgtE (contains CBS domain) (MgtE) (PDB:2YVX)	MgtE		+										
	COG1262	Formylglycine-generating enzyme, required for sulfatase activity, contains SUMF1/FGE domain	YfmG		+										
	COG0071	Small heat shock protein IbpA, HSP20 family	IbpA									-		-	
	COG0526	Thiol-disulfide isomerase or thioredoxin	TrxA												+
	COG0542	ATP-dependent Clp protease ATP-binding subunit	ClpA												+
	COG0316	Fe-S cluster assembly iron-binding protein	IscA												-
Replication, recombination and repair	COG0513	Superfamily II DNA and RNA helicase	SrmB		+										
	COG0776	Bacterial nucleoid DNA-binding protein	HimA										-		-
Secondary metabolites biosynthesis, transport and catabolism	COG4242	Cyanophycinase and related exopeptidases	CphB		+		+		+						
	K03802	Cyanophycin synthetase	CphA		+		+		+						

				D-C		RW1-C		RW2-C		RW3-C		RW2-D		RW3-D	
Category	**ID**	**Protein**	**Gene**	**008**	**180**	**008**	**180**	**008**	**180**	**008**	**180**	**008**	**180**	**008**	**180**
Signal transduction mechanisms	COG3476	Tryptophan-rich sensory protein (mitochondrial benzodiazepine receptor homolog)	TspO	+	+										
	COG1352	Methylase of chemotaxis methyl-accepting proteins (CheR) (PDB:1AF7)	CheR		+	+	+	+							
	COG5592	Hemerythrin domain-containing protein		+	+										
	COG0784	chemotaxis protein or a CheY-like REC (receiver) domain	CheY		+										
	COG1366	Anti-anti-sigma regulatory factor (antagonist of anti-sigma factor)	SpoIIAA		+										
	COG0745	DNA-binding response regulator, OmpR family, contains REC and winged-helix (wHTH) domain	OmpR	-											
Stress response	COG3861	Stress response protein YsnF (function unknown) (YsnF)	YsnF												-
Transcription	COG1191	DNA-directed RNA polymerase specialized sigma subunit	FliA	+	+										
	COG0568	DNA-directed RNA polymerase, sigma subunit (sigma70/sigma32)	RpoD											-	
Translation, ribosomal structure and biogenesis	COG0724	RNA recognition motif (RRM) domain (RRM) (PDB:1HL6)	RRM	-	-									-	

				D-C		RW1-C		RW2-C		RW3-C		RW2-D		RW3-D	
Category	**ID**	**Protein**	**Gene**	**008**	**180**	**008**	**180**	**008**	**180**	**008**	**180**	**008**	**180**	**008**	**180**
Translation, ribosomal structure and biogenesis	COG1544	Ribosome-associated translation inhibitor	RaiA		+									+	
	COG0222	Ribosomal protein L7/L12	RplL											+	
	COG2890	Methylase of polypeptide chain release factors (HemK) (PDB:1NV8)	HemK												
	COG1189	Predicted rRNA methylase YqxC, contains S4 and FtsJ domains	YqxC												+

REFERENCES

Andriuzzi, W. S., Adams, B. J., Barrett, J. E., Virginia, R. A., & Wall, D. H. (2018). Observed trends of soil fauna in the Antarctic dry valleys: Early signs of shifts predicted under climate change. Ecology, 99, 312– 321.

Archer, S.D., De los Ríos, A., Lee, K.C., Niederberger, T.S., Cary, S.C., Coyne, K.J., Douglas, S., Lacap-Bugler, D.C. and Pointing, S.B., 2017. Endolithic microbial diversity in sandstone and granite from the McMurdo Dry Valleys, Antarctica. Polar Biology, 40, pp.997-1006.

Archibald, J.M., 2015. Endosymbiosis and eukaryotic cell evolution. *Current Biology*, *25*(19), pp.R911-R921.

Banerjee, S., Schlaeppi, K. and van der Heijden, M.G., 2018. Keystone taxa as drivers of microbiome structure and functioning. *Nature Reviews Microbiology*, *16*(9), pp.567-576.

Barberán, A., Bates, S.T., Casamayor, E.O. and Fierer, N., 2012. Using network analysis to explore co-occurrence patterns in soil microbial communities. *The ISME journal*, *6*(2), pp.343-351.

Bekker, A., Holland, H.D., Wang, P.L., Rumble Iii, D., Stein, H.J., Hannah, J.L., Coetzee, L.L. and Beukes, N.J., 2004. Dating the rise of atmospheric oxygen. *Nature*, *427*(6970), pp.117-120.

Bendia, A.G., Signori, C.N., Franco, D.C., Duarte, R.T., Bohannan, B.J. and Pellizari, V.H., 2018. A mosaic of geothermal and marine features shapes microbial community structure on deception Island Volcano, Antarctica. *Frontiers in Microbiology*, *9*, p.899.

Bergstrom, D.M., Woehler, E.J., Klekociuk, A.R., Pook, M.J. and Massom, R.A., 2018. Extreme events as ecosystems drivers: ecological consequences of anomalous Southern Hemisphere weather patterns during the 2001/02 austral spring-summer. Advances in Polar Science, 29(3), pp.190-204.

Berry, D. and Widder, S., 2014. Deciphering microbial interactions and detecting keystone species with co-occurrence networks. *Frontiers in microbiology*, *5*, p.219.

Bockheim, J.G. and Hall, K.J., 2002. Permafrost, active-layer dynamics and periglacial environments of continental Antarctica: periglacial and permafrost research in the Southern Hemisphere. South African Journal of Science, 98(1), pp.82-90.

Boenigk, J., Ereshefsky, M., Hoef-Emden, K., Mallet, J. and Bass, D., 2012. Concepts in protistology: species definitions and boundaries. *European Journal of Protistology*, *48*(2), pp.96-102.

Brooks, S.T., Jabour, J., van den Hoff, J., Bergstrom, D.M., 2019. Our footprint on Antarctica competes with nature for rare ice-free land. Nat. Sustain. 2, 185–190.

Cannone, N., Malfasi, F., Favero-Longo, S.E., Convey, P. and Guglielmin, M., 2022. Acceleration of climate warming and plant dynamics in Antarctica. *Current biology*, *32*(7), pp.1599-1606.

Castenholz, R.W., Wilmotte, A., Herdman, M., Rippka, R., Waterbury, J.B., Iteman, I. and Hoffmann, L., 2001. Phylum BX. cyanobacteria. In *Bergey's Manual® of Systematic Bacteriology* (pp. 473-599). Springer, New York, NY.

Chaffron, S., Rehrauer, H., Pernthaler, J. and Von Mering, C., 2010. A global network of coexisting microbes from environmental and whole-genome sequence data. *Genome research*, *20*(7), pp.947-959.

Chown, S.L. and Convey, P., 2007. Spatial and temporal variability across life's hierarchies in the terrestrial Antarctic. *Philosophical Transactions of the Royal Society B: Biological Sciences*, *362*(1488), pp.2307-2331.

Chown, S.L., Clarke, A., Fraser, C.I., Cary, S.C., Moon, K.L. and McGeoch, M.A., 2015. The changing form of Antarctic biodiversity. *Nature*, *522*(7557), pp.431-438.

Chrismas, N.A., Williamson, C.J., Yallop, M.L., Anesio, A.M. and Sánchez-Baracaldo, P., 2018. Photoecology of the Antarctic cyanobacterium Leptolyngbya sp. BC1307 brought to light through community analysis, comparative genomics and in vitro photophysiology. *Molecular ecology*, *27*(24), pp.5279-5293.

Coleine, C., Stajich, J.E., de Los Ríos, A. and Selbmann, L., 2021. Beyond the extremes: Rocks as ultimate refuge for fungi in drylands. *Mycologia*, *113*(1), pp.108-133.

Coleine, C., Biagioli, F., de Vera, J.P., Onofri, S. and Selbmann, L., 2021. Endolithic microbial composition in Helliwell Hills, a newly investigated Mars-like area in Antarctica. *Environmental Microbiology*, *23*(7), pp.4002-4016.

Collins, G.E. and Hogg, I.D., 2016. Temperature-related activity of Gomphiocephalus hodgsoni (Collembola) mitochondrial DNA (COI) haplotypes in Taylor Valley, Antarctica. *Polar Biology*, *39*, pp.379-389.

Convey, P., Biersma, E.M., Casanova-Katny, A. and Maturana, C.S., 2020. Refuges of Antarctic diversity. In Past Antarctica (pp. 181-200). Academic Press.

Convey, P., Gibson, J.A., Hillenbrand, C.D., Hodgson, D.A., Pugh, P.J., Smellie, J.L. and Stevens, M.I., 2008. Antarctic terrestrial life–challenging the history of the frozen continent?. Biological Reviews, 83(2), pp.103-117.

Convey, P., Chown, S.L., Clarke, A., Barnes, D.K., Bokhorst, S., Cummings, V., Ducklow, H.W., Frati, F., Green, T.A., Gordon, S. and Griffiths, H.J., 2014. The spatial structure of Antarctic biodiversity. *Ecological monographs*, *84*(2), pp.203-244.

Cornet, L., Bertrand, A.R., Hanikenne, M., Javaux, E.J., Wilmotte, A. and Baurain, D., 2018. Metagenomic assembly of new (sub) polar Cyanobacteria and their associated microbiome from non-axenic cultures. *Microbial Genomics*, *4*(9).

Cowan, D.A. and Tow, L.A., 2004. Endangered antarctic environments. Annu. Rev. Microbiol., 58, pp.649-690.

De Los Ríos, A., Wierzchos, J. and Ascaso, C., 2014. The lithic microbial ecosystems of Antarctica's McMurdo Dry Valleys. *Antarctic Science*, *26*(5), pp.459-477.

DeSantis, T.Z., Hugenholtz, P., Larsen, N., Rojas, M., Brodie, E.L., Keller, K., Huber, T., Dalevi, D., Hu, P. and Andersen, G.L., 2006. Greengenes, a chimera-checked 16S rRNA gene database and workbench compatible with ARB. Applied and environmental microbiology, 72(7), pp.5069-5072.

De Smet, W.H. and Gibson, J.A., 2008. *Rhinoglena kutikovae* n. sp. (Rotifera: Monogononta: Epiphanidae) from the Bunger Hills, East Antarctica: a probable relict species that survived Quaternary glaciations on the continent. *Polar Biology*, *31*, pp.595-603.

Dsouza, M., Taylor, M.W., Turner, S.J. and Aislabie, J., 2015. Genomic and phenotypic insights into the ecology of Arthrobacter from Antarctic soils. *BMC genomics*, *16*, pp.1-18.

Effendi, D.B., Sakamoto, T., Ohtani, S., Awai, K. and Kanesaki, Y., 2022. Possible involvement of extracellular polymeric substrates of Antarctic cyanobacterium Nostoc sp. strain SO-36 in adaptation to harsh environments. *Journal of Plant Research*, *135*(6), pp.771-784.

Ertekin, E.; Meslier, V.; Browning, A.; Treadgold, J.; DiRuggiero, J. Rock Structure Drives the Taxonomic and Functional Diversityof Endolithic Microbial Communities in Extreme Environments.Environ. Microbiol.2021,23, 3937–3956

Field, C.B., Behrenfeld, M.J., Randerson, J.T. and Falkowski, P., 1998. Primary production of the biosphere: integrating terrestrial and oceanic components. *science*, *281*(5374), pp.237-240.

Fox, A.J., Paul, A. and Cooper, R., 1994. Measured properties of the Antarctic ice sheet derived from the SCAR Antarctic digital database. *Polar Record*, *30*(174), pp.201-206.

Gooseff, M.N., Barrett, J.E., Adams, B.J., Doran, P.T., Fountain, A.G., Lyons, W.B., McKnight, D.M., Priscu, J.C., Sokol, E.R., Takacs-Vesbach, C. and Vandegehuchte, M.L., 2017. Decadal ecosystem response to an anomalous melt season in a polar desert in Antarctica. *Nature ecology & evolution*, *1*(9), pp.1334-1338.

Greening, C., Islam, Z.F. and Bay, S.K., 2022. Hydrogen is a major lifeline for aerobic bacteria. Trends in Microbiology, 30(4), pp.330-337.

Guidetti, R., Rebecchi, L., Cesari, M. and McInnes, S.J., 2014. Mopsechiniscus franciscae, a new species of a rare genus of Tardigrada from continental Antarctica. *Polar Biology*, *37*, pp.1221-1233.

Hanson, C.A., Fuhrman, J.A., Horner-Devine, M.C. and Martiny, J.B., 2012. Beyond biogeographic patterns: processes shaping the microbial landscape. *Nature Reviews Microbiology*, *10*(7), pp.497-506.

Hawes, T.C., Torricelli, G. and Stevens, M.I., 2010. Haplotype diversity in the Antarctic springtail Gressittacantha terranova at fine spatial scales-a Holocene twist to a Pliocene tale. *Antarctic Science*, *22*(6), pp.766-773.

Higo, A., Suzuki, T., Ikeuchi, M. and Ohmori, M., 2007. Dynamic transcriptional changes in response to rehydration in Anabaena sp. PCC 7120. Microbiology, 153(11), pp.3685-3694.

Higo, A., Katoh, H., Ohmori, K., Ikeuchi, M. and Ohmori, M., 2006. The role of a gene cluster for trehalose metabolism in dehydration tolerance of the filamentous cyanobacterium Anabaena sp. PCC 7120. Microbiology, 152(4), pp.979-987.

Hughes, K.A., Pescott, O.L., Peyton, J., Adriaens, T., Cottier-Cook, E.J., Key, G., Rabitsch, W., Tricarico, E., Barnes, D.K., Baxter, N. and Belchier, M., 2020. Invasive non-native species likely to threaten biodiversity and ecosystems in the Antarctic Peninsula region. *Global change biology*, *26*(4), pp.2702-2716.

Jancusova, M., Kovacik, L., Pereira, A.B., Dusinsky, R. and Wilmotte, A., 2016. Polyphasic characterization of 10 selected ecologically relevant filamentous cyanobacterial strains from the South Shetland Islands, Maritime Antarctica. *FEMS Microbiology Ecology*, *92*(7), p.fiw100.

Ji, M., Greening, C., Vanwonterghem, I., Carere, C.R., Bay, S.K., Steen, J.A., Montgomery, K., Lines, T., Beardall, J., Van Dorst, J. and Snape, I., 2017. Atmospheric trace gases support primary production in Antarctic desert surface soil. *Nature*, *552*(7685), pp.400-403.

Jungblut, A.D. and Vincent, W.F., 2017. Cyanobacteria in polar and alpine ecosystems. *Psychrophiles: from biodiversity to biotechnology*, pp.181-206.

Katoh, H., Asthana, R.K. and Ohmori, M., 2004. Gene expression in the cyanobacterium Anabaena sp. PCC7120 under desiccation. Microbial ecology, 47, pp.164-174.

Kim, M., Cho, A., Lim, H.S., Hong, S.G., Kim, J.H., Lee, J., Choi, T., Ahn, T.S. and Kim, O.S., 2015. Highly heterogeneous soil bacterial communities around Terra Nova Bay of northern Victoria Land, Antarctica. *PLoS One*, *10*(3), p.e0119966.

Komárek, J., Nedbalová, L. and Hauer, T., 2012. Phylogenetic position and taxonomy of three heterocytous cyanobacteria dominating the littoral of deglaciated lakes, James Ross Island, Antarctica. *Polar Biology*, *35*(5), pp.759-774.

IPCC. Climate Change 2013: The Physical Science Basis. Contribution of Working Group I to the Fifth Assessment Report of the Intergovernmental Panel on Climate Change (eds Stocker, T.F. et al.) (IPCC, Cambridge Univ. Press, 2013).

IPCC. (2021). Summary for policymakers. In V. Massondelmotte-Delmotte, P. Zhai, A. Pirani, S. L. Connors, C. Péan, S. Berger, N. Caud, Y. Chen, L. Goldfarb, M. I. Gomis, M. Huang, K. Leitzell, E. Lonnoy, J. B. R. Matthews, T. K. Maycock, T. Waterfield, O. Yelekçi, R. Yu, & B. Zhou (Eds.), Climate Change 2021: The physical science basis. Contribution of working group I to the sixth assessment report of the intergovernmental panel on climate Change (pp. 3–32). Cambridge University Press.

Lefler, F.W., Berthold, D.E. and Dail Laughinghouse IV, H., 2023. CyanoSeq: a database of cyanobacterial 16S rRNA sequences with curated taxonomy. Journal of Phycology.

Lefler, F.W., Berthold, D.E. and Laughinghouse, D., 2022. CyanoSeq: a new curated reference database of cyanobacterial 16S rRNA sequences.

Lee, J.R., Raymond, B., Bracegirdle, T.J., Chadès, I., Fuller, R.A., Shaw, J.D. and Terauds, A., 2017. Climate change drives expansion of Antarctic ice-free habitat. *Nature*, *547*(7661), pp.49-54.

Lee, C.K., Laughlin, D.C., Bottos, E.M., Caruso, T., Joy, K., Barrett, J.E., Brabyn, L., Nielsen, U.N., Adams, B.J., Wall, D.H. and Hopkins, D.W., 2019. Biotic interactions are an unexpected yet critical control on the complexity of an abiotically driven polar ecosystem. *Communications biology*, *2*(1), p.62.

Lee, J.R., Waterman, M.J., Shaw, J.D., Bergstrom, D.M., Lynch, H.J., Wall, D.H. and Robinson, S.A., 2022. Islands in the ice: Potential impacts of habitat transformation on Antarctic biodiversity. *Global Change Biology*, *28*(20), pp.5865-5880.

Lee, C.K., Barbier, B.A., Bottos, E.M., McDonald, I.R. and Cary, S.C., 2012. The inter-valley soil comparative survey: the ecology of Dry Valley edaphic microbial communities. *The ISME journal*, *6*(5), pp.1046-1057.

Lee, J.Z., Burow, L.C., Woebken, D., Everroad, R.C., Kubo, M.D., Spormann, A.M., Weber, P.K., Pett-Ridge, J., Bebout, B.M. and Hoehler, T.M., 2014. Fermentation couples Chloroflexi and sulfate-reducing bacteria to Cyanobacteria in hypersaline microbial mats. *Frontiers in Microbiology*, *5*, p.61.

Lenton, T.M. and Daines, S.J., 2017. Matworld–the biogeochemical effects of early life on land. *New Phytologist*, *215*(2), pp.531-537.

Li, X., Huo, S., Zhang, J., Ma, C., Xiao, Z., Zhang, H., Xi, B. and Xia, X., 2019. Metabarcoding reveals a more complex cyanobacterial community than morphological identification. *Ecological Indicators*, *107*, p.105653.

Liu, Y., Jeraldo, P., Herbert, W., McDonough, S., Eckloff, B., Schulze-Makuch, D., De Vera, J.P., Cockell, C., Leya, T., Baqué, M. and Jen, J., 2022. Whole genome sequencing of cyanobacterium Nostoc sp. CCCryo 231-06 using microfluidic single cell technology. Iscience, 25(5).

Løvenskiold, H.L., 1960. The Snow Petrel *Pagodroma nivea* nesting in Dronning Maud Land. Ibis 102: 132–134.

Mareš, J., Strunecký, O., Bučinská, L. and Wiedermannová, J., 2019. Evolutionary patterns of thylakoid architecture in cyanobacteria. *Frontiers in Microbiology*, *10*, p.277.

Martineau, E., Wood, S.A., Miller, M.R., Jungblut, A.D., Hawes, I., Webster-Brown, J. and Packer, M.A., 2013. Characterisation of Antarctic cyanobacteria and comparison with New Zealand strains. *Hydrobiologia*, *711*, pp.139-154.

Matsuoka, K., Skoglund, A., Roth, G., de Pomereu, J., Griffiths, H., Headland, R., Herried, B., Katsumata, K., Le Brocq, A., Licht, K. and Morgan, F., 2021. Quantarctica, an integrated mapping environment for Antarctica, the Southern Ocean, and sub-Antarctic islands. *Environmental Modelling & Software*, *140*, p.105015.

Meslier, V. and DiRuggiero, J., 2019. Endolithic microbial communities as model systems for ecology and astrobiology. In Model ecosystems in extreme environments (pp. 145-168). Academic Press.

Mieth, M., Jacobs, J., Ruppel, A., Damaske, D., Läufer, A. and Jokat, W., 2014. New detailed aeromagnetic and geological data of eastern Dronning Maud Land: Implications for refining the tectonic and structural framework of Sør Rondane, East Antarctica. *Precambrian Research*, *245*, pp.174-185.

Namsaraev, Z., Mano, M.J., Fernandez, R. and Wilmotte, A., 2010. Biogeography of terrestrial cyanobacteria from Antarctic ice-free areas. *Annals of Glaciology*, *51*(56), pp.171-177.

Napoli, A., Micheletti, D., Pindo, M., Larger, S., Cestaro, A., De Vera, J.P. and Billi, D., 2022. Absence of increased genomic variants in the cyanobacterium Chroococcidiopsis exposed to Mars-like conditions outside the space station. Scientific Reports, 12(1), p.8437.

Niederberger, T.D., Sohm, J.A., Gunderson, T.E., Parker, A.E., Tirindelli, J., Capone, D.G., Carpenter, E.J. and Cary, S.C., 2015. Microbial community composition of transiently wetted Antarctic Dry Valley soils. *Frontiers in Microbiology*, *6*, p.9.

Nübel, U., Garcia-Pichel, F. and Muyzer, G., 1997. PCR primers to amplify 16S rRNA genes from cyanobacteria. *Applied and environmental microbiology*, *63*(8), pp.3327-3332.

Osanai, Y., 1996. Explanatory text of geological map of Brattnipene, Sor Rondane Mountains, Antarctica. *Antarctic Geological Map Series (Sheet 34, Brattnipene)*.

Osanai, Y., Nogi, Y., Baba, S., Nakano, N., Adachi, T., Hokada, T., Toyoshima, T., Owada, M., Satish-Kumar, M., Kamei, A. and Kitano, I., 2013. Geologic evolution of the Sør Rondane Mountains, East Antarctica: collision tectonics proposed based on metamorphic processes and magnetic anomalies. *Precambrian Research*, *234*, pp.8-29.

Ortiz, M., Leung, P.M., Shelley, G., Van Goethem, M.W., Bay, S.K., Jordaan, K., Vikram, S., Hogg, I.D., Makhalanyane, T.P., Chown, S.L. and Grinter, R., 2020. A genome compendium reveals diverse metabolic adaptations of Antarctic soil microorganisms. bioRxiv.

Parks, D.H., Chuvochina, M., Rinke, C., Mussig, A.J., Chaumeil, P.A. and Hugenholtz, P., 2022. GTDB: an ongoing census of bacterial and archaeal diversity through a phylogenetically consistent, rank normalized and complete genome-based taxonomy. *Nucleic acids research*, *50*(D1), pp.D785-D794.

Partensky, F., Hess, W.R. and Vaulot, D., 1999. Prochlorococcus, a marine photosynthetic prokaryote of global significance. *Microbiology and molecular biology reviews*, *63*(1), pp.106-127.

Partensky, F. and Garczarek, L., 2011. Arms race in a drop of sea water. *Nature*, *474*(7353), pp.582-583.

Pearce, D.A., Bridge, P.D., Hughes, K.A., Sattler, B., Psenner, R. and Russell, N.J., 2009. Microorganisms in the atmosphere over Antarctica. FEMS Microbiology Ecology, 69(2), pp.143-157.

Pessi, I.S., Maalouf, P.D.C., Laughinghouse IV, H.D., Baurain, D. and Wilmotte, A., 2016. On the use of high-throughput sequencing for the study of cyanobacterial diversity in Antarctic aquatic mats. Journal of Phycology, 52(3), pp.356-368.

Pessi, I.S., Lara, Y., Durieu, B., Maalouf, P.D.C., Verleyen, E. and Wilmotte, A., 2018. Community structure and distribution of benthic cyanobacteria in Antarctic lacustrine microbial mats. FEMS Microbiology Ecology, 94(5), p.fiy042.

Peeters, K., Verleyen, E., Hodgson, D.A., Convey, P., Ertz, D., Vyverman, W. and Willems, A., 2012. Heterotrophic bacterial diversity in aquatic microbial mat communities from Antarctica. *Polar Biology*, *35*, pp.543-554.

Pinseel, E., Janssens, S.B., Verleyen, E., Vanormelingen, P., Kohler, T.J., Biersma, E.M., Sabbe, K., Van de Vijver, B. and Vyverman, W., 2020. Global radiation in a rare biosphere soil diatom. Nature communications, 11(1), p.2382.

Pinseel, E., Van de Vijver, B., Wolfe, A.P., Harper, M., Antoniades, D., Ashworth, A.C., Ector, L., Lewis, A.R., Perren, B., Hodgson, D.A. and Sabbe, K., 2021. Extinction of austral diatoms in response to large-scale climate dynamics in Antarctica. Science advances, 7(38), p.eabh3233.

Pointing, S.B., Chan, Y., Lacap, D.C., Lau, M.C., Jurgens, J.A. and Farrell, R.L., 2009. Highly specialized microbial diversity in hyper-arid polar desert. Proceedings of the National Academy of Sciences, 106(47), pp.19964-19969.

Prabha, R., Singh, D.P., Somvanshi, P. and Rai, A., 2016. Functional profiling of cyanobacterial genomes and its role in ecological adaptations. Genomics Data, 9, pp.89-94.

Pugh, P.J. and Convey, P., 2008. Surviving out in the cold: Antarctic endemic invertebrates and their refugia. Journal of Biogeography, 35(12), pp.2176-2186.

Pushkareva, E., Pessi, I.S., Namsaraev, Z., Mano, M.J., Elster, J. and Wilmotte, A., 2018. Cyanobacteria inhabiting biological soil crusts of a polar desert: Sør Rondane Mountains, Antarctica. Systematic and applied microbiology, 41(4), pp.363-373.

Quince, C., Walker, A.W., Simpson, J.T., Loman, N.J. and Segata, N., 2017. Shotgun metagenomics, from sampling to analysis. Nature biotechnology, 35(9), pp.833-844.

Ray, A.E., Zaugg, J., Benaud, N., Chelliah, D.S., Bay, S., Wong, H.L., Leung, P.M., Ji, M., Terauds, A., Montgomery, K. and Greening, C., 2022. Atmospheric chemosynthesis is phylogenetically and geographically widespread and contributes significantly to carbon fixation throughout cold deserts. The ISME Journal, pp.1-14.

Richards, S., 2015. It's more than stamp collecting: how genome sequencing can unify biological research. Trends in Genetics, 31(7), pp.411-421.

Richter, I., Herbold, C.W., Lee, C.K., McDonald, I.R., Barrett, J.E. and Cary, S.C., 2014. Influence of soil properties on archaeal diversity and distribution in the McMurdo Dry Valleys, Antarctica. FEMS Microbiology Ecology, 89(2), pp.347-359.

Robinson, S. A., Klekociuk, A. R., King, D. H., Pizarro Rojas, M., Zúñiga, G. E., & Bergstrom, D. M. (2020). The 2019/2020 summer of Antarctic heatwaves. Global Change Biology, 26, 3178–3180

Robinson, S. A., Klekociuk, A. R., King, D. H., Pizarro Rojas, M., Zúñiga, G. E., & Bergstrom, D. M. (2020). The 2019/2020 summer of Antarctic heatwaves. Global Change Biology, 26, 3178–3180.

Ruppel, A.S., Läufer, A., Jacobs, J., Elburg, M., Krohne, N., Damaske, D. and Lisker, F., 2015. The Main Shear Zone in Sør Rondane, East Antarctica: Implications for the late-Pan-African tectonic evolution of Dronning Maud Land. *Tectonics*, *34*(6), pp.1290-1305.

Sahade, R., Lagger, C., Torre, L., Momo, F., Monien, P., Schloss, I., Barnes, D.K., Servetto, N., Tarantelli, S., Tatián, M. and Zamboni, N., 2015. Climate change and glacier retreat drive shifts in an Antarctic benthic ecosystem. Science Advances, 1(10), p.e1500050.

Scambos, T.A., Campbell, G.G., Pope, A., Haran, T., Muto, A., Lazzara, M., Reijmer, C.H. and Van den Broeke, M.R., 2018. Ultralow surface temperatures in East Antarctica from satellite thermal infrared mapping: the coldest places on Earth. Geophysical research letters, 45(12), pp.6124-6133.

Schirrmeister, B.E., Antonelli, A. and Bagheri, H.C., 2011. The origin of multicellularity in cyanobacteria. BMC evolutionary biology, 11, pp.1-21.

Sen, S., Rai, S., Yadav, S., Agrawal, C., Rai, R., Chatterjee, A. and Rai, L.C., 2017. Dehydration and rehydration-induced temporal changes in cytosolic and membrane proteome of the nitrogen fixing cyanobacterium Anabaena sp. PCC 7120. Algal research, 27, pp.244-258.

Shakya, M., Lo, C.C. and Chain, P.S., 2019. Advances and challenges in metatranscriptomic analysis. Frontiers in genetics, 10, p.904.

Shiraishi, K., Y., Osanai, Y., Tainosho, Y., Takahashi, N., Tsuchiya, S., Kojima, K., Yanai, and K., Moriwaki, 1992. Geological map of the Sør RondaneMountains, Antarctica. Antarctica Geological Map Series, sheet 32, scale 1 : 25 0000. National Institute of Polar Research, Tokyo.

Sinclair, L., Osman, O.A., Bertilsson, S. and Eiler, A., 2015. Microbial community composition and diversity via 16S rRNA gene amplicons: evaluating the illumina platform. PloS one, 10(2), p.e0116955.

Stevens, M.I., Frati, F., McGaughran, A., Spinsanti, G. and Hogg, I.D., 2007. Phylogeographic structure suggests multiple glacial refugia in northern Victoria Land for the endemic Antarctic springtail Desoria klovstadi (Collembola, Isotomidae). *Zoologica Scripta*, *36*(2), pp.201-212.

Stevens, M.I. and D'Haese, C.A., 2014. Islands in ice: isolated populations of Cryptopygus sverdrupi (Collembola) among nunataks in the Sør Rondane Mountains, Dronning Maud Land, Antarctica. Biodiversity, 15(2-3), pp.169-177.

Stuart, R.K., Mayali, X., Lee, J.Z., Craig Everroad, R., Hwang, M., Bebout, B.M., Weber, P.K., Pett-Ridge, J. and Thelen, M.P., 2016. Cyanobacterial reuse of extracellular organic carbon in microbial mats. *The ISME journal*, *10*(5), pp.1240-1251.

Strunecký, O., Ivanova, A.P. and Mareš, J., 2023. An updated classification of cyanobacterial orders and families based on phylogenomic and polyphasic analysis. *Journal of Phycology*, *59*(1), pp.12-51.

Tang, J., Du, L.M., Liang, Y.M. and Daroch, M., 2019. Complete genome sequence and comparative analysis of Synechococcus sp. CS-601 (SynAce01), a cold-adapted cyanobacterium from an oligotrophic Antarctic habitat. *International Journal of Molecular Sciences*, *20*(1), p.152.

Taton, A., Grubisic, S., Brambilla, E., De Wit, R. and Wilmotte, A., 2003. Cyanobacterial diversity in natural and artificial microbial mats of Lake Fryxell (McMurdo Dry Valleys, Antarctica): a morphological and molecular approach. Applied and environmental microbiology, 69(9), pp.5157-5169.

Taton, A., Grubisic, S., Balthasart, P., Hodgson, D.A., Laybourn-Parry, J. and Wilmotte, A., 2006a. Biogeographical distribution and ecological ranges of benthic cyanobacteria in East Antarctic lakes. *FEMS microbiology ecology*, *57*(2), pp.272-289.

Taton, A., Grubisic, S., Ertz, D., Hodgson, D.A., Piccardi, R., Biondi, N., Tredici, M.R., Mainini, M., Losi, D., Marinelli, F. and Wilmotte, A., 2006b. Polyphasic study of Antarctic cyanobacterial strains 1. *Journal of Phycology*, *42*(6), pp.1257-1270.

Terauds, A., Chown, S.L., Morgan, F., J. Peat, H., Watts, D.J., Keys, H., Convey, P. and Bergstrom, D.M., 2012. Conservation biogeography of the A ntarctic. *Diversity and distributions*, *18*(7), pp.726-741.

Terauds, A. and Lee, J.R., 2016. Antarctic biogeography revisited: updating the A ntarctic C onservation B iogeographic R egions. *Diversity and Distributions*, *22*(8), pp.836-840.

Vaulot, D., Geisen, S., Mahé, F. and Bass, D., 2022. pr2-primers: An 18S rRNA primer database for protists. *Molecular Ecology Resources*, *22*(1), pp.168-179.

Van Horn, D.J., Okie, J.G., Buelow, H.N., Gooseff, M.N., Barrett, J.E. and Takacs-Vesbach, C.D., 2014. Soil microbial responses to increased moisture and organic resources along a salinity gradient in a polar desert. *Applied and environmental microbiology*, *80*(10), pp.3034-3043.

Van Horn, D.J., Van Horn, M.L., Barrett, J.E., Gooseff, M.N., Altrichter, A.E., Geyer, K.M., Zeglin, L.H. and Takacs-Vesbach, C.D., 2013. Factors controlling soil microbial biomass and bacterial diversity and community composition in a cold desert ecosystem: role of geographic scale. *PLoS One*, *8*(6), p.e66103.

Velasco-Castrillón, A., Gibson, J.A. and Stevens, M.I., 2014. A review of current Antarctic limno-terrestrial microfauna. *Polar Biology*, *37*, pp.1517-1531.

Vick-Majors, T.J., Priscu, J.C. and A Amaral-Zettler, L., 2014. Modular community structure suggests metabolic plasticity during the transition to polar night in ice-covered Antarctic lakes. *The ISME journal*, *8*(4), pp.778-789.

Vincent, W. F. Evolutionary origins of Antarctic microbiota: invasion, selection and endemism. *Antarctic Science* **12,** 374–385 (2000).

Wang, L., Lei, X., Yang, J., Wang, S., Liu, Y. and Liang, W., 2018. Comparative transcriptome analysis reveals that photosynthesis contributes to drought tolerance of Nostoc flagelliforme (Nostocales, Cyanobacteria). Phycologia, 57(1), pp.113-120.963

Whitton, B.A. and Potts, M., 2012. Introduction to the cyanobacteria. *Ecology of cyanobacteria II: their diversity in space and time*, pp.1-13.

Wynn-Williams, D.D., 1996. Antarctic microbial diversity: the basis of polar ecosystem processes. *Biodiversity & Conservation*, *5*, pp.1271-1293.

Yoshimura, H., Okamoto, S., Tsumuraya, Y. and Ohmori, M., 2007. Group 3 sigma factor gene, sigJ, a key regulator of desiccation tolerance, regulates the synthesis of extracellular polysaccharide in cyanobacterium Anabaena sp. strain PCC 7120. DNA research, 14(1), pp.13-24.

CURRICULUM VITAE

Valentina Savaglia

Department of Life Sciences, University of Liège, Allée du Six Août 13, 4000 Liège - Belgium
Department of Biology, Ghent University, K.L. Ledeganckstraat 35, 9000 Gent - Belgium
email: v.savaglia@gmail.com

I am interested in extreme environment ecology and so far I have focused my research on polar ecosystems.
I am intrigued by the complex processes that are hidden behind life and understanding the threats that climate change poses to the most vulnerable communities is one of my main concerns. Since 2016 I have taken part to four field expeditions in Antarctica and in many outreach activities while also chairing APECS (Association of Polar Early Career Scientists) Belgium between 2018 to 2021. I have strong interests in pursuing a career in research within a multidisciplinary and stimulating environment by also integrating outreach, communication and education in my scientific activities. After starting a joint PhD within the Belgian MICROBIAN project at the Universities of Liège and Ghent in 2017, I obtained a personal doctoral fellowship by the FRIA - F.N.R.S. (National Fund for Scientific Research) of four additional years.

EDUCATION

University of Liège | **Ghent University** - Belgium
PhD student in Biology (2017-2023)
Thesis: Microbiome diversity and function in the Sør Rondane Mountains, East Antarctica
Skills: genomics, transcriptomics, multivariate statistics, network analysis, cyanobacterial isolation and culturing, experimental design & maintenance
Supervisor: Dr. Annick Wilmotte (ULiège)
Co-supervisor: Prof. Elie Verleyen (UGhent)

Sorbonnes Universités (Université de Pierre et Marie Curie) - Paris
M.Sc. Oceanography and Marine Environments

Thesis: Effects of interspecific competition and global warming on two endemic Antarctic *Desmarestia* and two Antarctic red macroalgae

Supervisor: Dr. Katharina Zacher, Alfred Wegner Institute (Bremerhaven, Germany)

Università degli Studi di Catania, Italy

B.Sc. (Honors) Environmental and Natural Sciences

Thesis: A contribution to the knowledge of macrophytobenthos of Monte Cofano Littoral, TP (Italy)

Supervisor: Dr. Donatella Serio

PUBLICATIONS

*a. Peer-review journals (*Corresponding authors)*

Pessi I*, Popin RV, Durieu B, Lara Y, **Savaglia V**, Roncero Ramos B, Hultman J, Verleyen E, Wyverman W, Wilmotte A (2023). Novel diversity of polar Cyanobacteria revealed by genome-resolved metagenomics (submitted). doi: 10.1101/2023.02.03.526606

Vanhellemont Q*, Lambrechts S, **Savaglia V**, Tytgat B, Verleyen E & Vyverman W (2021). Towards physical habitat characterisation in the Antarctic Sør Rondane Mountains using satellite remote sensing. Remote Sensing Applications: Society and Environment, 23, 100529. doi: 10.1016/j.rsase.2021.100529

Beyer T, Mélanie C, Durieu B & **Savaglia V**, 2021. Chercheurs, médiateurs et musées universitaires: une relation à (dé) construire, des pratiques à systématiser. Cahiers de Muséologie.

Bradley A*, Höfer J, **Savaglia V** & Eayrs C (2020). Survey on early career travel support shows geographic, career stage, and indigenous status inequality in access to polar science events. Advances in Geosciences, 53, 73-85. doi: 10.5194/adgeo-53-73-2020

Savaglia V*, Matula C V, Quartino M L, Valli Francione M & Zacher K (2019). Physiological response to irradiance, temperature and co-cultivation in Antarctic engineering brown algae (*Desmarestia menziesii* and *D. anceps*). Polar Biology, 42(11), 2031-2044. doi: 10.1007/s00300-019-02578-1

Zacher K*, **Savaglia V** & Bartsch I (2016). Effects of temperature and interspecific competition on growth and photosynthesis of two endemic Antarctic *Desmarestia* species. Algological studies. doi: 10.1127/algol_stud/2016/0269

b. other publications

Roncero Ramos B, Vanhellemon Q & **Savaglia V** (2020) Microbiome diversity and function in the Sør Rondane Mountains, East Antarctica (MICROBIAN) field report 2020

Savaglia V, Vanhellemon Q, Verleyen E (2019) Microbiome diversity and function in the Sør Rondane Mountains, East Antarctica (MICROBIAN) field report 2019

Savaglia V, Lambrecht S, Verleyen E (2018) Microbiome diversity and function in the Sør Rondane Mountains, East Antarctica (MICROBIAN) field report 2018

c. Publications submitted or in preparation

Savaglia V, Lambrechts S, Vanhellemont Q, Willems A, Wilmotte A, Tytgat B, Verleyen E & Vyverman W. Geology defines microbiome structure and composition in Antarctic ice-free areas. *In prep*

Savaglia V, Roncero Ramos B, Pessi I, Cornet L, Wilmotte A & Verleyen E. Ecophysiological and transcriptomic response to desiccation and rehydration of *Nostoc* sp. from Antarctic freshwater and terrestrial habitats. *In prep*

Savaglia V, Durieu B, Verleyen E & Wilmotte A. Unveiling resistance mechanisms to extreme conditions from comparative genomics of three closely related pairs of cyanobacteria strains isolated from Polar terrestrial and aquatic habitats. *In prep*

Savaglia V, Durieu B, Tytgat B, Vanhellemont Q, Lambrechts S, Verleyen E, Willems A, Wilmotte A & Vyverman W. Diversity of cyanobacteria in terrestrial and aquatic habitats of the Sør Rondane Mountains, East Antarctica. *In prep*

Roncero-Ramos B, **Savaglia V**, Durieu B, Van de Vreken I, Wilmotte A. A cyanobacterial hardening method based on multiple stress factors for soil restoration: an ecophysiological and genomic approach. *In prep*

d. Conferences

October 2022 9th International Conference on Polar and Alpine Microbiology, Potzdam, Berlin, Germany. **Savaglia V**, Lambrechts S, Vanhellemont Q, Willems A, Wilmotte A, Tytgat B, Verleyen E & Vyverman W. Disentangling terrestrial microbial community composition in the Sør Rondane Mountains, East Antarctica

August 2022 Virtual SCAR 2022 'Antarctica in a changing world'. Wilmotte A, Savaglia V, Durieu B, Tytgat B, Lambrechts S, Willems A, Van De Putte A, Van Hellemont Q, Van De Vijver B, Verleyen E & Vyverman W. The science-policy link in practice: how to propose an Antarctic Specially Protected Area (ASPA)?

June 2021 World Microbe Forum (American Microbiology Society), online. **Savaglia V**, Lambrechts S, Durieu B, Vanhellemont Q, Tytgat B, Verleyen E, Willems A, Vyverman W. & Wilmotte A Elucidating microbial community composition in the Sør Rondane Mountains, East Antarctica.

June 2021 World Microbe Forum (American Microbiology Society), online. Roncero Ramos B **Savaglia V** & Wilmotte A Different resistance to salinity and UVR of a pair of *Nostoc* commune strains from cold and warm deserts.

October 2020 Belgian Society for Microbiology Symposium "Microbiology 2020 horizon", Belgium. Roncero Ramos B, **Savaglia V** & Wilmotte A. (16 October 2020). Physiological performance under high salinity conditions of Nostoc commune from hot and cold deserts.

August 2020 SCAR 2020 Open Science Conference Online. **Savaglia V**, Lambrechts S, Durieu B, Vanhellemont Q, Tytgat B, Verleyen E, Willems A, Vyverman W & Wilmotte A. Understanding the microbiome diversity through a combination of remote sensing and close-range field observation techniques in the Sør Rondane Mountains, East Antarctica.

August 2020 SCAR 2020 Open Science Conference Online, Hobart, Australia. Wilmotte A, **Savaglia V**, Durieu B, Lambrechts S, Willems A, Vanhellemont Q, Van de putte A, Van De Vijver B, Tytgat B, Verleyen E & Vyverman W. MICROBIAN: Microbial diversity in the Sør Rondane Mountains in a context of climate change.

April 2020 EGU General Assembly 2020: Sharing Geoscience Online. **Savaglia V**, Bradley A, Höfer J & Eayrs C. Survey on early career travel support shows geographic, career stage, and indigenous status inequality in access to polar science events.

October 2019 Belgian Society for Microbiology Symposium 2019, Bruxelles, Belgium. **Savaglia V**, Lambrechts S, Tytgat B, Verleyen E, Willems A, Vyverman W & Wilmotte
A. MICROBIAN: Microbiome diversity and function in the Sør Rondane Mountains, East Antarctica

June 2018 POLAR 2018 Conference - Where the Poles come together, Davos, Switzerland. **Savaglia V**, Namsraev Z, Mano M J & Wilmotte A (2018). Highest diversity
of cyanobacterial on granite substrates in the Sør Rondane Mountains.

e. Books

Savaglia V, Christiansen H, Gan M Y, Pinseel E, Jacques C & Durieu B (2019). Imagine l'Antarctique, Denkbeeldig Antarctica. APECS Belgium

WORKSHOPS

November 2019 Latex Training, University of Liège, Belgium

July 2019 Determination Course of Freshwater and Terrestrial Cyanobactreria - Department of Botany, University of South Bohemia, České Budějovice, Czech Republic

December 2018 Intensive training to exploit data from the PAM fluorometer of cyanobacteria, University of South Boemia, Czech Republic

September 2018 EMBO: Hands-on training in prokaryotic and eukaryotic metagenomics (ICME9), Bruxelles, Belgium

August 2018 Symposium: Resolving Microbial Communities At Strain-Level Resolution (Anvi'o) with Tom Delmont and A. Murat Eren, University of Exeters, Wales, UK

FELLOWSHIPS, PRIZES AND AWARDS

July 2021 Awarded the Adrian Dahood-Fritz Memorial Fund to cover the registration fees of the online World Microbe Forum organized by the American Microbiology Society

October 2018 Awarded a FRIA/FNRS PhD fellowship (4 years) for the study of "Life on the edge: a comparative study of ecophysiological and genetic adaptations of Antarctic cyanobacteria to aquatic and terrestrial habitats" salary for 4 years + € 10,000

June 2018 Awarded an AntEco-SCAR travel funding to attend POLAR 2018 Conference in Davos, Switzerland

FIELDWORK CAMPAIGNS

January-February 2020 takes part to the Antarctic fieldwork BELARE 2019-20 at the Belgian Princess Elisabeth station within the Belgian MICROBIAN project (funded by BelSPO). Leads a team of 4.

January-February 2019 takes part to the Antarctic fieldwork BELARE 2018-19 at the Belgian Princess Elisabeth station within the Belgian MICROBIAN project. Leads a team of 2 during half campaign.

January-February 2018 takes part to the Antarctic fieldwork BELARE 2019-20 at the Belgian Princess Elisabeth station within the Belgian MICROBIAN project. Team leader: Prof. Elie Verleyen.

December 2015 - March 2016 takes part to the Antarctic fieldwork campaign CAV 2015-16 at the German Dallmann Laboratory in the Argentinean Carlini station within the EU project Interdisciplinary Modelling of Climate Change in Coastal Western Antarctica (IMCONet) for her M.Sc. (experiments with freshly collected macroalgae with remote supervising from Dr. Katharina Zacher, AWI, Germany).

April 2015 takes part to a 3-day Oceanografic cruise within the academic course "UE 4UM14 - Diversité et écologie des écosystèmes marins" at Villefranche sur Mer to learn oceanographic sampling techniques.

LANGUAGES

Italian	mother tongue
English	fluent
French	fluent
Spanish	fluent
German	beginner

ADDITIONAL SKILLS

Photographer (III and last year of professional school: Saint-Luc Prom-Soc Liège)
II star certified **CMAS diver**
B driving license
Adobe suite (InDesign, Illustrator, Lightroom) proficiency